JUL 12 1948

VOLUME 107 NUMBER 3

THE ASTROPHYSICAL JOURNAL

AN INTERNATIONAL REVIEW OF SPECTROSCOPY AND ASTRONOMICAL PHYSICS

MAY 1948

SPECTROPHOTOMETRY OF THE WOLF-RAYET STAR HD 45166 — *F. J. Neubauer and Lawrence H. Aller* 281

THE ULTRAVIOLET SOLAR SPECTRUM, λλ 2935–3060 — *Harold D. Babcock, Charlotte E. Moore, and Mary F. Coffeen* 287

WAVE LENGTHS OF ATOMIC ABSORPTION LINES IN THE SPECTRA OF LONG-PERIOD VARIABLE STARS — *Paul W. Merrill* 303

THE SPECTRUM OF Z ANDROMEDAE IN 1946 AND 1947 — *Paul W. Merrill* 317

J. S. PLASKETT'S STAR OF LARGE MASS, HD 47129 — *Otto Struve* 327

THE SPECTRUM OF γ PEGASI — *Anne B. Underhill* 337

THE INTENSITIES AND PROFILES OF LINES IN SOME B-TYPE STARS — *Anne B. Underhill* 349

A POLARIGRAPHIC STUDY OF THE REFLECTION NEBULA NGC 6729 — *Walter T. Whitney and Edwin B. Weston* 371

STARS IN DIFFUSE NEBULAE — *Jesse L. Greenstein* 375

SOME *f*-VALUES FOR IONIZED OXYGEN AND IONIZED SILICON — *D. R. Bates and Agnete Damgaard* 383

VIBRATIONAL ENERGY LEVELS OF THE CARBON DIOXIDE MOLECULE — *Robert C. Herman* 386

A NEW BAND SYSTEM OF THE C_3 MOLECULE — *John G. Phillips* 389

METHANE IN THE EARTH'S ATMOSPHERE — *Marcel V. Migeotte* 400

ANHARMONIC PULSATIONS OF THE CEPHEID VARIABLE — *H. K. Sen* 404

NOTES

NOTE ON THE PECULIAR SPECTRUM OF HD 25878 — *W. P. Bidelman* 413

LIGHT-CURVE OF A NEW VARIABLE OF R CORONAE BOREALIS TYPE — *Chang Yuin* 413

REPLY TO D. TER HAAR'S REMARKS ON MY PAPER, "THE PHYSICS OF COSMIC GRAINS" — *F. Carnuschi* 417

A FAINT S-TYPE STAR IN THE CLEAR REGION IN CYGNUS — *J. J. Nassau and G. B. van Albada* 418

A NEW BAND IN THE INFRARED SPECTRA OF S-TYPE STARS — *J. J. Nassau and G. B. van Albada* 418

ON THE OCCURRENCE OF LANTHANUM OXIDE IN S-TYPE STARS — *Philip C. Keenan* 420

NOTICE CONCERNING Be STARS — *Paul W. Merrill and Cora G. Burwell* 421

REVIEWS 422

INDEX 425

THE UNIVERSITY OF CHICAGO PRESS
CHICAGO, ILLINOIS, U.S.A.

May 1948 Vol. 107, No. 3

THE ASTROPHYSICAL JOURNAL

AN INTERNATIONAL REVIEW OF SPECTROSCOPY AND ASTRONOMICAL PHYSICS

Edited by

W. W. MORGAN, *Managing Editor*
S. CHANDRASEKHAR
Yerkes Observatory of the University of Chicago

PAUL W. MERRILL
Mount Wilson Observatory of the Carnegie Institution of Washington

HARLOW SHAPLEY
Harvard College Observatory
Cambridge, Massachusetts

N. U. MAYALL
Lick Observatory
University of California

With the Collaboration of the American Astronomical Society

Collaborating Editors:

1946-48
C. S. BEALS
Dominion Astrophysical Observatory, Victoria
LUIS E. ERRO
Astrophysical Observatory, Tonanzintla
O. C. WILSON
Mount Wilson Observatory

1947-49
LYMAN SPITZER, JR.
Princeton University Observatory
A. N. VYSSOTSKY
Leander McCormick Observatory
ALBERT E. WHITFORD
Washburn Observatory

1948-50
CECILIA H. PAYNE-GAPOSCHKIN
Harvard College Observatory
H. N. RUSSELL
Princeton University
ANDREW McKELLAR
Dominion Astrophysical Observatory, Victoria

The Astrophysical Journal is published bimonthly by the University of Chicago at the University of Chicago Press, 5750 Ellis Avenue, Chicago, Illinois, during July, September, November, January, March, and May. ¶The subscription price is $12.00 a year; the price of single copies is $3.00. Orders for service of less than a full year will be charged at the single-copy rate. ¶Postage is prepaid by the publishers on all orders from the United States and its possessions, Argentina, Bolivia, Brazil, Chile, Colombia, Costa Rica, Cuba, Dominican Republic, Ecuador, Guatemala, Haiti, Republic of Honduras, Mexico, Morocco (Spanish Zone), Nicaragua, Panama, Paraguay, Peru, Rio de Oro, El Salvador, Spain (including Balearic Islands, Canary Islands, and the Spanish Offices in Northern Africa; Andorra), Spanish Guinea, Uruguay, and Venezuela. ¶Postage is charged extra as follows: for Canada and Newfoundland, 42 cents on annual subscriptions (total $12.42); on single copies, 7 cents (total $3.07); for all other countries in the Postal Union, 96 cents on annual subscriptions (total $12.96), on single copies 16 cents (total $3.16). ¶Patrons are requested to make all remittances payable to The University of Chicago Press, in United States currency or its equivalent by postal or express money orders or bank drafts.

The following is an authorized agent:

For the British Empire, except North America and Australasia: The Cambridge University Press, Bentley House, 200 Euston Road, London, N.W. 1, England. Prices of yearly subscriptions and of single copies may be had on application.

Claims for missing numbers should be made within the month following the regular month of publication. The publishers expect to supply missing numbers free only when losses have been sustained in transit, and when the reserve stock will permit.

Business correspondence should be addressed to The University of Chicago Press, Chicago 37, Illinois.

Communications for the editors and manuscripts should be addressed to: W. W. Morgan, Editor of THE ASTROPHYSICAL JOURNAL, Yerkes Observatory, Williams Bay, Wisconsin.

Line drawings and photographs should be made by the author, and all marginal notes such as co-ordinates, wave lengths, etc., should be included in the cuts. It will not be possible to set up such material in type.

One copy of the corrected galley proof should be returned as soon as possible to the editor, Yerkes Observatory, Williams Bay, Wisconsin. Authors should take notice that the manuscript will not be sent to them with the proof.

The cable address is "Observatory, Williamsbay, Wisconsin."

The articles in this journal are indexed in the *International Index to Periodicals*, New York, N.Y.

Applications for permission to quote from this journal should be addressed to The University of Chicago Press, and will be freely granted.

Entered as second-class matter, July 31, 1940, at the Post-Office at Chicago, Ill., under the act of March 3, 1879.
Acceptance for mailing at special rate of postage provided for in United States Postal Act of October 3, 1917, Section 1103, amended February 28, 1925.

[PRINTED IN U.S.A.]

THE ASTROPHYSICAL JOURNAL

AN INTERNATIONAL REVIEW OF SPECTROSCOPY AND ASTRONOMICAL PHYSICS

VOLUME 107 MAY 1948 NUMBER 3

SPECTROPHOTOMETRY OF THE WOLF-RAYET STAR HD 45166*

F. J. NEUBAUER AND LAWRENCE H. ALLER

Lick Observatory and Kirkwood Observatory

Received February 1, 1948

ABSTRACT

The star HD 45166 shows Balmer absorption lines in a continuous spectrum, upon which is superposed an emission spectrum of narrow Wolf-Rayet lines. Spectrophotometric measures of the continuum, of the emission, and of absorption lines were made upon plates taken at the Lick and McDonald observatories. The confluence of the Balmer absorption lines and the intensities of $H\beta$, $H\gamma$, and $H\delta$ suggest that $\log N_e = 14.7$ in the atmosphere of the star, which may be taken to be a main-sequence object. The emission spectrum appears to be what would be observed if an atmosphere having the same relative abundances of helium, carbon, nitrogen, and oxygen as in 10 Lacertae or τ Scorpii, were excited to a sufficiently high temperature to emit a Wolf-Rayet spectrum.

The Wolf-Rayet star HD 45166—$\alpha = 6^h20^m.8$; $\delta = +8°13'$ (1900); mag. 9.6; spectrum W7n—shows narrow emission lines of hydrogen, helium, nitrogen, oxygen, carbon, and silicon superposed upon a continuum crossed by strong absorption lines of the Balmer series. At first glance one might suppose that the composite spectrum is produced by a "conventional" Wolf-Rayet star with narrow lines and an ordinary B-type companion with absorption lines. The fact that the star shows no variation of radial velocity with time does not favor this hypothesis.

We shall be concerned here mainly with a photometric study of the spectrum. For those plates which were measured for line wave length and intensity, Table 1 gives the number, date, wave-length region covered, telescope and spectrograph combination, and observer. The star was observed at the McDonald Observatory with the 82-inch reflector and at the Lick Observatory with both the 36-inch refractor and the Crossley reflector. The McDonald observations were obtained by W. A. Hiltner with the Cassegrain spectrograph and 500-mm camera, while the Lick 36-inch refractor plates were obtained with the two-prism spectrograph with a 6-inch camera. The Mills spot sensitometer (plus diaphragm exposures on suitable comparison stars for the Crossley observations) provided the photometric calibration of the Lick plates. At the McDonald Observatory the spectrograph slit was replaced by a wedge slit, illuminated by a lamp plus a diffusing screen for calibration purposes.

Table 2 lists the lines in the photographic region measured upon the Lick 36-inch re-

* *Contributions from the Lick Observatory*, Ser. II, No. 22.

fractor plates. We give the wave length as measured by both authors, eye-intensity estimates on an arbitrary scale (Aller), and identifications (Neubauer).

One may measure the equivalent widths of the absorption lines directly; but, in order to obtain the true relative intensities of the emission lines (which can be expressed in terms of equivalent angstroms of the underlying continuum), we must measure the energy distribution of the continuous spectrum. Plates 330 and 331, kindly obtained for

TABLE 1

LIST OF OBSERVATIONS

Plate No.	Date	Wave-Length Region	Instrument	Observer
29280 M	Jan. 16, 1944	λλ 4900–4000	36-inch 2-prism, 6-inch camera	F.J.N.
28621 M	Mar. 2, 1943	4900–3970		F.J.N.
28622		4900–3970		F.J.N.
28676	April 2, 1943	4900–4340		F.J.N.
28677		4900–4080		F.J.N.
312 LHA	Mar. 20, 1944	4900–3400	Crossley, quartz, 2-prism, slitless	L.H.A.
319	Mar. 21, 1944	4000–3200		L.H.A.
321	Mar. 21, 1944	3500–3200		L.H.A.
323	Mar. 21, 1944	4900–3200		L.H.A.
330	Apr. 30, 1944	4900–3450		G.H.
331	Apr. 30, 1944	4900–3800		G.H.
437	Oct. 16, 1944	4900–3400		L.H.A.
438	Oct. 16, 1944	4900–3200		L.H.A.
CQ 4383	.....	5900–3400	82-inch Cass., 500-mm camera	W.A.H.

TABLE 2

LINES IN THE PHOTOGRAPHIC REGION

Neubauer	Identification			Neubauer	Identification		
	Aller	Int.	Elem.		Aller	Int.	Elem.
3887.5	.....	.....	*He* II	4199.9	4199.7	(5)	*He* II
3886.6	.....	.....	*He* I	4267.2	.....	.....	*Ca* II
3889.1	.....	.....	*H*8	4338.7	4339.4	(0)	*He* II
3930	.....	.....	.....	4340.5			*H*γ
3933.7	3934	(wk)	*Ca* II	4387.9	.....	.....	*He* I
3968.5	3970	(3d)	*He* II	4471.5	4471.7	.....	*He* I
3970.1			*H*7	4481.6	.....	.....	*Mg* II
4009.3	.....	.....	*He* I	4540.8	4541.4	.....	*He* II
4026.2	.....	.....	*He* I	4603.2	4605.0	.....	*N* V
4057.8	4057.7	(5)	*N* IV	4619.4	.....	.....	*N* V
4088.9	4088.7	(3d)	*Si* IV	4634.2	4633.7	(3)	*N* III
4097.3	4097.0	(2)	*N* III	4640.6	4640.2	(3)	*N* III
4100.0	.....	.....	*He* II	4641.9	.....	.....	*N* III
4101.8	4102.4	(7)	*H*δ	4648.5	4648.7	(15)	*O* II
4103.4	.....	.....	*N* III	4658.4	4659.1	(2)	*O* II
4116.1	4116.3	(0)	*Si* IV	4686.4	4686.0	(50)	*He* II
4120.8	.....	.....	*He* I	4860.6	4860.6	(20)	*He* II
4143.8	.....	.....	*He* I	4861.3	.....	.....	*H*β

us by Mr. George Herbig with ν Geminorum as a comparison star, and plates 437 and 438 were best suited for this purpose. In each instance sky fog introduced an uncertainty, estimated to amount to 0.05 in log I. The results from plates 330 and 331 are in good agreement; and, although the October 15 observations show greater accidental errors, they indicate a similar variation of intensity with wave length. Table 3 gives the adopted intensity of the continuous background expressed as log I/I_0, where I_0 is the intensity at λ 4000. The discontinuity at the Balmer limit, log I (λ > 3700) — log I (λ < 3700), is 0.05. We have adopted the energy distribution in the continuous spectra of the comparison stars from the photometric work of Barbier and Chalonge.[1]

The earlier members of the Balmer series show strong emission components, and the intensities of the underlying absorption lines are therefore uncertain. Some of the later members show profiles with definite cusps, indicating that the lines are not broadened

TABLE 3

INTENSITY OF THE CONTINUOUS BACKGROUND

Wave Length	log $I/I_{\lambda\ 4000}$	Wave Length	log $I/I_{\lambda\ 4000}$
3200	+0.36	4200	−0.06
3300	+ .31	4300	− .08
3400	+ .26	4400	− .11
3500	+ .22	4500	− .13
3600	+ .14	4600	− .16
3700	+ .07	4700	− .18
3800	+ .06	4800	− .21
3900	+ .04	4900	− .23
4000	.00	5000	− .25
4100	−0.03	5100	−0.27

TABLE 4

CENTRAL INTENSITIES AND EQUIVALENT WIDTHS OF THE HYDROGEN LINES

Wave Length	R_c	W	Wave Length	R_c	W
4861	.....	4.52 A	3797	0.24	3.82 A
4340	.....	3.90	3770	.17	2.15
4101	.....	3.50	3750	.15	1.35
3970	0.28	4.10	3734	.09	0.64
3889	.27	4.10	3722	0.09	0.50
3835	0.23	3.82			

by any rotational effects. Table 4 gives the measured central depths and the intensities of the lines. The high central intensities suggest that the absorption lines are to some degree filled in by an overlying continuous emission. For early-type stars with pure absorption spectra, R_c is of the order of 0.45, and, if this is true of the absorption "component" of HD 45166, we may estimate that the overlying continuous emission contributes about 60 per cent as much light as does the star which gives the absorption spectrum.

In Table 5 we list the emission lines for which the intensities have been measured on plates listed in Table 1. The first column gives the approximate wave length, the second the identifications, and the third the intensity in terms of 1 A of the continuum at λ 4000. The intensities were first expressed in terms of equivalent angstroms of the underlying continuum and were then reduced to a scale of true relative intensities with the aid of

[1] *Ann. d'ap.*, Vol. **3**, No. 2, 1940.

Table 3. A number of the weaker lines and λλ 5411, 5809, 5812, and 5876 were measured only on the plate CQ 4383. To reduce the intensities of the lines in the visual region of the spectrum to the scale of the others, we assumed a color temperature of 28,000° K for the continuum on the basis of the energy distribution observed in the photographic region of the spectrum. The strongest emission lines are λ 4686 and λ 3203 of *He* II; and, since the latter is nearly as strong as the former, we may infer that a considerable amount of self-reversal takes place, as appears to be true for other Wolf-Rayet stars. Lines of nitrogen, oxygen, and carbon are all prominent, although the strength of the characteristic lines of nitrogen has led to the object's being classified as a star of the nitrogen sequence.

Aside from the interstellar line of *Ca* II at λ 3933, the only absorption lines are those of hydrogen. The members of the Balmer series can be counted up to $n_m = 14$. If we

TABLE 5

INTENSITIES OF THE EMISSION LINES

Wave Length	Elem.	Int.	Wave Length	Elem.	Int.	Wave Length	Elem.	Int.
3202.....	*He* II	12.00	3968.....	*He* II	0.38	4541.....	*He* II+*N* III	1.28
3411.....	*O* IV	1.65	4025.4.....	*He* II	0.08	4634.....	*N* III	0.51
3443.....	*O* III	0.84	4057.8.....	*N* IV	1.33	4640.....	*N* III	1.30
3478.....	*N* IV	3.16	4069.6.....	*C* III	0.16	4648.7....	*O* II	3.10
3483.....	*N* IV	2.84	4080.2.....	*O* III	0.15	4658.....	*O* II	0.81
3706.0.....	*O* III	0.30	4088.8.....	*Si* IV	0.44	4686.....	*He* II	14.0
3714.3.....	*O* III	0.35	4097.....	*N* III	1.60	4861.....	*Hβ*	3.80
3754.6.....	*O* III	0.72	4103.7.....	*H*, *N* III	1.62	5411.....	*He* II	2.54
3759.4.....	*O* III	0.80	4200.....	*He* II	0.96	5400.....	*C* IV	4.72
3791.....	.....	0.14	4340.....	*H*	2.94	5412.....	*C* IV	3.05
3889.....	*He* II	0.38	4380.....	*N* III	0.74	5875.....	*He* I	0.95
3965.....	*He* I	0.28	4513.1.....	*N* III	0.96			

apply the Inglis-Teller formula[2] for the number, N, of broadening charges per cubic centimeter,

$$\log N = 23.26 - 7.5 \log n_m ,$$

we find $\log N_i = \log N_e = 14.66$. From the intensities of the higher members of the Balmer series we can estimate the number of hydrogen atoms in the second level and "above the photosphere" by the method suggested by Unsöld.[3] Thus, from the intensities of Table 4, we find $\log N_{02} H = 16.00$, while, if we assume that the true central intensities of the hydrogen lines ought to be 0.45, we find that $\log N_{02} H$ ought to be increased to 16.20. Once the value of $\log N_{02} H$ has been established, we can employ the earlier members of the Balmer series $H\beta$, $H\gamma$, and $H\delta$ to get an independent check on the number of electrons per cubic centimeter. The intensities of these lines will depend not only on the number of atoms in the second level but also on the broadening, which, in turn, depends on the charge density. The relation between the equivalent width and the effective number of broadening particles can be written in the following form:

$$N = 6.5 \times 10^{12} \frac{W_\lambda^{5/2}}{C_n N_{02} H} ,$$

where C_n is a constant for each line. If we take the equivalent widths of $H\beta$, $H\gamma$, and $H\delta$ (corrected for superposed continuum) as 7.25, 6.25, and 5.60 A, respectively, and if we

[2] *Ap. J.*, **90**, 439, 1939. [3] *Zs. f. Ap.*, **21**, 22, 1941.

assume, following Unsöld, that $N = 1.5N_e$, we find that $\log N_e = 14.51$, 14.76, and 14.80 respectively. The electron density in the atmosphere of "the absorption-line component" appears to be somewhat greater than in τ Scorpii or 10 Lacertae; this result suggests that HD 45166 is definitely not a supergiant but probably is a main-sequence star.

We have analyzed the emission-line intensities by a method given by one of us in a previous discussion of the Wolf-Rayet stars.[4] If we define an excitation temperature by means of the relative population of the upper levels of a given ion, we can derive a "temperature" of that ion from the relative intensities of the emission lines arising from levels of different excitation potentials. Table 6 summarizes the excitation temperatures derived in this way. We list for each ion its ionization potential, the lines employed, the excitation potential of the upper level, the observed intensity, and, finally, the excitation temperature. In good agreement with previous results, the excitation temperature increases with the ionization potential of the ion.

Our next task is to see what we can infer about the chemical composition of the Wolf-Rayet envelope from the relative intensities of the emission lines and the aforementioned relation between the excitation temperature and the ionization potential. For this purpose we employ equations (14) and (15) of Aller's article to estimate the quantity $N_{i+1}N_e$ for the layers in which a given line is produced. Here N_{i+1} refers to the number of ions in the next higher stage of ionization. Thus the λ 4069 line of *C* III gives $N(C\ \text{IV})N_e$, λ 3708 of *O* III gives $N(O\ \text{IV})N_e$, etc.

TABLE 6

EXCITATION TEMPERATURES OF VARIOUS IONS

Ion	I.P.	Wave Length	E.P. (Volts)	Int.	Temperature
O III	54.62	3707+3715	40.41	0.65	56,000°
		3760	36.30	1.52	
N III	47.20	4097+4100	30.28	2.40	38,000
		4380	41.31	0.745	37,600
		4634+4640	32.95	1.45	
N IV	77.04	4057	52.90	1.34	66,500
		3483	50.00	6.0	

To obtain the abundance of *He* II we use the Pickering lines at λ 4542 and λ 5411, since λ 4686 appears to be affected by self-absorption.

Table 7 gives the basis of the abundance estimates. For each ion we list the lines employed, the ionization potential, and, finally, the ratio $\overline{N_{i+1}N_e}/\overline{N(He\ \text{II})N_e}$. The recombination lines of each ion give an estimate of the mean value of the number of ions in the next higher stage of ionization, multiplied by the electron density and by a numerical factor which is the same for all lines observed in the spectrum. Thus the recombination lines of *O* III give an idea of the number of *O* IV ions multiplied by the mean value of the electron density in the layers in which the *O* IV lines are emitted. We estimate the relative abundances of the different elements by the method given by one of us.[4] If we plot $N_{i+1}N_e$ for each element against the ionization potential, we obtain pairs of points which indicate that $N_{i+1}N_e$ increases as the ionization potential increases (see Fig. 4 of n. 4). The results suggest that carbon, nitrogen, and oxygen are all of comparable abundance in this star; and, if we can suppose that helium becomes doubly ionized in the layers where the observed lines of carbon, nitrogen, and oxygen are produced, then helium is

[4] *Ap. J.*, **97**, 135, 1943.

about one hundred and fifty times as abundant as oxygen. In other words, if we take an atmosphere of the same chemical composition as that of 10 Lacertae[5] (in so far as the proportions of helium, carbon, nitrogen, and oxygen are concerned) and excite it so as to produce a Wolf-Rayet type spectrum, we would expect an emission spectrum with just about the same relative intensities as are observed.

The ratio of hydrogen to helium is more difficult to find. We compare λ 4861 corrected for the effect of *He* II, λ 4859 with *He* II, λ 5411 and λ 4542. The emission in a transition n–n' per unit volume is[6]

$$E_{nn'} = N_i N_e \frac{hKZ^6R}{T_e^{3/2}} b_n \frac{2 g_{nn'} e^{X_n}}{n^3 n'^3}, \quad X_n = \frac{hRZ^2}{n^2 kT_e},$$

where g is the Gaunt factor, K is a numerical factor, R is the Rydberg constant, and b_n is a factor expressing the deviation from thermodynamic equilibrium for level n at tem-

TABLE 7

IONIC ABUNDANCES RELATIVE TO HELIUM

Ion	Line	I.P	$\log \left(\frac{\overline{N_{i+1} N_e}}{\overline{N(He\ II) N_e}} \right)$
C III	4069	47.6	−3.10
C IV	5800+12	64.2	−1.85
O III	3708	54.6	−2.17
	3760	.....	−2.18
N III	4097+4100	47.2	−2.48
	4380	.....	−2.55
	4638	.....	−2.48
N IV	4057	77.0	−1.49
	3483	.....	−1.49

perature T_e. With our present assumptions we take $b_n = 1$. The *He* II λ 5411 and λ 4542 transitions represent jumps from $n = 7$ and $n = 9$ to $n = 4$, respectively. If the intensity of *H* λ 4861 (after correction for *He* II λ 4859) is taken as 1.6, then we find $N(H)/N(He) = 1.0$ by assuming that both hydrogen and helium are completely stripped of electrons. This result assumes that the same electron temperature can be assumed for both *H* and *He* II. In this star, at least, both *H* and *He* appear to be of comparable abundance; helium does not appear to be overwhelmingly abundant.

We are indebted to Mr. George Herbig, who obtained plates 330 and 331 and made microphotometer tracings of plates 28621, 28622, and 29280. We are grateful to Dr. W. A. Hiltner, of the Yerkes and McDonald observatories, who kindly placed his plate CQ 4383 at our disposal for photometric measurements.

[5] *Ap. J.*, **104**, 347, 1946.

[6] *Ap. J.*, **85**, 336, 1937.

THE ULTRAVIOLET SOLAR SPECTRUM, λλ 2935–3060*

HAROLD D. BABCOCK, CHARLOTTE E. MOORE,† AND MARY F. COFFEEN
Mount Wilson Observatory
Received January 26, 1948

ABSTRACT

Solar spectrograms, obtained with a 21-foot concave grating, show better detail below λ 3100 than has been reported previously. New measurements of wave length and visual estimates of intensity have been made for 665 lines, λλ 2935–3060. Solar standards of wave length near λ 4500 were observed in the second order for fixing the scale in the overlapping third order. Final measurements were made in the second-order ultraviolet. The new intensities are consistent with those found in the region of greater wave lengths; many of them differ widely from the early values. From a thorough study of laboratory data, identifications have been found for three-fourths of the tabulated lines. The lower E.P. is given for every classified line.

Additional measurements (500 lines, λλ 3060–3150), not presented in detail, show that differences between our interpretation of solar spectrograms and that made by Jewell from Rowland's plates occur even where it is easy to obtain excellent spectrograms.

The text is accompanied by tables and reproductions of spectra.

INTRODUCTION

Almost simultaneously, E. Becquerel[1] and J. W. Draper[2] photographed the prismatic solar spectrum on daguerreotype plates and found a rather surprising extent of the ultraviolet region, in view of their use of flint-glass prisms. The first ultraviolet photographs of the solar spectrum to be made with a diffraction grating were those of Draper,[3] extending to wave lengths less than 3360 A and having a scale of wave lengths for designating the positions of the Fraunhofer lines. Among the numerous investigations which followed, it is interesting to note that Henry Draper,[4] continuing his father's work, obtained grating spectrograms extending to λ 3047 which far surpassed all earlier results. Difficulties of reproduction restricted his published spectrograms to λ 3440 at the limit.

A great extension of the observable solar spectrum was made by A. Cornu[5] by means of a quartz spectrograph with small dispersion. On collodion plates, exposed at comparatively low altitude above the sea, he recorded the principal features of the ultraviolet region as far as λ 2947. Later, from gelatin dry plates, exposed at the summit of Teneriffe (altitude 11,000 feet) by O. Simony, Cornu[6] confirmed his earlier results and sketched the stronger lines of the spectrum as far as λ 2922. He showed that the observable limit of the solar spectrum is dependent on the amount of terrestrial atmosphere traversed by the light.

After more than one hundred years of photographic observation of the ultraviolet solar spectrum, during which H. A. Rowland[7] published his *Preliminary Table* and Fabry and Buisson[8] established the ozone layer in the upper atmosphere as the absorbent

* *Contributions from the Mount Wilson Observatory, Carnegie Institution of Washington*, No. 745.

† National Bureau of Standards, Washington, D.C.

[1] *Bibliothèque universelle de Genève*, **40**, 341, 1842.

[2] *Phil. Mag.*, (3) **22**, 360, 1843.

[3] *Ibid.*; also (3) **26**, 465, 1845.

[4] *Amer. J. Sci.*, (3) **6**, 401, 1873; *Phil. Mag.*, **46**, 417, 1873.

[5] *C.R.*, **86**, 1101, 1878; **89**, 808, 1879.

[6] *Anz. d. K. Akad. Wiss., Wien, Math.-nat. Cl.*, p. 37, 1889; *C.R.*, **111**, 941, 1890.

[7] Ultraviolet Section: *Ap. J.*, **4**, 106, 1896.

[8] *J. de phys.*, (6) **2**, 197 and 297, 1921; *Ap. J.*, **54**, 297, 1921.

responsible for the abrupt fading of the spectrum below λ 3000, the purpose of a new investigation may well be asked. The answer is that, in the spectral region which we discuss here, Rowland's spectrograms were comparatively poor; that Fabry and Buisson used a resolving power insufficient for the examination of fine details and did not refer their wave lengths to a comparison spectrum for standardization; and, finally, that structural analysis of atomic spectra has now reached a stage that aids materially in the identification of the solar lines.

It will be recalled also that, in preparing the revision of Rowland's table,[9] the original wave lengths from λ 2975 to λ 3560 were corrected to the modern scale by an indirect method, in contrast with the procedure in the region of greater wave lengths, where the correction could be based on new solar measurements. Furthermore, small corrections are still required, throughout the range λλ 3500–7330, to adapt the Rowland revision to later improvements in the scale of solar wave lengths. These corrections[10] become practically negligible near λ 3400, but, so far as we know, they have not yet been evaluated in the region discussed here.

In the preceding paragraphs some of the purposes of our investigation are suggested; but, since this work was begun, special interest has been directed to the problem by the successful photography of the spectrum from high-altitude rockets.[11] The extent of the observable ultraviolet is now so great (to λ 2200) that the range of our studies is only an introduction to the problem. Since low dispersion is still a necessary feature of the data obtainable from rockets, it is hoped that our data may be useful in linking the more remote region to that which is easily accessible from ground stations.

INSTRUMENTS

Our observations were made at the Hale Solar Laboratory in Pasadena (altitude 730 feet) with a fixed telescope, which consists essentially of a spherical concave mirror and a convex hyperboloid of the "off-axis" type. Two plane mirrors, a coelostat, and a directing flat are used to bring sunlight to the vertical telescope, and a small auxiliary plane mirror is required, near the focus, for projecting light into the slit of the spectrograph. The aperture of the concave mirror is 18 inches, its radius of curvature, 60 feet. Two hyperboloids of silica are available, giving equivalent focal lengths of about 150 feet and 60 feet, respectively. All the optical surfaces are aluminized.

The concave grating was ruled in 1924 on the large ruling machine at the Mount Wilson Observatory. It is of speculum, with a radius of curvature of 21 feet, and has 66,100 grooves, each about 10 cm long, spaced 600 per millimeter. Before the present investigation was begun, the surface of the grating was covered with evaporated aluminum, markedly increasing the brilliance of the ultraviolet spectra, yet retaining the original resolving power. The grating is used in a modified Eagle mounting, which is sufficiently stable to permit exposures of at least nine hours without loss of definition. In the second order the dispersion is about 1.268 A/mm, and in the third order 0.845 A/mm, near λ 3000. Slit widths ranged from 18 to 12 μ for the definitive plates.

At the bottom of the atmosphere the available solar energy below λ 3000 is only a small fraction of that in the range λλ 3000–3200; and, since instrumental losses steepen this gradient, it is essential to restrict the radiation entering the slit as closely as possible to the region which is to be recorded. Otherwise, the scattering of undesired radiation by the surface of the grating produces fog when the exposure time is sufficient to bring out the spectrum below λ 2990. Few filters are suitable. The mixture of nickel sulphate and cobalt sulphate recommended by H. L. J. Bäckström[12] proved inadequate, perhaps be-

[9] St. John, Moore, Ware, Adams, and Babcock, *Carnegie Inst. Washington Pub.* 396, p. vi, 1928.

[10] *Trans. I.A.U.*, **4**, 60, 1932; see also Table 2 below.

[11] Durand, Oberly, and Tousey, *Phys. Rev.*, **71**, 827, 1947.

[12] *Naturwiss.*, **21**, 251, 1933.

cause the best cobalt sulphate available contained too much iron. A strong solution of nickel sulphate, 5 cm thick, used with a 5-mm plate of Corning glass, No. 986, forms a filter through which the sun is invisible. Spectrograms show that with high sun the radiation transmitted through our apparatus in conjunction with this filter is nearly zero at λ 3400, reaches a maximum near λ 3250, and extends well into the region of ozone absorption. Nevertheless, exposures of several hours on fast emulsions show some fog on the spectrum below λ 2990.

Eastman spectroscopic plates of types IV-O, II-O, and 103-O were used, and exposures ranged up to 6 hours at the center of the solar disk, where most of the observations were made. A small number of spectra were obtained at points along a radius, R, of the image, ranging between $0.75R$ and $0.98R$ from the center. The greater part of the spectrograms were made in the summer of 1943.

TABLE 1

REFERENCE STANDARDS OF WAVE LENGTH IN THE SOLAR SPECTRUM

λ in Air 15°; 760 mm	Int.	λ in Air 15°; 760 mm	Int.	λ in Air 15°; 760 mm	Int.
2995.841	2	3018.143	3	3064.379	1
96.398	5	22.749	3	64.715	1
96.590	5	24.804	3	66.696	−2
97.224	2N	29.992	3	67.783	1
97.980	2	30.609	2	68.946	−1
98.499	1	33.107	2	71.431	−1
3004.122	3	33.819	3	82.628	2
04.632	3	42.265	3	86.402	1
05.054	4	42.488	3	89.507	−1
05.310	3	43.131	1	91.878	0
05.970	2	43.357	2	95.080	0
06.742	3	46.048	1	98.455	2
06.870	3	46.505	0	3104.169	0
08.803	−2	46.807	0	09.624	1
10.182	2	48.221	3	17.770	1
10.630	1	52.493	1	18.143	1
11.169	0	56.112	1	18.255	0
11.279	1	56.342	2	18.829	0
12.452	3	58.708	3	22.081	0
13.972	−1	60.347	−1	25.922	0
14.322	2	60.457	1	33.493	0
15.204	6				

WAVE LENGTHS

Since no standards of wave length have been adopted in the region under discussion, temporary standards in the ultraviolet third-order spectrum were derived by comparison with adopted standards in the blue of the overlapping second order. A simple occulting arrangement, mounted more than a meter in front of the slit because of the astigmatism of the spectrograph, permits the exposure of either a central strip of the plate or two flanking strips, without touching any part of the spectrograph or telescope. When the blue region is being photographed, the ultraviolet filter is replaced by one that is opaque to ultraviolet and transparent to the desired light, such as aesculin, with a Zeiss blue glass, 1 mm thick, No. 17436. The comparison spectrum was put on in equal time-intervals preceding and following the ultraviolet exposure. No attempt was made to extend these spectrograms in the third-order ultraviolet to the limit that could be reached in the second order, since the exposures would have been prohibitive.

The temporary standards derived in the foregoing manner are listed in Table 1, where

the observed wave lengths have been corrected (+0.001 A) to the values which they would have had if the observations had been made in air at 15° C and 1 atm. pressure. Table 1 is based mainly on four excellent spectrograms, though a few lines were not measured on all plates. All the adopted solar standards between λ4534.785 and λ4700.162, inclusive, were utilized in the comparison spectra, and the plates were measured twice in opposite directions. On the average the wave lengths in Table 1 are systematically greater by +0.0008 A than those given for the same lines in the *Revised Rowland* table. Without regard to sign, the mean difference is ±0.005 A.

In Table 2 the corrections required for changing wave lengths from the scale of 1922 to the scale of 1928, which were cited[7] above, are augmented by the result derived from Table 1 and by additional values for the deep-red region.

With reference standards of wave length from Table 1 the positions of intermediate lines (first column, Table 3) were determined by interpolation from second-order spectrograms. But, since the second-order plates extend beyond the lower limit of Table 1, extrapolation was necessary beyond λ 2995.841. Satisfactory measurements could be made with micrometers as far as λ 2959 on the lines best seen. The more difficult lines

TABLE 2

CORRECTIONS FOR CHANGING WAVE LENGTHS FROM THE SCALE OF 1922 TO THE SCALE OF 1928

Region*	Correction to 1922 λ	Region*	Correction to 1922 λ
2995–3133 A	+0.0008 A	6125–6290 A	−0.006 A
3370–3705	−0.0006	6290–6455	−0.007
3719–3849	−0.0015	6455–6630	−0.008
3850–3969	−0.0015	6630	−0.009
4000–5600	−0.002	6800	−0.010
5600–5780	(−0.003)†	6900	−0.012
5780–5960	(−0.004)†	7000	−0.014
5960–6125	−0.005	7100	−0.016

* For the interval λλ 3133–3370 the correction is probably negligible.

† Values in parentheses are interpolated.

below λ 3000 and a majority of all below λ 2975 were measured with a scale on contrasty enlargements. A few lines were measured more easily on spectra of the solar limb, where the marked suppression of the wings of strong lines rendered near-by weak lines more readily visible than on spectrograms of the center of the disk. At the same time the cores of the strongest lines were much easier to measure than in the central region of the disk.

Reduction of the measurements was facilitated by the use of the relation $\lambda = \lambda_0 \pm A \cdot \Delta S - B \cdot \Delta S^2 \mp C \cdot \Delta S^3$, in which λ is the desired wave length, λ_0 the wave length of a known or chosen standard, and ΔS the linear distance between the two lines. Upper signs apply when $\lambda > \lambda_0$. The quantities A, B, and C are functions of the constants of the grating and of the angle of diffraction associated with λ_0. Their computed values were combined with observed values of ΔS corresponding to a succession of known wave lengths, and the small differences between the wave lengths thus derived and the known values were plotted against wave length. From the smoothed curve the corrections to other derived wave lengths were obtained.

The numbers in the first column of Table 3 are stated to three decimal places or to two, according to their estimated reliability. The best results are thought to be significant to the nearest 0.003 A, but those given to two places may be in error, on the average, by 0.02 A.

TABLE 3

THE SOLAR SPECTRUM, λλ 2935.9–3062.875

λ 15°; 760 mm	Int.	Ident.	Low E.P. (Volts)	Notes	λ 15°; 760 mm	Int.	Ident.	Low E.P. (Volts)	Notes
2935.9.....	5?	*V*	0.04	1	2953.36*...	− 1	*Cr* II	3.70	
		Fe II?	4.13		53.48....	− 1	*Fe*	2.75	
36.20....	5?	*Ti* II?	3.81	1	53.84....	25	*Fe* II—	1.04	21
		Fe?	1.60				***Fe***	0.09	
36.5.....	5?	*Mg* II	4.41	1	54.31*...	− 3	*V*	0.02	
36.8.....	5?	*Fe*	0.00	1	54.58*...	2N	—*Fe*	2.27	
37.2.....	5?	*Ti*	0.02	1	54.89....	0	*Ti* II	4.29	
37.65....	5	*V*	0.00	20	55.11....	0	*Cr* II	4.15	
			0.02		55.33....	− 3	*Co*?	.....	
38.41....	5	*Mg*	2.70		55.61....	− 2	*V* II	3.74	
39.23....	20?	*Mn* II	1.17	1	55.79....	− 2	*Zr* II—	1.74	
39.6.....	2?	*Fe* II	1.04	1			*V*	0.07	
40.13....	2	*Fe* II	.....		55.92....	− 3	.....	.....	
40.50....	3	*Mn*?—	2.31		56.08....	2	*Ti*	0.05	
		Mn	2.31		56.34....	− 1	*Cr*	0.00	20
41.29....	10d?	*Fe*	0.09	1				0.94	
42.31*...	5d?	*Ti*	0.00	1	56.64*...	8N	*Cr* II—	4.14	
		Mg—	2.70		56.82*...	2	***Ti***—	0.02	
		V—	0.00	20			*Fe*	2.42	
			0.07		56.95*...	− 3	.....	.....	
42.85*...	5d?	.....	.....	1	57.17*...	− 1	*V*?	1.19	
43.10....	3	*V*	0.00		57.24*...	− 1	*Cr*?	.....	
43.59....	3	*Fe*	.....		57.38*...	10	*Fe*	0.11	
43.87....	5	*Ni*	0.03		57.52*...	− 1	*V* II	0.33	
44.09*...	0	.....	.....				*Fe*	2.27	
.....	0?	.....	.....	18	57.64*...	− 1	*Co*	2.07	
.....	0?	*Fe* II	1.69		58.07....	− 3	*Fe*?	.....	
44.54*...	0	*V* II	0.37		58.26....	− 1	*Ni*?	1.93	
44.98....	0	—*Fe*	.....		58.45....	0N	—*Fe* II?	5.49	
45.37....	− 1	*Fe* II—	1.04	2	58.73....	0N	.....	.....	
45.42....	− 1	*Ti* II	3.86		58.98....	0N	*Ti* II	4.26	
45.65....	− 1	.....	.....		59.32....	1N	*Fe*	.....	
45.79....	− 1	*Fe* II	.....		59.62....	3N	***Fe*** II	3.37	
46.08*...	− 1	.....	.....				*Fe*	2.80	
46.80*...	− 1	*Cr* II	4.30		59.95....	2N1	*Fe* II	5.54	
47.04*...	− 1	.....	.....				*Cr* II—	4.15	
47.70*...	30	*Fe* II—	1.66	21			***Fe***	2.68	
		Fe	0.05		60.28....	1	*Fe*	2.47	
48.22*...	− 1	*Ti*	0.02		60.52....	0	*Fe*	.....	
48.44....	− 1	*Fe*	2.72		60.65....	1NN	*Fe*—	2.94	
48.66....	− 1	—*Fe*?	2.19		61.09*...	1N	*V*—	1.21	
48.95....	3	*Cr*?—	.....				*Fe* II	5.55	
		Fe	.....		61.27*...	3	*Fe* II	1.07	
49.18....	5	*Fe* II	3.75		61.40*...	− 1N	.....	.....	
49.62....	3	*V*	0.02		61.56....	− 1N	.....	.....	
50.22....	5	*Fe*	2.17		61.71....	3	*Cr* II	3.74	20
50.62....	− 1	.....	.....					4.16	
50.77....	− 1	.....	.....		61.91....	− 3	.....	.....	
50.87....	− 1	*Cb* II	0.51		62.12....	3	*Fe*	1.48	
51.09....	0	*Fe* II	3.18		62.38....	0	.....	.....	
51.37....	0	*Cr* II	4.14		62.59....	− 1	*Fe*	.....	
51.53*...	0	*Fe*	.....		62.67....	− 2	*Zr* II	0.36	
52.03*...	2	*V* II	0.35		62.77....	− 2	*V*	0.04	
52.24*...	0	*Zr* II—	0.16		62.93....	− 3	*Fe* II	5.53	
52.86*...	− 1	*Mn* II?	4.05		63.05....	− 1	.....	.....	

* The asterisk is used in the first column to designate lines which, because of their proximity, probably influence one another both as to wave length and as to intensity. This designation might well be placed on most of the lines, for, since the average separation of adjacent lines is 0.16 A (λλ 2975–3060) and many lines are wider than this, nearly every line is a blend. Probably no true continuous background is observed on our spectrograms.

TABLE 3—*Continued*

λ 15°; 760 mm	Int.	Ident.	Low E.P. (Volts)	Notes	λ 15°; 760 mm	Int.	Ident.	Low E.P. (Volts)	Notes
2963.27....	− 2	*V* II	2.59		2975.280...	3	.....	.....	
63.52*...	3N	*Cr* II—	4.15		75.482...	4	*Cr*	0.96	
63.68*...	3	*Fe*—	2.85		75.667...	3	*V* II	1.67	
		Cr?	.....		75.825*..	0	*Fe*?	.....	
63.80....	− 2	*V*	1.21		75.926*..	5	*Fe* II	1.09	
64.13....	6N	*Fe* II	3.37		76.158...	7	*Fe*—	2.27	
64.52*...	0	—*Zr* II	0.09				*V* II	1.67	
64.606*..	6N	*Fe* II	1.72		76.37....	− 2	.....	.....	
64.84*...	1N	*C*	0.00		76.542...	7	*V* II	1.68	
65.02*...	4	*Fe* II	1.69		76.726...	3	*Cr* II	3.81	
65.26*...	10	*Fe*	0.12		76.915...	5	*Ce* II?—	0.53	6
65.41....	− 1	*Fe* II	3.41				***Fe***?	2.82	
65.81....	4ns	*Ti*—	1.06	20	77.238...	− 3	.....	.....	
			1.04		77.535...	2	*V*	0.07	
		Fe	2.42		77.687...	− 1	.....	.....	
66.08....	2	*Cr* II	3.85		77.84....	− 3	*Fe*?	.....	
66.26....	2	*Fe*	2.21		78.057...	3	*Zr* II	0.41	
66.93*...	30	*Fe*	0.00	21	78.206*..	0	—*V* II?	2.36	
67.23*...	0N	*C*	0.01		78.296*..	0	.....	.....	
		Ti	0.05		78.458*..	1	.....	.....	
67.664...	3	*Cr*	1.00		78.559*..	1	.....	.....	
68.092...	1	*Fe* II	5.56		78.694*..	1	.....	.....	
68.20....	− 3	*Ti*	0.00		78.850...	1	*Fe* II	3.75	
68.391*..	3	*V* II	1.70		79.122...	6	*V* II	2.02	
68.518*..	2N	*Fe*—	2.41				*Fe* II	3.95	20
68.742...	1	*Cr* II	4.16					5.55	
		Fe II	3.37		79.372...	8	*Fe* II	1.09	
68.97....	− 1	*Zr* II	0.46		79.59....	− 3	.....	.....	
69.04....	− 3	*Fe*?	.....		79.744...	2	*Cr* II	3.74	
69.19....	1	—*Ni*	1.94		79.88*...	1	.....	.....	
69.35*...	1	*Fe*	0.11		80.02*...	1	.....	.....	
69.46*...	8	*Fe*	0.86		80.221...	1	.....	.....	
69.67*...	− 1N	*Cr* II	4.30		80.398...	0	.....	.....	
69.96*...	3	*Fe* II	3.80	3	80.560...	5	*Fe*	2.75	
70.12*...	8	*Fe*	0.11	20	80.797...	4	*Cr*	0.96	
			0.09		80.981...	4	***Fe*** II	3.41	
70.36*...	3	.....	.....	3			*Zr* II	0.56	
70.521*..	5	*Fe* II	1.07		81.20*...	0	*V* II	2.37	
70.68*...	1N	*Fe* II	3.75		81.460*..	6N	*Fe*	0.05	
70.92*...	1N	—*Fe* II?	.....		81.660*..	3	*Ni*	0.11	
71.120*..	2	*Cr*	0.98		81.868...	3	*Fe*	2.17	
71.24....	0	.....	.....		82.069...	3	*Fe* II	4.46	
71.624*..	0	*Fe* II	3.37	3	82.245...	3	*Fe*	2.98	
71.77*...	1	*Fe*	.....				***Fe*** II	3.80	
71.938*..	3	*Cr* II	3.75		82.395*..	1	.....	.....	
72.03....	− 1	*Fe* II	5.58		82.490*..	1	.....	.....	
72.276...	4	*V* II	2.36		82.770*..	2	*V* II	1.67	22
		Fe	2.19		82.98*...	− 2	*V* II	1.67	20
72.417*..	− 1	.....	.....					1.68	
72.65*...	− 2	*Cr* II	3.73		83.20*...	− 1	—*Ti*	0.02	
73.203*..	40	*Fe*	0.09	21	83.578*..	40	*Fe*	0.00	21
		Fe	0.05		83.84*...	1	.....	.....	
73.747*..	2	*Ni*?—	1.67		84.146*..	4	*Ni*	0.00	
73.93*...	− 1N	*V* II	3.78		84.35....	− 2	*Ti* IIp	1.08	
74.225*..	1	.....	.....		84.576...	2	.....	.....	4
74.43....	− 1N	*Fe* II	.....		84.71*...	1	*Cr* II	3.74	4
74.642...	0	.....	.....		84.842*..	7N	***Fe*** II	1.66	
74.793...	3	*Fe*	2.82				*Fe*	0.86	
74.92....	− 2	*Ti*	1.06		85.19*...	− 3	*V* II	3.78	5
75.040...	2	.....	.....		85.326...	0	*Cr* II	3.73	

TABLE 3—*Continued*

λ 15°; 760 mm	Int.	Ident.	Low E.P. (Volts)	Notes	λ 15°; 760 mm	Int.	Ident.	Low E.P. (Volts)	Notes
2985.49*...	1	*Ti*	0.02		2995.262...	3	.....	.....	
85.56*...	5Nd	*Fe* II	1.72		95.375...	− 1	.....	.....	
85.73....	1	.....	.....		95.496*..	2	.....	.....	
85.874...	4	*Cr*	0.98		95.590*..	− 2n	.....	.....	
86.006...	4	*Cr*	1.00		95.841...	2	*Fe*	3.00	
86.147...	2	*Cr*	0.96		96.010...	4n1	*V* II	1.67	
86.300...	2	*Fe*	.....		96.398...	5	*Fe*	2.41	
86.480...	6	*Cr*	1.03		96.590...	5	*Cr*	0.98	
		Fe	0.11		96.73....	− 2N	*V* II	1.70	
86.643...	6	*Fe* II—	3.41		96.851...	2	—*Ti* II?	1.08	22
		Fe	2.42		97.00....	− 3N	*V*	2.02	
86.875...	0N	*Fe* II?p	3.87		97.224...	2N	.....	.....	
87.054...	2	.....	.....		97.32....	3	*Ca*	1.88	
87.20*...	2	*Co*	0.00				*Fe* II—	4.48	
87.293*..	10	*Fe*	0.91				*Cu*	1.64	
87.664...	10N	*Si*	0.78		97.54....	− 3	.....	.....	
88.035...	6	*V* II—	1.68		97.72....	− 3	*Fe* II	3.89	
		Cr II	3.75		97.864*..	− 2	*V*	2.03	
		Ni II	3.09		×97.980*..	2	(*Pt*)	0.10	
88.197...	0	.....	.....		98.154...	2	*Cr*?	3.43	
88.31....	− 3	.....	.....		98.338...	1	.....	.....	
88.483...	1	*Fe*	1.48		98.499...	1	.....	.....	
88.646...	2	*Cr*	0.94		98.797...	4	*Cr*	0.94	
88.776...	0	.....	.....		98.968...	2	.....	.....	
88.928...	1d?	*Fe*	2.72		99.04....	− 3	*Gd* II	0.03	
		Sc	0.02		99.207...	3	*Fe*—	.....	
		Sc II	3.22				*V*?	1.19	
89.14....	3	*Cr* II	3.72		99.368*..	4	*Cr* II—	3.84	
89.32....	− 1N	*V* II	2.37		99.523*..	10	*Fe*	0.86	
89.632...	4	*V* II	1.70		99.67*...	2	*Ca*	1.88	22
		Co	0.00		99.945...	2	*Cr* II	3.99	
89.78....	0N	*V* II	2.37		3000.067...	2	*Fe* II	3.80	2
90.037...	0	.....	.....		00.21....	− 3	.....	.....	
90.392...	6	*Fe*	2.72	2	00.341...	2	.....	.....	
90.620...	− 2N	.....	.....		00.464*..	3	*Fe*	1.48	
90.878...	2	.....	.....		00.578*..	2	*Co*	0.10	
91.098...	5	*Ni*	0.27	20	00.75*...	0	*Fe* II—	.....	
			1.93				*Ti*	0.05	
91.244...	1	*Fe* II	3.41		00.948*..	25	*Fe*	0.09	21
91.413...	1	*Zr* II	0.00		01.232*..	5N	*V* II	1.70	
91.637...	5	*Fe*	.....		01.434*..	1N	—*Fe* II	.....	
91.776...	4	—*Fe* II	5.49		01.660...	2	*Fe*	3.00	
91.884...	4	*Cr*	0.96		01.793...	3	*V* II?	2.55	
92.100...	1	.....	.....		01.934...	− 2	*V*	2.05	
92.409...	5	*Cr* II	3.74		02.043...	− 2	.....	.....	
92.602...	7	*Ni*	0.03		×02.195...	− 2	(*Mo*)	0.00	
92.960*..	− 1	.....	.....				*Fe* II	.....	
93.048*..	0	.....	.....		02.343*..	− 3	*Fe* II	3.93	
93.25....	1d?	.....	.....		02.488*..	25	*Ni*	0.03	21
93.400...	2	*Fe* II	4.48		02.662*..	10	*Fe* II	1.69	
93.800...	4	.....	.....		03.047...	8	*Fe*	0.95	
94.076*..	4	*Cr*	0.94		03.465*..	3N	*V* II	1.68	22
94.438*..	40	*Fe*	0.05	20, 21	03.651*..	8	*Ni*	0.11	5
			0.12		03.897*..	5	*Cr* II	3.85	
		Ni	0.03		04.122...	3	*Fe*	2.42	
94.760...	3	*Cr* II	3.73		04.273*..	2	*Fe* II	3.80	
94.953...	4	*Ca*	1.87		04.364*..	0	.....	.....	
95.115...	3	*Cr*—	0.94		04.482...	− 2	*Cr* II	4.39	
		Co?	2.13				*Fe*?p	2.21	
					04.632...	3	*Fe*	1.55	

TABLE 3—*Continued*

λ 15°; 760 mm	Int.	Ident.	Low E.P. (Volts)	Notes	λ 15°; 760 mm	Int.	Ident.	Low E.P. (Volts)	Notes
3005.054...	4	*Cr*	1.03		3013.972...	− 1	—*Fe*?	.....	
05.310...	3	*Fe*	2.39		14.107*..	2	*Fe*	2.94	
05.496...	− 1N	*Zr*	0.99		14.166*..	3	*Fe*	0.95	
05.757...	4d?	*Co*—	1.87		14.322...	1	*V*	2.12	
		V II?	2.36		14.459...	0N	.....	.....	
05.970...	2	*Fe*?	.....		14.650*..	0	*Mn*	3.12	
06.181...	0	—*V*	2.07	4	14.783*..	9	*Cr*—	0.96	
06.320...	0N	—*Fe*	.....				*V* II	1.68	
06.436...	0N	.....	.....		14.921*..	8	*Cr*	0.98	
06.575...	4d	.....	.....	8, 22	15.204...	6	*Cr*	0.96	
06.742...	3	.....	.....	7	15.368...	− 2	*Sc*	0.00	
06.870...	3	*Ca*	1.89		15.510...	4	*Cr* II	4.40	
07.154*..	5	*Fe*	1.48		15.690...	− 1	*Co*	1.87	
07.293*..	6	*Fe*—	0.09		15.820...	− 1	.....	.....	
		V II	1.67		15.931*..	5	*Fe*	2.42	
07.499...	1	*Ti*?	.....		15.991*..	0N	*V* II	2.03	
07.65*...	0	*Mn*	3.12		16.198*..	10	*Fe*	0.99	
07.77*...	− 1	*Fe* p	2.58		16.451*..	2	*Mn*	3.12	
07.96*...	3NN	.....	.....	2	16.524*..	0	.....	.....	
08.154*..	15	*Fe*	0.11	21	16.786*..	5	*V* II	1.70	
08.295*..	2	*Mn*—	3.12		16.874*..	3	.....	.....	
		Ti II	1.56		17.08....	− 2	.....	.....	
08.472...	3	—*V* II?	2.53		17.189*..	4	*Ti* II	1.58	
08.650...	4d	*V* II—	1.67		17.257*..	4	*Co*	1.87	
		Cr II	4.36		17.420*..	3	.....	.....	
08.803...	− 2	*Ce* II?	0.32		17.633*..	12	*Fe*	0.11	
08.924...	− 3	.....	.....				*Cr*	1.00	
09.104...	3	*Fe*	2.39				*Co*	0.10	
09.216...	2	*Ca*	1.89		17.856*..	2	.....	.....	
09.36....	1N	.....	.....		17.955...	0	*Ni*	1.93	
09.584...	12	*Fe*	0.91		18.033...	0	*Os*?	0.00	
09.923...	− 3	*Fe* II?—	.....		18.143...	3	*Fe*	2.39	
10.031...	− 3	*Fe*	.....		18.256...	1	*Fe* p	2.55	
10.182...	2	*Fe*?	.....		18.498...	4	*Cr*	0.96	
		Fe II	5.80		18.601...	− 2	.....	.....	
10.423...	0	*Ti*?p	1.87		18.703...	− 2	.....	.....	
10.630...	1	*Fe*	.....		18.823*..	4	*Cr*	0.98	
10.849...	0	*Cu*	1.38		18.994*..	7	*Fe*	0.95	
11.169...	0	*Mn*	3.12		19.156*..	7	*Ni*	0.00	
11.279...	1	.....	.....		19.315*..	4	*Fe*	2.44	
11.371...	0N	*Mn*—	3.12				*Sc*	0.02	
		Cr II	3.81		19.56*...	− 2	.....	.....	
11.480...	4	*Fe*	2.75	8	19.913*..	0d	.....	.....	
11.634...	− 2	.....	.....		20.017*..	5	*Fe* II	4.06	2
11.738...	0	*Zr*—	0.07		20.27*...	− 1	.....	.....	
11.88*...	0N	.....	.....		20.492*..	20	*Fe*	0.09	21
12.014*..	12	*V* II	2.04	4	20.658*..	40	*Fe*	0.00	21
		Ni	0.42		21.079*..	30	*Fe*	0.05	4, 21
12.348*..	− 3	*Cr* II	3.99		21.22*...	− 1	*OH*	0.84	9
12.452...	3	*Fe*	.....				*OH*	0.92	
12.60....	− 3	*Fe* IIp	3.80		21.574*..	5	*Cr*	1.03	
12.738...	− 2	.....	.....		21.721*..	0	*OH*	0.76	9
12.939...	3	.....	.....				*OH*	1.00	
13.050*..	3	*Cr*	0.96		21.885*..	1	.....	.....	
13.103*..	3	*V* II	1.67		22.12....	− 3	*V* II	2.37	
13.333...	1N	*Zr* II—	0.56		22.268...	1	.....	.....	
13.499...	1	.....	.....		22.361...	2	*Co*	1.70	
13.597...	2	*Co*	0.00		22.474...	− 1	.....	.....	
13.732*..	6	*Cr*	0.96		22.604...	3N	*V* II	1.67	
13.833*..	0	*Fe* II	4.14		22.749...	3	*Mn*	3.12	

TABLE 3—*Continued*

λ 15°; 760 mm	Int.	Ident.	Low E.P. (Volts)	Notes	λ 15°; 760 mm	Int.	Ident.	Low E.P. (Volts)	Notes
3022.91....	— 3	.....	.....		3031.213...	6	*Fe*	2.44	
23.070...	3	.....	.....	4	31.348...	6	—*Cr*	0.98	
23.30....	— 3	.....	.....		31.476*..	1	*Cr*	2.97	
23.440...	0	.....	.....		31.670*..	10	*Fe*	1.01	
23.697...	1N	.....	.....		31.869*..	5	*Ni*	0.00	
23.853*..	4N	*Fe* II—	3.87		32.038...	— 2	.....	.....	
		V II	2.04		32.230...	— 2N	.....	.....	
24.062*..	12	*Fe*	0.11		32.471...	1	*Ni* II	2.85	
24.244*..	2	.....	.....		32.647...	— 3N	.....	.....	
24.355*..	6	*Cr*	0.98		32.857*..	— 2	*Gd* II	0.08	
24.579...	— 2	.....	.....		32.931*..	3	*Cr* II	2.69	
24.679...	1	*Cr*	2.95		33.107...	2	*Fe*	2.41	
24.804...	3	.....	.....		33.436...	4d?	*V* II	2.51	
24.983...	2N	*V* II	2.36	2	33.609...	1N	*Mn* II?	.....	
25.288...	6	*Fe*	0.91		33.819...	3	*V* II	1.81	
25.646*..	8	*Fe*	2.39		33.951...	— 2N	.....	.....	
25.868*..	18	*Fe*	0.12		34.063...	— 1	*Cr* II	4.36	
26.223*..	— 1N	.....	.....				*Gd* II	0.03	
26.379*..	3	*Co*	1.87		34.12....	— 3	*Sn*	0.21	
26.497*..	8	*Fe*	0.99		34.198...	3	*Cr*	1.00	
26.647*..	6	*Cr* II	4.41		34.45*...	3	*Co*	0.17	12
26.838...	2	*Cr* II	3.99		34.50*...	3	*Fe*	1.60	
26.944*..	2	*Fe*?	.....		34.55*...	3	*Cr* II	3.84	
27.018*..	2	.....	.....		34.60*...	3	.....	.....	
27.215...	— 2N	.....	.....		34.814...	0	*Mn* II	.....	22
27.35....	— 2	*Fe* IIp	3.93		34.990...	1	*Cr* II	4.02	
27.609...	1	*V* II	2.37		35.120...	— 3	.....	.....	
		Gd II	0.14		35.234...	1	*NH*	1.28	13
27.701...	2	.....	.....				*Fe*p	3.06	
27.892...	— 1N	*OH*	0.51	9	35.362...	2	.....	.....	
		Pd	0.96		35.458...	— 2	.....	.....	
28.022*..	4	*V* II—	2.37	4	35.749...	4	*Fe*	.....	
		Zr II	0.97		35.888...	0	.....	.....	
28.129*..	4	*Cr* II	4.39		36.001...	— 3	.....	.....	
28.289...	0	.....	.....		36.110...	1N	*Cu*	1.64	
28.447...	— 2N	*Cb* II	0.44		36.254...	0	.....	.....	
28.606*..	1	.....	.....		36.399...	2	*Zr* II	0.56	
28.688*..	1	.....	.....	10	36.511...	0	*Zr* II	0.52	
28.871...	2	.....	.....		36.62....	— 2N	*Y* II	3.55	
29.002*..	2N	.....	.....		36.756...	2N	—*Ti* II	1.56	
29.071*..	2N	*Mn* II	5.35		36.94*...	— 2	*Fe* II	5.80	
29.157*..	4	*Cr*	0.98		37.046*..	8	*Cr*	1.03	
29.229*..	3	*Fe*	1.55		37.23*...	3	.....	.....	
29.290*..	2	*Ni*	1.67	20	37.398*..	30	*Fe*	0.11	21
			1.94		37.64*...	0	.....	.....	
29.347*..	— 2	.....	.....		37.790*..	3	*Fe*	0.99	
29.432*..	— 3	.....	.....	8	37.948*..	15	*Ni*	0.03	
29.550...	— 2N	*Zr*—	0.15		38.093*..	1	*Cr* II	4.91	
		V II	1.70		38.314...	3	*Co*?	0.92	
29.736...	5n1	*Ti* II	1.56		38.515...	2	*V* II	2.46	
		Sb	2.02				*Cr* II	3.99	
29.992...	3	.....	.....		38.749...	3d	*Ti* II—	1.58	
30.149*..	5	*Fe*	2.42				*Fe* II	3.87	
30.256*..	5	*Cr*	1.00		38.980*..	1	.....	.....	2
30.486...	— 3	*OH*	0.46	9	39.068*..	3	*Ge*	0.88	14
30.609...	2	*Fe*p—	2.27		39.204...	— 3	.....	.....	
30.762...	— 2	*Fe*	2.98		39.327*..	3n1	*Fe*	2.42	
		Sc	0.02		39.38*...	— 3	*In*	0.00	15
30.85....	— 3	.....	.....		39.599...	4ns	*Co*	1.70	
30.943...	2d?	*Zr* II	0.00				*Mn* II—	5.37	
31.054...	2	.....	.....		39.763...	3	*Cr*	1.00	

TABLE 3—*Continued*

λ 15°; 760 mm	Int.	Ident.	Low E.P. (Volts)	Notes	λ 15°; 760 mm	Int.	Ident.	Low E.P. (Volts)	Notes
3040.022...	− 2N	*Sc* II?	3.99		3048.005*..	0	.....	.....	
40.220...	− 3	.....	.....		48.096...	0	*Co*	1.95	
40.35*...	− 3	*OH*	0.34	9	48.221...	3	*V* II	2.50	
40.43*...	10	*Fe*	0.91		48.354...	− 1N	.....	.....	
40.608*..	2	*Mn*	3.12		48.456...	5	*Fe*	.....	
40.763*..	2	.....	.....		48.571...	− 3	*OH*	0.29	9
40.845*..	4	*Cr*	1.00	16	48.653...	− 3	*V* II	2.26	
40.940*..	4	*Cr* II	4.28		48.764...	2	*Ti* II	1.57	
41.040*..	2	.....	.....		48.889...	4	*Co*	0.17	
41.138...	− 3	*Fe* II?	.....				*V* II	2.03	
41.222...	0	*Mn*	3.12		49.017...	2	*Fe* II	5.85	
41.414...	2n1	*V* II	2.02				*Mn* II	.....	
41.627*..	5	*Fe*	1.55		49.158...	− 2	*Fe* IIp	4.06	
41.756*..	5	*Cr* II	4.40		49.351...	3	.....	.....	
		Fe	0.95		49.548...	2	.....	.....	
41.903*..	1	.....	.....		49.756...	− 3N	.....	.....	
42.028*..	7	*Fe*	1.01		49.902...	− 3N	*Cr*	1.03	
42.265...	3	*V* II	2.02		50.076...	2	*Al*	3.59	
42.488*..	3	*Co*	0.10		50.134...	3	*Cr* II	4.30	
42.666*..	10	*Fe*	0.99		50.275...	− 2	.....	.....	
42.856*..	3	*NH*	1.28	13	50.398...	− 2	*V*	1.37	
43.019...	− 3	.....	.....		50.506*..	0	*Co*	1.95	
43.131...	1	*V*	0.02		50.67*...	1N	*Mn* II	.....	
43.265...	− 2	.....	.....		50.817*..	10	*Ni*	0.03	8
43.357...	2	*Mn*	3.12		51.04*...	3	.....	.....	
43.545...	3	*V*	0.00		51.24....	− 3	.....	.....	
		V II	2.03		51.418...	2	.....	.....	
43.761...	− 2n	*Mn*	3.12		51.61....	− 3N	.....	.....	
43.855...	2	*Ti* II—	1.56		51.796...	− 1N	*Fe*?	.....	
		Cr II	4.05		51.989...	− 3d?	.....	.....	
44.011...	5	*Co*	0.00		52.150...	− 1	*V*	0.02	
44.126...	2	*Zr* II—	0.56		52.215...	0	*Cr*	3.07	
44.230...	2N	*Cr* II	4.92		52.270...	0d?	.....	.....	
44.335...	− 2	*OH*	0.31	9	52.493...	1	.....	.....	
44.44....	− 3	.....	.....		52.582...	− 1	.....	.....	
44.570...	3	*Mn*	2.11		52.67....	− 3	.....	.....	
44.722...	− 3	.....	.....		52.790...	0	*Fe* p	2.55	
44.839...	2	*Fe* II	3.95		52.928...	− 1	*Sc* II	3.41	
44.94....	− 2	*V*	0.04		53.070...	3	*Fe*	2.41	
45.01*...	4	*Ni*	0.16	2	53.248...	− 3	*V* II	3.53	
45.07*...	4	*Fe*	0.91		53.422...	7d	*V* II—	1.80	
45.342...	− 3	*Fe* II	5.54				*Fe*	1.01	20
45.48....	− 2N	.....	.....					2.93	
45.584...	2	*Mn*	3.12		53.55....	− 2	.....	.....	
		Fe	2.44		53.671...	1	*V*	0.00	
45.725...	1	*Sc* II	3.39		53.746...	2	.....	.....	
45.780...	1	*Mn*	3.12		53.882...	4	*Cr*	1.03	
45.96....	− 3	.....	.....				*V* II	2.04	
46.048...	1	*Fe*	.....		54.317...	12	*Ni*—	0.11	
46.17....	− 3	.....	.....				*Mn*	2.13	
46.268...	0N	*Mn* II	5.38	22	54.700...	2Ns	*Al*—	3.58	
46.505...	0	.....	.....				*Co*	0.17	
46.674...	3	*Ti* II	1.16		54.832...	1	*Zr* II	1.01	
46.807...	0	*Fe*	2.72		54.942...	1	*Fe*	2.60	
46.937...	2	*Fe*	2.42				*Eu* II	0.21	
47.050...	2	*Fe*	2.94		55.118...	1	.....	.....	
		Mn	3.12		55.298...	6d	**Fe**—	1.55	
47.202*..	0	*Fe*	2.83				*Fe* II	5.88	
47.43*...	1	*Cr*?	3.07		55.459...	1	*Cr* II	3.84	
47.616*..	35	*Fe*	0.09	21	55.596...	− 3	.....	.....	11
47.79*...	3?	*Cr* II	2.69		55.722...	4d	*Fe*—	.....	

TABLE 3—*Continued*

λ 15°; 760 mm	Int.	Ident.	Low E.P. (Volts)	Notes	λ 15°; 760 mm	Int.	Ident.	Low E.P. (Volts)	Notes
3055.936...	− 3N	*V* II	2.51		3060.041...	0d	*Fe* II?	4.06	
56.112...	1	.....	.....				*Co*	1.95	
56.235...	2	*Fe*	.....		60.12....	− 1	*Zr* II	0.04	
56.342...	2	*V*	0.02		60.24....	− 1	.....	.....	
56.463...	− 3	.....	.....		60.347...	− 1	.....	.....	
56.583...	1N	.....	.....		60.457...	0	*V*	0.04	
56.770...	5d	*Ti* II—	1.16		60.550...	0	*Fe*	2.98	
		Fe II	4.06		60.635...	0	*Cr*	3.09	
57.006*..	0N	.....	.....		60.775...	2	.....	.....	
57.136*..	2	*Al*	3.60		60.991...	2	*Fe*	1.55	
57.438*..	25	*Ti* II—	0.00	21	61.12....	− 1	*Cr* IIp—	4.46	5
		Fe	0.86		61.28....	− 3	.....	.....	
57.645*..	10	*Ni*	0.21		61.35....	− 1	*Zr* II	0.09	
57.790*..	2	*Fe*p	0.95		61.40....	− 1	.....	.....	
57.875...	− 3	*Cr* II	4.30		61.57....	1	*Cr* II	4.02	
57.965*..	3	.....	.....		61.66....	0	*Cr*	2.53	
58.077*..	7	*Ti* II	1.18	2	61.827...	3	*Co*	0.10	
58.242...	− 2N	.....	.....		61.974...	0	—*Co*	1.73	
58.358...	3	*Cr* II	4.06		62.12*...	1	*Mn*	2.15	
58.490...	4	*Fe*	.....		62.18*...	2	*Co*	0.10	
58.708*..	3	.....	.....	17	*	2?	*Fe* II	4.06	19
59.096*..	25	*Fe*	0.05	21	62.29*...	2	.....	.....	
59.385...	0	*Cr* II	2.69		62.52....	− 1	*OH*	0.24	9
59.518...	2d?	*Cr* II	2.69	20	62.70....	0	*V* II	1.81	
			2.69		62.83*...	0	.....	.....	
59.740...	3	*Ti* II	0.01	20	62.875*..	4	*Fe*	2.94	
			1.16						

NOTES TO TABLE 3

1. For 10 lines, λλ 2935.9–2942.85, the question mark after the intensity is used to indicate that the absorption is probably due in each case to an unresolved group of lines, each weaker than the tabular value.

2. Diffuse absorption bands of atmospheric O_3, each roughly 10 A wide, occur near the wave lengths designated. No fine structure is known. The wave lengths have been taken from Wulf and Melvin (*Phys. Rev.*, **38**, 330, 1930; see also footnotes 13, 14, 15, p. 299).

3. Diffuse absorption is noticeable from λ 2969 to λ 2971. It seems structureless but is superposed by the definite tabular lines, among which λ 2970.36 coincides closely with a line of *Si*, λ 2970.35, E.P. 0.78; but this particular detail of the solar absorption is too weak and much too sharp to permit its unqualified identification with *Si*. The other member of the multiplet, λ 2987.664, has solar intensity 10N and corresponds in position with its laboratory counterpart. Without doubt, the line of *Si* at λ 2970.35 is present in the solar spectrum and would appear much like λ 2987.664 if it were not confused with superposed detail. Higher dispersion than that which we have used would permit a more accurate description of these solar details.

4. In the original *Rowland Table* the lines corresponding to those marked here by this note were given footnotes which stated that their violet portions were due partly to lines of the overlapping first-order yellow spectrum.

5. In the original *Rowland Table*, footnotes stated that the red portions of these lines were due partly to lines of the overlapping first-order spectrum (see n. 4).

6. The observed intensity is not accounted for by *Ce* II? and *Fe*?.

7. No line corresponding to this wave length was seen on Rowland's plates because it was covered by the strong first-order line of *Mn* λ 6013.503.

8. Band heads degrading to shorter wave lengths are suspected near the positions marked by this note number.

9. Eight lines having this note are members of the satellite branch of a band of *OH* which was discussed by Mulliken (see footnote 17, p. 299). The other seven members of comparable rotational energy are masked. The E.P. is computed from molecular constants given by H. L. Johnston, D. H. Dawson, and

M. K. Walker (*Phys. Rev.*, **43**, 473, 1933). The range of solar intensities among these *OH* lines is smaller than that observed for emission in the laboratory, an analogy with the red system of *CN*.

10. A line of *Ca* III, E.P. 30.32 volts, nearly coincides with this solar line, λ 3028.688, but other evidence of *Ca* III is not found. *Ca* is perhaps the most likely element to appear in the solar spectrum in the doubly ionized state, since the I.P. of *Ca* II is only 11.82 volts and the abundance is favorable. The apparent coincidence of several weak solar lines, otherwise unidentified, with known lines of *O* III is probably fortuitous, since no lines of *O* II, I.P. 35 volts, have been recognized.

11. A line of *Ce* III λ 3055.585, E.P. 2.25, is probably not producing this solar line (see preceding note).

12. This group of lines is too poorly resolved for satisfactory measurement, although the principal details can be counted.

13. The R head of the 1, 0 band of the $^1\Pi \leftarrow {}^1\Delta$ system of *NH* degrades toward the red from λ 3035.234. The Q head is at λ 3042.856. Both are strengthened in sunspots. The $^1\Delta$ state is not the ground state of *NH*. The tabulated E.P. for *NH* does not include rotational energy.

14. Other *Ge* lines of low E.P. occur in the solar spectrum at λ 3269.505 and λ 4226.567.

15. Evidence of the occurrence of the *In* line here is supported by our unpublished observations of the raie ultime at λ 4511.34 and of λ 3256.01 (solar wave lengths), both of which are found to have intensities −2 in the disk and −1 in the spot. Of the remaining sensitive lines, λ 4101.764 is masked by *Hδ*, and the weakest, λ 3258.565, is absent.

16. Resolution of the group at λ 3040.8 is incomplete.

17. A line of *Os*, E.P. 0.00 volts, is probably masked by this solar line, λ 3058.708.

18. Leaders in the wave-length column indicate unresolved lines. These are so closely defined by the measurements of adjacent lines that the identification of *Fe* II with part of the observed absorption, as given in the third column, appears reasonable.

In the $^2\Sigma \leftarrow {}^2\Pi$ system of *OH* bands, the clearest head of the $v' = 3$, $v'' = 2$ member, E.P. 1.1 volts, lies near λ 2945. The solar absorption here is no doubt in part due to this molecule. Other bands from the same (ground-state) term have been observed in the solar spectrum, e.g., the 2, 2 head near λ 3185.

19. The leaders in the wave-length column indicate the presence of a solar line between the adjacent lines, but no maximum of absorption is seen on which significant measurements can be made (see preceding note).

20. The numbers in the "E.P." column indicate that two lines of the same element but of different E.P. coincide here.

21. In the spectra of the central part of the solar disk and of integrated sunlight, these lines of *Fe* and *Ni* have wide wings, so diffuse that they may be nearly invisible when the spectral background is weak or when fog reduces the contrast. Some of these lines were described as faint in Rowland's table; and for similar reasons others are wide and weak on our plates but show great strength on the low-dispersion spectrogram of Fabry and Buisson.

22. The following lines weaken about 2 intensity units near the solar limb: λλ 2982.770, 2996.851, 2999.67, 3003.465, 3006.575, 3034.814, 3046.268.

INTENSITIES

For most of the lines in Table 3, visual estimates of intensity were made from the original spectrograms. The results were checked and extended by further estimates from enlarged positive prints, which could be used more easily in the region originally underexposed. It is recognized that the data obtained in these ways may be influenced by errors of undesirable magnitude, but valid photometric measurements are so difficult in this region that they could not be attempted. Enlarged positive prints of the region λλ 3652–3720 were made in the same manner as were those of shorter wave length from which intensities were to be derived. From these prints a scale of Rowland's intensities was selected containing typical lines from intensity −1 to 40, and the type lines were then compared with each of the lines below λ 3000 in Table 3. The spectra used for these estimates of intensity were representative of the central region of the solar disk, and the resulting intensities therefore may differ somewhat in meaning from those of Rowland, which refer to sunlight more or less completely integrated over the disk. Some of the numbers in the second column are accompanied by symbols: "d," double; "N," nebulous, diffuse; "NN," very diffuse; "Nl," diffuse more noticeably on the side toward longer wave length; "Ns," diffuse toward smaller wave lengths; "n," slightly diffuse; "?," stated result is doubtful. Near the beginning of the table a few fairly strong intensities are given the symbol "?" to indicate that even on the best plates it cannot be determined whether these objects are strong individual lines or, much more probably, close groups of weaker lines unresolvable against the faint background (see n. 1 to Table 3).

As would be expected, spectrograms made with the slit very near to the solar limb show marked changes in the intensities of some lines, when compared with the data of Table 3. The most striking effects are associated with the strong lines of *Fe* and *Ni*, which are very wide and diffuse when seen in the central part of the disk but at the limb lose their great wings and present narrow cores. This phenomenon is more pronounced in the ultraviolet than in the visual region and can be traced to a greater distance from the limb in the shorter wave lengths. Further discussion of intensities is given below.

IDENTIFICATIONS

The lines of Table 3 without exception are considered to originate in the solar atmosphere, although terrestrial ozone is known to have diffuse absorption bands near the positions indicated in note 2 to this table. Densitometer-curves from our best spectrograms show no diffuse absorption that can be related to the separate bands of ozone. Sir William and Lady Huggins[13] first observed these telluric bands in low-dispersion spectra of hot stars; Fowler and Strutt[14] showed them to be due to ozone and observed them in the solar spectrum, with a dispersion of 58 A/mm, at very low sun. E. Pettit[15] concluded that, even with low dispersion, these bands would be masked in the spectrum of the high sun.

The identifications given in Table 3 result from a thorough comparison of the solar data with the wave lengths and intensities from laboratory spectra and with the structural analyses of the spectra. Part of the laboratory data has been compiled from the original sources and published by C. E. Moore.[16] The remainder is from her forthcoming ultraviolet multiplet table. It is probable that these identifications are as definitive as existing knowledge permits.

For the identification of molecular lines the results of H. D. Babcock[17] have been utilized and supplemented by additional laboratory data for *OH* and *NH*.

When a solar line is associated with more than one element, the symbols are placed one below the other, with the upper one corresponding to the violet component of the blend. A dash preceding or following a chemical symbol indicates the presence on the violet or on the red, respectively, of an unknown component. A boldface symbol indicates the dominant component in a blend. For weak components which are supposed to be wholly masked by lines too strong to have been appreciably modified by them, the identifications have been omitted. A few lines not yet observed in the laboratory but predicted from known term values are identified and indicated by the symbol "p" following the element.

EXCITATION POTENTIALS

For classified atomic lines the lower excitation potentials (fourth column, Table 3) are those adopted by C. E. Moore.[16] For molecular lines the excitation potential has been computed from the molecular constants.

Approximate values of the high excitation potentials are found by adding 4.10 volts to the tabular values. A closer approximation is found with the aid of Table 4, or by reference to the *Revised Multiplet Table*, or by multiplying the wave number of a line by 12395×10^{-8}.

Notes referred to in the final column of Table 3 are given at the end of the table.

[13] *Proc. R. Soc.*, **48**, 216, 1890.

[14] *Proc. R. Soc., A*, **93**, 577, 1917.

[15] *Mt. W. Contr.*, No. 622; *Ap. J.*, **91**, 159, 1940.

[16] *A Multiplet Table of Astrophysical Interest* (rev. ed.; Princeton, 1945).

[17] *Mt. W. Contr.*, No. 708; *Ap. J.*, **102**, 154, 1945.

DISCUSSION

Most of the differences between our observational data and those of Rowland are due to the improved contrast afforded by modern filters and by our use of a large, stable, achromatic image of the sun. In notes 7 and 21 (Table 3), attention is called to some special points of interest in comparison with Rowland's table. Many less striking differences will also be found, such as our omission of some false lines.

The relatively low dispersion and resolving power used by Fabry and Buisson[8] account for the differences between their data and ours. From their descriptive text the reader will note that most of the wave lengths in the tabular data of Fabry and Buisson are not from solar measurements but are merely the positions of laboratory lines which they considered responsible for the observed solar absorption. The solar intensities assigned by those writers are reasonably similar to ours, when the diverse conditions of observation are kept in mind.

The identifications of solar lines in this spectral region, as given by Rowland and by Fabry and Buisson, were based on approximate coincidences of solar and laboratory lines. In the *Revised Rowland*[9] the identifications were rediscussed with the aid of the analyses of atomic spectra available twenty years ago. Such analyses are now much

TABLE 4

FOR FINDING THE HIGH E.P.

λ	Add to Low E.P.	λ	Add to Low E.P.
2936	4.21 volts	3047	4.05 volts
2974	4.15	3063	4.03
3010	4.10		

further advanced, yet many of the earlier identifications are confirmed, and comparatively few are rejected. Numerous additions to the list of identified solar lines are now made, as a result of improved and extended data. Three-fourths of the lines in Table 3 are identified, and, of these, nearly half are associated with singly ionized elements. A search has been made for elements in the second stage of ionization, but in notes 10 and 11 to Table 3 we conclude that the data provide no certain evidence of their occurrence in the sun.

Additional evidence of the occurrence of *In* in the sun is summarized in note 15 to Table 3, a new line of *Pt* is recognized at λ 2997.980, and a probable line of *Os* at λ 3018.033. Two weak, diffuse solar lines due to *C*, at λ 2964.84 and λ 2967.23, are associated with the lowest term of this element. Absorption by *OH* has been identified with the aid of extensions to the well-known $^2\Sigma \leftarrow {}^2\Pi$ system, which were recognized by R. S. Mulliken.[18] The absorption ascribed to band heads of *NH* is discussed in note 13 to Table 3. The lower molecular state involved here is not the ground state but is more than 1 volt higher. Other solar bands arising from the same state were found by H. D. Babcock.[17] No doubt numerous additional weak molecular lines occur in the spectral region of Table 3, but their identification must await further study. Some of the strongest unidentified lines of Table 3 are collected in Table 5.

While the present investigation was in an early stage and before the observations for Table 1 had been completed, the disk spectrum was measured from λ 3060 to λ 3150 on a second-order plate of high quality. Reference lines were selected for their measurability and were assigned the wave lengths given them in the *Revised Rowland*. The purpose of this special study was not so much to verify the relative values of the wave lengths as to examine the correspondence between Rowland's description of the lines and their appearance on our plates. Over 500 lines were observed on the spectrogram. Of these,

[18] *Phys. Rev.*, **32**, 410, 1928.

37 lines are not listed by Rowland, the strongest being λ 3119.584, of intensity 1. On the other hand, 15 lines were recorded by Rowland which we could not distinguish as separate objects on our plate. The strongest is λ 3075.240, of intensity 3. Rowland described 9 lines as single, each of which we find resolved into two; but 31 lines which appear single on our spectrogram were each given two wave lengths by him. These include such objects as λ 3081.280, whose intensity is 25Nd but which he described as a pair, with intensities 2 and 3; and λ 3077.203, whose intensity is 25 but which Rowland saw as a pair with intensities −3 and −1. These examples illustrate some of the peculiarities in the data of Rowland. To them may be added his treatment of the Q branches of the 0, 0 band in the system $^2\Sigma \leftarrow {}^2\Pi$ of *CH*. These branches have their principal absorption in the range λλ 3143.4–3145.2, where the superposition of numerous lines produces a wide, sharp stripe across the spectrum. Although the absorption is not uniform, there

TABLE 5

THE STRONGEST UNIDENTIFIED LINES FROM TABLE 3

λ	Int.	λ	Int.
2942.85	5?	3023.070	3
2975.280	3	3024.804	3
2993.800	4	3029.992	3
2995.262	3	3034.60	3
3006.575	4d	3037.23	3
3006.742	3	3049.351	3
3007.96	3NN	3051.04	3
3012.939	3	3057.965	3
3016.874	3	3058.708	3
3017.420	3		

is no possibility of observing any individual spectral line with this stripe; yet L. E. Jewell, who measured Rowland's plates, recorded 16 wave lengths and separate intensities within this space. It appears that Jewell, with all his skill in measuring, was overzealous in describing unresolved details. T. Heimer[19] showed that *CH* has about 50 lines in the interval considered, and 19 atomic lines are potentially present there as well, as may be seen from the *Revised Multiplet Table*.

Other less striking differences between Rowland's data and the results of later work are found scattered through the range of his observations. These call for careful redescription, most of which is easily available in the Utrecht *Atlas*.[20] Lest we appear hypercritical, we hasten to remark that our experience has taught us a vast respect for Rowland's genius and that discrepancies like those noted above are probably due to Jewell's interpretations of the spectrograms, in which he disagreed with Rowland, as he himself pointed out[21] and we have noted elsewhere.[22]

Besides the observations described above, numerous spectrograms of sunspots have been obtained, each having a comparison spectrum from the normal disk. But though our filters permit the direct photography of spots in satisfactory contrast against the disk by means of a narrow range of radiation with maximum energy near λ 3250, the

[19] *Zs. f. Phys.*, **78**, 771, 1932.

[20] *A Spectrophotometric Atlas of the Solar Spectrum*, by M. Minnaert, G. F. W. Mulders, and J. Houtgast (Amsterdam, 1940).

[21] L. E. Jewell, *Ap. J.*, **21**, 28, 1905.

[22] H. D. Babcock and Charlotte E. Moore, "The Solar Spectrum, λ 6600 to λ 13495," *Carnegie Inst. Washington Pub.* 579, p. 3, 1947.

difficulty of making representative spectrograms of sunspots is very great. Exposure times for the spot spectrum seem consistent with the appearance of the direct photographs, and the effects of atmospheric and instrumental scattering are apparently not always too bad; yet critical study of the spectrograms is required for discerning the changes that occur when passing from disk to spot, especially for wave lengths shorter than λ 3200.

The seeing is always much worse in the ultraviolet than in visible light, and atmospheric refraction introduces displacements, at the slit of the spectrograph, of the ultraviolet image of the spot with reference to the visible image. Apart from these and other technical difficulties, the possibility may be suggested that some solar factor may operate to obscure, in the ultraviolet, phenomena that are more accessible in other radiation.

In passing from the center of the solar disk to the limb, definite changes of intensity are found for some lines of weak and medium intensity, a phenomenon distinct from the suppression of the wide wings of intense lines. The effect for weak lines amounts to a weakening of about two intensity units at the limb, and, among the few observations that are collected in note 22 to Table 3, most of the affected lines are identified with ionized metals. In the visible and infrared this phenomenon has long been familiar.

From the foregoing paragraphs it appears that the spectral region studied here is not likely to yield results on the temperature effect in spots or on the limb effect commensurate with those more easily found in the region of greater wave length.

To Professor J. C. Duncan, director of Whitin Observatory, we extend sincere thanks for assistance in obtaining some of our most useful spectrograms.

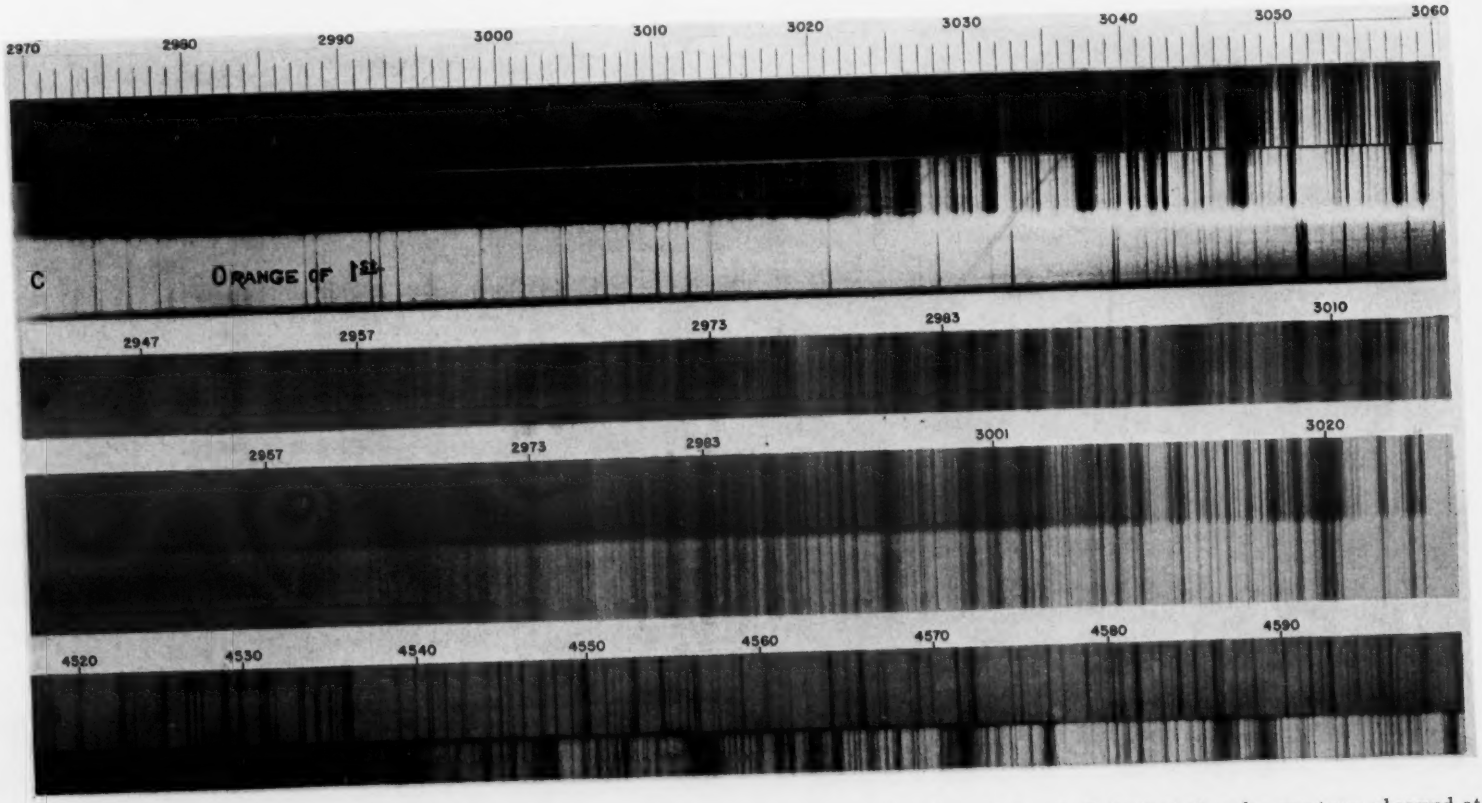

FIG. 1.—Portions of the solar spectrum: *A*, *B*, *C*, minified copy of Rowland's map (wave-length scale above); *D*, limit of the solar spectrum observed at Hale Laboratory (el. 700 ft.)—for 3010 *read* 3001; *E*, at center of disk; *F*, near the limb; *G*, *H*, second-order blue and third-order ultraviolet (wave lengths in *H* are $\frac{2}{3}$ of those in *G*).

WAVE LENGTHS OF ATOMIC ABSORPTION LINES IN THE SPECTRA OF LONG-PERIOD VARIABLE STARS*

PAUL W. MERRILL
Mount Wilson Observatory
Received December 24, 1947

ABSTRACT

Lists of wave lengths measured during recent investigations of the spectra of long-period variable stars are in Tables 1 (R Leonis, type Me) and 2 (R Andromedae, type Se). The wave lengths, based on spectrograms having a dispersion of 10 A/mm (20 A/mm in the red), should have relatively few errors in excess of 0.02 A, although blending and actual displacements will cause many larger differences from corresponding laboratory wave lengths. Estimates of intensity made at the microscope are included. Data for the corresponding laboratory lines include the element, multiplet number, and wave length.

The regions covered in the spectrum of R Leonis are λλ 3442–4575; in R Andromedae, λλ 3342–5064 and λλ 5797–6832.

The wave lengths of lines recorded in Tables 1 and 2 were measured recently in the course of a general investigation of the spectra of long-period variable stars of types Me and Se. The spectrograms, dispersion 10 A/mm, were described and illustrated in *Mount Wilson Contributions*, Nos. 713, 717, 720, and 730,[1] which should be consulted for relevant data.

The probable error of the wave length of a sharp line measured on a single good plate is somewhat less than 0.01 A. Except for values in parentheses, relatively few of the wave lengths should have errors of measurement in excess of 0.02 A. Many of the wave lengths agree with the laboratory values within this limit; most of the residuals that are larger are probably caused either by blends or by actual displacements. The relative displacements of various classes of lines, some of which are due to emission components, have previously been discussed.[1]

The intensities in the second column of Tables 1 and 2 are estimates made at the measuring microscope; they have, of course, the well-known limitations of eye estimates. The scale is such that 1 corresponds to a narrow line of about optimum intensity for accurate settings.

The recorded identifications are limited to the more important lines involved; many minor contributors are omitted. Various columns give the chemical element, the multiplet number in the *Revised Multiplet Table*,[2] and the decimals of the laboratory wave length. Two or more contributing lines are listed in order of wave length. A line belongs to the neutral atom unless the ionized atom (II) is indicated.

R Leonis 094211.—R Leonis is a well-known red variable star, period 309 days, class M8e, whose spectrum is representative of the coolest known stars of the giant branch. Table 1 is based on measurements of six of the best spectrograms of R Leo, supplemented by data from two plates of R Aql and one each of R Hya, U Ori, R Ser, and R Cas. One strongly exposed plate of R Leo, Ce 3017, phase +49 days, was measured in great detail; it supplied most of the lines having but one measure; and the recorded intensities were largely estimates made on this plate. Most of the intensities were checked by comparison with microphotometer tracings, magnification 60.

Longward from λ 4200 the list is seriously incomplete because of increasing interference by the *TiO* band lines.

R Andromedae 001838.—R Andromedae is a red variable star, period 407 days, whose spectrum is a typical example of class Se. Most of the wave lengths in Table 2 were based on two to four spectrograms. For the spectral region λλ 3342–5064, plates Ce 3522 and 3526 (phase +10 days) and 3560 and 3564 (+45 days) were used; for the region λλ 5797–6832, plates Ce 4003 (+27 days), 4035 and 4040 (+53 days). The green region, unfortunately, was not photographed in this investigation.

* *Contributions from the Mount Wilson Observatory, Carnegie Institution of Washington*, No. 743.

[1] *Ap. J.*, **102**, 347, 1945; **103**, 6 and 275, 1946; **105**, 360, 1947.

[2] C. E. Moore, *Contr. Princeton U. Obs.*, No. 20, 1945.

TABLE 1

ATOMIC ABSORPTION LINES IN THE SPECTRUM OF R LEONIS

λ	Int.	No. Pl.	Ident. El.	Mult.	λ
3400					
42.80	2	1	Fe	26	.67
			Co	6	.92
43.79	2	1	Co	22	.64
			Fe	6	.88
.....	...	..	....	....	...
.....	...	..	....	....	...
51.95	0.5	1	Fe	81	.92
52.31	1	1	Fe	25	.28
52.86	1.3	1	Ni	17	.89
53.55	1.2	1	Co	22	.51
55.18	1.3	1	Co	6	.24
56.93	0.7s	1	Co	5	.92
58.47	3 n	1	Ni	19	.47
59.99	0	1	....	....	...
61.65	2	1	Ni	17	.65
62.81	2	1	Co	23	.80
(65.6)	1	1	Zr	17	.63
			Co	5	.79
(65.9)	1	1	Fe	6	.86
66.50	0.5s	1	Fe	24	.50
67.50	1	1	Ni	3	.50
69.45	1 s	1	Ni	8	.49
71.32	0.5s	1	Fe	82	.27
(72.5)	1.3	1	Ni	20	.54
73.95	1	1	Co	4,23	.02
75.54	3 n	1	Fe	6	.45
			Fe	78	.65
76.68	2	1	Fe	6	.70
83.05	1	1	Fe	24	.01
			Ti	22	.01
83.42	1	1	Co	23	.41
83.78	1.2	1	Ni	6	.77
85.87	2	1	Ni	17	.89
89.40	1	1	Co	36	.40
(90.61)	4	1	Fe	6	.58
(91.27)	2	1	Co	6	.32
(93.00)	4 n	1	Ni	18	.96
(95.70)	1	1	Co	22	.68
96.70	1	1	Co	19	.68
97.97	4	1	Fe	6	.84
98.95	1	1	Ru	4	.94
3500					
00.92	3	1	Ni	6	.85
02.47	4 n	1	Co	21	.28
			Ni	3	.60
			Co	6	.63
(03.8)	0.4	1	Ti	22	.76
06.32	2	1	Co	21	.31
06.62	1	1	Ti	22	.64
07.71	2	1	Ni	3	.69
09.87	1.5s	1	Co	22	.84
10.34	3	1	Ni	18	.34
(11.60)	0	1	Ti	22	.63
12.66	1	1	Co	21	.64
13.47	1.8	1	Co	5	.48
13.93	2	1	Ni	17	.93
15.00	4 n	1	Ni	19	.05
18.36	1	1	Co	36	.34
19.76	2	1	Ni	5	.77
20.06	2	1	Co	4	.08
21.42	3 n	1	Fe	24	.26
			Co	20	.57
(23.43)	1.5	1	Co	21	.42
			Ni	16	.44
24.56	6 n	1	Ni	18	.54
26.06	2.5	1	Fe	6	.04
26.80	2	1	Co	4	.85
27.93	2	1	Ni	6	.98
29.01	1.7	1	Co	5	.03
29.81	1.5s	1	Co	22	.81
(31.8)	0.4	1	Mn	18	.85
(32.1)	0.6	1	Mn	18	.00
			Mn	18	.12
33.33	1.7	1	Co	5	.36
(33.7)	(0.4)	1	V	53	.68
			V	53	.76
(35.0)	0	1	Fe	48	.91
(36.6)	0.3	1	Fe	326	.56
(37.5)	0.3	1	Fe	239	.49
(38.6)	1.5	1	Fe	137	.55
(40.1)	0	1	Fe	329	.12
40.72	1.5s	2	Fe	23	.71
(42.2)	0.3	1	Fe	326	.08
			Fe	128	.24
(45.8)	0.2	1	Gd II	2	.80
(47.0)	0.3	1	Ti	133	.03
(47.7)	0.6	1	Zr	13	.69
48.17	2	2	Ni	3,20	.18
(49.0)	0	1	Y II	9	.02
50.58	2	2	Co	4	.60
51.53	1.5	1	Ni	5	.53
52.70	2	1	Y	8	.69
			Co	6	.72
53.46	1.7	1	Ni	16	.49
54.14	0.6	2	Fe	23	.12
58.51	3	1	Fe	24	.52
58.78	1.6	1	Co	20	.78
60.89	2 s	4	Co	21	.89
61.72	2.5s	3	Ni	2	.75
64.95	1.5	1	Co	19	.95
65.42	2	2	Fe	24	.38
66.37	2.5	1	Ni	36	.37
67.72	0.5	1	Sc II	3	.70
69.42	2	1	Co	35	.37
70.15	3.5n	1	Fe	24	.10
			Fe	326	.24
71.25	0.5s	1	Fe	46	.23
71.86	3	1	Ni	5	.87
72.55	0.6	1	Zr II	1	.47
			Sc II	3	.52
74.94	1.5	1	Co	21	.96
75.36	2	1	Co	4	.36
(76.34)	0.4	1	Sc II	3	.34
77.24	1	1	Ni	3	.24
78.69	20. n	1	Cr	4	.69
81.21	5. n	1	Fe	23	.20
(82.6)	0.5	1	....	....	...
84.75	(3)	1	Co	6	.80
85.26	(3)	1	Co	21	.15
			Fe	23	.32
85.71	(3)	1	Fe	23	.71
(86.2)	0	1	Zr	12	.28
87.07	3 n	1	Fe	23	.99
			Co	35	.19
87.92	2.5	4	Ni	16	.93
89.11	2.5	3	Fe	23	.11
90.55	0.5	1	Sc II	3	.48
93.36	20.	1	Cr	4	.49
94.86	(3)	1	Co	4	.87
96.15	1	1	Ru	4	.18
			Rh	1	.19
			Fe	181	.20
97.69	3	3	Ni	18	.70
98.70	0.5	1	Ti	59	.71
3600					
00.72	0.3	1	Y II	9	.73
01.20	0.4	1	Zr	13	.19
02.13	3	3	Y II	9	.93
			Co	4	.08
			Ni	3	.28
03.25	(0.4)	1	Fe	295	.21
03.85	0.5n	1	Fe	496	.85
			Ti	20	.84
04.22	(1)	1	Ti	21	.28
05.30	15.	1	Cr	4	.33
06.72	1	2	Fe	294	.68
			Ti	20	.79
07.57	0.5	1	Mn	8	.54
08.86	2	1	Fe	23	.86
09.28	2.5	1	Ni	16	.31
10.38	4	1	Mn	8	.30
			Ni	18	.46
(11.01)	0.4	1	Y II	9	.05
11.54	1.5	1	Ni	2	.54
			....	....	...
12.74	3	1	Ni	6	.74
13.62	0	1	Ti	0	.60
13.82	0.4	1	Sc II	2	.84
15.64	2.5	5	Cr	3	.64
17.86	0.4	1	Fe	496	.79
			Co	36	.01
18.37	0	1	Fe	324 P	.30
			Fe	295,571	.39
18.77	3.5	1	Fe	23	.77
19.38	3	1	Ni	35	.39
20.01	1	1	Fe	324 P	.00
			Ni	0	.03
20.96	0.5	1	Y	8	.95
21.46	0.4	1	Fe	294	.46
23.18	0.4	2	Fe	180	.19
23.83	0.5	1	Zr	12	.86
24.12	1	1	Ca	9	.11
24.84	1.5	1	Ni	2	.73
			Co	21	.96
26.10	0.7s	3	Ti	20	.09
27.81	1.5s	4	Co	19	.81
28.64	0.4	1	Y II	9	.71
30.83	2 n	1	Sc II	2	.74
			Ca	9	.75
			Ca	9	.97
31.45	4	1	Co	4	.39
			Fe	23	.46
32.65	0	1	....	....	...
33.07	0.4	1	Y II	2	.12
34.23	0.3	1	....	....	...
34.91	1	1	Ni	33	.94
35.33	4	1	Ti	20	.20
			Cr	3	.28
			Ti	19	.46
37.97	1 s	3	Ti	18	.97
39.79	0.6	1	Cr	47	.80
40.42	0.7	2	Fe	295	.39
			Cr	47	.39
41.64	2	3	Ni	6	.64
42.70	3	2	Ti	19	.68
			Sc II	2	.78
43.31	0	1	....	....	...
43.80	0.6	1	Fe	46 P	.82

TABLE 1—Continued

λ	Int.	No. Pl.	Ident. El.	Mult.	λ
3600					
44.39	2 s	1	Ca	9	.41
44.79	1	1	Ca	9	.77
(45.0)	0	1	Ca	9	.99
45.38	0.5	1	Sc II	2	.31
45.85	0	1	Fe	496	.82
46.21	1	4	Ti	18	.20
47.82	5	1	Fe	23	.84
49.30	3	2	Fe	5	.30
49.96	0	1	....	.....	...
			Fe	394	.03
50.30	0.3	1	Fe	180	.28
50.95	0.4	1	....	.....	...
51.46	0.3	1	Fe	295	.47
51.82	0.6	1	Sc II	2	.80
52.56	1.7	8	Co	4	.54
53.47	3	1	Ti	19	.50
54.61	1.5	2	Ti	18	.59
(55.55)	0	1	Fe	369	.47
			....	.....	...
56.30	0	2	Cr	46	.26
56.97	1	1	Co	21	.96
57.50	0	1	....	.....	...
58.08	2.5	9	Ti	19	.10
59.53	0.5	1	Fe	180	.52
60.64	2	6	Ti	18	.63
61.35	1.7	7	Ru	3	.35
			Fe	179	.37
61.95	1.5	6	Ni	16	.95
63.64	0.3	1	Zr	12	.65
64.10	3	6	Ni	4	.10
(64.6)	0	1	Y II	9	.62
66.49	1 n	1	....	.....	...
			Sc II	2	.54
69.10	3 n	1	Ti	18	.97
			Ni	2	.24
70.42	3	5	Ni	4	.43
71.25	0	1	....	.....	...
71.68	2	3	Ti	19	.66
74.11	3	8	Ni	15 P	.06
			....	.....	...
			Ni	32 P	.15
(75.10)	(0.7)	1	....	.....	...
75.72	(0.7)	1	V	29	.70
77.10	(0.7)	1	V	.....	...
79.93	4	3	Fe	5	.92
82.26	0.5	2	....	.....	...
83.06	3 s	5	Fe	5	.06
87.43	3	2	Ti	19	.35
			Fe	21	.46
88.09	0.5	1	V	29	.07
88.41	2	2	Ni	5	.42
89.92	1	1	Ti	18	.91
90.31	1	1	V	29	.28
92.28	2	4	V	29	.22
			Rh	1	.36
92.74	0.5	1	....	.....	...
93.90	1.7	1	Ni	15	.93
95.88	1.5	1	V	29	.86
3700					
02.94	0.5n	3	Ti	132	.94
03.59	1 s	8	V	29	.58
04.09	0	1	Co	35	.06
04.70	1	2	V	29	.70
05.09	0.5	1	V	29	.04
05.58	4	2	Fe	5	.57
07.82	3	7	Fe	5	.83
09.25	2.5	5	Fe	21	.25
09.98	0	1	Ti	83	.96
10.35	0	1	Y II	7	.29
11.27	0.4	2	Fe	228	.22
12.47	0.5	1	....	.....	...
13.07	0	1	Cb	3	.01
13.95	1	1	V	11	.97
(14.8)	0	1	Zr II	18	.77
(15.9)	0.3n	1	Fe	124	.91
17.39	2	4	Ti	17	.40
17.88	0	1	....	.....	...
20.01	8	1	Fe	5	.94
21.39	0.5	2	V	11	.36
			Fe	131	.40
22.55	4	3	Ni	18	.48
			Fe	5	.56
			Ti	17	.57
24.49	1	3	Fe	124	.38
			Ti	131	.57
25.06	1 n	2	Eu II	2	.94
			Ti	83	.16
26.96	1.2s	2	Fe	385	.92
			Ru	2	.93
27.60	2	4	Fe	21	.62
28.02	1	4	Ru	2	.03
29.81	1	2	Ti	17	.82
30.46	0.5	1	Co	62	.48
30.77	2	1	Ni	2	.75
			Cr	2	.81
32.00	2.5	8	Cr	2	.03
32.40	0	1	Fe	76	.40
			Co	62	.40
33.31	3	1	Fe	5	.32
34.82	3	1	Fe	21	.87
37.11	6 n	1	Fe	5	.13
39.24	1	4	Ni	2	.23
39.74	0.6	1	Cb	3	.80
41.05	3	6	Ti	17	.06
41.88	0	1	....	.....	...
42.32	0	1	Ru	2	.28
42.60	0	1	Fe	387	.62
43.38	3	4	Fe	21	.36
(45.51)	3	1	Co	34	.50
			Fe	5	.56
(45.85)	3.5	1	Fe	5	.90
48.25	3.5	2	Fe	5	.26
48.98	2	1	Ni	1	.04
49.52	3	1	Fe	21	.49
52.84	2 s	7	Ti	17	.86
53.64	1 s	7	Ti	17	.62
56.39	0.5	1	....	.....	...
58.23	4	4	Fe	21	.24
59.40	0.3	1	....	.....	...
60.06	0.5	1	Ru	2	.03
			Fe	177	.05
(60.70)	?	1	....	.....	...
61.38	0.5	1	Ti II	13	.32
			Fe	227	.41
63.80	3	4	Fe	21	.79
67.20	3	3	Fe	21	.19
(68.4)	0.3	1	....	.....	...
70.47	(2)	4	Fe	177	.40
			V	.....	.53
71.64	1.5n	10	Ti	17	.66
72.53	1	7	Ni	15	.53
73.25	0 n	1	....	.....	...
74.26	0.6n	1	Y II	7	.33
			Ti	16	.33
75.64	3	10	Ni	33	.57
			Ti	1	.72
77.14	0.5	1	....	.....	...
78.06	2 s	8	Ni	15	.06
78.68	1 s	2	V	28	.68
			Fe	73	.70
83.54	1.5	7	Ni	30	.53
84.62	1 n	1	....	.....	...
85.47	0.3	1	....	.....	...
86.04	1	1	Ti	57	.04
86.70	1.5	3	Fe	22	.68
87.87	2.5	3	Fe	21	.88
88.77	1.5	3	Y II	7	.70
			Ti	16	.80
89.69	0.3	1	Cr	24	.72
(90.14)	1.5	1	Fe	22	.10
(90.40)	1	1	V	28	.32
			....	.....	...
91.32	0.6	2	V	10	.33
			Zr	8	.40
92.36	1 s	4	Ni	2	.34
93.59	2 s	9	Ni	4	.61
			V	9	.61
95.00	1.5	4	V	9,28	.96
			Fe	21	.00
(97.66)	(1.8)	4	Fe	607	.52
			Cr	139	.72
98.39	3	1	Mo	1	.25
			Ti	115	.28
			Fe	21	.51
98.88	1	1	Ru	1	.90
99.44	4	2	Ru	1	.35
			Fe	21	.55
99.91	0.5	1	V	28	.91
3800					
03.49	1	6	V	28	.47
03.90	1.5	6	V	10	.90
05.45	0.6	2	Fe	608	.35
			....	.....	...
06.69	1	4	Fe	607	.70
			Mn	6	.72
07.14	1.5	7	Ni	33	.14
07.55	(1)	3	V	28	.50
			Fe	73	.53
08.10	1	3	Co	17	.11
08.52	2.5	5	V	9	.52
09.64	0.6	1	Mn	6	.59
			V	28	.60
10.36	0	1	....	.....	...
(11.09)	1	1	Co	31	.07
11.29	1.5	1	Ni	15	.32
12.97	2	9	Fe	22	.96
13.49	2.5	9	V	9	.49
14.53	2	1	Fe	22	.52
15.52	0	1	V	28	.51
15.86	2.5	2	Fe	45	.84
17.84	2	3	V	10	.84
18.25	3	3	V	9	.24
18.99	0	1	....	.....	...
19.67	1	1	Eu II	1	.67
20.37	7	3	V	44	.30
			Fe	20	.43
21.49	0.4	1	V	28	.49

TABLE 1—Continued

λ	Int.	No. Pl.	Ident. El.	Mult.	λ
3800					
21.99	2	9	V	9	.01
22.42	0	1	Zr	10	.41
22.89	0.8	1	V	28	.89
23.24	1	1	V	28	.21
23.52	1	1	Mn	6	.51
			Cr	24	.52
23.94	0	1	Mn	6	.89
24.47	8	1	Fe	4	.44
25.89	5	6	Fe	20	.88
27.83	2	5	Fe	45	.82
28.55	3	11	V	9	.56
31.06	1	1	Cr	24	.03
31.71	3	9	Ni	31	.69
(32.35)	1	2	Mg	3	.31
32.92	1.5	2	Ni	1	.87
			Y II	7	.89
			Sc II	1	.06
(34.27)	5	4	Fe	20	.22
(35.6)	1	3	V	44	.56
(38.34)	0.8	3	Mg	3	.29
39.00	0.5	1	V	44	.00
40.42	3	1	Fe	20	.44
40.72	2	1	V	9	.75
41.08	1	1	Fe	45	.05
41.97	3	6	V	8	.89
			Co	33	.05
44.46	3	7	V	7	.44
45.50	1.5	1	Co	34	.47
47.30	3	6	V	7	.33
49.45	0.6	1	Cr	138	.36
			Cr	24	.53
50.00	3	5	Fe	20	.97
50.87	4	7	Fe	22	.82
			Co	17	.95
(52.22)	(1)	1	Cr	24	.22
(52.64)	(1)	2	Fe	73	.57
55.34	4	7	V	7	.37
55.83	4	2	V	9	.84
56.39	7	2	Fe	4	.37
58.30	2	9	Ni	32	.30
59.94	12	1	Fe	4	.91
61.20	1	1	Co	33	.16
62.21	2	8	V	8	.22
62.86	0.5s	1	Ti	175	.83
64.10	2	1	Mo	1	.11
64.85	3	11	V	7	.86
65.53	2.5	7	Fe	20	.53
67.59	3	3	V	7	.60
72.52	4	5	Fe	20	.50
73.11	4	6	Co	18	.12
73.92	3	3	Co	18	.96
75.11	5	6	V	7	.08
75.97	6	6	V	7	.90
			Fe	22	.04
			V	8	.09
76.91	3 n	4	Co	17,62	.84
			....	.....	...
78.03	4	3	Fe	20	.02
78.60	5	1	Fe	4	.58
81.41	1	4	Ti	15	.40
81.86	2.5s	10	Co	18	.87
83.27	3	3	Cr	23	.29
85.19	3	2	Cr	23	.22
85.56	0	1	Fe	124	.51
(86.01)	3	1	Fe	4	.28
(86.52)	3.5	1	Fe	4	.28
(87.01)	4	1	Fe	20	.05
(88.53)	(1)	8	Fe	45	.52
(89.70)	0	1	Ni	15	.67
90.13	4	1	V	8	.18
91.10	1 n	1	V	.....	.12
92.82	4	11	V	7	.86
94.06	3	5	Cr	23	.04
			Co	34	.08
94.99	2	1	Co	18	.98
95.65	6	11	Fe	4	.66
98.00	2.5	6	Fe	20	.01
98.50	1.5	2	Ti	13	.49
99.72	7 n	8	Ti	15	.67
			Fe	4	.71
3900					
(00.62)	0	1	Zr	6	.51
00.98	1.5	3	Ti	15	.96
02.24	3 s	10	V	7	.25
03.02	2 n	6	Fe	45	.95
			Mo	1	.96
			Cr	23	.16
(04.76)	1 n	2	Ti	56	.78
06.45	8	10	Fe	4	.48
07.53	1	5	Sc	8	.48
08.76	2.5	9	Cr	23	.76
09.91	3.5	9	V	7,63	.89
			Co	3	.93
10.78	0	1	V	42	.79
11.83	2	4	Sc	8	.81
12.26	0	1	V	42,43	.21
12.98	2.5	3	Ni	15	.98
14.35	0	7	Ti	15	.33
14.78	1	4	Ti	14	.74
15.88	1	1	Ti	15	.88
16.20	1.5	2	Cr	23	.24
17.20	2	6	Fe	20	.18
19.15	3	8	Cr	23	.16
20.26	6	11	Fe	4	.26
21.03	1.5	5	Cr	23	.02
21.44	1.7	9	Ti	14	.42
21.88	0	1	V	42	.90
22.47	0	1	V	42	.43
22.92	7	10	Fe	4	.91
24.52	3	10	Ti	13	.53
25.24	2	5	V	8	.24
25.91	1	1	Fe	364	.95
27.91	7	10	Fe	4	.92
28.70	1	1	Cr	23	.64
29.85	1.5	4	Ti	13	.88
30.30	6	7	Fe	4	.31
(33.78)	25	1	Ca II	1	.67
40.90	2	5	Fe	20	.88
(41.53)	1	1	Cr	23	.49
(41.74)	2.5	1	Co	17	.73
44.03	14	8	Al	1	.03
(45.45)	1	1	Co	29	.33
46.21	0.5n	1	Ni	1 P	.18
47.78	2	11	Ti	14	.78
48.75	4	6	Ti	13	.67
			Ca	6	.90
(50.27)	0.5	1	Y II	6	.36
51.05	0.5n	1	Cr	136	.10
52.31	0.8	5	Co	16	.33
52.95	1	2	Co	28	.92
56.29	4	11	Co	2	.2
			Ti	13	.5
57.05	2	7	Ca	6	.0
(58.02)	2	1	Co	18	.9
58.17	3 n	3	Ti	13	.2
61.52	12	8	Al	1	.5
62.86	2	1	Ti	12	.8
64.29	1.5	1	Ti	12	.2
66.10	1.5	1	Fe	45	.0
(68.50)	16	2	Ca II	1	.4
70.61	1.5n	1	Ca	41	.5
73.64	5	7	Ni	31	.5
			Ca	6	.7
74.73	1.5	4	Co	18	.7
(76.68)	0.5	1	Cr	38	.6
78.68	1	1	Co	17	.6
79.51	3	8	Co	3	.5
81.76	3	9	Ti	12	.7
82.51	1.7	6	Ti	11	.4
86.81	0	1	Zr	.....	.8
87.14	0.5	1	Co	16	.1
87.97	2	3	Yb	2	.9
89.75	4	9	Ti	12	.7
(91.11)	0	1	Cr	38	.1
91.76	0.5	1	Co	17	.6
93.86	0	1	....	.....	...
94.57	1	1	Co	17	.5
95.35	1	1	Co	31	.3
96.40	0	1	....	.....	...
96.64	1	2	Sc	7	.6
97.43	0.5	1	Fe	278	.3
(97.98)	1	1	Co	32	.9
98.62	4	9	Ti	12	.6
4000					
05.26	2	11	Fe	43	.2
07.94	1	1	Co	.....	.9
08.92	2	8	Ti	12	.9
09.70	0.7	3	Ti	11	.6
			Fe	72	.7
11.11	1	1	Co	2	.0
18.02	1 n	1	Mn	5	.1
20.42	2	9	Sc	7	.4
20.94	1	4	Co	16	.9
23.71	2	8	Sc	7	.6
24.58	2.5	9	Ti	12	.5
27.07	2	3	Co	3	.0
30.73	6	12	Mn	2	.7
33.02	6	12	Mn	2	.0
34.50	5	12	Mn	2	.4
35.83	1	11	Mn	5	.7
40.83	0.7	1	Co	.....	.8
41.38	0.7	4	Mn	5	.3
44.10	4 s	10	K	3	.1
(45.47)	0	2	Co	31	.3
45.87	4	11	Fe	43	.8
47.18	3	10	K	3	.2
47.78	1	10	Sc	7	.7
48.70	1.5	5	Mn	5	.7
54.57	1	6	Sc	6	.5
57.21	1.5	6	Co	3	.2
63.62	2	12	Fe	43	.6
70.35	1	1	Mn	5	.2
70.77	1	2	Fe	558	.7
71.77	2	12	Fe	43	.7
77.74	2	12	Sr II	1	.7

TABLE 1—Continued

λ	Int.	No. Pl.	Ident. El.	Mult.	λ
4000					
.44	2	2	Sc	6	.40
			Ti	80	.46
.99	0.5	1	Mn	5	.94
.72	1.5	2	Mn	5	.63
			Y	6	.71
.54	1.5	2	V	41	.58
.43	1	2	Co	29	.39
			V	52	.41
.68	1.5	2	V	27	.69
.52	1	1	V	41	.49
.81	2	5	V	27	.80
4100					
.76	1.5	2	Fe	18	.74
.79)	?	2	In	1	.77
.86	1	1	....	.....	...
.16	2	4	V	27	.17
.73	1.5	8	Co	1	.71
			V	27	.79
.58	1	1	Co	29	.54
.82	2.5	7	V	27	.78
.72	1	5	Ti	9	.71
.17	2	5	V	27	.18
.59	3	3	V	27	.47
			V	27	.70
.78	1	2	Co	28	.77
.37	1	1	Co	28	.32
			Zr	32	.45
.51	2	5	....	.....	...
			V	27	.57
.08	1	1	V	27	.07
.29	0	1	Y	5	.30

λ	Int.	No. Pl.	Ident. El.	Mult.	λ
29.75	1	1	Eu II	1	.73
32.06	2	4	V	27	.02
			Fe	43	.06
34.37	4	7	Fe	3	.34
			V	27	.49
43.90	1.5	2	Fe	43	.87
47.68	1	3	Fe	42	.67
49.76	3	11	Fe	3 P	.76
(51.12)	1	1	....	.....	...
52.19	1.5	4	Fe	18	.18
59.70	1	1	V	25	.69
72.06	1	6	Ga	1	.06
72.77	2	6	Fe	19	.75
73.92	3	1	Fe	19	.93
74.96	2	2	Fe	19	.92
77.61	1.5	5	Y II	14	.55
			Co	2	.59
			Fe	18	.60
79.46	2	1	V	25	.42
90.71	3	2	Co	1	.71
4200					
00.00	3	8	Fe	3	.98
(02.11)	1	1	Fe	42	.03
06.70	2	12	Fe	3	.70
11.72	1	1	Ti	279	.73
			Mn	.....	.75
15.53	1	9	Sr II	1	.52
16.18	2.5	12	Fe	3	.19
26.72	30 n	1	Ca	2	.73
32.74	1	2	Fe	3	.73
34.02	2	2	Co	1	.00
			V	6,111	.00
50.18	1	5	Fe	152	.13

λ	Int.	No. Pl.	Ident. El.	Mult.	λ
50.79	1.5	5	Fe	42	.79
52.27	3	3	Co	1	.31
54.30	10	10	Cr	1	.35
58.32	1.5	2	Fe	3	.32
71.77	1.5	1	Fe	42	.76
74.77	6	9	Cr	1	.80
89.67	6	6	Cr	1	.72
91.49	1.5	1	Fe	3,41	.47
4300					
44.52	1	4	Cr	22	.51
47.20	4	7	Fe	2	.24
52.81	1.5	1	V	5	.87
75.96	2	5	Fe	2	.93
79.21	2	1	V	22	.24
89.23	3	5	Fe	2	.25
4400					
(27.29)	1	2	Fe	2	.31
(35.10)	2	2	Ca	4	.96
			Fe	2	.15
45.50	1	1	Fe	2	.48
54.80	1	1	Ca	4	.78
(61.63)	1	1	Fe	2	.65
4500					
45.96	2	4	Cr	10	.96
54.00	2	4	Ba II	1	.04
(71.06)	2	3	Mg	1	.11
75.44	3	3	Mn	.....	.41
			Zr	5	.52

TABLE 2

ATOMIC ABSORPTION LINES IN THE SPECTRUM OF R ANDROMEDAE

λ	Int.	Ident. El.	Mult.	λ
3300				
42.74	1	(Ti	25	.71)
43.74	1	(Mn	9	.73)
57.22	1	(Zr II	3	.26)
62.80	1	(Ni	23	.81)
67.09	1.5	Co	22	.11
82.91	1	Ag	1	.89
3400				
16.51	1	....	....	....
17.86	1.5	Co	19	.80
		Fe	81	.84
18.62	1	Gd II	7	.73
19.14	0.6	Zr II	2	.10
19.67	1	Fe	377	.71
20.77	0.5	Ni	9	.74
23.74	1	Ni	20	.71
24.88	0.6	Zr II	2	.82
28.27	0.8	(Fe	81	.19)
		....	....	....
31.59	0.9	Co	6	.58
34.91	1	Rh	2	.89
36.71	1	Ru	4	.74
38.28	1.5	Zr II	1	.23
43.87	2	Fe	6	.88
44.46	0.5	....	....	....
47.38	1.2	Zr	16	.36
50.45	0.9	(Gd II	22	.38)
51.91	1	Fe	81	.92
52.31	1	Fe	25	.27
52.89	1.5	Ni	17	.89
53.52	1.6	Co	22	.51
54.35	1	....	....	....
55.18	1.4	Co	6	.24
55.96	1.2	....	....	....
61.59	2	Ni	17	.65
62.82	0.9	Co	23	.84
65.71	2	Zr	17	.63
		Co	5	.79
		Fe	6	.86
66.58	1	Fe	24	.50
67.41	1 n	....	....	....
		Ni	3	.50
68.47	0.5	Ca	10	.48
69.05	1	....	....	....
71.21	1 n	Zr	15	.18
		Fe	82	.27
(78.88)	1.5	Rh	6	.91
		Ti	84	.92
(79.39)	1	Zr II	46	.39
80.51	1	Ti	84	.52
82.90	1.5	Mn II	3	.90
85.84	1	Ni	17	.89
96.73	1	Co	19	.68
97.18	0.4	Fe	78P	.12
99.06	1.2	Ru	4	.94
		Ti	84	.10
3500				
00.35	0.5	Ti II	6	.34
00.84	1.2	Ni	6	.85
01.41	1.2d?	Zr	14	.33
		....	....	....
02.29	1	Co	21	.28
02.61	1.2	Ni	3	.60
		Co	6	.63
03.77	1	Ti	22	.76
05.69	1 s	Zr II	1	.67
09.30	1	Zr	15	.32
(10.33)	1.5	Ni	18	.34
11.62	0.6	Ti	22	.63
12.67	0.8	Co	21	.64
.....	....	....	....	....
.....	....	....	....	....
21.24	1	Fe	24	.26
21.56	1	Co	20	.57
(26.97)	?	Co	4	.85
		Fe	6	.04
		Fe	24	.17
(27.70)	0.5	Sun	....	.61
		Fe	326	.79
(27.93)	1.5	Ni	6	.98
28.60	0.2	Os	1	.60
29.07	1	Co	5	.03
29.82	1.7	Co	22	.82
30.24	0.5	Zr	52	.22
30.55	0.8	Ti	22	.58
		Ni	121	.60
31.21	0.4	....	....	....
31.75	1.8	Mn	18	.85
32.09	1.4	Mn	18	.00
		Mn	18	.12
33.24	3	Zr	14	.22
		Co	5	.36
(33.68)	1.4	V	53	.68
		V	53	.76
34.96	0	Fe	48	.91
35.26	1.6	Zr	59	.16
		Cb	4	.30
35.72	0.7	Sc II	11	.73
36.05	0.5	....	....	....
36.57	0.6	Fe	326	.56
36.99	0.8	Zr II	10	.94
37.47	1.3	Fe	239	.49
37.94	0.6n	Fe	327	.90
38.56	1.5	Fe	137	.55
39.14	1.5n	....	....	....
39.38	0.5	....	....	....
40.15	0.7	Fe	329	.12
40.72	1.2	Fe	25	.71
41.16	0.6	Fe	326	.08
41.67	0.5	....	....	....
42.18	0.8	Fe	326	.08
		Fe	128	.24
43.42	0.8	Fe	183	.39
		V	53	.50
43.98	0.2	Rh	6	.95
(45.28)	0.6	....	....	....
45.79	0.6	Gd II	2	.80
47.02	2 n	Ti	133	.03
47.68	2.5	Zr	13	.69
48.17	2.5	Ni	3,20	.18
48.99	2.3	Y II	9	.02
49.40	0	....	....	....
(49.75)	0.8	Fe	48	.87
(50.50)	?	Co	4	.59
51.10	0	(Fe	321P	.11)
51.55	1.7	Ni	5	.53
51.97	1.7	Zr II	1	.94
52.72	1.8	Y	8	.70
		Co	6	.72
53.47	1.7	Ni	16	.48
54.13	1	Fe	23	.12
54.64	0.9	(Fe	154P	.65)
55.04	0.7	Fe	326	.92
		....	....	....
55.38	0.5	....	....	....
55.83	0.8	....	....	....
56.78	1.5d?	Zr II	9	.61
		Fe	325	.68
		Fe	327	.88
58.55	2.5	Fe	24	.52
		Sc II	3	.54
58.92	1.3	Co	20	.77
		....	....	....
60.03	1 n	(Fe	321P	.07)
60.89	1.5	Co	21	.89
61.70	2.5	....	....	....
		Ni	2	.75
62.47	0.5	....	....	....
63.12	0.7s	....	....	....
63.56	1.2	....	....	....
64.20	0.3	Fe	48	.11
64.57	0.6	Fe	183P	.56
64.96	1	Co	19	.95
65.42	1.8	Fe	24	.38
66.12	1.5	Zr	15	.10
66.42	1.5	Ni	36	.37
67.27	0.8	....	....	....
		Fe	183	.36
67.74	1	Sc II	3	.70
68.53	0.5	Fe	321	.42
		Co	61	.43
		....	....	....
68.92	0.8	V	122	.94
69.43	1	Co	35	.37
		Mn	18	.49
70.10	3 n	Fe	24	.10
71.6	bh	....	....	....
.....	....	....	....	....
74.97	0	Co	21	.97
75.38	0.3	Co	4	.36
75.77	0.5	Zr	12	.79
76.35	0.8	Sc II	3	.34
78.	....	Cr	4	.69
.....	....	....	....	....
81.15	2 n	Fe	23	.20
.....	....	....	....	....
.....	....	....	....	....
86.25	1	Zr	12	.28
87.07	1.5	Fe	23	.98
		Co	35	.19
87.88	1	Ni	16	.93
89.11	1	Fe	23	.11
89.67	0.9	Sc II	3	.64
(90.41)	0.8	Sc II	3	.48
93.5	20	Cr	4	.49
94.86	0.9	Co	4	.87
96.14	1	Ti II	15	.05
		Ru	4	.18
		Rh	1	.19
(97.67)	1	Ni	18	.70
98.04	0.4	....	....	....
98.69	1	Ti	59	.71
3600				
00.74	1.2	Y II	9	.74
01.18	1	Zr	13	.18
01.93	1	Y II	9	.93
02.21	0.5	Co	4	.08
		Ni	3	.28
03.83	0.8	Ti	20	.84
04.25	0.8	Ti	21	.28
05.33	5 n	Cr	4	.33

TABLE 2—Continued

λ	Int.	Ident. El.	Mult.	λ
3600				
06.74	1	Ti	20	.79
07.62	0.3	Mn	8	.54
08.84	0.8	Fe	23	.86
(09.36)	1	Ni	16	.31
10.33	1.5d?	....	....	....
		Mn	8	.30
		Ni	18	.46
11.03	0.8	Y II	9	.06
11.61	0.5	Ni	2P	.54
12.69	1	Ni	6	.74
13.09	1.2	Zr II	1	.08
(13.72)	3	Zr	33	.70
		Sc II	2	.84
14.78	0.8	Zr II	9	.79
15.13	0.3	....	....	....
		(Fe	569	.19)
15.62	1	Cr	3	.64
16.64	0.6	....	....	....
18.76	1.8	Fe	23	.77
19.43	1	Ni	35	.39
20.05	0.7	Ni	⊙	.03
(20.97)	1.5	Y	8	.95
23.25	0.4	Fe	180	.19
23.95	2.8d?	Zr	12	.87
		Ca	9	.11
24.82	1.8d?	Ni	2	.73
		Co	21	.96
26.08	1.2s	Ti	20	.08
27.07	0	....	....	....
27.82	1	Co	19	.81
28.72	1	Y II	9	.71
(30.11)	0.5	Zr II	10	.03
30.80	1.5	Sc II	2	.74
		Ca	9	.74
(31.00)	0	Ca	9	.97
31.46	2.5d?	Co	4	.39
		Fe	23	.46
33.13	1.5	Y II	2	.13
33.53	0	....	....	....
34.20	1.2	(Zr	....	.15)
34.97	1	Ni	33	.94
35.41	3	(Ti	20	.20)
		(Cr	3	.28)
		Ti	19	.46
36.13	0.7	Fe	77	.19
36.59	0.7	Cr	47	.59
37.25	0	Fe	180	.25
37.96	1.5	Ti	18	.97
38.79	0.3	....	....	....
39.02	0	V	83	.02
39.73	1.2n	....	....	....
		Cr	47	.80
40.47	0.4n	Cr	47	.39
		....	....	....
40.67	0.5	....	....	....
41.60	1.8n	(Cr	47	.47)
		Ni	6	.64
42.68	3.5d?	Ti	19	.68
		Sc II	2	.78
43.82	0.5d?	Fe	233	.72
		V	83	.86
44.40	1 s	Ca	9	.41
44.77	0.9s	Ca	9	.76
45.35	1.5s	Sc II	2	.31
46.18	1.5s	Ti	18	.20
47.82	2.8n	Fe	23	.84
48.48	0	Cr	47	.53
49.25	3	Fe	5	.30
49.88	0	....	....	....
50.34	0.3	Fe	180	.28
51.00	0.7	....	....	....
51.52	0	Fe	295	.47
51.82	1 s	Sc II	2	.80
52.57	1	Co	4	.54
53.50	3 n	Ti	19	.50
54.59	1.5	Ti	18	.59
		Gd II	4	.62
54.98	0.2	....	....	....
55.53	0.3	Fe	369	.46
56.27	0.7	Cr	46	.26
56.93	1.5n	Co	21	.96
57.50	0.7s	(Ru II	1	.57)
58.06	2 d?	Rh	1	.99
		Ti	19	.10
59.00	0	....	....	....
60.61	1.8	Ti	18	.63
61.30	2.2	Zr	12	.20
		Ru	3	.35
61.96	0.8s	Ni	16	.95
62.30	0	....	....	....
62.96	0.2	....	....	....
63.62	1.6s	Zr	12	.64
64.10	1.5	Ni	4	.10
64.66	1.2	Y II	9	.62
65.22	0.8	(La II	....	.22)
66.20	0.3	Rh	3	.22
66.64	1	Sc II	2	.54
		(Cr	46	.64
67.11	0.3	Zr II	8	.06
68.91	1.5	Ti	18	.96
69.24	0.8	Ni	2	.24
70.42	1.2	Ni	4	.43
70.86	0.3	Fe	133	.81
71.26	0.6	V	70	.20
		Zr II	45	.28
71.67	1.5	Ti	19	.67
72.37	0	V	115	.40
72.72	0.4	Zr II	1	.65
		Fe	180	.69
73.18	0	....	....	....
74.12	2.5	Ni	15P	.06
		Ni	32P	.15
		....	....	....
74.76	1	Zr II	9	.74
75.29	0.3	Sc II	10	.26
75.74	0.8	V	29	.70
77.08	0.8	V	....	....
79.5	bh	....	....	....
80.0	4	Fe	5	.92
82.0	bh	....	....	....
(82.24)	1.2	(Hf	1	.25)
83.02	1.2	Fe	5	.05
85.21	0.7	Ti II	14	.19
87.37	2	Ti	19	.35
		Fe	21	.46
88.10	0.5	V	29	.07
88.42	0.5	Ni	5	.42
		Eu II	2	.42
89.86	1	Ti	18	.92
		band line?		
90.31	1	V	29	.28
		band line		
90.75	0.5	band line		
91.12	0.5	band line		
91.53	0.5	band line		
91.91	0	band line		
92.27	1.5	band line		
		V	29	.22
92.68	1	band line		
93.09	0	band line		
93.52	0.5	band line		
93.94	1.5	band line		
		Ni	15	.93
		Sm II	2	.99
94.30	1	band line		
94.86	0.7	band line		
95.29	0.6	band line		
95.86	1.6	V	29	.86
		band line		
96.24	0	band line		
96.68	0.5	band line		
97.19	0	band line		
97.73	2.5	(Gd II	4	.73)
		band line		
98.18	0	band line		
98.70	0.5	band line		
99.18	0.5	band line		
99.68	0.7	band line		
3700				
00.22	0.6	band line		
00.87	0	band line		
01.44	0	band line		
01.91	0.5	band line		
02.34	2	band line		
		....	....	....
02.99	1	band line		
		....	....	....
03.57	2	V	29	.58
		band line		
04.19	1.5	....	....	....
		band line		
04.65	0.5	V	29	.70
05.00	0	....	....	....
05.54	4	Fe	5	.57
06.61	1.5	....	....	....
07.81	3.5	Fe	5	.83
09.23	1.8	Fe	21	.25
09.95	0.6s	Ti	83	.96
10.31	1.2	Y II	7	.30
11.30	1	....	....	....
11.99	0.6	Zr II	8	.95
13.00	0.5	Cb	3	.02
14.06	1.5n	V	11	.96
		Zr	12	.13
14.80	1	Zr II	18	.77
17.38	1	Ti	17	.39
17.88	0.2	....	....	....
(20.1)	15	Fe	5	.94
21.33	0.4	V	11	.36
22.50	3.5	Ni	18	.48
		Fe	5	.56
		Ti	17	.57
24.56	0.8s	Ti	131	.57
25.04	1 d?	Eu II	2	.94
		Ti	83	.16
26.28	1 n	Cb	3	.24
26.95	1	Ru	2	.93
27.59	1.2	Fe	21	.62
28.06	1.2	Ru	2	.03
29.74	2 n	Zr II	8	.74
		Ti	17	.81
30.47	0.9	Ru	2	.43
		Co	62	.48

TABLE 2—Continued

λ	Int.	Ident. El.	Mult.	λ
3700				
30.81	1.4	Ni	2	.75
		Cr	2	.81
31.28	0.8	....	....	....
31.99	1.8	Cr	2	.03
32.43	0.4	Co	62	.39
		Fe	76	.40
(33.36)	3.5	Fe	5	.32
(34.81)	2.5	Ti	21	.87
(37.13)	4 n	Fe	5	.13
39.26	0.7	Ni	2	.23
		Fe	74	.32
39.80	0.6	Cb	3	.80
(41.02)	2	Ti	17	.06
43.41	1.5	Fe	21	.36
45.75	5 d	Fe	5	.56
		Fe	5	.90
47.56	0.8s	Y II	8	.55
48.26	3	Fe	5	.26
49.01	0.8	Ni	1	.04
(49.51)	1.5	Fe	21	.49
51.73	0.8n	....	....	....
52.80	3	Ti	17	.86
53.61	1.5	Fe	73	.61
		Ti	17	.62
57.44	0.3	....	....	....
(58.29)	2.5	Fe	21	.24
59.00	0	(Gd II	2	.00)
59.31	0.5	Ti II	13	.29
59.58	0.5	Cb	3	.56
60.05	0.6	Ru	2	.03
		Fe	177	.05
(60.71)	1	....	....	....
61.36	1	Ti II	13	.32
63.40	1.2	Mn	24	.38
63.79	1.2	Fe	21	.79
64.36	1	Zr	10	.38
65.15	1	....	....	....
66.69	1	Zr	10	.71
67.20	0.8	Fe	21	.19
67.53	0.3	....	....	....
68.41	0.5	(Gd II	2	.39)
(69.72)	0.5	....	....	....
71.61	2	Ti	17	.65
72.51	1	Ni	15	.53
73.31	0.5	....	....	....
74.33	1	Y II	7	.33
		Ti	16	.33
75.65	1.5	Ni	33	.57
		(Ti	1	.72)
76.55	1.4	Y II	8	.56
77.15	0.6	....	....	....
(77.63)	0.2	Hf	1	.64
78.08	1	Ni	15	.06
78.69	0.8	V	28	.68
		Fe	73	.70
78.97	0.3	....	....	....
79.45	0.5	Fe	74	.49
79.86	0.4n	....	....	....
80.49	1.2	Zr	8	.53
83.55	0.5s	Ni	30	.53
83.89	0 s	....	....	....
84.23	0.6	....	....	....
(84.73)	0.7n	....	....	....
86.10	1	Ti	57	.04
86.71	0.5	Fe	22	.68
(87.62)	1	....	....	....
87.99	1	Fe	21	.88
88.70	3	Y II	7	.70
89.33	0.5	Ti	115	.29
89.70	0.3	Cr	24	.72
90.34	2.5n	V	28	.32
		....	....	....
90.83	0	Fe	73,127	.76
91.31	2	V	10	.33
		Zr	8	.39
91.89	0	....	....	....
92.40	1.2	Ni	2	.34
93.63	1.2	Ni	4	.61
		V	9	.61
93.96	0	....	....	....
94.99	1.8	V	9,28	.96
		Fe	21	.00
96.41	0.6	(Gd II	2	.37)
96.81	0.3	....	....	....
		Ti II	12	.90
97.73	?	Cr	139	.72
(98.36)	3	Ti	115	.28
		Fe	21	.51
98.91	0.8	Ru	1	.90
99.42	2	Ru	1	.35
		Fe	21	.55
99.89	0.4	V	28	.91
3800				
00.27	0.2	....	....	....
01.14	0.5n	Ti	165	.09
(02.27)	0.4	(Fe	666	.28)
02.94	1	Cb	3	.93
03.48	1	V	28	.47
03.92	1.2	V	10	.90
04.87	0.2n	Cr	139	.80
05.46	1.8n	....	....	....
06.70	1.2n	Mn	6	.72
07.14	1 s	Ni	33	.14
07.51	0.8s	V	28	.50
		Fe	73	.53
(08.44)	2 n	V	9	.52
09.65	1	Mn	6	.59
		V	28	.60
(11.31)	0.5	Ni	15	.32
(11.81)	0.3	....	....	....
12.96	1.6	Fe	22	.96
13.47	2	V	9	.49
14.04	0.8	(Gd II	2	.97)
14.65	1.4	Fe	22	.53
		Ti II	12	.58
15.48	0.5	V	28	.51
15.87	1	Fe	45	.84
16.32	0	Fe	73	.34
16.73	0	Mn	6	.75
17.82	1 s	V	10	.84
18.24	2	V	9	.24
19.02	0.5	....	....	....
19.63	0.6	Eu II	1	.67
19.97	....	V	28	.96
20.35	2.6	Fe	20	.43
21.50	0.6s	V	28	.49
21.97	1 s	V	9	.01
22.40	1 s	Zr	10	.41
22.89	0.4s	V	28	.89
23.22	0.4s	V	28	.21
23.56	0	Mn	6	.51
		Zr	24	.52
24.42	5.5	Fe	4	.44
25.85	1.2	Fe	20	.88
26.43	?	Cr	70	.42
(27.92)	0.5	Fe	45	.82
28.54	1.8	V	9	.56
29.36	0.6	Mg	3	.35
31.72	0.8	Ni	31	.69
32.33	0.6	Mg	3	.30
32.99	1.2	Ni	1	.87
		Y II	7	.89
		Sc II	1	.06
(34.29)	3	Fe	20	.22
		Mn	6	.36
35.96	1.5	Zr	8	.96
38.30	0.8	Mg	3	.29
38.99	0.8	(V	44	.00)
40.57	3 d?	Fe	20	.44
		V	9	.75
41.06	0.5	Fe	45	.05
41.89	0.9	V	8	.89
(42.10)	?	Co	33	.05
43.08	0.5	Sc II	1	.00
		Zr II	7	.03
44.42	1.4	V	7	.44
45.50	0.4	Co	34	.47
46.99	1	Zr	10	.01
47.33	1	V	7	.32
49.22	0.9	Zr	6	.26
49.59	0	Cr	24	.53
50.03	1	Fe	20	.97
50.88	1	Fe	22	.82
		Co	17	.94
(51.70)	1	....	....	....
(52.2)	0.5	Cr	24	.22
(52.54)	?	Fe	73	.57
54.29	0.5	Cr	69	.22
55.31	0.7	V	7	.37
(55.8)	0.3	V	9	.84
(56.3)	11	Fe	4	.37
58.32	0.5	Ni	32	.30
(59.94)	9	Fe	4	.91
62.23	1	V	8	.22
62.90	0.6	....	....	....
63.37	0.9	....	....	....
63.96	2 d?	Zr	8	.88
		....	....	....
64.26	1	....	....	....
		Zr	10	.33
64.83	1.5	V	7	.86
65.55	0.9	Fe	20	.53
66.07	0.3	....	....	....
66.51	0.4	(Ti	176	.45)
66.88	0	....	....	....
67.59	1.8	V	7	.60
68.46	0.4s	Ti	175	.40
69.08	? n	....	....	....
69.62	0.5s	Fe	284	.59
71.11	0.6	V	66	.08
71.71	0.7n	....	....	....
72.11	0.5s	....	....	....
72.55	1.8	Fe	20	.50
73.13	1.5	Co	18	.12
(74.0)	2 n	Co	18	.95
		Fe	120	.05
75.12	2.6n	V	7	.08
		Ti	15,175	.26
75.97	2.8d?	V	7	.90
		Fe	22	.04
		V	8	.09
77.04	1.2n	....	....	....
77.59	0.4s	Ti	175	.59
		Zr	58	.60

TABLE 2—Continued

λ	Int.	Ident. El.	Mult.	λ
3800				
3.01	0.5	Fe	20	.02
3.7)	4 n	Fe	4	.58
3.05	?	Zr	6	.04
0.43	0.5	....	....	....
0.79	0.3	....	....	....
1.38	1 s	Ti	15	.40
1.86	0.6	Co	18	.87
3.29	0.6	Cr	23	.29
3.34	2.2	Cr	23	.22
		Co	31	.28
		Zr	7	.41
5.98	0.5	(Ni	1P	.87)
7.95	?	....	....	....
8.5)	0.8	Fe	45	.52
0.05)	4	Ti	15	.95
		V	8	.18
0.97	0.3	....	....	....
2.82	1.2	V	7	.86
4.05	1	Cr	23	.04
		Co	34	.07
4.62	0.5	....	....	....
5.04)	0	Co	18	.98
5.64	1.8	Fe	4	.66
6.52	0.7	Zr	9	.53
6.95	0.4	(Sm II	5	.98)
7.86	0.3	(Cr	....	.65)
8.07	0.8	Fe	20	.01
8.49	1.2	Ti	13	.49
8.69	2.2d?	Fe	4	.71
3900				
1.49	0.7s	Zr	6	.51
1.94	0.7s	Ti	15	.96
2.23	1.5	V	7	.25
3.0)	1.2n	Fe	45	.95
		Cr	23	.16
4.79)	1	Ti	56	.78
5.86	0.6	....	....	....
6.45	1.6n	Co	17	.29
		Fe	4	.48
6.77	0.4	V	42,43	.75
7.13	0.2	Eu II	5	.10
7.48	1	Sc	8	.48
8.40)	0.7	....	....	....
8.76	0.5	Cr	23	.76
9.91	2	V	7,63	.89
		Co	3	.93
3.80	0.3	V	42	.79
4.19	0.4	Ti	175	.18
4.79)	1	Sc	8	.81
5.24	0.2	V	42,43	.21
5.99	1	Ni	15	.98
6.30	1 s	Ti	15	.33
6.73	1 s	Ti	14	.75
6.87	0.8	Ti	15	.88
7.25	0.5s	Cr	23	.24
8.66	0.9	Zr	6	.64
9.27	0.9n	Fe	20	.18
9.49	0.6	Cr	23	.16
0.28	2.2n	Fe	4	.26
2.04	0.6	Cr	23	.02
2.39	1	Ti	14	.42
2.89	1.2d?	Zr	8	.80
		V	42	.90
3.38	0.4	V	42	.43
3.90	2 n	Fe	4	.91

λ	Int.	Ident. El.	Mult.	λ
(24.49)	1.5n	Ti	13	.53
25.22	0.5	V	8	.24
25.93	0.8	Fe	364	.95
(27.90)	2	Fe	4	.92
.....	.....	....	....	....
.....	.....	....	....	....
.....	.....	....	....	....
44.07	5 n	Al	1	.01
47.68	1.2	....	....	....
		Ti	14	.77
48.68	2.5	Ti	13	.67
50.35	1	Y II	6	.35
51.17	0.6	....	....	....
(51.63)	0.3	(Y II	16	.59)
52.27	0.8	Co	16	.33
52.95	0.4	Co	28	.92
53.47	0.4	....	....	....
56.27	2.5	Co	2	.27
		Ti	13	.34
57.05	0.8n	Ca	6	.05
58.17	1.2n	Ti	13	.21
(61.53)	5	Al	1	.52
(64.23)	0.3	Ti	12	.27
66.61	0.3	Zr	8	.65
.....	.....	....	....	....
.....	.....	....	....	....
73.57	1	Ni	31	.56
76.82	0.5	....	....	....
79.49	1	Co	3	.52
80.54	0	....	....	....
81.64	2	....	....	....
		Ti	12	.76
82.51	1.8	Ti	11	.48
		Y II	6	.59
83.95	0.3	Cr	38	.91
84.76	0.5	Zr II	7	.76
84.98	0.3	....	....	....
85.65	0.2	(Ti	188	.58)
86.78	1	Mg	17	.75
87.95	1	Yb	2	.98
88.67	0.3	Zr	46	.68
89.23	0.4	Zr	6	.29
89.70	2.5	Ti	12	.76
90.62	0.8	V	89	.57
91.15	0.8	Cr	38	.12
91.75	1	Cr	38	.67
		Co	17	.68
		(Co	3	.01)
92.81	0	V	89	.80
93.32	0.4	....	....	....
94.73	1.2	(Co	17	.54)
		(Ti	188	.68)
95.34	0.5	Co	31	.31
96.62	1.2s	Sc	7	.61
98.53	1.8n	(Co	33	.55)
		(Ti	12	.64)
99.89	0.3	....	....	....
4000				
00.54	0.6	....	....	....
(01.14)	0.6	....	....	....
02.58	0.6	Zr	46	.55
04.01	0.6	....	....	....
04.74	0	....	....	....
05.27	0.4	Fe	43	.25
06.60	0	Fe	488	.63
06.84	0	Fe	320	.77
07.53	0.8	....	....	....

λ	Int.	Ident. El.	Mult	λ
07.97	0.7	(Ti	187	.05)
08.88	2.5n	Ti	12	.93
09.65	1 s	Ti	11	.65
11.08	0.5	Co	2	.09
11.54	0.8	Ti	10	.53
12.62	1 n	....	....	....
13.26	0.4	....	....	....
14.55	0.4s	Sc II	8	.49
15.35	0.8w	Ti	185	.38
17.76	0.2	Ti	185	.77
18.14	0.6	Mn	5	.10
18.81	0.7	....	....	....
19.37	0	Co	16	.29
		(Co	18P	.30)
19.78	0	....	....	....
20.37	2	Sc	7	.40
20.93	0.6	Co	16	.90
21.36	0.5	....	....	....
(21.81)	0.5n	Ti	185	.81
23.66	1 n	Sc	7	.69
24.55	1.5	Ti	12	.57
24.88	0.8	Zr	46	.92
26.19	0	Cr	37	.17
26.58	0.2	Ti	185	.54
27.16	1.2	Co	3	.03
		Zr	46	.20
28.95	1	Zr	....	.95
(29.94)	2	....	....	....
		Zr	46	.03
(30.75)	5	Mn	2	.76
31.68	1 n	....	....	....
		Ti	185	.75
(33.01)	5	Mn	2	.07
(34.48)	4	Mn	2	.49
35.87	1.8	Mn	5	.73
37.40	0	....	....	....
38.19	0.3	....	....	....
38.48	0.5	....	....	....
39.40	0	....	....	....
39.81	1.5s	Y	5	.83
40.80	0.8s	(Co	....	.80)
41.08	0 s	....	....	....
41.40	0.5	Mn	5	.36
42.35	0.7n	Cr	36	.25
		....	....	....
(42.84)	0.9n	....	....	....
43.58	0.9s	Zr	32	.57
44.10	0.6	K	3	.14
(44.61)	0.4	Zr	46	.57
(44.96)	.....	....	....	....
45.88	2	Fe	43	.82
47.24	0.5	K	3	.21
47.72	4	....	....	....
		Sc	7	.79
48.68	1.6	....	....	....
		Mn	5	.76
50.50	1	Zr	....	.48
51.14	0.4n	....	....	....
52.44	1	Fe	563	.47
53.58	0	....	....	....
53.88	0	Fe	485	.82
54.51	3	Sc	6	.56
55.02	1.8	Ti	80	.01
		Zr	46	.03
55.66	1	Mn	5	.54
		Zr	....	.71
56.57	0.3	Fe	320	.53
57.20	1	Co	3	.20
57.83	0	....	....	....

TABLE 2—Continued

λ	Int.	Ident. El.	Mult.	λ
4000				
58.24	0.8	Co	16	.18
58.94	1.5	Cb	1	.93
		Mn	5	.93
59.32	0.8	Co	2	.32
(59.98)	0	....	....	....
60.23	1 n	Ti	80	.26
60.76	0.3n	....	....	....
61.11	0.5s	....	....	....
61.54	0.8	Zr	....	.53
62.84	0.7	....	....	....
64.17	1.4s	Zr	46	.16
		Ti	80	.20
64.61	0	....	....	....
65.11	1	Ti	80	.09
66.40	0.8n	Co	30	.36
66.80	0.4n	....	....	....
67.37	0.5	Fe	217	.28
67.92	1.8	....	....	....
		Mn	5	.00
68.41	0	....	....	....
68.90	0.8	....	....	....
69.26	1.1	....	....	....
70.30	0.2	Mn	5	.28
70.77	0.9	Fe	558	.77
71.17	0.7	....	....	....
71.77	1.6	Fe	43	.74
72.68	1	Zr	46	.71
(73.72)	0.5n	....	....	....
74.05	0	....	....	....
74.36	0	Ti	254	.36
(74.97)	1	Ni	28	.90
75.23	1	....	....	....
77.62	5 n	Sr II	1	.71
(78.64)	1 n	Ti	80	.47
		....	....	....
79.34	0.3	Mn	5	.24
		Mn	5	.42
79.74	1	Cb	1	.73
80.24	0.4	Cr	66	.22
		Fe	558	.23
80.58	0.4	Cr	156	.56
		Ru	7	.60
81.27	2 n	Zr	46	.22
82.39	2.5	Sc	6	.40
		Ti	80	.46
83.01	0.4	Mn	5	.94
83.70	1.5	Mn	5	.63
		Y	6	.71
84.47	0.7	(Fe	698	.50)
85.41	0.4n	....	....	....
85.81	0.5n	....	....	....
86.7	0.8n	....	....	....
87.64	0.2	....	....	....
88.00	0.5	....	....	....
88.32	0.9	Co	2	.29
88.74	0.4	....	....	....
89.23	0.2	Fe	422	.22
90.55	1	V	41	.58
91.97	0.5	V	52	.94
92.32	0.5	Sm II	1	.27
		Co	29	.39
92.72	1 s	V	27	.69
93.21	0.3	Zr	....	.16
93.60	0.5	Ni	1P	.62
94.22	0.4	Zr	....	.27
95.01	0.5	Ca	25	.93
95.59	1.8n	V	41	.49
(95.95)	?	Fe	217	.98
96.26	0.4	Fe	18P	.21
98.21	0.8n	Fe	558	.18
99.25	2.5	....	....	....
99.80	1.8	V	27	.80
4100				
00.35	1	SiH	....	.33
(00.84)	1	Fe	18	.74
		....	....	....
(01.75)	?	In	1	.76
(02.32)	3.5	....	....	....
		Y	7	.38
(02.91)	?	Si	2	.93
03.31	1	....	....	....
03.76	0.4	....	....	....
04.37	0.6	SiH	....	.32
04.85	0.5	V	112	.78
		....	....	....
05.18	2	V	27	.17
05.87	0.4	SiH	....	.82
06.30	0.5	Fe	217	.27
		SiH	....	.30
06.65	0.3	SiH	....	.62
07.44	0.8	SiH	....	.41
		Fe	354	.49
07.86	0	SiH	....	.76
		SiH	....	.87
08.43	1 n	Zr	32	.39
		Co	2	.49
09.07	0.6s	Fe	558	.07
		SiH	....	.05
09.49	0.3	....	....	....
		SiH	....	.60
09.78	1	Co	1	.71
		V	27	.79
10.61	0.6n	Co	29	.53
		....	....	....
11.39	0	SiH	....	.43
11.84	1.8	V	27	.78
12.68	2	Ti	9	.71
13.52	0.6	V	52	.52
13.84	0.3	....	....	....
14.16	0.3	SiH	....	.13
(14.58)	0.3	....	....	....
15.16	0.8	V	27	.18
16.61	2 n	V	27	.47
		V	27	.70
17.51	0.5	SiH	....	.47
17.96	0.7	SiH	....	.91
18.54	1	Fe	801	.55
18.79	0.5	Co	28	.77
19.18	0	....	....	....
19.61	1.5n	SiH?	....	....
20.23	0.2	Fe	423	.21
20.72	0.5	....	....	....
21.52	2.2n	Zr	32	.45
22.68	0.4n	Fe	356	.52
		....	....	....
23.48	0.8s	....	....	....
		V	27	.57
23.83	0.6	Cb	1	.81
24.97	0.6	Y II	14	.91
25.43	0.5	....	....	....
26.25	0	Fe	695	.19
26.56	0	Cr	35	.52
27.03	0.3	....	....	....
27.55	0.3	Y II	15	.57
28.18	3.6n	V	27	.07
		Y	5	.31
29.75	0.8	Eu II	1	.73
30.65	0.5n	Ba II	4	.65
		SiH	....	.66
31.27	0.8n	(Ti	253	.24)
32.03	1.1	V	27	.02
		SiH	....	.05
		Fe	43	.06
33.44	0.4	....	....	....
33.87	0 s	....	....	....
34.35	2.9	Fe	3	.34
34.94	0	SiH	....	.91
35.30	0.2	....	....	....
35.73	0.6	Zr	50	.68
36.48	1 n	V	26	.39
		Fe	694	.51
37.08	0.5s	Cb	1	.09
37.60	0.5	....	....	....
39.69	2.5	Cb	1	.70
		....	....	....
42.80	3	V	26	.66
		Y	5	.86
		....	....	....
43.88	0.4	Fe	43	.87
44.60	0	SiH	....	.6
44.99	0	....	....	....
45.37	0.2	SiH	....	.3
45.71	0.2	SiH	....	.68
46.29	0.7	SiH	....	.3
46.72	0.6	....	....	....
47.30	0.5	....	....	....
		Zr	....	.37
47.72	0.8	Fe	42	.87
(48.42)	0.9	....	....	....
(48.87)	0.7	V	26	.86
49.77	1.5s	Fe	3P	.76
50.37	0.4	....	....	....
		Co	16	.43
51.13	1 n	....	....	....
52.00	0.4	....	....	....
52.17	1	Fe	18	.18
52.61	0.9	Cb	1	.58
53.04	0.5	Cr	35	.07
53.29	?	V	26	.33
53.79	0.5	Cr	35	.82
54.54	0.3	Fe	355	.50
55.06	0.5n	SiH	....	.06
55.74	0.6	SiH	....	.72
56.17	1	....	....	....
57.27	0.3	SiH	....	.24
57.84	0.6n	Fe	695	.79
58.41	0.3	....	....	....
58.93	0.4	SiH	....	.88
59.65	0.8	V	25	.69
60.51	0.5n	Fe	419	.56
61.15	0	....	....	....
(62.0)	1.5n	SiH	....	.07
63.07	0.6	....	....	....
63.65	1	Cb	1	.65
64.21	0.7	Ti	163	.13
		....	....	....
64.75	0.8	Ni	28	.64
		Cb	1	.65
		....	....	....
65.15	0.4	Sc	20	.12
66.01	0	Ba II	4	.00
66.37	1 s	Ti	163	.31
		Zr	45	.37

TABLE 2—Continued

λ	Int.	Ident. El.	Mult.	λ
4100				
67.50	1.2	Y	7	.52
68.11	1	Cb	1	.12
68.49	0.2	SiH	....	.44
68.94	0.3	(Fe	694	.94)
69.76	? n	....	....	....
71.09	0	(Ti	206	.02)
72.07	1.2	Ga	1	.05
72.76	1	Fe	19	.75
74.08	1.5	Fe	19	.93
		Y	6	.14
74.95	1	Fe	19	.92
75.58	0.3s	....	....	....
		Fe	354	.64
76.12	0.3n	....	....	....
76.78	0.9s	V	6	.79
77.52	2.2n	....	....	....
		Y II	14	.55
		Co	2	.59
		Fe	18	.60
78.19	0	SiH	....	.25
78.65	0.2	....	....	....
79.47	2	V	25	.42
81.17	0.2	....	....	....
81.81	0.3	Fe	354	.76
82.61	0.8	V	24	.59
83.34	1	Zr	51	.31
83.80	0.4	....	....	....
84.37	0.3	....	....	....
84.90	0.6	Fe	355	.90
86.14	1	Ti	129	.12
86.83	0.3	....	....	....
87.10	0.4s	Fe	152	.04
87.55	0.8s	Zr	45	.56
(87.88)	0.3n	Fe	152	.80
88.84	0	....	....	....
89.48	0.5s	Co	2	.50
89.86	0.6s	V	24	.84
90.74	1.8	Co	1	.71
91.56	0.3	V	24	.56
92.11	0.4	Zr	....	.10
94.12	0.5	....	....	....
94.96	1 n	....	....	....
(97.3)	0.6n	....	....	....
98.46	1 n	Co	2	.42
		V	24	.61
99.22	1.3n	....	....	....
		Y II	5	.27
4200				
00.02	1.2n	Fe	3	.97
00.90	0.6	V	6	.89
01.43	0.6	Zr	45	.45
02.06	0.7	Fe	42	.03
03.11	0.3	....	....	....
03.58	0.4	Fe	19	.57
04.22	0	....	....	....
04.67	0.7	Y II	1	.69
05.04	0.4	Eu II	1	.05
05.31	0.3	....	....	....
05.68	0.2n	....	....	....
(06.2)	0.2	....	....	....
06.69	2	Fe	3	.70
09.90	0.6	V	24	.86
10.41	0.4	Fe	152	.35
11.32	0	Cr	133	.35
11.74	0	Ti	279	.73
13.89	1	Zr	43	.86
15.48	4	Sr II	1	.52
16.10	3.5	Fe	3	.19
26.70	50	Ca	2	.73
32.54	1 n	....	....	....
34.01	0.8s	Co	1	.00
		V	6,111	.00
34.56	0.8n	V	6	.52
35.89	1.8n	Y II	5	.73
		Y	5	.94
		Fe	152	.94
36.55	0.8	....	....	....
38.21	1	....	....	....
38.89	0	Fe	693	.82
39.31	1 s	Zr	45	.31
39.89	0.4	Fe	18,273	.85
40.36	0.9	Zr	45	.35
41.18	0.8	Zr	45	.20
41.67	0.7	Zr	45	.68
42.04	1	(Zr	....	.01)
43.02	0.6	....	....	....
43.62	0.3	....	....	....
45.22	1 n	Fe	352	.26
46.85	1	Sc II	7	.83
47.45	1.1	(Fe	693	.43)
49.20	0	....	....	....
49.58	0.5	....	....	....
50.21	1.1	Fe	152	.13
		....	....	....
50.81	1	Fe	42	.79
51.31	0.2	....	....	....
52.29	1.2	Co	1	.30
54.31	4.5n	Cr	1	.35
56.01	0.8	Zr	....	.04
		Ti	252	.04
56.46	0.4	....	....	....
57.28	0.2	....	....	....
58.32	1.7	Fe	3	.32
59.31	0.9s	V	6	.31
59.66	0.2	....	....	....
60.06	0.3	....	....	....
60.49	0.6	Fe	152	.48
61.03	0.6n	....	....	....
61.68	0.4	(Ti	252	.61)
62.29	2.2	(Cr	84,178	.13)
		(Cr	154	.38)
63.31	0.5n	....	....	....
64.05	0.4n	....	....	....
64.49	0.3	....	....	....
65.75	0.8	Ti	162	.72
		....	....	....
(66.7)	0.3	....	....	....
67.13	0.3	....	....	....
68.07	1.1	Zr	45	.01
		Co	1	.03
68.71	0.5	....	....	....
69.20	0	....	....	....
69.76	0	....	....	....
70.17	0	Ti	251	.14
70.56	0.3	....	....	....
71.16	0.6	Fe	152	.16
71.79	1.8	Fe	42	.76
(72.5)	0.8	Ti	44	.44
72.75	0.2	....	....	....
74.77	4.5n	Cr	1	.80
76.69	0.6n	Ti	252	.66
77.62	0.5s	....	....	....
		Fe	172	.68
78.57	0.6n	....	....	....
80.55	0.3n	Fe	598	.53
81.38	0.8	Ti	44	.37
82.23	0.5	Zr	45	.20
82.61	0.2	....	....	....
		Ti	162	.70
83.01	0.8	Ca	5	.01
(83.85)	0.9n	Fe	19P	.87
84.55	0	....	....	....
84.99	0.5	Ti	148	.99
85.96	2.3	Co	1	.78
		Ti	44	.01
86.61	0	....	....	....
87.07	0.5	....	....	....
87.45	2	Ti	44	.40
		....	....	....
88.17	0.7	Ti	43,79	.16
89.05	0.6s	Ti	44	.07
89.61	5 n	Cr	1	.72
90.91	0.3	Ti	44	.94
91.44	3	Fe	3,41	.47
91.88	0.4	V	120	.82
		....	....	....
92.76	0.5	Ti	79	.68
93.38	0.5n	....	....	....
94.16	0.8	Fe	41	.13
94.79	0.8	Sc II	15	.77
		Zr	45	.78
95.75	1	Ti	44	.75
96.17	0 s	....	....	....
96.75	0.4	....	....	....
97.02	3	CH	....	....
97.87	0.8	....	....	....
(98.8)	2 n	Ti	44	.66
		Ni	28	.77
		Ca	5	.99
99.16	1	....	....	....
99.64	1 s	Ti	43	.64
4300				
00.11	0	Ti II	41	.05
00.54	1.8	Ti	44	.57
01.09	1.6	Ti	44	.09
(02.1)	0.7n	....	....	....
02.51	1.1	Ca	5	.53
02.89	0.2s	Zr	45	.88
03.28	0 s	Co	1	.24
03.60	1	CH?	....	....
04.74	0.7	(Zr	....	.68)
05.84	2	Sc II	15	.72
		Ti	44	.91
06.21	1.8	V	5	.21
(07.11)	1.5	Ti	43	.94
		V	5	.18
07.90	1	Fe	42	.91
08.63	0.6	....	....	....
09.06	0	(Fe	849	.04)
09.73	2.5	Y II	5	.62
		V	5	.80
13.16	bh	CH	....	....
14.40	0.4s	Ti	45	.36
14.81	0.7s	Ti	43	.80
15.53	0	....	....	....
18.66	0.9s	Ca	5	.65
(19.04)	0.3	(Zr	....	.05)
20.82	0	Sc II	15	.74
21.15	0.8s	(Ti II	41	.96)
		(Cr	83	.24)
23.28	0.4n	....	....	....

TABLE 2—Continued

λ	Int.	Ident. El.	Mult.	λ
4300				
25.08	0.7	Sc II	15	.01
25.73	3	Fe	42	.76
26.39	1	Ti	43	.36
27.05	0.8	Ti	43	.99
28.04	0.4	(Fe	597	.92)
		....	.....	....
28.66	0	....	.....	....
29.08	0.2	....	.....	....
29.55	1	(Zr	.....	.56)
30.02	1.7	V	5	.02
(31.82)	0.3	....	.....	....
32.82	1.8	V	5	.82
34.87	0.3	Ti	43	.84
37.04	0.4	Fe	41	.05
		....	.....	....
(37.5)	0.7	Cr	22	.57
(39.47)	0.7	Cr	22	.45
(41.03)	0.8	V	5	.01
41.49	0.2	....	.....	....
44.49	1	Cr	22	.51
45.17	0	....	.....	....
46.49	0.3	....	.....	....
47.20	1.6s	Fe	2	.24
47.90	0.8s	Zr	.....	.89
51.14	0.8n	Cr	22	.05
		....	.....	....
(51.80)	0.5	Cr	22	.77
52.88	2	V	5	.87
55.07	0.5n	....	.....	....
55.95	1	V	5	.94
(56.6)	0.4n	....	.....	....
57.76	0	....	.....	....
58.22	0.6	....	.....	....
58.75	1	Y II	5	.73
59.65	0.6	Cr	22	.63
60.82	0.8	Zr	31	.80
61.97	0.8	Co	1	.91
63.60	0.2	V	23	.52
		....	.....	....
66.46	0	Zr	61	.45
68.06	0.8	(Fe	41	.91)
		V	5	.04
71.31	0.6	Cr	22	.28
72.46	0.7n	....	.....	....
75.02	1	Y II	13	.94
75.87	3	Fe	2	.93
79.20	2	V	22	.24
83.55	1.5	Fe	41	.55
84.20	0.3	V	.....	....
84.67	0.7	V	5,22	.72
84.94	0.6	Cr	22	.98
85.69	0.4	....	.....	....
89.23	2	Fe	2	.24
89.97	1	V	22	.97
91.72	0	Cr	22	.75
(92.12)	0.3	V	23	.07
(94.04)	0.8	....	.....	....
94.39	0.8	....	.....	....
95.22	1	V	22	.23
98.04	0.8	Y II	5	.02
99.00	0.4	....	.....	....
99.86	0	Ti II	51	.77
4400				
00.58	1	V	22	.58
00.80	0.5	....	.....	....
02.97	0.4	(Zr	.....	.95)
04.36	0.5	Ti	78	.40
04.97	3	Fe	41	.75
		V	23	.01
		Fe	2P	.02
06.65	1.2	V	22	.64
07.64	1	V	22	.64
08.20	0.9	V	22	.20
08.53	1.5n	V	22	.51
08.76	0.9	....	.....	....
09.23	0	....	.....	....
11.11	0.5n	....	.....	....
12.24	1 n	Cr	22	.25
13.06	0	Zr	61	.04
13.79	0	....	.....	....
(14.20)	0.6n	....	.....	....
(14.48)	0	....	.....	....
15.15	0.3	Fe	41	.12
15.57	0.3	Sc II	14	.56
15.95	0	....	.....	....
16.48	1	V	22	.47
17.30	0.3	Ti	161	.27
19.95	0.8	V	21	.94
20.51	0.6	Zr	61	.45
21.60	1.1	V	22	.57
22.55	1	V	79	.48
		Fe	350	.57
		Y II	5	.59
22.78	1	Ti	78	.82
23.20	0	V	40	.21
25.44	1	Ca	4	.44
26.01	1	V	22	.00
		Ti	161	.05
27.26	2.8	Fe	2	.31
28.52	0.8	V	21	.52
29.19	0.8n	....	.....	....
29.83	0.9	V	22	.80
30.50	0.8n	Ti	113	.37
		Fe	68	.62
31.53	0.2	Zr	61	.48
32.26	0	....	.....	....
33.00	0	....	.....	....
34.00	0.6s	Ti	113,161	.00
34.36	0	....	.....	....
35.06	2.8	Ca	4	.96
		Fe	2	.15
35.66	0.8s	Eu II	4	.58
		Ca	4	.69
36.16	0.8s	V	21	.14
36.66	0	Ti	160	.59
37.19	?	....	.....	....
37.92	2.2	V	21	.84
		Sr	6	.04
40.38	0.3	Ti	159	.34
41.28	0.3	Ti	160	.27
41.69	1	V	21	.68
42.43	0.2	Fe	68	.34
44.22	1.4	V	21	.21
45.12	0.3	....	.....	....
45.46	1.5	Fe	2	.48
46.49	1 n	....	.....	....
47.22	0	....	.....	....
47.76	0.3	Fe	68	.72
(49.05)	0.8	Ti	160	.14
49.81	0.7n	....	.....	....
50.41	0	....	.....	....
50.92	0.6s	Ti	160	.90
51.59	0.6	Mn	22	.59
52.02	0.5	V	87	.01
52.76	0.4	....	.....	....
53.31	0.6	Ti	113	....
53.71	0.4	Ti	160	....
54.77	1.2	Ca	4	....
55.33	0.7	Ti	113	....
55.91	0.8	Ca	4	....
56.57	0.8n	Ca	4	....
57.47	1.2	V	21	....
58.54	0.4	....	.....	....
59.08	0.8	Fe	68	....
59.75	0.8	V	21	....
(60.33)	1	V	21	....
(61.65)	1	Fe	2	....
62.07	0.9	Ti	8	....
62.38	0	V	87	....
63.03	0.5	....	.....	....
(64.96)	?	....	.....	....
(65.78)	0.4	....	.....	....
66.55	1.2	Fe	2P	....
66.90	0	Co	150	....
(69.6)	bh	ZrO	.....	....
(71.3)	bh	ZrO	.....	....
71.67	1 n	Fe	2P	....
79.68	0.3	....	.....	....
81.33	0.6	....	.....	....
82.19	1.2	Fe	2	....
82.69	0.3	Ti	113	....
89.08	0.6	Ti	146	....
89.76	1.6	Fe	2	....
(93.7)	bh	ZrO	.....	....
(96.2)	bh	ZrO	.....	....
96.86	0.5	Cr	10	....
4500				
07.20	1.3	Zr	31	....
		....	.....	....
12.75	0.6n	Ti	42	....
18.05	1	Ti	42	....
19.63	0.4n	ZrO?	.....	....
22.82	1.1	Ti	42	....
23.94	0 s	....	.....	....
24.58	0	....	.....	....
27.36	2	Ti	42	....
		Ti	7	....
28.73	0.4	Fe	68	....
33.23	1.7	Ti	42	....
(34.2)	bh	ZrO	.....	....
(34.7)	4 n bh?	ZrO	.....	....
		Ti	42	....
(34.9)	?	Ti	42	....
37.68	0.5n	V	82	....
40.04	0.3n	V	100	....
40.49	1	Ti	8	....
42.21	0.8	Zr	49	....
44.69	1.2	Ti	42	....
46.01	0.8	Cr	10	....
(46.80)	0.4	....	.....	....
48.76	1.6	Ti	42	....
52.48	1	Ti	42	....
52.64	0	....	.....	....
53.04	0.8	Zr	31	....
54.00	4	Ba II	1	....
55.51	1	Ti	42	....
62.61	1.5	Ti	7	....
65.03	0.3	....	.....	....
65.54	0.5	Cr	21	....
66.25	0.4	....	.....	....
70.10	0.4	....	.....	....

TABLE 2—Continued

λ	Int.	Ident. El.	Mult.	λ
4500				
71.13	2	Mg	1	.10
75.46	3	Mn	.....	.41
		Zr	5	.52
77.17	1.8	V	4	.17
77.73	0	....	.....	....
80.06	0.8	Cr	10	.06
80.35	1	V	4	.39
81.34	1 n	Y	15	.32
		Ca	23	.40
(84.1)	bh?	....	.....	....
(84.5)	?	....	.....	....
85.88	0.9	Ca	23	.87
		Ca	23	.92
86.35	1.5	V	4	.36
90.51	0.8	(Zr	.....	.55)
91.42	1 s	Cr	21	.39
94.10	2.5	V	4	.10
4600				
00.75	1	Cr	21	.75
02.98	0.3	Fe	39	.94
04.36	1	Zr	29	.42
(06.1)	1.4	V	4	.15
07.30	4	Sr	2	.33
12.21	0.4	....	.....	....
13.40	1	Cr	21	.37
15.69	0.3	....	.....	....
16.14	1	Cr	21	.14
16.94	0	....	.....	....
17.28	1	Ti	145	.27
(19.6)	bh	ZrO	.....	....
24.15	1	....	.....	....
26.29	? n	Cr	21	.19
		....	.....	....
.....	.....	....	.....	....
.....	.....	....	.....	....
33.97	2.5	Zr	5	.99
35.22	1	V	4	.18
(37.7)	bh	ZrO	.....	....
(39.1)	bh	(ZrO)	.....	....
43.68	0.8	Y	4	.69
.....	.....	....	.....	....
(50.3)		end of band?		
51.29	1	Cr	21	.28
52.21	0.6	Cr	21	.16
.....	.....	....	.....	....
.....	.....	....	.....	....
56.42	2	Ti	6	.47
67.52	2	Ti	6	.58
74.78	2.5	Y	4	.84
81.83	2	Ti	6	.91
87.80	0.8	Zr	43	.80
88.43	1	Zr	5	.45
91.34	0.7	Ti	75	.34
(93.6)	2.5	Ti	6	.67
98.09	0.8n	....	.....	....
98.76	1	Ti	75	.77
4700				
06.58	0.4s	V	119	.57
(09.71)	0.4	Mn	21	.72
10.12	1.4	Zr	43	.08
		Ti	75,203	.19
15.29	1.6	Ti	6	.30
17.63	0.4	V	119	.69
22.62	0.8	Ti	75	.60

λ	Int.	Ident. El.	Mult.	λ
23.18	0.7	Ti	75	.17
32.28	1	Zr	48	.34
(36.9)	bh	ZrO	....	....
39.45	0.9	Zr	43	.48
41.02	0.5	Sc	14	.02
41.86	0.5	Sr	5	.92
42.78	0.3	Ti	233	.79
43.81	0.5	Sc	14	.81
53.15	1 s	Sc	5	.15
54.02	0.4	Mn	16	.02
58.83	0.6	(V	51	.74)
		Ti	41	.91
59.26	0.4	Ti	233	.27
60.97	2	Y	4	.98
71.10	0.7	Ti	41	.10
72.28	1	Zr	43	.32
76.12	0.3	....	....	....
77.74	0.3	....	....	....
79.33	2	Sc	5	.35
81.00	0.3	Y	13	.04
81.72	0.6	Ti	41	.72
83.37	0.5	Ti	41	.31
84.44	0.6	V	3	.48
84.92	0.6	Zr	44	.94
88.66	0.4	Zr	43	.69
89.28	0.8	Cr	31	.35
91.50	0.7	Sc	5	.50
99.39	0.7	Y	13	.30
4800				
05.86	0.3	Zr	43	.88
15.05	1	Zr	44	.05
15.67	2	Zr	43	.62
		....	....	....
(17.2)	bh	YO	....	....
20.44	0.7	Ti	126	.41
24.29	1	Zr	43	.29
25.49	0.4	Ti	250	.44
27.41	4	V	3	.46
28.09	0.4	Zr	44	.05
31.59	2	V	3	.64
32.39	2	V	3	.43
35.89	1 n!	....	....	....
39.86	0.5n	Y	13	.87
40.82	1	Ti	53	.87
51.45	3	Zr	43	.36
		V	3	.48
64.68	1	V	3	.74
66.11	0.4	Zr	44	.07
70.12	0.3	Ti	231	.13
75.47	1.5	V	3	.46
81.50	2.5	V	3	.55
83.64	0.8	Zr	44	.61
(90.86)	0.3	Fe	318	.76
(91.51)	0.3	Fe	318	.50
4900				
00.00	2	Ti	157	.91
		Ba II	3	.93
		Y II	22	.13
09.08	0.6	Ti	39	.10
13.54	0.4	Ti	157	.62
20.66	0.8	....	....	....
34.04	5	Ba II	1	.09
(54.4)	bh	TiO	....	....
(67.39)	1	Ti	5	.30
(81.81)	1	Ti	38	.73
(82.9)	?	....	....	....
(89.3)	0.9	....	....	....

λ	Int.	Ident. El.	Mult.	λ
(91.15)	1.5	Ti	38	.07
(94.26)	1	Fe	16	.13
		....	....	....
(97.12)	3	Ti	5	.10
(99.58)	2	Ti	38	.50
5000				
(07.26)	2	Ti	38	.21
(09.65)	3	Ti	5	.65
(12.14)	1	Fe	16	.07
(14.20)	4	Ti	5	.18
		Ti	38	.28
(16.22)	1	Ti	38	.16
(20.07)	2	Ti	38	.03
(22.89)	1	Ti	38	.87
(24.94)	3	Ti	38	.84
.....	.....	....	....	....
.....	.....	....	....	....
(60.03)	2	(Fe	1	.08)
(64.56)	3	Ti	5	.65
.....	.....	....	....	....
.....	.....	....	....	....
.....	.....	....	....	....
5700				
(97.77)	1.3	Zr	4	.76
5800				
(90.0)	?	Na	1	.95
(96.1)	?	Na	1	.92
5900				
(35.19)	1	Zr	2	.23
(40.72)	0.7	Ti	2	.68
(44.64)	1	Ti	2	.65
(55.4)	1	Zr	3	.37
6000				
(21.6)	1	ZrO	....	....
(22.4)	0.5	....	....	....
(23.48)	1	Y	3	.41
31.6	0.5	Ti	2	.68
(39.9)	0.5	V	34	.69
61.8	0.3	....	....	....
62.87	1	Zr	3	.88
90.30	1	V	34	.18
6100				
01.6	0.3	....	....	....
02.75	1	Ca	3	.72
10.1	0.5n	....	....	....
11.8	0.3	V	34	.62
22.20	1	Ca	3	.22
24.9	0.5s	(Zr	24	.86)
25.4	0.4	....	....	....
26.3	0.5n	....	....	....
27.51	1	Zr	2	.49
34.58	1	Zr	2	.58
43.24	1	Zr	2	.23
91.78	1	Y	2	.73
(99.25)	1 n	V	19	.20

TABLE 2—Continued

λ	Int.	Ident. El.	Mult.	λ
6200				
10.75	1 s	Sc	2	.68
(14.0)	0.7	V	20	.84
(14.9)	0.3	....	....	....
15.6	0.6	....	....	....
16.40	1	V	19	.37
22.65	1	Y	2	.59
(29.7)	2 bh	ZrO	....	....
30.91	1	V	19	.74
(39.7)	0.7	Sc	3	.78
43.09	1	V	19	.11
51.9	0.5	V	19	.83
58.97	1	Sc	3	.96
68.8	0	V	20	.84
74.7	0	V	19	.77
76.3	0	Sc	2	.31
(85.2)	0.6	V	19	.18
92.92	1.4	V	19	.85
		(ZrO)	....	....
95.3	1 n	Ti	1	.25
96.59	1.5	V	19	.51
		Ti	1	.65
6300				
05.71	1.7	Sc	2	.67
(14.4)	0.5	....	....	....
25.1	1	ZrO	....	....
		Ti	1	.22
78.8	1 bh	ZrO	....	....
		Sc	1	.82
6400				
00.02	0.7	Y	2	.00
(12.4)	1 bh	ZrO	....	....
13.28	1.2	Ti	1	.13
		Sc	1	.53
35.03	1.2	Y	2	.02
38.9	0.5	....	....	....
		Ca	18	.07
47.9	0.4	....	....	....
		Sc	1	.10
62.56	2	Ca	18	.56
.....	....	....	....	....
.....	....	....	....	....
6500				
57.4	....	Y	1	.40
72.84	1	Ca	1	.78
6600				
87.57	1.2	Y	1	.57
6700				
07.7	1 n	Li	1	.74
		Li	1	.89
51.9	1	....	....	....
62.30	2	Zr	1	.38
93.71	1	Y	1	.71
6800				
32.84	2	Zr	1	.93

THE SPECTRUM OF Z ANDROMEDAE IN 1946 AND 1947*

PAUL W. MERRILL
Mount Wilson Observatory
Received January 8, 1948

ABSTRACT

This study is based chiefly on five spectrograms with a dispersion of 10 A/mm. Dark lines observed in the rich shell spectrum of 1946 are recorded in Table 2; the relatively large numbers of lines of *Ti* II and *Cr* II are noteworthy; the displacements of various groups of lines differed among themselves and changed from plate to plate. The displacements of dark lines in the Balmer series showed a progression with quantum number. In 1947 no dark lines were present. The displacements of the bright lines exhibited very complicated behavior (Table 4). Lines in the triplet series of *He* I had systematically greater displacements than did the singlet lines. Radial velocities derived from bright lines of *H* and *He* I in the interval 1940–1947 suggest damped oscillations with an approximate period of 700–750 days. The fluctuations shown by forbidden lines *follow* those by permitted lines by about 200 days. Various observed effects may arise from the differences in the motions of various levels of the extensive stellar atmosphere. Wave lengths measured for a few lines of [*Fe* V] and [*Fe* VII] may be more accurate than the calculated values.

In August, 1946, the spectrum of the peculiar variable star Z Andromedae, 232848, was photographed with dispersion 10.3 A/mm. In addition to about 60 bright lines from λ 3312 to λ 6678, the plates showed a well-developed early-type shell spectrum with

TABLE 1

JOURNAL OF OBSERVATIONS

Plate Ce	Date	JD 243	Exposure (Minutes)	Phot. Mag.*
4370	1946 Aug. 16	2049	430	10.5
4460	Oct. 12	2106	430	10.0
4482	Dec. 2	2157	282	9.9
4779	1947 Aug. 3	2401	364	10.3
4928	Oct. 24	2483	432	10.6

* Balfour S. Whitney, University of Oklahoma.

more than 200 sharp dark lines.[1] Four later spectrograms (Table 1) of the region shortward from λ 5000 showed many changes in both bright and dark lines.

The light-curve in Figure 1 was prepared from numerous photographic observations by Mr. Balfour S. Whitney, of the University of Oklahoma. I am indebted to Mr. Whitney for his courtesy in forwarding these data.

SHELL SPECTRUM

In August and October, 1946 (plates Ce 4370, 4460), the absorption spectrum consisted of numerous well-defined lines, chiefly of hydrogen and ionized metals. It had a considerable resemblance to the recent shell spectrum of Pleione. In October many of the lines showed emission edges, chiefly on their shortward sides. In December, 1946 (Ce 4482), numerous *H* lines toward the head of the Balmer series looked about the same as on the previous plates; but at longer wave lengths all shell lines, with the

* *Contributions from the Mount Wilson Observatory, Carnegie Institution of Washington*, No. 744.

[1] *Mt. W. Contr.*, No. 728; *Ap. J.*, **105**, 120, 1947.

exception of those of *Fe* I, were weaker and the bright edges less conspicuous. On the 1947 plates, Ce 4779 and 4928, the shell spectrum was not seen.

The measured lines with their probable identifications are listed in Table 2. Lines shortward from λ 3450 were measured on plate Ce 4460 only; for most of the lines of longer wave length, measures of one or two additional plates were available. The average probable error of the stellar wave lengths is about ±0.02 A. The displacements adopted for correcting the measured wave lengths were those found from the enhanced lines; hence the recorded wave lengths of lines of neutral metals will be systematically larger than the corresponding laboratory values. The large numbers of lines of *Ti* II and of *Cr* II are noteworthy. The relative intensities in various shell spectra of lines of elements in the iron group deserve much further investigation.

The behavior of the hydrogen lines in 1946 is indicated in Figure 2. The first diagram is the same as that in Figure 2 of *Mt. W. Contr.*, No. 728.[1] The absorption components evidently are not quite symmetrical with respect to the broad emission lines. Since the dark lines have the slower decrement, the bright lines have less and less effect as the head of the series is approached. Accordingly, the measured positions of the dark lines show a progression with increasing quantum number. This phenomenon, found also in a number of other shell spectra, may be of help in analyzing the excitation and stratification of the extensive atmospheres of these stars.

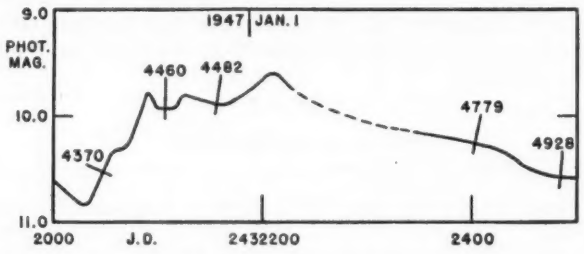

FIG. 1.—Light-curve of Z Andromedae showing dates of spectrograms (see Table 1)

A small but definite progression in the mean displacements of those ultraviolet lines presumably little affected by emission was shown by successive plates in 1946 (Fig. 2). On the 1947 plates no absorption components were visible; radial velocities derived from the emission lines showed no progression with quantum number, but the mean velocity changed by 8 km/sec.

Measured displacements of various groups of lines are summarized in Table 3. Poor lines were assigned weight ½, all others weight 1; hence the recorded weights are equal to, or less than, the number of lines measured. The displacements of neutral lines of *Mg* and *Fe* differ systematically from the displacements of lines of ionized metals. Lines of *Fe* II seem to differ somewhat from other ionized lines. Differences between the mean displacements of ionized lines on the three plates, although small, are greater than the errors of measurement.

Lines of *Ca* II and the *He* I line λ 3888 yield velocities differing substantially from those of other lines; hence these lines may be circumstellar.

BRIGHT LINES

Hydrogen lines.—In 1946 the Balmer series exhibited both bright and dark components, whose complex behavior has already been described. On the 1947 plates no absorption components are visible; radial velocities derived from the emission lines show no progression with quantum number. Tracings of $H\zeta$, $H\delta$, $H\gamma$, and $H\beta$ are reproduced in Figure 3.

TABLE 2

ABSORPTION LINES IN THE SHELL SPECTRUM OF Z ANDROMEDAE

λ	Int.	Identification			λ	Int.	Identification		
		Element	Mult.	λ			Element	Mult.	λ
3222.8	.....	*Ti* II	2	.84	3382.74	2	*Cr* II	3	.68
27.0	.....	.....	.....	.....	83.74	3	*Ti* II	1	.76
29.3	.....	*Ti* II	2	.19	87.76	2	*Ti* II	1	.83
		Ti II	36	.40	88.74	0.5	*Ti* II	53	.76
34.5	.....	*Ti* II	2	.52	91.48	0.6	*Cr* II	3	.43
52.9	.....	*Ti* II	2	.91	93.09	0.5	*Cr* II	21	.00
61.6	.....	*Ti* II	66, 89	.60	.....	.....	.....	.....	.....
82.41	1.5	*Ti* II	66	.33	93.82	0.5	*Cr* II	21	.86
89.34	1	*Fe* II	65	.35?	94.33	1s	*Cr* II	21	.32
95.35	1	*Cr* II	51	.43	94.57	0.5s	*Ti* II	1	.57
3308.79	1.5	*Ti* II	7	.81	3402.46	1	*Ti* II	53	.42
18.09	1	*Ti* II	7	.02			*Cr* II	21	.43
21.65	1s	*Ti* II	65	.70	03.33	1.5	*Cr* II	21	.32
22.92	1	*Ti* II	7	.94	07.30	1.5	*Ni* II	4	.30
24.21	1n	*Cr* II	4	.06	08.79	1	*Cr* II	3	.76
		Cr II	80	.35	09.81	1	*Ti* II	1	.81
26.79	1	*Ti* II	7	.76	.....	.....	.....	.....	.....
27.78	0.6s	.....	.....	.....	14.87	0.3	*Ni* I	19	.76
28.40	1	*Cr* II	4	.35	.....	.....	.....	.....	.....
29.5	1	*Ti* II	7	.46	21.26	1.5	*Cr* II	3	.20
32.09	1.5	*Ti* II	65	.11	22.74	1	*Cr* II	3	.74
35.28	2	*Ti* II	7	.19	33.34	1.5	*Cr* II	3	.30
		Cr II	80	.28	38.96	0	*Mn* II	1	.98
		Cr II	92	.46	42.05	1.5	*Mn* II	3	.98
36.33	0.5	*Cr* II	4	.33	44.28	1	*Ti* II	6	.31
39.88	1.5	*Cr* II	4	.80	46.40	0	*Co* II	2	.40
		Cr II	92	.90	56.38	0.7	*Ti* II	99	.39
40.36	0.5s	*Ti* II	7	.34	60.2	2	*Mn* II	1	.04
41.89	2	*Ti* II	16	.88			*Mn* II	3	.31
42.7	0.5	.....	.....	.....	61.51	2	*Ti* II	6	.50
43.81	2	*Ti* II	7	.77	65.65	0.4	*Ti* II	99	.56
46.78	1.5	*Ti* II	7	.72			*Ni* II	4	.62
47.88	1	*Cr* II	4	.84	68.71	0.5	*Fe* II	114	.68
49.26	3d	*Ti* II	7	.84	71.39	0.3	*Ni* II	4	.35
		Ti II	16	.04	74.07	2	*Mn* II	3	.04
		Cr II	4	.34			*Mn* II	3	.12
		Ti II	1	.40	75.12	0	*Cr* II	2	.13
52.09	0.5s	*Ti* II	54	.07	77.19	2	*Ti* II	6	.18
53.82	0.6	*Sc* II	12	.73	82.93	1	*Mn* II	3	.90
.....	.....	.....	.....	.....	88.68	1	*Mn* II	3	.68
57.4	1	*Cr* II	79	.40	89.02	0	.....	.....	.....
58.4	1	*Cr* II	4	.50	89.79	1	*Ti* II	6	.74
60.35	1.5	*Cr* II	21	.30	91.1	1.5	*Ti* II	6	.05
61.23	1	*Ti* II	1	.21	93.48	0.5	*Fe* II	114	.47
61.95	0.5	*Sc* II	4	.94	94.66	0.5	*Fe* II	16	.67
63.71	0.4s	*Cr* II	3	.71	95.38	0.6	*Cr* II	2	.37
66.20	0.6	*Ti* II	54	.18	95.88	0.7	*Mn* II	3	.83
68.12	2	*Cr* II	4	.05	96.88	0.5	*Mn* II	3	.81
.....	.....	.....	.....	.....	97.60	1	*Mn* II	3	.54
69.04	1	*Cr* II	68	.05	3500.34	0.5	*Ti* II	6	.34
72.18	1	*Ti* II	16	.21	01.78	0	*Co* II	2	.73
72.77	1.2	*Ti* II	1	.80	04.89	1.5	*Ti* II	88	.89
74.21	1	*Ni* II	1	.98	10.87	1.5	*Ti* II	88	.84
		Ti II	54	.35	11.84	0.4	*Cr* II	2	.84
78.40	2	*Cr* II	21	.34	13.85	0.5	*Fe* I	24	.82
.....	.....	.....	.....	.....	14.3	0.5	*Co* II	1	.21
79.35	1s	*Cr* II	21	.37	17.32	0.7	*V* II	6	.30
79.80	1s	*Cr* II	21	.82	20.28	0.5	*Ti* II	98	.25
80.23	1	*Ti* II	1	.28	23.54	0.3s	.....	.....	.....

TABLE 2—*Continued*

λ	Int.	Identification			λ	Int.	Identification		
		Element	Mult.	λ			Element	Mult.	λ
3524.57	0.4	*Ni* I	18	.54	3658.0	0.8	*H*	35	.93
30.80	0.5	*V* II	5	.76	58.7	1	*H*	34	.64
35.4	1	*Ti* II	98	.41	59.4	?	*H*	33	.42
45.2	0.6	*V* II	5	.19	59.72	0.8	*Ti* II	75	.76
56.81	1	*V* II	5	.80	60.3	1	*H*	32	.28
58.53	0.4	*Fe* I	24	.52	61.3	1.2	*H*	31	.22
61.11	0.4				62.3	1.5	*H*	30	.26
65.28	0.4	*Ti* II	76	.33	63.4	1.5	*H*	29	.40
		Fe I	24	.38	64.7	1.8	*H*	28	.68
66.18	0.4	*V* II	4	.18	65.01	0	*Cr* II	156	.95?
67.75	0.3s	*Sc* II	3	.70	66.1	2	*H*	27	.10
70.16	0.7	*Fe* I	24	.10	66.7	2.5	*H*	26	.68
72.51	0.7	*Sc* II	3	.52	69.4	2.5	*H*	25	.47
73.72	0.4	*Ti* II	15	.74	71.5	2.5	*H*	24	.48
76.28	0.5	*Sc* II	3	.34	73.8	3	*H*	23	.76
76.76	0.3	*Ni* II	4	.76	76.4	3	*H*	22	.36
78.76	0	*Cr* I	4	.69	77.79	1	*Cr* II	12	.69
		Ti II	117	.69			*Cr* II	12	.86
81.13	1.5n	*Sc* II	3	.93			*Cr* II	12	.93
		Fe I	23	.20	79.3	3	*H*	21	.36
85.37	1.3n	*Cr* II	13	.31	82.8	3	*H*	20	.81
		Cr II	13	.54	85.17	3	*Ti* II	14	.19
87.10	0.3	*Ti* II	15	.13	86.8	3	*H*	19	.83
89.70	1	*Sc* II	3	.63	91.5	3	*H*	18	.56
		V II	4	.74	97.1	3	*H*	17	.15
90.52	0	*Sc* II	3	.48	3703.8	3	*H*	16	.86
92.04	0.5	*V* II	4	.01	06.22	0.6	*Ti* II	73	.22
93.41	0.6	*V* II	4	.32	09.27	0.4	*Fe* I	21	.25
		Cr I	4	.49	11.8	3	*H*	15	.97
96.04	1	*Ti* II	15	.05	12.12	0.6			
3603.76	0.7	*Cr* II	13	.61	12.95	0.5	*Cr* II	12	.97
		Cr II	13	.80	15.43	0.4	*V* II	15	.48
		Cr II	13	.86	19.97	0.7	*Fe* I	5	.93
08.91	0.4	*Fe* I	23	.86	21.61	0.5	*Ti* II	13	.63
13.18	0	*Cr* II	13	.21	21.9	3	*H*	14	.94
		Cr II	13	.26	27.40	0.6	*V* II	21	.35
13.81	1	*Sc* II	2	.84			*Cr* II	117	.37
18.83	0.8	*Fe* I	23	.77	32.80	0.7	*V* II	15	.76
21.34	0.6	*Fe* II	144	.27	34.3	3	*H*	13	.37
					34.88	0.5	*Fe* I	21	.87
24.87	1	*Ti* II	52	.83	37.2	0.6	*Fe* I	5	.13
		Fe II	144	.89	38.35	0.4	*Cr* II	20	.38
30.74	1	*Sc* II	2	.74	41.65	1.5	*Ti* II	72	.63
31.56	1	*Fe* I	23	.46	43.45	0	*Fe* I	21	.36
		Cr II	12	.49	45.56	0.5	*Fe* I	5	.56
		Cr II	12	.72	45.82	0.5	*V* II	15	.81
41.32	1.2	*Ti* II	52	.33	48.5	0.4	*Fe* II	154	.49?
42.76	0.8	*Sc* II	2	.78	49.5	0.3	*Fe* I	21	.49
45.36	0.3n	*Sc* II	2	.31	50.2	3	*H*	12	.15
					57.67	1s	*Ti* II	72	.68
47.92	0n	*Fe* I	23	.84	58.30	0.7	*Fe* I	21	.24
49.53	0	*Fe* I	291	.51?	59.28	2	*Ti* II	13	.29
51.78	1n	*Sc* II	2	.80	60.52	?			
55.6	0	*H*	39	.60	61.30	2	*Ti* II	13	.32
56.1	0.3	*H*	38	.11	61.91	0.4	*Cr* II	11	.90
56.7	0.4	*H*	37	.67	63.83	0.4	*Fe* I	21	.79
57.3	0.5	*H*	36	.27	65.66	0.3	*Cr* II	20	.62

TABLE 2—*Continued*

λ	Int.	Identification			λ	Int.	Identification		
		Element	Mult.	λ			Element	Mult.	λ
3767.27	0.3	*Fe* I	21	.19	4233.10	0.5	*Fe* II	27	.17
69.50	1	*Ni* II	4	.46	42.35	0	*Cr* II	31	.38
70.5	3	*H*	11	.63	44.42	0.4			
76.12	0	*Ti* II	72	.06	46.81	1s	*Sc* II	7	.83
97.8	3	*H*	10	.90	50.11	0	*Fe* I	152	.12?
3813.38	0.3s	*Ti* II	12	.39	50.84	0	*Fe* I	42	.79
14.62	0.5s	*Ti* II	12	.58	54.42	0	*Cr* I	1	.35
15.94	0.8	*Fe* I	45	.84	61.93	0	*Cr* II	31	.92
20.50	1	*Fe* I	20	.43	67.95	0.6n			
25.89	0.7	*Fe* I	20	.88	71.77	0.6	*Fe* I	42	.76
27.86	0.3	*Fe* I	45	.82	87.8	0.4	*Ti* II	20	.89
29.38	1	*Mg* I	3	.35	90.25	1	*Ti* II	41	.22
32.33	2	*Mg* I	3	.30	94.09	1	*Ti* II	20	.10
34.24	0.4	*Fe* I	20	.22	96.63	0	*Fe* II	28	.57
35.2	1	*Hη*		.39	4300.05	1.5	*Ti* II	41	.05
36.17	0.3	*Ti* II	12	.08?	01.92	0.5	*Ti* II	41	.93
38.32	2	*Mg* I	3	.29	03.21	0.4	*Fe* II	27	.17
40.3	0.3	*Fe* I	20	.44	07.92	1	*Ti* II	41	.90
41.10	0	*Fe* I	45	.05	12.89	0.5	*Ti* II	41	.86
56.68	0.8n				14.09	0.3	*Sc* II	15	.08
59.92	0.7	*Fe* I	4	.91	14.96	1	*Ti* II	41	.98
77.98	0	*Fe* I	20	.02	20.80	0.5	*Sc* II	15	.75
78.73	0.4	*V* II	33	.72	25.00	0	*Sc* II	15	.01
86.34	0	*Fe* I	4	.28?	25.80	0.3	*Fe* I	42	.76
88.1	2	*He* I		.65	26.61	0			
96.11	1.5	*V* II	10	.16	37.90	1	*Ti* II	20	.92
3900.54	1.5	*Ti* II	34	.54	40.0	?	*Hγ*		.47
13.48	2	*Ti* II	34	.46	44.26	0.3	*Ti* II	20	.29
30.31	0	*Fe* I	4	.31	51.78	0.6	*Fe* II	27	.76
32.00	0	*Ti* II	34	.01	68.38	1.5n	*O* I	5	.30?
33.5	3	*Ca* II	1	.66	74.47	0	*Sc* II	14	.46
47.5	0.6	*O* I	3	bl?	83.59	1	*Fe* I	41	.55
52.05	0	*V* II	10	.97	85.4	0	*Fe* II	27	.38
61.8	0				94.02	0	*Ti* II	51	.06
68.4	3	*Ca* II	1	.47	95.01	3	*Ti* II	19	.03
69.8	1	*He*		.08	99.75	0.7	*Ti* II	51	.77
73.61	0s	*V* II	9	.64	4400.45	0	*Sc* II	14	.36?
4002.09	0	*Fe* II	29	.07?	04.82	0.4	*Fe* I	41	.75
12.39	0.7	*Ti* II	11	.37	15.58	0.6	*Sc* II	14	.56
24.57	0s	*Fe* II	127	.55?	16.79	1	*Fe* II	27	.82
25.15	0s	*Ti* II	11	.14	17.71	1.2	*Ti* II	40	.72
27.12	0.7n				37.93	0			
28.3	0.3	*Ti* II	87	.33	43.77	2	*Ti* II	19	.80
35.6	0.4	*V* II	32	.63	50.48	0.5	*Ti* II	19	.49
45.87	0.8	*Fe* I	43	.81	64.42	0	*Ti* II	40	.46
53.85	0	*Ti* II	87	.81	68.47	1.5	*Ti* II	31	.50
63.65	0.5	*Fe* I	43	.60	81.3	1n	*Mg* II	4	.23
71.84	0.3	*Fe* I	43	.74	89.14	0	*Fe* II	37	.18
77.73	0.5	*Sr* II	1	.71	91.38	0.3	*Fe* II	37	.40
4101.4	1	*Hδ*		.74	4501.25	1.5	*Ti* II	31	.28
28.12	0	*Si* II	3	.05	08.23	0.5	*Fe* II	38	.28
31.0	0.8	*Si* II	3	.88	15.3	0.5	*Fe* II	37	.34
63.63	0.5	*Ti* II	105	.65	16.5	0			
71.95	0.5	*Ti* II	105	.90	20.24	0	*Fe* II	37	.22
73.45	0.5	*Fe* II	27	.45	22.65	1	*Fe* II	38	.63
78.87	0.3	*Fe* II	28	.86	28.62	0	*Fe* I	68	.62

TABLE 2—*Continued*

λ	Int.	Identification			λ	Int.	Identification		
		Element	Mult.	λ			Element	Mult.	λ
4533.94	1	*Ti* II	50	.97	4589.96	0	*Ti* II	50	.96
49.56	1.5	*Fe* II	38	.47	4618.80	0	*Cr* II	44	.83
		Ti II	82	.62	19.62	0			
55.91	0	*Fe* II	37	.89	29.28	0.3	*Fe* II	37	.34
58.67	1	*Cr* II	44	.66	35.30	0	*Fe* II	186	.33?
63.72	1.5	*Ti* II	50	.76	4728.56	0			
71.95	2	*Ti* II	82	.97	4805.2	0	*Ti* II	92	.10
76.26	0	*Fe* II	38	.33	24.13	0.5	*Cr* II	30	.13
77.15	0.6n				61.0	5	*Hβ*		.33
83.78	0	*Fe* II	38	.83	4923.85	0.5	*Fe* II	41	.92
88.24	0.5	*Cr* II	44	.22	5018.46	0	*Fe* II	42	.43

Helium lines.—The ionized line λ 4686 is extremely intense on all plates. The over-all width measured on the tracings (Fig. 3) varies from 5 to 8 A, and the structure changes somewhat. On plates Ce 4460, 4779, and 4928 the line is nearly symmetrical. On Ce 4370 there is a maximum with a wing or a diffuse weaker component on the shortward side; on Ce 4482 the line appears to consist of two diffuse overlapping components, the shortward one being slightly stronger. Other *He* II lines observed in emission are : λ 4542, low intensity; λ 4200, trace.

Several emission lines of neutral helium are fairly strong. Lines of the triplet series have algebraically greater displacements than singlet lines (see Table 4). The same effect is present on the low-dispersion spectrograms described in *Mt. W. Contr.*, No. 688;[2] on four plates the measured difference exceeded 20 km/sec, the average difference (triplets *minus* singlets) for all plates being +16 km/sec. A possible interpretation is that the higher and more tenuous portions of the atmosphere are moving outward with respect to the denser lower layers.

Permitted metallic lines.—On the 1947 plates, metals are represented by the following permitted lines in emission: *Mg* I, *Mg* II, *Si* I, *Si* II, *Ca* II (edges), *Ti* II, *Cr* II, *Mn* II (trace), *Fe* I, *Fe* II, *Ni* II (trace). The mean displacements of most of these groups are recorded in Table 4.

An example of fluorescence with Lyman β as the exciting line[3] may perhaps be presented by the bright line λ 3848.24 of *Mg* II, which appears to be several times as intense as the only other line, λ 3850.40, of multiplet (5). The weaker line from the same upper level, λ 3613.80 *Mg* II (2), was not observed.

Forbidden iron lines.—Among the most remarkable peculiarities of combination spectra is the frequent presence of lines of [*Fe* V] and [*Fe* VII]. These lines have not been observed in the laboratory but can be predicted from the known structure of the iron ions. The calculated wave lengths of lines astronomically observable cannot be very precise because the terms on which they depend are based on lines in the extreme ultraviolet. Hence it will be desirable, as opportunity occurs, to determine the wave lengths in spectra of astronomical sources. The spectrum of Z And is not ideal for this purpose because the lines are somewhat diffuse and because their displacements may not correspond exactly to those of other lines on the same plates; nevertheless, the available measurements (Table 5) may for a few lines yield mean wave lengths somewhat more

[2] *Ap. J.*, **99**, 15, 1944.

[3] I. S. Bowen, *Pub. A.S.P.*, **59**, 196, 1947.

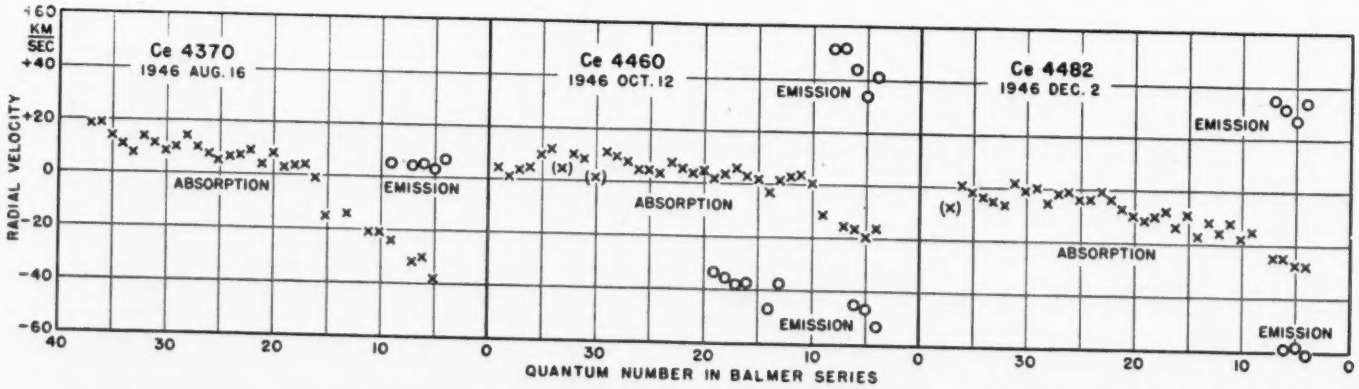

FIG. 2.—Radial velocities derived from hydrogen lines

TABLE 3

RADIAL VELOCITIES FROM ABSORPTION LINES
(Km/Sec)

LINES	1946 AUG. 16		1946 OCT. 12		1946 DEC. 2	
	Rad. Vel.	Wt.	Rad. Vel.	Wt.	Rad. Vel.	Wt.
H	+ 9.3	17	(+ 6.2)	.....	(− 3.0)	.....
He I λ 3888	−24	1	−45	1	.....	.....
Ca II	−14	1	− 9	1	−12.8	2
Mg I	+ 8.7	3	+ 5.6	3	+ 5.5	3
Fe I	+ 9.4	27	+ 6.1	13	+ 6.6	19
Mean *M* I	+ 9.3	30	+ 6.0	16	+ 6.4	22
Sc II	+ 7.4	8	+ 0.8	9.5	+ 3.5	1
Ti II	+ 7.1	45	+ 0.5	56	+ 3.3	28
V II	+ 7.8	9	+ 1.7	5.5	0.0	2.5
Cr II	+ 7.3	12	+ 2.4	24	+ 4.2	7
Mn II	+ 6.8	1.5	+ 3.8	6.5	.....	.....
Fe II	+ 8.0	12	− 1.0	13	+ 9.5	4
Ni II	+ 6.4	2	+ 1.9	2	+ 6.5	1
Mean *M* II	+ 7.3	89.5	+ 1.0	116.5	+ 3.9	43.5

TABLE 4

RADIAL VELOCITIES FROM EMISSION LINES
(Km/Sec)

Lines	1946 Aug. 16	1946 Oct. 12	1946 Dec. 2	1947 Aug. 3	1947 Oct. 24
H	(+ 5)	Abs.	Abs.	− 8.6	−0.2
He I (sing.)	−76, +4	− 1.9	− 5.3	− 7.6	+0.9
He I (trip.)	+16	+ 9.2	+ 6.4	− 3.6	+6.4
Mg I	Abs.	Abs.	.....	− 9	−2
Fe I	Abs.	Abs.	Abs.	− 7.9	−4.6
He II	−76, +3	(−15)	(−16)	(−10)	(0)
Si II	Abs.	(− 3)	(−20)*	− 4	0
Ti II	Abs.	Abs.	Abs.	− 5.6	−4.9
Cr II	Abs.	Abs.	Abs.	− 9.2	(−4)
Fe II	Abs.	Abs.	(−21.9)*	− 5.3	−0.4
N III	(+ 9)	(− 1)	?	− 8.7	+1.9
O III	(+17)	(+29)	−23.8	−12	+8
[*S* II]	(0)	.....	.....	.....	.....
[*Fe* II]	+ 4	+ 6	+ 2.0	− 2.8	−2.8
[*O* III]	−34, +3	−45, +12	+ 7.3	− 0.3	−0.4
[*Ne* III]	−36, +8	+12	+12.4	− 3	−4
[*Ne* V]	−72, +24	(+31)	−17	− 5.6	+1.2

* Bright edges.

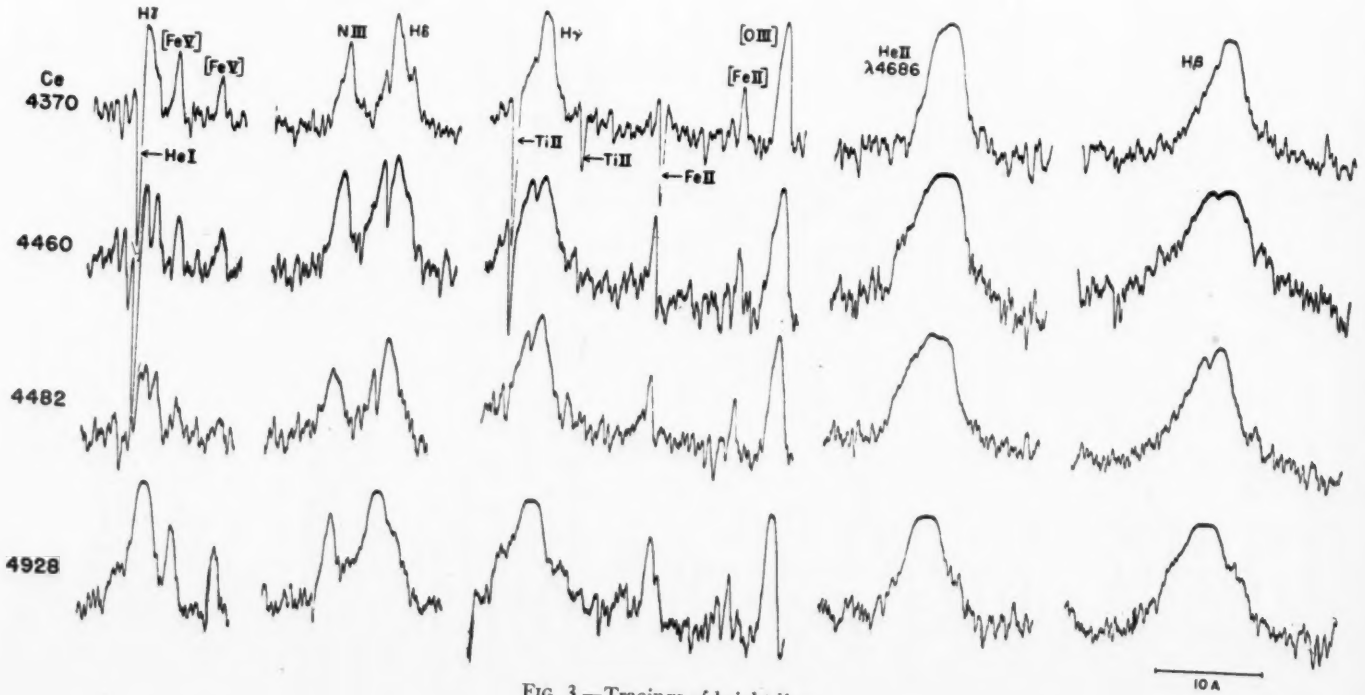

FIG. 3.—Tracings of bright lines

accurate than the computed values. The wave length of the red line [*Fe* VII] λ 6086.9 A, previously measured in the spectrum of Z And,[1] agrees well with the value λ 6086.8 A measured by R. F. Sanford[4] in the spectrum of T CrB, but it differs appreciably from the computed value λ 6085.5.

Radial velocities.—Radial velocities derived from various groups of emission lines are recorded in Table 4. As in previous observations, various lines yield different velocities and appreciable changes occur from plate to plate. A study of the available measures of radial velocity from emission lines[5] for the interval 1940–1947 suggests the occurrence of

TABLE 5

MEASURED WAVE LENGTHS OF FORBIDDEN IRON LINES

Plate Ce	[*Fe* V]					[*Fe* VII]	
4370	.....	3839.72	3891.66	3895.79	.....	3586.58	3759.89
4779	3783.42	(9.84)	1.57	5.70	(4071.66)	.....	9.73
4928	3.45	9.55	1.57	5.67	(1.62)	6.56	9.86
Mean	(3783.44)*	3839.7	3891.60	3895.72	4071.6	3586.57	(3759.83)†
Swings and Struve‡	4.2	9.3	1.4	5.4	1.4	6.6	9.2
Calculated	2.9	8.9	1.8	5.7	1.5	7.2	9.9

* Blend with *Fe* II?

† Blend with *O* III?

‡ [*Fe* V], *Ap. J.*, **97**, 214, 1943; [*Fe* VII], *Ap. J.*, **91**, 614, 1940.

oscillations with an approximate period of 700–750 days; the oscillations of the *H* and *He* I lines appear to diminish in amplitude. Fluctuations in the mean curve for forbidden lines, [*O* III] and [*Ne* III], *follow* those for permitted lines, *H* and *He* I, by about 200 days. In this connection it is interesting that on several occasions the light-curve has had the appearance of damped vibrations[6] and that the median value for the length of the cycle is about 714 days.

[4] *Pub. A.S.P.*, **59**, 87, 1947.

[5] Swings and Struve, *Ap. J.*, **91**, 608, 1940; P. W. Merrill, *Mt. W. Contr.*, No. 688; *Ap. J.*, **99**, 15, 1944.

[6] Campbell and Jacchia, *The Story of Variable Stars* (Philadelphia: Blakiston, 1941), p. 160; Cecilia Payne-Gaposchkin, *Ap. J.*, **104**, 362, 1946.

J. S. PLASKETT'S STAR OF LARGE MASS, HD 47129*

OTTO STRUVE
Yerkes and McDonald Observatories
Received January 24, 1948

ABSTRACT

Spectrographic observations at the McDonald Observatory confirm the general character of the velocity-curve of the primary star derived by Plaskett but show that the maximum of the curve is not always the same. There are also small, irregular changes in the intensities and profiles of the absorption lines. The secondary set of absorption lines shows very large and erratic fluctuations in velocity and intensity, so that it cannot have its origin in a normal, quiescent stellar atmosphere. Nor can its radial velocities be used to derive the mass ratio of the system. There are indications that this set of lines is affected by dilution of the exciting radiation and that it is produced in a rapidly moving stream of gas which is most conspicuous when it is seen projected against the receding hemisphere of the primary star. The spectrum exhibits other peculiar features, most of which are probably related to the unique value of the mass-function of this system, $\sin^3 i\, m_2^3/(m_1 + m_2)^2 = 13.1\ \odot$. It is not certain that any of the observed features are really due to the second component of this double-star system.

The spectroscopic binary, HD 47129 = BD+6°1309[1] was investigated by J. S. Plaskett in 1922. On December 16, 1921, he found double lines in its spectrum, both components belonging to about spectral class Oe5. The measurements of thirty Victoria spectrograms led him next to derive a period of 14.414 days. The semi-amplitude of the primary was 206 km/sec, that of the secondary, 247 km/sec. The eccentricity was 0.035, and the longitude of the line of apsides, 182°. With these elements Plaskett computed the mass-functions

$$m_1 \sin^3 i = 76\odot\,, \qquad m_2 \sin^3 i = 63\odot\,.$$

The total mass of more than 139 ⊙ was exceptional in 1922. It has remained unique to this day; all other known spectroscopic binaries have smaller mass-functions than $f(m) = 13.1\ \odot$. Plaskett investigated the possibility of a period of the order of $1 \pm 1/14.4$ days; but he concluded from observations on four nights with two spectrograms on each, separated by an interval of about 4 hours, that such a short period would not be consistent with his measurements. This is fully confirmed by observations at the McDonald Observatory. On December 1, 1947, four spectrograms were obtained, over an interval of 5 hours. The entire range in velocity was 10 km/sec. The phases in the 14.4-day period were 4.507, 4.555, 4.605, and 4.716 days. In the corresponding part of the velocity-curve the change is about 60 km/sec per day. Hence, if the period were close to 24 hours, we should have observed a change of 60 km/sec within an interval of about 2 hours. The change in 5 hours would have been about 150 km/sec. It is therefore certain that Plaskett's period is approximately correct.

Efforts to find variations in the brightness of this star were unsuccessful. J. Stebbins announced in 1928,[2] from a series of photoelectric observations made in 1923 and 1924, that the "results are discordant and unsatisfactory, but Plaskett's star is not an eclipsing variable. One or both comparison stars are suspicious, but no variation was established." Similarly, P. Guthnick[3] concluded from photoelectric observations made in 1922 and 1923 that the star "is not noticeably variable." Despite these negative results, S.

* *Contributions from the McDonald Observatory, University of Texas*, No. 147.

[1] *Pub. Dom. Ap. Obs., Victoria*, **2**, 147, 1922. The position for 1900 is $\alpha = 6^h32^m0$; $\delta = +6°13'$. The visual magnitude is 6.06.

[2] *Pub. Washburn Obs.*, Vol. **15**, 1928.

[3] *Vierteljahrsschr. der Astr. Gesellsch.*, **58**, 83, 1923.

Gaposchkin[4] has included Plaskett's star in his list of "some important eclipsing systems," with the remark: "It is very probable that this most massive spectroscopic binary (Plaskett's star) is an eclipsing variable with a range of about 0.10 mag." No observations have been published by Gaposchkin in support of this opinion.

The large mass-function of HD 47129 is so remarkable that a new study of its spectrum was undertaken at the McDonald Observatory during the winter of 1947–1948. The total number of spectrograms obtained was seventy-three. They were distributed over two complete cycles: November 25–December 9, 1947, and December 24, 1947–January 7, 1948. We shall designate these cycles as "I" and "III," respectively. The phases, in days, were computed with Plaskett's elements:

$$T = \text{JD } 2423031.870 + 14.414E\,.$$

All spectrograms were taken with the quartz spectrograph at the Cassegrain focus, giving a dispersion of 40 A/mm at λ 3933. Plaskett's dispersion was probably about twice as great. But this difference was not objectionable in the measurement of the star lines because of their intrinsic widths and, occasionally, shallow profiles. The McDonald plates have the advantage of extending beyond the Balmer limit into the ultraviolet and of requiring such short exposures that about one-third of them were made on Eastman Process emulsion. With the exception of a few II-O and 103*a*-F plates, the rest were exposed on emulsion 103*a*-O.

The general appearance of the spectrum is very similar to that described by Plaskett. The lines of the primary component are strong and are easily measurable. Those of *He* I, *Si* IV, and *N* III are not very broad. On some plates they are only slightly broader than the instrumental profile of the spectrograph. The *He* I series ($2^3P^o - n^3D$) is especially strong in absorption, and its members extend far into the ultraviolet as moderately narrow lines. The lines *He* I 3965 and *He* I 3889 are both present; the former is exceptionally narrow and weak, the latter is seen only on a few spectrograms distinct from $H\zeta$. On these plates it appears as a very narrow, but rather weak, absorption line. Neither shows any emission above the level of density of the neighboring continuous spectrum. Since the lower levels of both lines are metastable, the corresponding transitions are known to be sensitive to the dilution effect. Because both lines are weak, I believe that dilution plays no significant role in the atmosphere of the principal component of HD 47129. But the differences in the widths of the *He* I lines (in the order, $2^3S - n^3P$, $2^1S - n^1P$, $2^3P - n^3D$, and $2^1P - n^1D$, of increasing diffuseness) are undoubtedly real and must have some, as yet mysterious, explanation. The lines of the Pickering series of *He* II are somewhat more diffuse. Those of *H* are peculiar: $H\beta$ is very weak and often present only as a diffuse absorption feature between extremely wide and barely perceptible emission components; $H\gamma$ and $H\delta$ are strong and surprisingly well-defined absorption lines between excessively weak emission borders whose total widths may be estimated as 30 A. These double emission lines are seen only with difficulty, even on the Process plates; $H\epsilon$ is blended with interstellar *Ca* II H; $H\zeta$ and all the higher members of the Balmer series, as far as $H\beta$, are quite diffuse, though the degree of diffuseness varies with the phase. The series terminates rather abruptly at *H* 13. There are no *H* emission lines beyond $H\delta$. The Fowler line *He* II 4686 is, in accordance with Plaskett, seen only as a depression between two very weak and broad emission components.

The spectrum of Plaskett's second component was easily detected on the first spectrogram of the new series. Its absorption lines are weak and more diffuse than are those of the principal component. I have measured them on many plates, usually in the case of *H* and *He* I. Contrary to Plaskett's description, I find that this component is relatively weak in *He* II. Moreoever, I have found some very remarkable and unusual features among the lines of this spectrum which I shall describe farther on.

[4] *Variable Stars* ("Harvard Observatory Monographs," No. 5 [Cambridge, 1938]), p. 92.

Table 1 lists the star lines used for the determination of the radial velocities. Many lines are seriously blended: all *H* lines have violet components due to *He* II; *Hδ* is seriously blended with *N* III 4103. Despite these blends, I have used the wave lengths listed in the table, because the errors tend to cancel one another. Nevertheless, the velocity of the system cannot be accurately determined, and Plaskett's value of +24 km/sec is probably as good as can be determined with the help of the new material. The radial velocities are listed in Table 2. Those of the principal component are plotted in Figure 1. The character of the curve closely resembles that published by Plaskett. There is a shift of the entire curve in phase, by about +2.6 days. Since 660 cycles had elapsed between the mean dates of his and of my series of observations, this would correspond to a correction in the period of +0.0039 day, assuming, of course, that no complete cycles were lost or gained during the interval. Plaskett's series extended over an interval of 110 days, or about 8 cycles. Within a single cycle the period would be determined within about ±0.05 day. Hence the probable error of his final value, 14.414 days, was of the order of ±0.01 day.[5]

Between phases 0 and 6 days the measurements are in excellent accord, and the two cycles agree perfectly. Between phases 8 and 13 days, the results from cycle III are

TABLE 1

STAR LINES IN HD 47129

He I	3705.04	*Si* IV	88.86
H 12	50.15	*N* III	97.31
H 10	97.90	*Hδ*	4101.74
He I	3819.64	*Si* IV	16.10
He I+*Hζ*	88.85	*He* I	20.86
Ca II	3933.67	*He* I	43.76
He I	64.73	*He* II	99.83
Ca II	68.47	*Hγ*	4340.47
Hε	70.07	*He* I	87.93
N III	4003.64	*He* I	4471.51
He I	09.27	*He* II	4541.59
He I	26.22	*He* II (emission)	4685.80

systematically lower than those from cycle I. The effect is quite large—of the order of 30 km/sec—and, since care was taken in measuring the same lines on all plates, as nearly as was possible, I believe that the difference must be real. The maximum of the velocity-curve in cycle I (filled circles) was more peaked than in cycle III (open circles). Perhaps this phenomenon is connected with the well-known tendency of certain spectroscopic binaries to produce spuriously peaked maxima in their velocity-curves, which I have attempted to explain as the result of blending of the true stellar line with a line produced in a receding stream of gas, seen projected upon the disk of the principal component a short time prior to superior conjunction (or principal eclipse).[6] There is, however, no certain variation of a periodic nature in the relative intensities of the absorption lines. In view of this uncertainty concerning the maximum of the velocity-curve, I have decided not to derive a new set of orbital elements. Cycle I would suggest an appreciable eccentricity, perhaps of the order of 0.05 with a value ω close to 0°. Cycle III would give almost no eccentricity. The departure from Plaskett's value $\omega = 182°$ is probably not dynamically significant.

[5] It would seem that the procedure used by Plaskett of solving for *P* in his least-squares solution of the orbit was inadvisable and that the close agreement of his value with that found from the new material must have been largely accidental; perhaps he had already ascertained the second decimal place of the period by means of the conventional procedure.

[6] *Ap. J.*, **99**, 95, 1944.

TABLE 2

RADIAL VELOCITIES OF HD 47129

Plate (CQ)	Date	U.T.	Phase (In Days)	Vel. I (Km/Sec)	Vel. II (Km/Sec)	Vel. *Ca* II (Km/Sec)
	1947					
6305	Nov. 25	6^h50^m	12.916	+ 52	−225	+17.6
06	25	7:52	12.959	+ 62	.....	− 4.5
07	25	8:26	12.982	+ 68	−277	+17.7
26	26	7:59	13.963	− 33	.....	− 1.7
27	26	8:15	13.975	− 39	.....	+17.3
46	27	6:44	0.498	− 95	+ 55	+21.7
47	27	7:35	0.533	− 87	.....	+10.2
55	27	11:09	0.682	−110	.....	+17.8
67	28	6:14	1.477	−157	+163	+16.4
68	28	6:34	1.491	−165	+161	+11.8
69	28	6:55	1.505	−172	+ 55	+13.3
73	28	9:12	1.600	−162	+129	+15.7
85	29	6:45	2.498	−169	+164	+ 9.4
86	29	7:55	2.547	−177	+118	+12.4
87	29	9:10	2.599	−185	+143	+12.2
6403	30	6:05	3.471	−164	+157	+15.5
04	30	7:17	3.521	−167	+102	+ 9.4
05	30	8:26	3.568	−160	+169	+ 8.9
22	Dec. 1	6:57	4.507	−107	.....	+21.5
23	1	8:07	4.555	−103	.....	+25.9
24	1	9:19	4.605	−112	.....	+16.3
28	1	11:58	4.716	−114	.....	+ 6.5
33	2	8:23	5.566	− 27	.....	+14.5
34	2	9:27	5.611	− 38	.....	+ 9.8
46	4	9:25	7.609	+137	.....	+ 7.1
47	4	10:32	7.656	+148	.....	− 0.3
51	5	7:35	8.533	+224	−247	+25.7
52	5	8:46	8.582	+223	−243	+22.5
53	5	9:56	8.631	+177	−245	+14.8
63	6	6:43	9.497	+235	−167	+ 6.0
64	6	7:40	9.537	+273	−187	+26.5
65	6	8:34	9.574	+256	−207	+ 7.8
76	7	9:11	10.599	+242	−229	+12.1
77	7	10:10	10.640	+208	−268	+10.5
78	7	11:09	10.682	+224	−242	+28.9
93	8	9:56	11.631	+161	−219	+28.7
94	8	10:28	11.653	+172	.....	+33.4
95	8	11:06	11.680	+180	−221	+33.1
6505	9	11:08	12.681	+ 95	.....	+29.5
06	9	12:01	12.718	+ 89	−176	+ 9.3
15	24	10:38	13.247	+ 17	.....	+22.2
16	24	11:10	13.269	+ 11	.....	+14.7
34	26	10:17	0.818	−123	.....	+10.7
35	26	11:17	0.860	−137	+ 63	+ 9.0
44	27	6:53	1.677	−169	+ 91	+15.0
45	27	7:52	1.718	−160	+137	.....
46	27	8:57	1.763	−164	.....	.....
55	28	7:59	2.723	−163	.....	+23.2
56	28	8:56	2.762	−173	+146	+13.4
57	28	9:52	2.801	−161	+178	+ 9.7
67	29	8:35	3.748	−138	+157	+12.4
68	29	9:33	3.788	−161	.....	+16.8
69	29	10:40	3.835	−161	.....	+22.7
76	30	9:43	4.795	− 73	.....	+27.3
77	30	10:00	4.807	− 81	+178	+10.9
93	31	10:53	5.833	− 39	.....	+26.6
94	31	11:23	5.864	− 31	.....	+11.1

TABLE 2—*Continued*

Plate (CQ)	Date	U.T.	Phase (In Days)	Vel. I (Km/Sec)	Vel. II (Km/Sec)	Vel. *Ca* II (Km/Sec)
	1948					
6596	Jan. 1	7^h11^m	6.689	+ 59	−230	+15.2
97	1	8:08	6.729	+ 78	.....	+27.7
6614	3	6:06	8.644	+198	−260	+11.2
15	3	7:09	8.688	+213	−309	+10.0
16	3	8:37	8.749	+225	−332	+20.3
34	4	7:38	9.708	+216	−185	+17.0
35	4	8:25	9.741	+211	−175	+15.3
36	4	9:15	9.775	+192	−256	+ 9.2
46	5	9:38	10.791	+216	−195	+25.7
47	5	10:35	10.831	+183	.....	+ 5.5
63	6	9:21	11.780	+164	−251	+20.3
64	6	10:21	11.821	+166	−246	+17.2
65	6	11:26	11.866	+132	−195	+22.1
75	7	8:03	12.725	+ 55	.....	+23.4
76	7	9:20	12.779	+ 64	−178	+25.9
80	7	10:58	12.847	+ 40	.....	+10.6

The emission lines are so broad and so faint that I was not able to measure them. They are undoubtedly variable in intensity, and often these variations are erratic in character. It is probable that they are systematically stronger at phases between about 9 and 12 days than at other phases. The entire range of oscillation of the absorption lines is about 8 A; they are never far removed from the geometrical centers of the broad, double emission features. It is certain that the latter do not oscillate by any large amount, either in phase or out of phase with the absorption lines; I should estimate that, if such oscillation does take place, it must have a range of less than about 5 A. On several spectrograms taken near the minimum of the velocity-curve of the primary, the violet emission looks stronger than the red component; but this may mean only that the rise from the bottom of the absorption line to the top of the emission component is more abrupt. Similarly, near maximum radial velocity the red emission component is often more conspicuous.

Throughout the entire series of measurements I was struck by the fact that the blend of $H\zeta$ and *He* I 3889 is usually weaker than are several of the higher members of the Balmer series. Normally, we should expect the blend to be distinctly stronger, especially if *He* I 3889 is strengthened by the dilution effect. At phases 3.5 days of cycle I and 3.8 days of cycle III the line *He* I 3889 is visible as a very narrow, but weak, absorption on top of the diffuse absorption line $H\zeta$. There is no emission visible in either line. At other phases the *He* I line is not seen distinct from $H\zeta$, except in the case of the secondary's spectrum, at phases between 8 and 11 days. The blend seems to be especially weak between phases 2 and 6 days, that is, in the vicinity of the minimum of the velocity-curve.

A somewhat similar phenomenon is present at $H\epsilon$. This line is strong near the maximum of the velocity-curve; it is not much affected by the interstellar line of *Ca* II at phases around 13.5 days and 0.5 days; even at phases 1.6 and 1.7 days it is clearly visible on the violet side of the interstellar line. But at phases between 2.5 and 5 days it is exceedingly faint. The other *H* lines are not affected in this manner. It is probable that the narrow absorption lines of *He* I, λ 3965 and λ 3889, are in reality flanked by extended emission wings, which cut down the intensities of the *H* lines. This would, of course, be possible only if the emission features are stationary or if they oscillate opposite in phase to the absorption lines.

The diffuse character of the higher absorption members of *H* deserves attention. The profiles produced by the Stark effect in ordinary main-sequence O stars (for example, in 10 Lacertae) are of an entirely different character: as far as *H* 11 they are quite deep in their centers, and their wings have the usual exponential profiles. Even the higher members, to *H* 14, are narrower than in HD 47129.[7] Moreover, in the latter star $H\delta$ and $H\gamma$ do not have the exponential wings associated with the Stark effect. If we should attribute the diffuse character of the *H* lines to rotation, then the relatively narrow profiles of the *He* I lines would be unexplained. Similarly, there is no simple explanation for the differences between the profiles of the *He* I lines of different series. If we should attribute the very narrow lines λ 3965 and λ 3889 to dilution, then we should have to explain why there are no other, broader, lines present at these wave lengths which would correspond in origin to the rest of the *He* I spectrum. It would be tempting to investigate

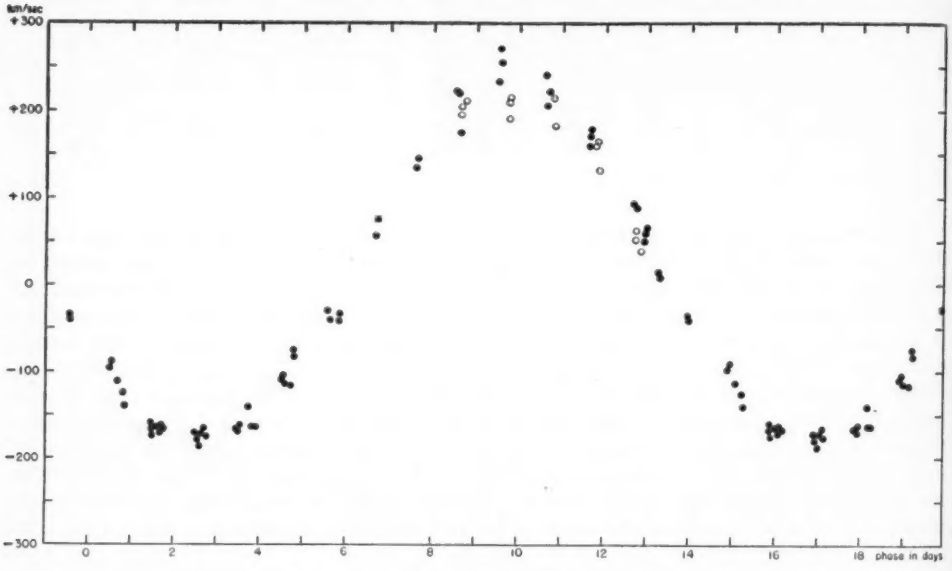

FIG. 1.—Velocity-curve of the primary component of HD 47129. The open circles near the maximum of the curve represent observations made 2 weeks later than the observations indicated by the filled circles.

whether differences in the formation of the *He* I lines, coupled with rapid axial rotation, could produce the observed effects.

The mean of all the interstellar *Ca* II velocities is +16.0 km/sec, in exact agreement with Plaskett's result.

The measurements of the fainter component show several interesting features (Figs. 2, 3, and 4).

1. Between my phases 0 and 4 days (when the primary is near minimum radial velocity) the velocities of the secondary are all systematically smaller than those predicted from Plaskett's elements, the average departure being about:

$$\text{Measured} - \text{computed} = -100 \text{ km/sec} .$$

A similar departure, though of a smaller amount, is clearly shown in Plaskett's velocity-curve. Since the lines are separated, near my phase 2.6 days, by about 325 km/sec, there can be no serious error resulting from the blending of the two components.

[7] See the spectrum of 10 Lacertae (*Ap. J.*, **90**, 699, 1939, Pls. XII and XIII).

2. Between my phases 6 and 13 days the velocities of the secondary show a large amount of scatter—far greater than can be attributed to errors of measurement—and the plotted points fail to show the curvature required by Plaskett's velocity-curve. The mean value is about -250 km/sec, which produces, over the interval of phases from 6 to 13 days, a large departure from Plaskett's curve in the sense

$$\text{Measured} - \text{computed} = -100 \text{ km/sec} .$$

This lack of curvature, with a general tendency of the plotted points to fall below the computed curve is also evident in Plaskett's results. We are faced with the peculiar conclusion that, on the average, the fainter component requires a γ-velocity which is about 100 km/sec less than that derived from the principal component.

3. The secondary spectrum was measured on four plates with phases between 12 and 13 days. The corresponding velocities of the primary are about $+60$ km/sec, which

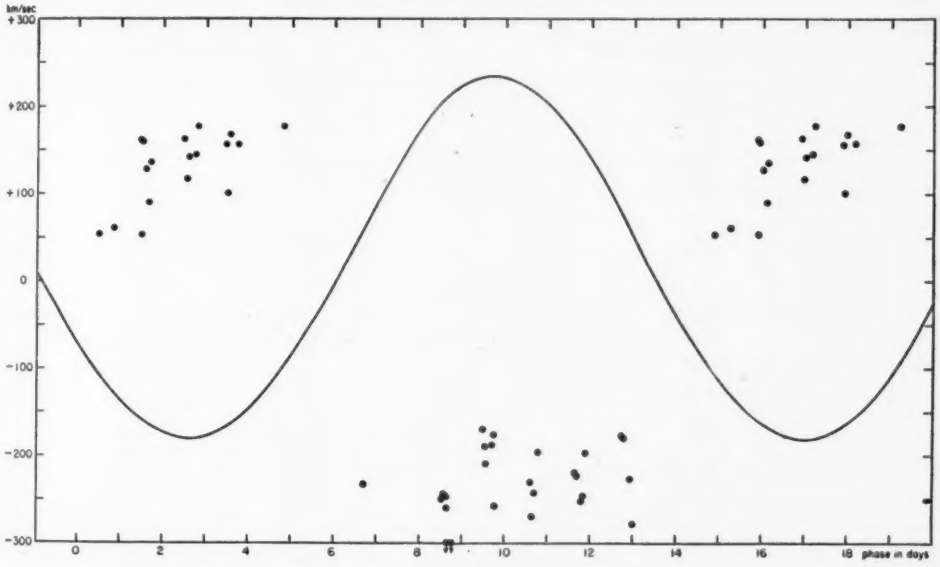

FIG. 2.—Radial velocities of the secondary component of HD 47129. The curve represents the average velocity-curve of the primary component.

differs by only 36 km/sec from the γ-velocity. Yet at these same phases the secondary gave an average velocity of the order of -220 km/sec, or about 244 km/sec less than the γ-velocity. It is clear that the ratio 36/244, which would normally be identical with the mass-ratio, m_2/m_1, has no real significance.

4. On all spectrograms between phases 0 and 4 days the lines of the secondary are weak. They are best seen in $H\gamma$, but they were also measured in the case of *He* I 4026, 4472, and several other lines. They were not seen in $H\delta$, probably because of the blending effect with *N* III 4103. Between phases 6 and 13 days the intensities of the secondary component are subject to very large variations. For example, in cycle I at phase 9.5 days (December 6) the secondary was very strong—almost as strong as the principal component. But on the following night, phase 10.6 days (December 7) the secondary was very weak. I estimate that the equivalent widths of these lines had decreased by a factor of 3 or 4. Yet from the velocity-curve it appears that both phases fall very close to the time of elongation (maximum radial velocity of the primary) so that the separa-

tion of the components on the plates should have been about the same. There is no dynamical interpretation of this result. Nor is it possible to attribute variations of brightness to the secondary, sufficient to produce the observed changes in the equivalent widths of the lines and at the same time consistent with the negative results of the photoelectric observers.

5. In cycle I the secondary component was very strong at phases 9.497, 9.537, and 9.574 days. In cycle III this component was weak at phases 9.708, 9.741, and 9.775 days. Instead, it was fairly strong at phases 8.644, 8.688, and 8.749 days of cycle III. The material is not sufficient to detect any periodicity in the recurrences of the large intensities of the secondary; but they certainly do not repeat themselves with $P = 14.4$ days. There are no such variations between phases 0 and 4 days.

6. The most unexpected result is perhaps obtained from a comparison of spectrograms taken near phase 9.5 days of cycle I with those taken near phase 8.7 days of cycle III. On both nights (December 6 and January 3) the secondary was strong—more so on the former than on the latter. Both sets of plates show several widely separated pairs of lines, especially of *He* I and *H*. From the velocity-curve we should expect that the separation of each pair of lines would be slightly larger at phase 9.5 than at phase 8.7 days. Figure 3 shows that, instead, the separation of the *He* I pairs is very much larger at phase 8.7 days than at phase 9.5 days. The separation of the *H* lines is also different on the two dates. If we take the two Process plates, CQ 6464 (phase 9.537 of cycle I) and CQ 6615 (phase 8.688 of cycle III), we obtain the summary given in the accompanying tabulation. This proves that the secondary component of the spectrum does not originate in an ordinary star. Its intensities and radial velocities vary from cycle to cycle in such an erratic manner that no confidence can be placed in the mean velocity-curve derived from its lines. The mass-ratio of HD 47129 must therefore be regarded as unknown. It is, however, important to realize that this result in no way invalidates Plaskett's conclusion concerning the large mass of this system. The mass function is

Line	Cycle I		Cycle III	
	Principal Component	Secondary Component	Principal Component	Secondary Component
	(km/sec)	(km/sec)	(km/sec)	(km/sec)
He I 3819	+265	.....	+209	−351
He I 4026	+247	−184	+214	−356
He I 4471	+267	−200	+179	−390
Mean *He* I	+260	−192	+201	−366
Separation	452		567	
Hδ	+174	−243	+158	−305
Hγ	+218	−204	+199	−355
Mean *H*	+196	−224	+178	−330
Separation	420		508	

$$\frac{m_2^3}{(m_1+m_2)^2}\sin^3 i = [3.01642-10]\,K_1^3 P(1-e^2)^{3/2} = 13.1\odot .$$

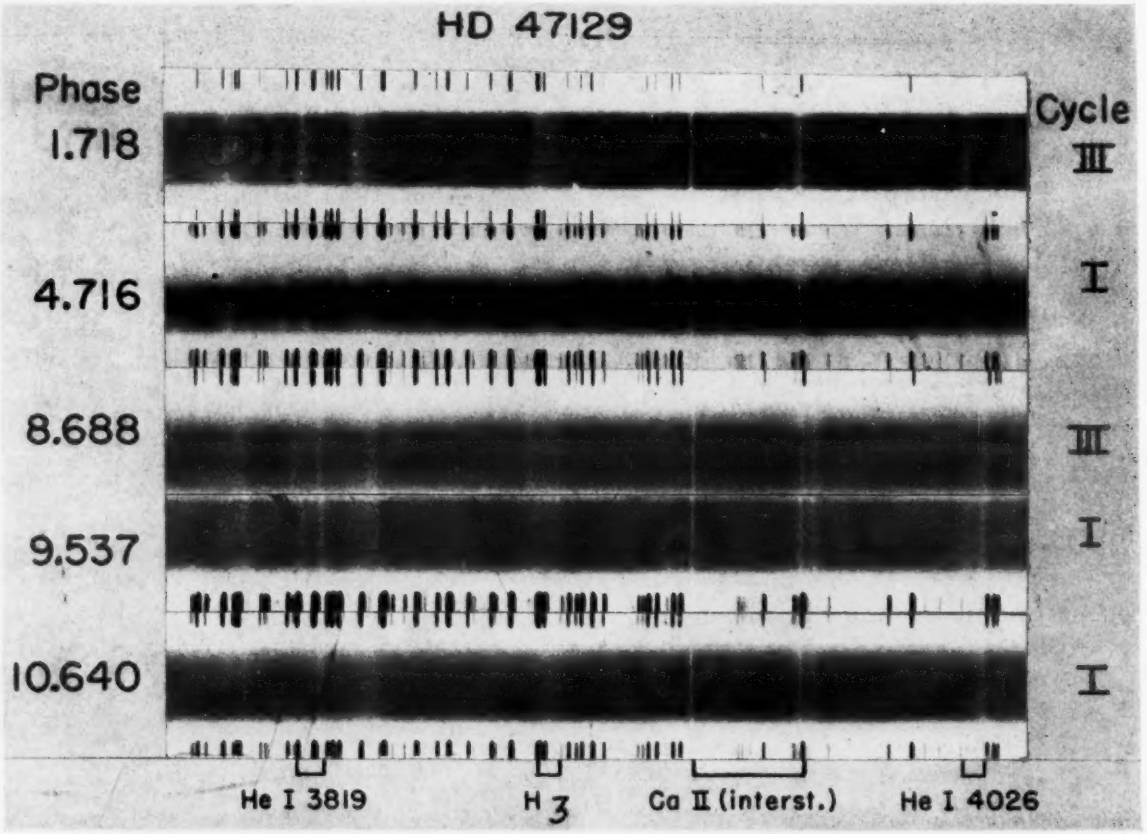

FIG. 3.—The spectrum of HD 47129. Notice that at phase 1.7 days the secondary is visible only as a faint, broad feature on the red sides of $H\zeta$, H 9, and H 10. The secondary is not clearly visible at *He* I. At phase 4.7 days the lines are almost single; notice that the blend $H\zeta$ + *He* I 3889 is weaker than H 9 or H 10. At phase 8.7 days of cycle III the lines are widely double, and the secondary is strong in *He* I; it is somewhat weaker and more diffuse in *H;* notice the strength of the violet component (secondary) for the blend $H\zeta$ + *He* I 3889. The velocity-curve predicts that at phase 9.5 days the separation of the components should be even greater than at phase 8.7 days. Yet, in cycle I, at 9.5 days the separation was much smaller than at phase 8.7 days of the same cycle. At the same time, the intensity of the secondary was exceptionally great. On the following night, phase 10.6 days, the secondary had become very weak.

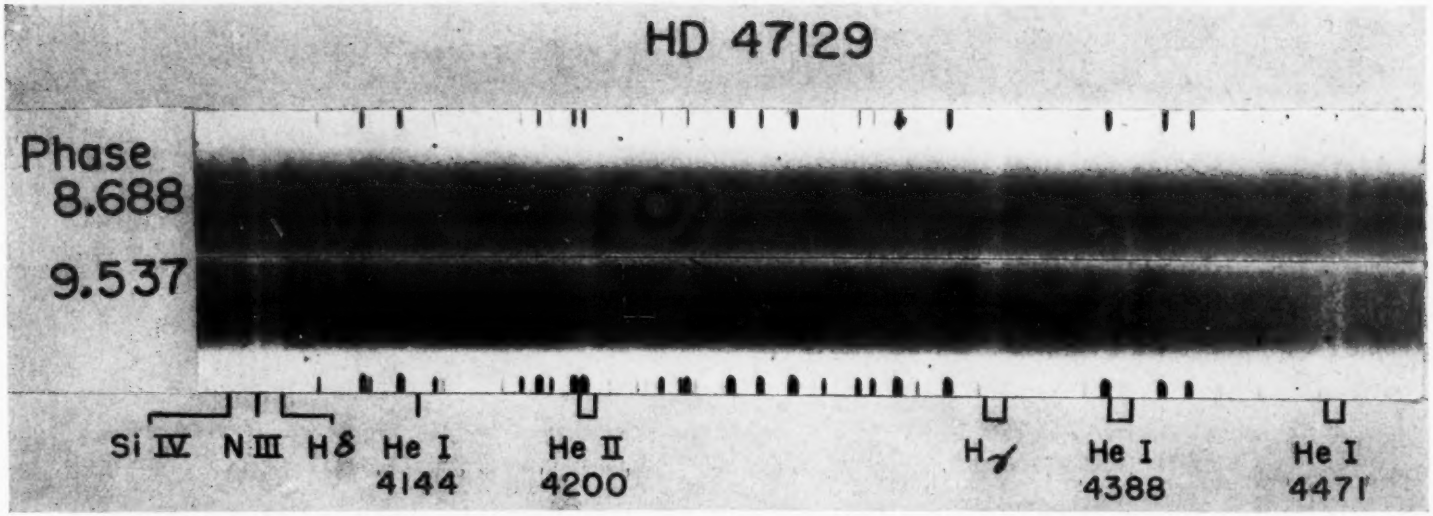

FIG. 4.—The spectrum of HD 47129. The difference in the separations of the two components is greater in the case of *He* I 4471 than in that of $H\gamma$

Plaskett's individual masses are obtained with $m_1/m_2 = 1.2$. This value is now under suspicion. But, even with $m_1 = m_2$, we should still have $m_1 = m_2 = 52\,\odot$. The only manner in which the mass of the principal component can be reduced below this value is to assume that the secondary is more massive than the primary. This might be possible if m_2 were a very red star, completely invisible in the photographic region of the spectrum. There is no observational evidence of the existence of such a red component. Several spectrograms on 103*a*-F emulsion show *Hα* and D3 of *He* I as fairly strong, widely separated, double emission lines. But there is no indication of a composite character in the spectrum, as far as *Hα*, which could be attributed to the blending with the light of a hypothetical red companion.

7. An interesting clue concerning the character of the source which gives rise to the erratic lines of the secondary spectrum appears in the blended line *Hζ* + *He* I 3889. On all those spectrograms which show double absorption lines of *H* and *He* I the lines of the secondary are always fainter than those of the primary. The only exception occurs near phases 9.5 of cycle I and 8.7 of cycle III, on both of which, as we have just seen, the lines of the secondary are *relatively* strong. Even on these dates all double lines show the violet component (secondary) as a fainter line than the red component (primary). The exception is λ 3889, in which the violet component is much the stronger. I have investigated the possibility that this may be caused by a blend. But the blending of *Hζ* with the *He* I line cannot of itself be the cause of this effect, because their separation is only 0.4 A. Nor can the blending with *He* II 3887.44 produce this effect, because the other *H* lines, all of which are blended with *He* II, are not affected in the same manner. It was at first disturbing that another absorption line appeared at phase 9.5 days of cycle I, just to the violet of the strong violet component of the *Hζ* + *He* I pair at λ 3889. This extra line gives to the entire feature the appearance of a triple line. Could the central component be the blend of the violet member of one pair and the red member of another pair? I believe that this is not the case. In the first place, we do not see the extra line at all in cycle III. In the second place, the undisturbed wave length of this extra line is λ 3879.4. Its identification is not known, but it can hardly represent the weaker (violet) component of a pair whose red component must, then, be even stronger. There is no such line to be found in the spectra of the normal O-type stars. It seems to me more plausible to suggest that the spectrum of the secondary component of HD 47129 is affected by the dilution of radiation, which results in the strengthening of the violet component of *He* I 3889. This spectrum is probably produced in a stream of gas not directly connected with any star.

8. The preceding section shows that there are unmistakable small differences in the appearance of the principal spectrum from cycle to cycle. These differences are erratic in character and occur rapidly—perhaps even between successive nights. They affect the relative intensities of the lines of different elements and, perhaps even more so, the profiles of the absorption lines. The latter are sometimes diffuse, while at other times they are quite narrow. These variations are, however, of a minor character and do not compare with those in the spectrum of the secondary. Together with the observed changes in the height of the maximum of the primary's velocity-curve, they suggest that the radial velocities of some O-type stars may be vitiated by streams of gas or perhaps by large masses of prominences whose integrated absorption effects need not always be symmetrical with respect to the undisplaced wave length of each line. It is possible that such a phenomenon is responsible for the anomalous velocities of such stars as 15 S Monocerotis,[8] and it may not be necessary to attribute to the Trumpler stars the very large masses required to explain the anomalous velocities as gravitational red shifts.

9. Because of the large variations in the intensities of the lines of the secondary spectrum, it is probable that the gaseous streams responsible for them absorb the light of the

[8] *Ap. J.*, **105**, 499, 1947.

principal star and not that of the secondary; the latter may be invisible in the region covered by my spectrograms. Otherwise, it would be difficult to explain the great intensity of the secondary at phase 9.537 days of cycle I, without a marked "filling-in" of the lines of the primary by the continuous spectrum of the secondary. In reality, the lines of the primary are no shallower than is normal for a star of spectral class O. There is no parallel to this conclusion among other binary systems with gaseous streams: in β Lyrae the secondary spectrum gives a more or less uniform velocity of expansion; in UX Monocerotis the stream can be roughly described as a ring of gas, rotating in the same direction as the system of the two stars and set in motion by prominences erupting from the advancing hemispheres of both stars. In HD 47129 the lines of the secondary are strongest when they have a relative velocity of -400 or -500 km/sec with respect to the receding hemisphere of the primary star. It would be premature to attempt a dynamical explanation of the conditions in such a stream. It would have been more satisfactory in this respect, if we could have connected the streams with the secondary star. In that case the motion of the stream would depart by a smaller amount from that of the star and could perhaps be explained by assuming an expanding mass of prominences surrounding the latter and having an average velocity of the order of -100 km/sec with respect to it. But there is probably no escape from the conclusion that the changes of intensity are caused by varying amounts of gas in front of the brighter source of continuous spectrum.

10. The lines of the secondary are usually broader than those of the primary, and on some spectrograms (for example, at phase 8.688 days of cycle III) the space between the two widely separated absorption components seems to be affected by a slight amount of uniform absorption.

I am grateful to Dr. A. Blaauw for assistance in securing the observational material; the spectrograms between November 25 and December 2 were obtained by us jointly; those after December 2 were taken by him alone.

THE SPECTRUM OF γ PEGASI*

ANNE B. UNDERHILL†
Yerkes and McDonald Observatories
Received November 19, 1947

ABSTRACT

Two coudé plates of γ Pegasi have been measured for wave length, and some new lines were found. About 70 per cent of the 877 lines measured between λ 3965 and λ 4921 have been identified. The results show generally that the spectrum of any element of reasonably high abundance on the earth may be found if its excitation potential is around 20–25 volts. Potassium has not been found, in spite of the fact that it is abundant on the earth, and the lines of the *K* II spectrum have very favorable wave length and excitation potential for appearance in γ Pegasi.

Small displacements, such as are qualitatively expected on the basis of Stark effect, are found for the *He* I lines. A quantitative comparison is made between theory and observation, and it is shown that the observed displacements of the diffuse-series lines are more nearly in agreement with those calculated by M. K. Krogdahl on the basis of collisional broadening than with those given by the theory of Stark effect from constant fields.

Some forbidden *He* I lines of the $2^1P - m^1P$ series are tentatively identified, and a possible explanation of a small luminosity effect at λ 4026 between dwarf and intermediate B-type stars is proffered.

I. THE MEASUREMENT AND IDENTIFICATION OF LINES IN γ PEGASI

The star γ Pegasi—$\alpha(1900) = 0^h08^m$; $\delta(1900) = +14°38'$; mag. 2.9—is classified on the system of the Yerkes spectral atlas[1] as B2.5 IV. The lines are very sharp and of excellent quality for measurement. Four plates of γ Pegasi taken by W. A. Hiltner with the coudé spectrograph of the McDonald Observatory in November and December, 1943, were very kindly offered for study. Three of the spectra run from about λ 3965 to λ 4713, and one goes from λ 4068 to λ 4935. The dispersion is 1.82 A/mm at $H\epsilon$, 2.29 at $H\delta$, 3.26 at $H\gamma$, and 5.82 at $H\beta$. The plates are of exquisite quality, the spectra being wide and in excellent focus and definition throughout their entire length. A visual inspection of the plates revealed so many more faint features than had previously been reported in the spectrum of γ Pegasi that it seemed worth while to measure the two best plates for wave length, attempting to record every feature. The plates were measured in one direction only, two independent series of measures being made and reduced separately. In compiling the final list of lines, the reality of each feature was checked by visual inspection of all the plates on which it should appear.

The settings, before reduction to wave length, were corrected for the radial velocity of the star as determined from the *He* I lines, the *H* lines, and the strong lines of *O*, *N*, and *Si*. Hence, if there are peculiar displacements of the *He* I and *H* lines with respect to the other lines, a systematic error will be introduced in the measured wave lengths. To investigate such peculiar displacements, which might arise from personal bias in bisecting very strong lines (this effect was not minimized by reversing the plate) or from physical causes, the lines were grouped as indicated in Table 1, and the average residual $\lambda_{star} - \lambda_{lab}$ found for each group. It is evident that the *H* and *He* I lines are displaced to the red with respect to the other lines and that a mean correction of +0.016 A is required to reduce the measured wave lengths to zero velocity. Such a correction has been incorporated in the table of wave lengths. The *He* displacements are discussed later; the *H* displacements may be fictitious because of personal bias.

* *Contributions from the McDonald Observatory, University of Texas*, No. 146.

† This work was completed during the author's tenure of a scholarship from the Canadian Federation of University Women.

[1] Morgan, Keenan, and Kellman, *An Atlas of Stellar Spectra* (Chicago: University of Chicago Press, 1943).

The estimated intensities, mean wave lengths, and identifications are given in Table 2. The intensity scale runs from 00 for lines on the verge of visibility to about 10 for strong sharp lines. Occasionally, the remark "diffuse, *n*," is made. In general, the lines are very sharp, diffuseness usually indicating a forbidden line or an unresolved blend. Lines marked as *n* in the laboratory appear to be as sharp as any of the other lines. In particular, the lines of *N* II, specially mentioned by Struve[2] because of their diffuse character in the laboratory, are found to be just as sharp as the other lines. Laboratory intensities are given in parentheses after the laboratory wave lengths.

Table 2 has been compared to the list of lines given by Kühlborn[3] in five wave-length regions: λλ 4050–4090, λλ 4267–4307, λλ 4395–4431, λλ 4612–4664, λλ 4792–4902. The average $\lambda_{star}-\lambda_{lab}$ for these regions in Table 2 is ±0.058 A; in Kühlborn's table it is ±0.080 A. Owing partly to the improved and increased spectroscopic knowledge now available, about 70 per cent of the lines in Table 2 have been identified, whereas Kühlborn identifies only about 50 per cent. In the region $4200 < \lambda < 4700$ the number of lines measured by both of us is about the same, the chief advantage of Table 2 being the greater number of identifications, mostly *Fe* III, that are made. For the region $\lambda < 4100$, Table 2 is notable for the very small number of unidentified lines remaining. In this

TABLE 1

AVERAGE RESIDUALS

Group	$\lambda_{star}-\lambda_{lab}$
1. All lines used for radial velocity	+0.003A
2. All *H* lines	+ .000
3. All *He* lines of intensity > 2	+ .040
4. All other lines of intensity > 2	− .016
5. All lines of intensity 1–2	− .017
6. All lines of intensity 0	− .022
7. All lines of intensity 00	− .015
8. All radial-velocity lines except *He* and *H*	−0.015

region Kühlborn lists twice as many lines as are given in Table 2 but makes only the same identification as in Table 2; thus half his lines are unidentified. In this region he has a density of lines which is three times what he finds (and approximately what I find) for $\lambda > 4100$. It would seem probable that some of Kühlborn's lines in the region $\lambda < 4100$ are spurious. For the region $\lambda > 4700$ Kühlborn's list of lines is very meager, the comparison having been made chiefly against lines that he measures in other B-type stars. The percentage of unidentified lines in Table 2 for this region is a little larger than it is for the rest of the table, being 39.6 per cent. The wave lengths are from the measurement of a Mount Wilson coudé plate of this region (dispersion 2.83 A/mm) taken by H. W. Babcock and from one McDonald coudé plate.

Figures 1 and 2 show the spectrum of γ Pegasi. Comparison with other published spectra of B-type stars[4] shows the superiority of the present material for studying faint features and for general definition and resolution.

All coincidences within ±0.08 A ($\lambda < 4700$ A) and ±0.15 A ($\lambda > 4700$ A) with lines in the finding list[5] were tabulated for elements of the expected level of ionization and excitation. The mean level of ionization and excitation in γ Pegasi lies near 21 volts,[2,3,4] and it is found that, if the ionization potential of an atom and the excitation potential of the lower levels of the lines in the next spectrum lie between 15 and about 25 volts,

[2] *Ap. J.*, **74**, 225, 1931.

[3] *Veröff. U.-Sternw. Berlin-Babelsberg*, Vol. **12**, No. 1, 1938.

[4] E.g., *Ap. J.*, **74**, 225, 1931; also R. K. Marshall, *Pub. Michigan Obs.*, **5**, 137, 1934.

[5] C. Moore, *Contr. Princeton U. Obs.*, No. 20, Parts I and II, 1945.

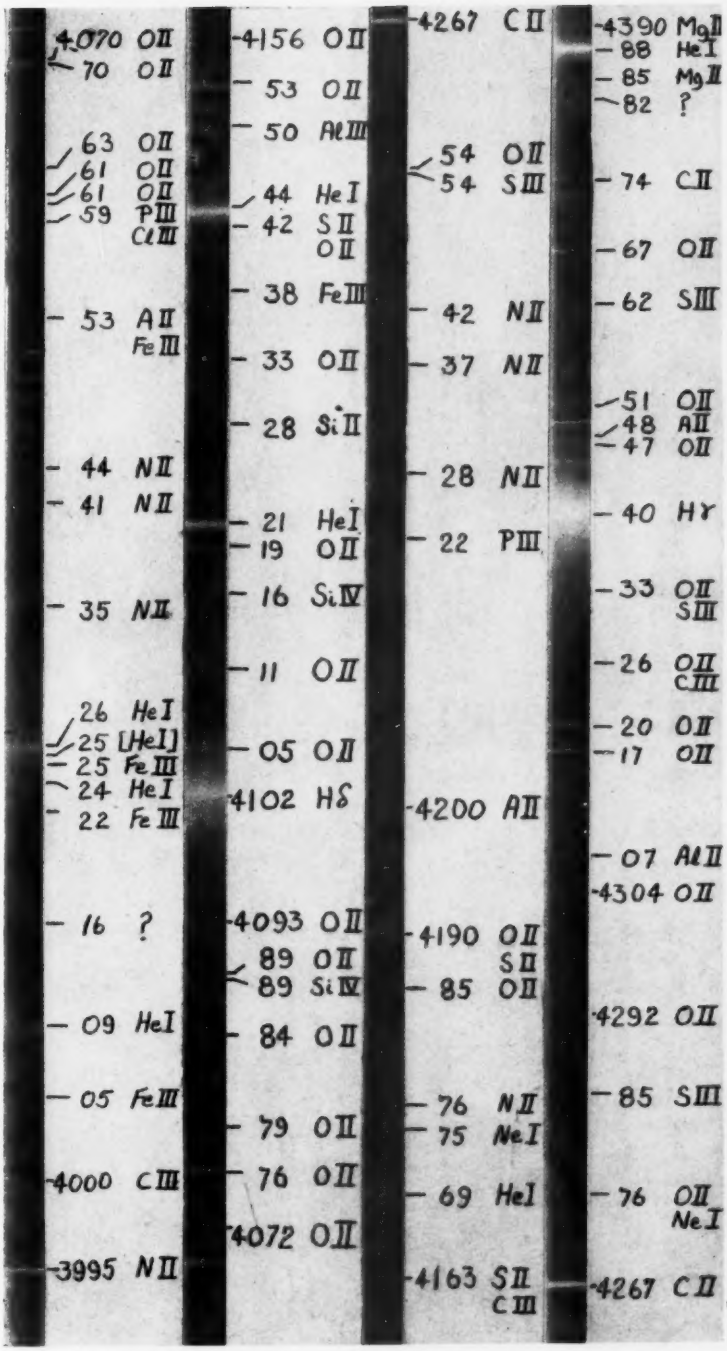

FIG. 1.—The spectrum of γ Pegasi

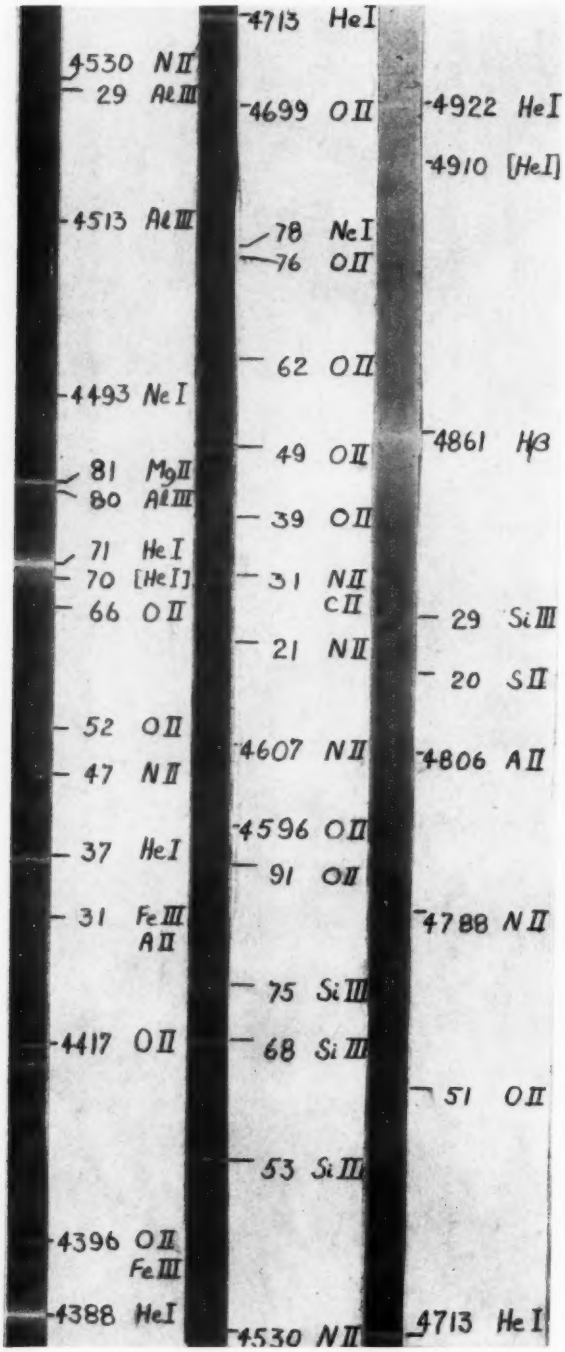

FIG. 2.—The spectrum of γ Pegasi

TABLE 2.

LINES IN γ PEGASI

λ	Int.	Identification	λ	Int.	Identification	λ	Int.	Identification
3964.68	10	He I .73(4)	4032.71	0	S II .81(7)	4087.72	00	FeIII .76(tr)
67.68	0	O II .44(1)	33.15	0	O II .18(0d)			NaII .60(0)
68.42	5	CaII .47(350)	33.74	00	P II .68(2)	88.31	00	FeIII .55(2)
70.15	100	H .07(Hε)			A II .83(6)			.16(tr)
72.42	0	C II .44(0)	35.04	1	N II .09(4n)	88.87	1	SiIV .86(10)
73.25	1	O II .26(10)			O II .09(0d)	89.34	2	O II .30(4n)
73.86	00	C II .84(1d)	35.37	0	A II .47(6)	92.96	2	O II .94(5)
74.26	00	A II .48(5)	39.05	0	FeIII .12(3)	93.50	00	FeIII .36(2)
74.64	00	A II .76(6)	41.40	2	N II .32(5n)	94.22	0	O II .18(0)
75.17	0	FeIII .13(4)			O II .31(0d)	94.80	00	....
75.76	00	....	41.92	0	....	95.17	0	S III .17(-)
77.25	00	C II .30(0)	42.90	0	A II .91(6)	95.71	0	O II .63(0n)
78.21	00	P III .28(8)	43.52	2	N II .54(3n)	96.17	00	O II .18(0d)
79.24	0	A II .36(7)	43.98	00	FeIII .05(4)	96.61	0	FeIII .76(3)
80.34	0	C II .35(3)	44.79	1	N II .75(1)			O II .54(3)
81.60	00	....			FeIII .79(1)	97.30	00	O II .26(4n,
82.18	00	....			O II .96(0d)			4n)
82.68	2	O II .72(5)	45.97	0	O II .15(00d)	98.37	00	O II .27(0n)
83.72	1	S III .77(3)	47.37	0	A II .51(3)	4099.61	00	FeIII .56(tr)
84.04	00	?Ne I .06(0.5)	48.06	0	O II .22(1n)			?A II .47(3)
85.99	0	FeIII .00(3)	48.91	0	FeIII .88(3)	4100.59	00	FeIII .52(3)
		S III .97(2)	51.09	0	FeIII .08(2)	01.73	100	H .74(Hδ)
87.14	0	....	52.18	0	ClII .22(12)	03.64	00	F II .53(15)
90.87	0	S II .94(3)	53.06	1	A II .94(5)			.72(7)
		FeIII .81(tr)			FeIII .28(5)			.87(7)
91.58	0	ClIII .50(7)	53.94	0	O II .10(0d)	04.09	00	A II .91(10,
93.33	00	FeIII .30(4)	55.20	0	....			10)
		S II .53(4)	56.13	00	C III .06(5)	04.39	00	ClIII .23(5)
94.98	9	N II .00(10)	56.86	0	N II .00(1)	04.89	0	O II .74(5)
		A II .81(5,5)			AlII .8 (0.5)			.00(7)
95.87	00	AlII .86(5)	58.60	0	S II .7 (00)	06.23	00	O II .03(0)
		FeIII .81(1)	59.28	1	P III .27(6)	07.50	0	FeIII .65(3)
96.18	00	AlII .16(4)			ClIII .07(6)	07.97	00	FeIII .12(2)
96.67	0	FeIII .65(tr)	60.58	1	O II .58(3n)	08.44	00	....
97.29	0	P III .17(5)	61.02	1	O II .98(2n)	08.76	00	O II .75(0n)
97.90	0	S III .97(-)	61.72	00	FeIII .70(2)	09.59	00	MgII .54(3)
		SiII .00(-)	62.87	1	O II .90(1n)	10.00	00	N II .00(0n)
98.82	0	S II .79(3)	63.91	00	Ne I .04(4)			FeIII .95(5)
3999.90	0	FeIII .83(4)	64.39	00	FeIII .34(1)	10.82	1	O II .80(3)
		C III .92(-)			S III .45(-)	11.46	0	S III .56(-)
4000.60	00	....	65.05	00	A II .14(3)	12.05	1	O II .03(4)
01.21	00	....	66.19	0	FeIII .11(4)			Ne I .10(2)
03.35	0	FeIII .41(4)	68.92	00	C III .97(9)	12.62	0	Ne I .69(2.5)
05.00	2	FeIII .04(-)			Ne I .84(3)	13.29	00	FeIII .45(7)
05.89	0	AlII .7 (0)	69.56	3	O II .64(4)			.23(7)
		FeIII .64(-)	69.89	3	O II .90(6)	13.89	0	O II .82(1)
07.27	0n	[Ne I] .81(-)	70.29	00	C III .30(10)	14.46	0	A II .52(2)
07.64	0	A II .66(1)	71.20	1	O II .20(0)	15.54	0	....
08.73	0	FeIII .81(5)	72.18	5	O II .16(8)	16.14	1	SiIV .10(8)
09.31	15	He I .27(-)	73.10	0	N II .06(2n)	16.59	00	F II .55(7)
09.96	0	C II .90(2)	74.54	2	C II .53(6)	16.82	0	FeIII .88(3)
11.28	00	A II .23(3)	74.85	2	C II .89(5)	17.45	0	....
13.71	00	?Ne I .75(0)	75.40	0	SiII .45(-)	18.31	0	....
15.80	0	....	75.88	5	O II .87(10)	18.82	0	F II .72(-)
16.43	0	FeIII .47(1)			FeIII .83(3)	19.26	8	O II .22(8)
17.51	0	FeIII .58(3)			C II .00(7)			F II .92(7)
19.96	0	?Ne I .02(0.5)	76.57	00	A II .64(5)	19.86	0	....
21.03	00	C II .13(0)	78.24	00	FeIII .28(1)	20.30	2	O II .28(3)
22.30	1	FeIII .36(4)	78.88	2	O II .86(4)	20.90	15	He I .86(3,1)
24.04	2	He I .99(-)	79.69	00	A II .60(5)			FeIII .97(8)
		O II .04(1n)	80.16	0	Ne I .15(4)	21.52	1	O II .48(4)
24.96	1	FeIII .07(3)			P III .04(7)	22.04	1	FeIII .06(8)
		FeIII .85(2)	81.02	1	?FeIII .19(7)			C III .05(3)
		F II .73(20)			?O III .10(1)	22.76	1	FeIII .98(8)
		F II .01(10)	81.62	0	CaIII .74(5)	23.18	0	Na II .07(3)
25.49	2n	[Ne I] .40(-)	82.30	1	N II .28(2n)	23.51	00	FeIII .50(2)
		.49(-)	82.95	00	N II .85(00)	27.26	00	....
		F II .50(15)	83.90	1	O II .91(2n)	28.06	2	SiII .05(8)
26.24	30	He I .20(5,1)	84.35	00	....			FeIII .06(3)
28.78	0	S II .79(7)	84.63	0	O II .66(1)			Ne I .07(3)
30.03	0	FeIII .04(tr)	85.14	1	O II .12(3)	28.59	00	A II .65(-)
31.35	0	A II .41(2)	87.16	1	O II .6(2n)	29.37	1	O II .34(2)

TABLE 2 -- Continued

λ	Int.	Identification
4129.92	0	FeIII .95(3)
30.38	00	?Ne I .51(2.5)
30.90	2	Si II .88(10)
		Ne I .05(5)
31.71	1	A II .73(8)
32.37	00	ClII .48(200)
32.83	2	O II .81(6)
33.63	0	N II .67(2)
35.31	00	....
36.97	00	FeIII .95(4)
37.80	1	FeIII .93(10)
38.27	00	....
39.37	1	FeIII .37(8)
39.99	00	....
40.40	0	FeIII .51(6)
40.95	00	O II .74(0)
41.46	0	[He I] .34(-)
42.20	0	AlIII .15(2n)
		FeIII .16(1)
		O II .08(1)
42.32	1	S II .29(8)
		O II .24(0)
42.92	0	?He I 2P-6D
43.32	0	[He I] .44(-)
43.86	25	He I .76(2)
		O II .77(2)
		FeIII .87(7)
45.08	1	S II .10(9)
45.91	0	O II .90(0)
46.77	0	FeIII .82(4)
		?S II .94(3)
47.88	00	....
48.56	00	....
49.21	00	....
50.07	2n	AlIII .90(10)
		.92(8)
53.26	3	O II .30(7)
53.91	00	....
54.30	00	....
54.92	0	FeIII .98(8)
55.87	0	FeIII .83(tr)
56.56	1	O II .54(3)
		C III .50(4)
57.11	0	....
58.31	00	FeIII .34(3)
60.42	00	P II .56(3)
62.71	1	S II .70(10, 10)
		C III .80(5)
63.19	0	....
64.02	00	....
64.79	1	FeIII .79(20)
		Ne I .80(4)
65.08	0	S II .11(1)
		S III .96(-)
65.60	0	FeIII .53(1)
66.18	0	FeIII .09(1)
		Ne I .09(3)
66.86	1	FeIII .86(9)
68.17	0	....
68.42	0	FeIII .41(4)
		S II .41(5)
69.10	5	He I .97(-)
69.76	0	....
70.32	00	FeIII .34(2)
70.53	00	....
71.65	1	N II .61(2n)
72.09	0	FeIII .09(1)
72.53	0	FeIII .58(1)
72.95	0	....
73.56	0	N II .51(0n)
73.94	0	S II .04(4)
		Ne I .97(0.5)
74.27	1	FeIII .27(10)
		S II .30(-)
		Ne I .37(5)
4175.12	0	Ne I .22(4.5)
75.38	0	Ne I .45(3.5)
76.20	2	N II .16(3n)
76.82	0	FeIII .79(4)
77.33	00	FeIII .19(2)
77.77	00	FeIII .63(3)
78.35	00	A II .39(5)
79.07	00	FeIII .25(5)
79.67	00	N II .67(1n)
80.23	00	....
80.75	00	S II .7 (00)
84.92	00	....
85.48	2	O II .46(8)
85.88	00	S II .95(-)
86.86	0	....
87.93	0	....
89.11	0	FeIII .10(7)
89.77	2	O II .79(10)
		S II .71(6n, 6n)
		A II .67(-)
91.08	0	FeIII .04(3)
91.53	0	?ClII .59(15)
91.81	00	FeIII .96(2)
92.28	00	FeIII .43(2)
92.57	0	O II .50(2)
93.32	0	....
94.23	00	FeIII .13(4)
94.92	00	....
95.99	0	....
97.18	00	FeIII .29(2)
97.78	00	....
98.66	00	....
99.44	00	....
4199.95	0	A II .93(3)
4200.82	00	FeIII .90(1)
01.89	00	A II .99(5)
02.43	00	AlII .4 (2)
03.73	00	....
04.72	00	FeIII .57(4)
05.41	00	....
07.44	00	FeIII .45(2)
08.66	00	FeIII .71(2)
10.63	00	....
11.77	00	....
12.57	00	SiIV .44(4)
14.47	00	....
15.06	00	....
15.79	00	?N III .69(3)
16.41	00	....
17.30	0	S II .23(3)
18.74	00	A II .69(5)
20.26	00	FeIII .32(5)
22.26	1	P III .15(7)
		FeIII .39(8)
23.56	00	....
24.00	00	....
24.71	00	....
25.43	00	FeIII .39(2)
26.85	00	AlII .83(8)
27.74	0	N II .75(3n)
29.45	00	....
30.97	00	S II .98(4)
31.55	00	FeIII .59(1)
		?NeII .60(4)
32.34	00	Ne I .32(0)
33.72	00	....
34.27	00	FeIII .25(tr)
35.56	0	FeIII .54(10)
36.29	0	....
37.00	2	N II .93(5)
		N II .05(4)
4237.44	00	AlII .57(-)
37.93	00	....
38.60	0	....
39.56	00	FeIII .53(1)
		?O III .5 (00)
40.00	00	FeIII .06(1)
		NeII .95(2)
40.74	0	AlII .75(3)
		FeIII .71(4)
41.27	00	....
41.82	1	N II .79(8n, 8n)
42.50	00	MgII .47(4)
43.59	00	?B III .60(3d)
44.27	00	?NeII .17(0)
45.54	00	....
46.08	00	FeIII .18(2)
		F II .16(15n)
46.77	0	FeIII .67(3)
		P III .68(7)
47.58	00	FeIII .56(2)
		C III .56(1)
48.15	00	FeIII .11(2)
50.78	00	NeII .68(4)
52.42	00	Ne I .42(0.5)
53.57	2	FeIII .62(4)
		S III .59(9)
54.12	1	FeIII .08(2)
		O II .98(4d)
55.02	0	S II .01(0)
55.82	00	....
57.41	00	S II .42(3)
58.84	00	FeIII .77(2)
59.68	00	ClII .52(35)
		Ne I .74(0)
60.24	00	....
61.47	00	FeIII .46(4)
62.68	00	....
63.71	00	FeIII .94(4)
		.52(4)
64.53	00	....
65.04	00	....
66.58	00	A II .53(10)
67.18	15	C II .02(19)
		.27(20)
67.89	0	FeIII .84(2)
		S II .80(5)
69.11	00	....
69.70	00	S II .76(3)
		Ne I .72(5)
71.63	00	....
73.39	0	FeIII .42(7n)
74.24	00	O II .13(00)
75.53	1	O II .52(4n)
		Ne I .56(5)
76.00	00	O II .90(0d)
76.74	0	O II .71(1n)
77.44	0	O II .40(1n, 1n)
77.98	0	O II .90(1n)
78.55	0	FeIII .62(1)
		S II .54(3)
79.56	0	FeIII .58(1)
80.66	00	FeIII .74(2)
81.35	0	O II .40(0n)
81.98	00	....
82.54	00	S II .63(3)
83.00	0	A II .90(7)
		O II .96(1n)
		O II .13(0d)
83.78	0	O II .75(0n)
		S III .70(-)
85.00	1	S III .99(5)
85.65	0	O II .70(3n)

TABLE 2 -- Continued

λ	Int.	Identification
4286.25	0	FeIII .13(10n)
87.54	00	FeIII .61(1)
88.19	00	FeIII .17(1)
		N III .21(-)
88.86	0	O II .83(1n)
89.58	00	....
90.55	00	N III .55(-)
91.21	0	FeIII .11(4)
		O II .25(1n)
92.26	0	O II .23(0n)
93.29	00	....
94.36	0	S II .43(6)
94.80	0	O II .82(3n)
95.70	00	....
96.92	0	FeIII .86(10n)
97.90	00	A II .99(-)
4298.96	00	?F II .18(10)
4300.14	00	....
00.90	00	....
01.52	00	FeIII .47(2)
03.00	0	O II .81(0d)
		.06(0d)
03.86	1	O II .82(5n)
04.76	0	FeIII .81(10n)
05.29	00	....
07.19	0	AlII .20(3)
08.26	00	....
08.98	0	O II .96(1n)
		ClII .06(50)
09.65	00	....
10.28	0	FeIII .37(12n)
12.07	00	FeIII .13(1)
		O II .10(0n)
13.12	00	....
13.58	00	C II .50(2)
15.48	00	O II .35(0d, 0d)
15.82	00	O II .80(00d)
16.59	00	....
17.18	3	O II .14(8)
17.95	00	....
18.62	0	S II .68(4)
19.13	00	....
19.67	3	O II .63(8)
20.66	00	....
21.10	00	....
22.40	00	FeIII .45(2)
24.19	00	....
24.60	00	....
25.75	1	O II .77(3)
		C III .70(8)
26.73	00	....
27.42	0	FeIII .41(1)
		O II .48(3)
28.59	0	O II .62(2)
30.05	00	....
31.01	00	....
31.15	0	O II .13(0d)
		A II .25(10)
31.87	0	O II .89(2)
32.76	1	O II .76(1n)
		S III .71(4)
33.66	00	FeIII .60(3)
34.83	00	....
36.82	1	FeIII .81(3)
		O II .86(6)
37.94	0	....
38.58	0	SiIII .52(1)
39.42	0	....
40.55	80	H .47(HY)
41.61	00	....
44.93	0	....
45.61	2	O II .56(7)
46.53	00	....
4347.40	0	FeIII .38(2)
		O II .42(5)
48.14	1	A II .11(20n)
48.73	00	....
49.44	3	O II .43(8)
50.31	0	FeIII .29(1)
51.26	2	O II .27(6)
51.98	00	....
52.50	1	?FeIII .70(4)
53.03	00	....
53.53	0	O II .60(1n)
54.49	0	S III .56(2)
55.48	0	....
56.52	00	....
57.23	00	O II .25(0)
		AlIII .24(-)
58.53	00	A II .53(1)
59.34	00	O II .38(1)
59.53	00	....
59.80	00	....
60.68	0	....
61.57	1	S III .53(2)
62.33	0	....
62.75	00	FeIII .68(1)
		Ne I .69(3)
63.27	00	FeIII .33(1)
		Ne I .23(0.5)
64.70	00	S III .73(1)
65.62	0	FeIII .56(3)
65.92	00	....
66.90	3	O II .90(7)
67.54	00	....
68.12	0	C II .14(4d)
		C III .14(-)
69.26	0	O II .28(4)
69.75	00	FeIII .80(2)
		NeII .77(5)
70.57	00	....
71.46	0	C II .59(3)
		A II .36(8)
72.30	1	C II .49(4)
		Ne I .16(3)
72.86	0	ClII .91(80)
73.49	00	....
74.30	1	C II .28(5)
75.02	00	N II .00(0)
		Ne I .00(0.5)
75.65	00	....
76.38	00	....
77.88	0	NeII .95(2)
		Ne I .75(0.5)
78.34	0	O II .41(0)
79.13	00	N III .09(10d)
79.64	0	A II .74(8)
		NeII .50(6)
80.74	00	....
81.63	00	....
82.52	1	....
83.36	0	[He I] .24(-)
		?C III .24(1)
83.83	00	A II .79(4)
84.65	0	MgII .64(8)
85.64	00	....
86.30	00	....
87.26	0	[He I] .30(-)
		.59(-)
87.99	30	He I .93(3)
88.73	00	FeIII .65(1)
89.84	00	FeIII .76(1)
90.56	1	MgII .58(10)
91.80	00	S II .84(3)
93.55	00	FeIII .52(tr)
95.88	2	O II .95(7)
		FeIII .78(6)
4396.51	00	....
97.68	00	....
98.50	0	....
99.19	00	ClII .14(15)
4399.89	00	A II .09(6)
4400.99	0	A II .02(7)
01.97	00	?P II .97(1n)
03.28	00	FeIII .27(1)
04.01	00	....
05.06	0	....
05.90	0	....
06.48	00	FeIII .41(2)
07.59	00	....
08.50	00	....
09.11	0	....
09.97	1	FeIII .04(3)
		C II .06(4)
11.12	1	C II .20(5)
11.47	1	C II .52(5)
12.28	00	Ne I .28(2.5)
13.22	00	NeII .20(4,4)
14.19	0	P II .29(6)
14.90	4	O II .91(10)
15.64	00	....
16.25	00	....
16.96	3	O II .98(8)
		Ne I .82(4)
17.61	00	....
18.53	00	FeIII .57(tr)
19.57	2	FeIII .59(10)
20.28	00	....
21.02	00	A II .90(7)
21.62	00	Ne I .56(4)
22.11	00	....
23.12	00	....
24.06	00	?P II .9 (3d)
24.96	00	Ne I .80(8)
25.57	0	FeIII .48(2)
		Ne I .40(7)
26.11	1	A II .01(15)
26.60	00	FeIII .56(tr)
27.25	0	N II .21(2)
27.91	0	N II .97(2)
		MgII .00(7)
		Ne I .98(2)
29.22	0	....
30.17	0	FeIII .18(1)
		A II .18(9)
30.98	1	FeIII .95(7)
		S II .02(1)
		A II .02(8)
31.89	00	FeIII .84(2)
		N II .82(0)
32.70	0	N II .74(6n)
34.00	00	FeIII .02(2)
		MgII .99(8)
34.54	00	FeIII .49(1)
35.40	00	....
36.19	00	....
37.62	8	He I .55(1)
38.24	00	A II .12(1)
38.87	00	....
39.84	0	S III .87(1)
40.53	00	FeIII .60(3)
		Ne I .36(2)
41.95	0	N II .99(3n)
43.09	0	O II .05(5)
44.38	00	FeIII .46(1)
47.04	2	N II .03(10)
48.23	0	O II .21(6)
48.94	00	FeIII .97(1)
		A II .88(6)
49.78	00	FeIII .63(3)
50.36	00	....

TABLE 2 -- Continued

λ	Int.	Identification	λ	Int.	Identification	λ	Int.	Identification
4451.60	0	....	4539.17	0	Ne I .17(4)	4605.59	00	....
52.38	2	O II .38(6)	40.38	0	Ne I .36(10)	07.22	1	FeIII .24(1)
54.27	00	Ne I .28(1)	41.77	0	FeIII .65(4)			N II .15(7)
55.54	00	Ne I .56(2)	44.02	00	FeIII .98(4)	08.28	00	ClIII .21(5)
56.79	00	....			A II .91(1)	09.53	1	A II .60(15)
58.47	00	....	44.21	0	NeII .11(1)			O II .42(4n)
59.09	00	....	45.09	0	A II .08(10)	10.27	0	O II .14(3n)
60.15	00	Ne I .18(6)	46.67	00	....	10.86	00	FeIII .83(1)
61.16	00	....	47.55	00	....	11.82	00	FeIII .80(1)
61.88	00	....	48.43	0	....	12.57	00	FeIII .48(1)
62.71	00	....	49.36	0	....	13.12	00	O II .11(0d)
63.50	00	S II .58(7)	51.12	0	FeIII .15(tr)	13.61	0	O II .67(1d)
64.40	0	S II .42(-)	51.88	0	FeIII .85(tr)			S III .47(00)
65.28	0	....	52.64	5	SiIII .65(9)	13.86	2	N II .87(6)
66.35	0	O II .32(2n)			Ne I .60(3)	15.28	00	....
67.68	0	....	53.83	00	FeIII .77(1)	15.73	00	....
68.53	00	FeIII .51(3)	55.22	00	....	16.42	00	....
69.87	5n	FeIII .92(1)	56.12	00	....	16.87	00	FeIII .95(1)
		[He I] .92(-)	57.82	0	FeIII .82(1)	18.09	00	....
71.56	40	He I .51(6,1)	58.84	00	....	18.83	00	C II .85(5d)
		FeIII .57(4)	60.56	00	....	19.57	0	....
		.16(4)	61.75	00	S II .88(-)	20.42	00	FeIII .39(1)
73.09	0	....	62.70	00	....	21.44	1	N II .39(7)
74.46	00	FeIII .46(3)	63.57	00	FeIII .56(1)			FeIII .39(3)
75.99	00	O II .08(0d)	64.74	00	N II .78(1)	22.35	1	....
77.80	00	N II .74(2)	65.99	00	Ne I .89(4.5)	23.93	00	....
		O II .88(2n)	66.99	00	Ne I .83(3.5)	26.56	00	FeIII .53(1)
79.00	00	....	67.88	5	SiIII .87(7)			P II .61(5)
79.96	2	AlIII .89(3)	69.05	00	FeIII .08(1)	27.29	00	....
		.97(4)			NeII .01(5)	27.91	00	FeIII .94(1)
81.24	5	MgII .33(100)	69.70	0	FeIII .82(4)			NeII .85(3)
		.13(100)	70.97	0	FeIII .85(4)	28.70	00	P II .71(4)
82.42	00	....	72.01	0	ClII .13(100)	30.56	2	N II .54(10)
83.57	00	S II .42(6)	73.26	0	FeIII .14(5)			C II .52(1d)
		FeIII .48(4)	73.78	0	Ne I .76(3)	32.65	0	....
		P II .67(4)	74.80	4	SiIII .78(4)	33.59	0	FeIII .69(2)
84.93	00	....	75.54	00	....	34.91	00	?NeII .73(2)
86.53	00	FeIII .55(1)	76.67	00	....	36.71	00	Ne I .63(5)
		S II .66(3)	77.74	0	....	37.57	0	....
87.70	00	O II .72(0n)	78.39	00	....	38.89	2	O II .85(6)
89.40	0	O II .48(1n)	79.32	0	A II .39(8)	39.78	0	AlII .72(2)
91.22	0	O II .25(3n)	79.94	00	....			.83(1.5)
92.33	00	FeIII .39(3)	80.57	0	....	40.31	0	AlII .36(4)
		S II .3 (00)	81.39	0	....			.38(3.5)
92.60	1	Ne I .69(2)	82.23	00	Ne I .03(7)	41.82	3	O II .81(9)
96.44	00	....			.45(7)			FeIII .90(3)
98.06	00	FeIII .02(tr)	82.93	00	....	43.10	1	N II .09(8)
4499.09	00	?P II .18(7)	83.74	00	....	43.96	00	....
4501.52	00	FeIII .58(2)	84.62	00	....	44.97	0	....
07.74	00	?N II .56(3)	85.32	00	....	45.74	00	FeIII .77(1)
10.91	00	N III .92(6)	86.51	00	....	46.49	00	FeIII .46(2)
12.61	2	AlIII .54(8)	87.36	00	....	47.32	0	C III .40(20)
13.94	00	FeIII .02(1)	87.85	00	P III .91(7)	48.26	00	S II .17(2)
17.47	00	....			P II .91(8)	49.16	4	O II .14(10)
22.08	00	....			A II .90(2)			A II .06(0n)
24.87	00	S II .68(2)	88.99	0	....	50.18	00	C III .16(19)
		.95(6)	90.13	0	....	50.88	2	O II .84(6)
27.70	00	FeIII .67(1)	91.02	2	O II .97(9)	51.60	00	FeIII .57(1)
		Ne I .72(2)	91.69	00	FeIII .84(4)	52.24	00	....
29.15	3	AlIII .18(10)			.35(3)	52.81	00	....
		.91(1)	93.05	00	....	54.27	00	FeIII .19(1)
29.92	00	....	93.86	00	....			SiIV .14(6)
30.44	1	N II .40(5)	94.43	00	....	55.60	00	....
31.67	0	FeIII .59(1)	95.14	00	Ne I .25(4)	56.73	00	S II .74(4)
32.11	00	FeIII .15(1)	96.19	2	O II .17(8)			FeIII .78(2)
32.62	00	....	97.28	0	FeIII .34(2)			SiII .80(-)
33.46	00	FeIII .51(1)	98.09	0	FeIII .98(1)	57.74	00	?A II .94(9)
		S II .3(00)	98.56	00	....	59.00	00	FeIII .00(tr)
34.25	0	MgII .26(4)	4599.38	00	FeIII .27(1)	59.97	00	....
35.15	0	N III .11(2)	4600.49	0	FeIII .43(2)	60.60	00	FeIII .56(tr)
36.56	00	Ne I .31(7)	01.50	2	N II .48(8)	61.64	2	O II .64(9)
37.71	00	Ne I .68(8)	02.21	0	O II .11(2n)	62.47	00	....
		Ne I .75(10)	03.72	00	....	63.12	0	FeIII .21(tr)
		A II .67(4)	04.54	0	....			?AlII .05(0)

TABLE 2 -- Continued

λ	Int.	Identification	λ	Int.	Identification	λ	Int.	Identification
4664.95	00	....	4721.55	00	N II .59(0)	4810.27	0	N II .29(2)
65.69	00	?SiIII .87(0)	22.50	00	....			ClII .06(225)
66.41	00	A II .28(2n)	23.55	00	FeIII .70(2)	11.42	0	ClII .57(12)
67.35	0	FeIII .34(2)	25.28	00	Ne I .14(5)	13.33	0	SiIII .29(2n)
		N II .28(2)	26.92	00	A II .91(10)	15.43	0	S II .52(10)
68.30	00	....	29.74	00	....	16.30	00	....
69.40	0	O II .33(0)	31.96	00	A II .08(5)	17.48	0	Ne I .64(8)
71.10	00	?FeIII .25(tr)	32.86	00	FeIII .70(1)			FeIII .36(1)
71.94	00	....	34.74	00	C II .75(2d)	19.62	1	S II .60(2n,
73.67	1	O II .75(4)	35.82	0	A II .93(15)			2n)
74.73	0	FeIII .79(1)	38.04	00	C II .11(0)			ClII .46(200)
76.25	2	O II .23(8)	40.08	00	....	23.91	00	S II .07(3)
77.01	00	FeIII .24(2)	40.76	00	....			P II .84(0)
		.74(2)	41.63	0	O II .71(3)	25.70	00	....
		O II .00(0)	44.99	0	C II .90(1)	28.95	1	SiIII .92(4n)
78.17	0	Ne I .22(8)	46.29	00	....	30.89	0	....
79.06	00	P II .95(6)	47.48	00	....	35.91	0	S II .85(-)
		Ne I .14(7)	48.17	00	....	36.83	00	ClII .79(20)
79.61	00	....	49.26	00	....	37.79	00	....
80.45	0	Ne I .36(6)	50.36	00	....	38.79	0	....
81.22	00	Ne I .20(4)	51.23	0	O II .34(4)	43.22	0	O II .26(1n)
		?S II .32(00)	52.70	00	Ne I .73(10)	45.10	00	O II .01(1)
82.24	00	A II .29(-)			O II .70(2)	45.85	0	....
		Ne I .15(2.5)	53.52	00	....	47.83	0	A II .90(8)
83.09	00	SiIII .02(2)	54.88	00	?S II .12(2)	48.33	0	....
84.38	00	....	55.53	00	ClII .64(50)	48.98	00	....
85.97	00	....	58.25	00	....	51.88	00	....
87.03	00	....	60.00	00	....	53.41	0	....
87.99	00	....	61.24	00	....	56.68	0	O II .49(2)
89.24	00	....	63.42	00	S II .38(1)			.76(2)
89.85	00	FeIII .87(tr)	64.53	00	....	57.06	00	ClII .04(10)
91.68	0	FeIII .63(1)	64.99	0	A II .89(10)			FeIII .06(tr)
		O II .47(1)	66.45	00	....	58.11	00	....
93.13	00	....	68.07	0	....	59.77	0	....
94.76	0	FeIII .57(4)	69.29	00	....	61.28	80	H .33(Hβ)
96.05	0	N II .91(1)	70.92	00	ClII .09(40)	62.74	0	FeIII .66(-)
96.45	00	O II .36(2)	73.94	00	N II .22(2)	64.33	00	Ne I .35(3)
97.68	0	FeIII .69(1)	75.17	00	....			P II .38(4)
4699.18	1	O II .21(7,7)	79.74	0	N II .71(4)	71.72	0	O II .58(3)
		FeIII .22(1)	80.94	00	Ne I .88(3)			FeIII .86(2)
4701.04	0	O II .23(2)	81.79	00	ClII .82(50)	80.02	0	A II .90(12)
03.10	0	O II .18(3)	83.42	00	....	82.11	00	A II .25(-)
04.26	00	Ne I .40(15)	84.35	00	....	83.41	0	....
		N II .33(0)	85.34	0	ClII .44(50)	85.70	0	S II .63(-)
05.40	2	O II .36(8)	86.32	00	....	4890.85	0	O II .93(4)
06.92	00	....	87.25	0	....	4902.45	1	....
08.02	0	....	88.05	0	N II .13(5)	04.55	0	A II .75(6)
08.75	00	Ne I .85(12)	88.93	0	Ne I .93(12)			ClII .76(135)
09.90	1	Ne I .06(10)	91.10	00	....	05.85	0	....
		O II .04(5)	91.95	00	ClII .04(12)	06.89	1	O II .88(5)
10.92	00	....			S II .02(3)			SiII .88(-)
11.99	0	FeIII .98(1)	93.18	0	....	09.15	00	....
		Ne I .06(10)	94.72	00	ClII .54(250)	10.66	0	[He I] .75(-)
13.23	10	He I .20(3,1)	96.85	0	....	14.20	0	ClII .32(12)
15.37	00	Ne I .34(15)	98.29	00	ClII .40(15)	16.27	00	....
16.64	1	SiIII .66(-)	4799.43	0	....	17.10	0	S II .15(7)
17.61	00	....	4800.69	0	....	17.77	00	ClII .72(125)
18.41	00	N II .43(2)	02.63	0	S III .81(-)	19.36	0	....
19.22	00	FeIII .12(2)	03.27	1n	N II .27(6)	19.96	00	....
		?NeII .37(1.5)	05.92	1	A II .07(20)	20.52	1	[He I] .35(-)
20.21	00	P II .26(3)	07.20	0	....	4922.02	10	He I .93(-)
			09.21	00	....			

two stages of ionization contribute lines. A survey of the *O* II lines shows that, when the excitation potential is higher than about 28 volts, only the strongest lines appear. Although for some elements lines of excitation potential greater than 30 volts have been identified, it is not felt that much weight should be given to these identifications because the general level of excitation is considerably lower than this.

When the wave-length coincidences had been found, the identifications were checked by an attempt to establish full multiplets. For this work Part I of the "Revised Multiplet Table"[5] was invaluable. If a series of reasonably full multiplets with estimated stellar intensities closely paralleling the laboratory intensities could be established for an element, the proposed identification was retained; if not, it was rejected. Additional lines of *Ne* I were identified from the wave lengths given by Meggers and Humphreys[6] (interferometer measures) and by Paschen.[7] A number of unclassified *Fe* III lines were identified from an unpublished list very kindly loaned to the writer by Mrs. Sitterly. In this manner about 70 per cent of the 877 lines measured were identified.

Use of the *M.I.T. Tables*[8] suggested *Rb* II, *Kr* II, and *Th* III as sources of the unidentified lines; but the multiplet structure of these spectra could not be adequately established in γ Pegasi; hence all coincidences found were considered as random and were disregarded. The lack of knowledge of the third and fourth spectra of the metals *Ti*, *V*, *Cr*, *Mn*, and *Ni* in the photographic region is to be deplored, as it would probably lead to the identification of many faint lines.

On the average, less than one and one-half lines per angstrom were measured. Since the reality of each feature was checked by visual inspection of all the plates, it is felt that the number of spurious lines and of random coincidences is low. The reality of many of the weak unidentified lines is supported by the fact that Kühlborn,[3] in most cases, gives practically identical wave lengths and intensities.

The elements for whose spectra comprehensive lists of lines in the region λλ 3965–4935 could be found are summarized in Table 3. The first four columns are self-explanatory. The abundances in the earth are taken from Von Klüber.[9] In column 5 "Yes" means that the spectrum is definitely present in γ Pegasi, most of the possible multiplets being represented; a question mark (?) means that the identifications are not too good but that the spectrum is probably present; (??) mean that some coincidences have been found suggesting this spectrum but that it is probably not present; "No" means that it is not present. The figures in column 6 refer to notes at the end of the table.

In general, it seems that all elements with the proper ionization and excitation potential will be found if they have lines in the region under consideration and if their abundance in the earth is reasonably high. The only exception of note is potassium. This element is very abundant in the earth, and the *K* II spectrum has many strong lines of favorable wave length and excitation potential for appearance in the spectrum of γ Pegasi. However, not one line could be identified with certainty; in fact, there was nothing at all where most of the strong lines should be. This result is in agreement with that obtained by Struve,[2] but contrary to that of Kühlborn.[3]

II. A STUDY OF THE *He* I LINES

PERMITTED LINES

A review of the material in Table 2 shows small redward displacements for the lines of the diffuse and sharp series of *He* I and a violet displacement for λ 3965, which is the only member of the principal series observed. Similar displacements have been observed in τ Scorpii by Adams and Merrill[10] from measurements on coudé plates.

[6] *J. Research Nat. Bur. Standards*, **13**, 293, 1934.

[7] *Ann. d. Phys.*, **60**, 405, 1919.

[8] *M.I.T. Wavelength Tables* (New York: Technology Press, John Wiley & Sons, Inc., 1939).

[9] *Das Vorkommen der chemischen Elemente im Kosmos* (Leipzig: Johann Ambrosius Barth, 1931), p. 29.

[10] *Ap. J.*, **97**, 98, 1943.

The theory of Stark effect for constant electric fields has been developed by Foster[11] and investigated by him in the laboratory. According to theory and experiment, the *He* I lines are displaced, the amount and direction of the displacement depending on the field strength and the levels between which the line arises. In stellar atmospheres the electric field is caused by random encounters of the helium atoms with charged particles. Thus only qualitative agreement of stellar displacements with those predicted by con-

TABLE 3

SPECTRA IDENTIFIED IN γ PEGASI

Element (1)	Abundance in Earth (2)	Spectrum (3)	I.P. (Volts) (4)	Spectrum Found (5)	Remarks (6)	Element (1)	Abundance in Earth (2)	Spectrum (3)	I.P. (Volts) (4)	Spectrum Found (5)	Remarks (6)
H	8.8×10^{-3}	I	13.54	Yes		*Si*	2.6×10^{-4}	I	8.11	No	2
								II	16.27	Yes	
He	4.2×10^{-9}	I	24.48	Yes				III	33.32	Yes	
		II	54.17	No	1			IV	44.95	Yes	
Li	5.0×10^{-5}	I	5.37	No	2	*P*	1.2×10^{-3}	I	10.9	No	2
		II	75.31	No	1			II	19.57	?	8
								III	30.03	Yes	
Be	5.0×10^{-6}	I	9.28	No	2	*S*	4.8×10^{-4}	I	10.31	No	2
		II	18.13	No	3			II	23.3	Yes	
								III	34.9	Yes	
B	1.4×10^{-5}	I	8.26	No	2	*Cl*	1.9×10^{-3}	I	12.95	No	2
		II	25.02	??	4			II	23.70	Yes	
		III	37.77	??	5			III	39.69	?	8
C	8.7×10^{-4}	I	11.20	No	2	*A*	3.6×10^{-6}	I	15.69	No	2
		II	24.28	Yes				II	27.76	Yes	
		III	47.67	Yes				III	40.75	No	1
N	3.0×10^{-4}	I	14.49	No	2	*K*	2.4×10^{-2}	I	4.32	No	2
		II	29.49	Yes				II	31.7	No	9
		III	47.24	??	5						
O	1.9×10^{-1}	I	13.56	No	2	*Ca*	3.4×10^{-2}	I	6.09	No	2
		II	35.00	Yes				II	11.82	Yes	10
		III	54.71	??	5			III	51.00	??	11
F	2.4×10^{-4}	I	17.35	No	2	*Sc*	7.5×10^{-7}	I	6.7	No	2
		II	34.84	Yes				II	12.8	No	2
Ne	5.0×10^{-5}	I	21.47	Yes				III	24.61	??	3
		II	40.91	?	5						
Na	2.6×10^{-2}	I	5.12	No	2	*Fe*	4.7×10^{-2}	I	7.86	No	2
		II	47.10	?	6			II	16.16	No	2
								III	30.48	Yes	
Mg	1.9×10^{-2}	I	7.61	No	2	*Rb*	3.4×10^{-6}	I	4.16	No	2
		II	14.97	Yes				II	27.36	??	8, 3
Al	7.5×10^{-2}	I	5.96	No	2	*Kr*	2.0×10^{-10}	I	13.93	No	2
		II	18.75	?	7			II	26.4	??	8, 3
		III	28.33	Yes		*Th*	2.5×10^{-8}	III	29.5	??	8, 3

NOTES TO TABLE 3

1. The excitation potential is too high for this spectrum to appear.
2. The ionization potential is too low for this spectrum to appear.
3. The terrestrial abundance is low.
4. Only one line is possible, λ 4191.95, and it would be blended with *Fe* III.
5. A few coincidences were found, but the excitation potential is rather high.
6. Two out of three possible coincidences found, but the excitation potential is rather high.
7. A good many coincidences found, but the ionization potential is rather low.
8. Quite a few coincidences were found, but the multiplet structure could not be adequately established in the star.
9. The absence of this element cannot be attributed to unfavorable excitation potential or unfavorable wave length of the strong lines.
10. Only the H line is measured.
11. Only one line of rather high excitation potential occurs in the region under study, giving a poor coincidence with a stellar line.

[11] *Proc. R. Soc., London, A*, **117**, 137, 1927.

stant field-strength theory is to be expected. M. K. Krogdahl[12] gives theoretical results for the broadening and displacement of the *He* I lines in the case of a fluctuating field.

Data on the observed and theoretical displacements are given in Table 4. Column 3 gives the observed displacements $\lambda_{star} - \lambda_{lab}$ for γ Pegasi and column 4 those for τ Scorpii, measured by Adams and Merrill. For the triplet lines I have chosen a mean wave length, weighted according to the statistical weights of the two components. Adams and Merrill use the wave length of the strongest component alone. In order to compare results, Adams and Merrill's displacements have been adjusted to my system of wave lengths for the triplet lines. Column 5 gives the mean displacement calculated by Foster for a constant field of 10 kv/cm, the lowest field strength for which Foster calculates displacements. A field strength of 1–10 kv/cm is suggested[13,14] by the relative strengths of the

TABLE 4

DISPLACEMENTS OF *He* I LINES $\lambda_{STAR} - \lambda_{LAB}$

Transition	λ	Observed*		Theoretical	
		γ Peg	τ Sco	Foster 10 Kv/Cm	Krogdahl (For τ Sco)
(1)	(2)	(3)	(4)	(5)	(6)
2^3P-4^3D	4471	+0.05 A	−0.02 A	+0.22 A	+0.04 A
2^3P-5^3D	4026	+ .02	+ .00	+ .87	+ .12
2^1P-4^1D	4921	+ .09	.....	+ .42	+ .07
2^1P-5^1D	4388	+ .06	+ .04	+1.29	+ .28
2^1P-6^1D	4144	+ .10	+ .07	.....	.....
2^1P-7^1D	4009	+ .04	+ .05	.....	.....
2^3P-4^3S	4713	+ .03	− .02	+ .01	+ .005
2^3P-5^3S	4121	+ .04	− .02	+ .06	+ .011
2^1P-5^1S	4437	+ .07	+ .02	+ .04	.....
2^1P-6^1S	4169	+ .13	.....	.....	.....
2^1P-7^1S	4024	+ .05	.....	.....	.....
2^1S-4^1P	3965	−0.09	−0.02	−0.08	−0.017

* Weighted mean laboratory wave length used for the triplets. If the wave length of the strongest component is used, the displacements for λ 4471, λ 4026 should be increased by +0.03 A, that for λ 4713 by +0.06 A, and that for λ 4121 by +0.04 A.

forbidden lines. Column 6 gives the mean displacements calculated by M. K. Krogdahl[15] according to the fluctuating-field collisional theory for the lines in τ Scorpii.

Only the diffuse-series lines are displaced enough by low electric fields for a comparison of theory and observation to yield significant results. The data of Table 4 show that the displacements of the *He* I lines are small and not of the order of magnitude predicted and found experimentally for a constant field of 10 kv/cm. If we adopt the mean field in stars as 5 kv/cm,[13,14] interpolation from the graphs in Foster's paper[11] (Pls. 7–13) would suggest displacements only half those quoted in Table 4, but still there is no agreement with observation. The displacements calculated by M. K. Krogdahl for the diffuse-series lines seem more nearly in agreement with observation; however, the displacements observed for 2^3P-5^3D (λ 4026) and 2^1P-5^1D (λ 4388) are significantly less than the predicted values; for, since the lines are strong and sharp, the accidental error of measurement is less than ±0.01 A. The results from the triplet lines should be given low weight because of the uncertainty of what to use for the "laboratory wave length." The smallness of

[12] *Ap. J.*, **100**, 333, 1944; **102**, 64, 1945; **105**, 327, 1947.

[13] Struve, *Ap. J.*, **70**, 90, 1929.

[14] Goldberg, *Ap. J.*, **89**, 623, 1939.

[15] *Ap. J.*, **105**, 327, 1947.

the observed displacements of λ 4026 and λ 4388 may be partly due to the blending effect of the forbidden lines which occur to the violet. For the principal and sharp series lines the smallness of the predicted and observed displacements makes it difficult to decide whether the agreement between theory and observation is significant or merely fortuitous. One possible additional factor not included in either theory of the displacements is the effect of stratification, particularly for the diffuse-series lines. Since these lines are very strong, the cores are formed at the top of the atmosphere in regions of low density, whereas the forbidden lines are formed and the shifts occur at lower, more dense levels. Since the cores of the *He* I lines are measured, the observed shifts might be expected to be less than those predicted. This effect would not be so important for the principal and sharp series lines, since they are fairly weak.

FORBIDDEN LINES

The probability of the occurrence of a forbidden transition ($\Delta l = 0, 2, 3$) depends upon the strength of the electric field. Foster[11] has calculated the intensities of the forbidden components for various field strengths for some lines. Table 5, derived from the

TABLE 5

THEORETICAL RELATIVE STRENGTHS OF *He* I LINES

Transition	Triplets			Singlets		
(1)	λ (2)	10 Kv/Cm (3)	40 Kv/Cm (4)	λ (5)	10 Kv/Cm (6)	40 Kv/Cm (7)
2P–4D	4471.5	10	10	4921.9	10	10
2P–4F	4469.9	1.4	6	4920.4	2	4
2P–4P	4517.4	00	0	4910.7	0	1.6
2P–5D	4026.2	10	10	4387.9	10	10
2P–5F	4025.5	7	14	4387.6	6	4
2P–5G	4025.4	4	12	4387.3	2.4	1
2P–5P	4045.2	0	2	4383.2	1.5	7.5

results of his calculations at fields of 10 and 40 kv/cm, gives a guide to the expected relative strengths of the forbidden lines in main-sequence B stars. The strengths of the forbidden lines are expressed in terms of that of the permitted line, which has been arbitrarily put equal to 10. Since, theoretically, the sum of the strengths of all the component lines must be constant, the strength of the permitted line decreases as the field increases, to allow for the increasing strengths of the forbidden lines. In stars, however, owing to the saturation of the permitted lines, the strengths of the permitted lines will probably remain more or less the same with increasing field, whereas the forbidden lines will increase in strength in the manner indicated in Table 5. In comparing forbidden lines with permitted lines, it should be remembered that a forbidden line is intrinsically deeper than a permitted line;[16] hence the same apparent strength can be obtained with fewer active atoms. Qualitative agreement with the intensities in Table 5 (cols. 3 and 6) is expected.

Although fields of less than 10 kv/cm are expected in stars, the inclusion of the values for fields of 40 kv/cm in Table 5 brings out some interesting points. Because of the weakness of the 2^3P-m^3P transitions it seems unlikely that these lines will occur in stellar

[16] *Ap. J.*, **104**, 327, 1946.

spectra. The 2^1P-m^1P lines have greater relative strength and might possibly be seen. Secondly, the 2^3P-m^3F and 2^3P-m^3G lines appear to be much more sensitive to field strength than are the corresponding singlet lines. If this effect were pronounced enough, it could introduce a luminosity effect between intermediate and dwarf B-type stars. Since the dwarf stars have denser atmospheres, the average electric field will be greater, thus the observed line at λ 4026, which is a blend on most dispersions of 2^3P-5^3D, 2^3P-5^3F, and 2^3P-5^3G, will be strengthened, whereas the line λ 4388, which is a blend of 2^1P-5^1D, 2^1P-5^1F, and 2^1P-5^1G, will remain much the same as in a star of intermediate luminosity.

Since the forbidden lines are rather weak and diffuse, a comparison of the observed displacements with those calculated by Foster or by M. K. Krogdahl is not very significant. The relatively strong forbidden lines 2^3P-4^3F λ 4469.92; 2^3P-5^3F, 2^3P-5^3G λ 4025.49, λ 4025.40; 2^1P-4^1F λ 4920.35; 2^1P-5^1F, 2^1P-5^1G λ 4387.59, λ 4387.30, have been measured near their theoretical zero-field positions. Weak lines have been found close to the zero-field positions of 2^1P-6^1F λ 4143.44, 2^1P-4^1P λ 4910.75, 2^1P-5^1P λ 4383.24, 2^1P-6^1P λ 4141.34, 2^1P-7^1P λ 4007.81. A search was made for the lines 2^3P-4^3P λ 4517.43 and 2^3P-5^3P λ 4045.16. There is a faint line at λ 4517.45; but, in view of the intensity relations in Table 5, it seems unlikely that this line is [*He* I]. No line attributable to [*He* I] could be found at λ 4045.16.

The luminosity effect predicted in λ 4026 is indicated by equivalent widths derived from high-dispersion plates. Measurements of good internal consistency are provided by my measurements[17] of the equivalent widths of *He* I lines from high-dispersion plates taken at the Dominion Astrophysical Observatory, and by Unsöld's[18] measurements in the spectrum of τ Scorpii. The latter used coudé plates taken at the McDonald Observatory. Comparison of the strength of λ 4026 to that of the other *He* I lines for η Ursae Majoris and τ Scorpii, which are in luminosity class V (dwarfs) on the system of the Yerkes spectral atlas,[1] shows that λ 4026 is significantly stronger than any other *He* I line in the spectrum. In the intermediate stars, γ Pegasi and ι Herculis, class IV, λ 4026 is about the same strength as λ 4471. It does not seem possible to explain the increased relative strength of λ 4026 in the dwarf stars by blends with lines of other elements. An exact explanation of the strengths of the helium lines in dwarf and giant stars requires the solution of the problem of radiative transfer complicated by Stark effect. In the case of λ 4026 the blending of the near-by forbidden lines will likely contribute to the observed line strength; and, since these lines are quite sensitive to field strength, it is possible that they may be significant in producing the final observed equivalent width. It is doubtful whether the luminosity effect mentioned here is pronounced enough to be useful on low-dispersion plates.

I am indebted to Dr. Otto Struve for suggesting this problem and for his constant advice on the problems involved in the study of a B star; and to Dr. W. A. Hiltner, who very kindly loaned the excellent plates of γ Pegasi used. My special thanks are due to Dr. J. L. Greenstein, whose criticism and advice have been invaluable. Dr. W. S. Adams very kindly lent me some coudé spectrograms of γ Pegasi in the λ 4900 region taken by H. W. Babcock at the Mount Wilson Observatory.

[17] *J.R.A.S. Canada*, **38**, 385, 1944.

[18] *Zs. f. Ap.*, **21**, 22, 1941.

THE INTENSITIES AND PROFILES OF LINES IN SOME B-TYPE STARS*

ANNE B. UNDERHILL†
Yerkes and McDonald Observatories
Received February 24, 1948

ABSTRACT

The equivalent widths and central absorptions of $H\gamma$, $H\delta$, the *He* I lines λλ 4471, 4026, 4388, 4144, 4009; the *Mg* II line λ 4481; the *Si* II lines λ 4128, λ 4130; and the *Si* III lines λλ 4552, 4568, 4574 have been found from McDonald coudé plates for the B-type supergiants ρ Leo, χ^2 Ori, o^2 CMa, χ Aur, η CMa, and β Ori, and for the less luminous stars ε CMa, γ Peg, τ Her, and ζ Dra. The central absorptions are corrected for instrumental distortion. Profiles of $H\gamma$ are given for all the stars studied. Profiles of the other lines are given only for o^2 CMa, ε CMa, and γ Peg.

The interpretation of the hydrogen-line profiles is discussed, and model atmospheres with $\theta_0 = 0.30$ and $\log g = 2.00$ and 4.09 are calculated. The line intensities predicted from these models are compared with the observed intensities in o^2 CMa, and γ Peg; and it is shown how such models can be used to derive relative abundances of the elements and the shape of the line-absorption coefficient. The line-absorption coefficient is found to have a Doppler half-width $\Delta\lambda_D$ of 37 ± 2 km/sec in the supergiant o^2 CMa, and 27 ± 2 km/sec in the giant ε CMa.

The strength and shape of the absorption lines in a stellar spectrum reflect the physical properties of the stellar atmosphere. For this reason line profiles are an additional important source of information about conditions in the stellar atmosphere. The purpose of this investigation is to obtain profiles of some of the strongest lines in B-type stars and to show how they may be interpreted. The profile of a stellar absorption line obtained from a microphotometer tracing of the spectrum is distorted by the spectrograph. However, it turns out that for lines which are broad compared to the instrumental profile the correction to the measured central absorption is small; hence the true central absorption of the line can be determined quite accurately with only a relatively crude method of correction. Inspection of high-dispersion coudé plates of B-type stars shows that most of the strong lines are broad; thus the instrumental correction will be small for these lines, and the profiles obtained will be very similar to the true profiles.

1. *Procedure.*—Table 1 lists the stars studied and the plates used. The spectral type and luminosity class are according to unpublished work of W. W. Morgan. The star ζ Dra is peculiar in some respects,[1] and at present there is no luminosity classification for it, other than the statement that it is not a high-luminosity star. The estimated rotation classes ("Rot.") for the stars are according to Struve.[2] An effort has been made to select only stars with zero or low rotation, though the list of objects studied has been influenced by the coudé plates available. The range of spectral type from B8 to B1 is well covered in the supergiants and more sketchily for the stars of lower luminosity. The serial numbers of the plates used are tabulated with a symbol indicating the type of calibration used: "T" means the tube sensitometer of the McDonald Observatory, "W" means a linear wedge calibration. I am indebted to Dr. Jesse L. Greenstein for the use of Cd96, 126, 134, 255, 263, 680, 684, 689, 690, 691, 719, 720, 721; and to Dr. W. A. Hiltner for Cd461, 481, 555. The remaining plates I took myself at the McDonald Observatory.

* *Contributions from the McDonald Observatory, University of Texas*, No. 149.

† This work was completed during tenure of a scholarship from the Canadian Federation of University Women.

[1] Morgan, Keenan, and Kellman, *An Atlas of Stellar Spectra* (Chicago: University of Chicago Press, 1943), p. 12.

[2] *Ap. J.*, **74**, 225, 1931.

The lines chosen are those which are strong over the whole spectral range studied and which appear in the limited wave-length range of the available plates. They are, for hydrogen, $H\gamma$ and $H\delta$; for *He* I the triplet diffuse-series lines λ 4471, λ 4026, and the singlet diffuse-series lines λλ 4388, 4144, 4009; for *Mg* II λ 4481; for *Si* II λ 4130, λ 4128; and for *Si* III λλ 4574, 4568, 4552. The *Si* II lines and *Si* III lines appear equally strong at about B3; for later types, only *Si* II is measured and for earlier types only *Si* III.

All the plates were taken with the coudé spectrograph of the McDonald Observatory on Eastman 103*a*-O emulsion and were calibrated according to the system in use when they were obtained. The McDonald coudé spectrograph and the wedge-slit method of calibration are described by Hiltner and Williams.[3] The dispersion is about 3.2 A/mm at $H\gamma$. From plates on which two methods of calibration were used it was found that the same calibration-curve is obtained with the tube sensitometer as with the wedge slit, though the latter method of calibration is to be preferred. From the wedge-slit calibration it can be shown that over the wave-length range used, λλ 4000–4600, the

TABLE 1

STARS STUDIED

Star	Type	Rot.	Plates Used
ρ Leo	B1 Ib	3	Cd255(T), 263(T)
χ^2 Ori	B2 Ia	1	Cd680(T,W), 734(W), 738(W)
σ^2 CMa	B3 Ia	1	Cd691(T,W), 728(W)
χ Aur	B3 Ib	0	Cd684(T,W)
η CMa	B5 Ia	.....	Cd96(T), 126(T), 134(T), 719(T,W), 720(T,W), 730(W)
β Ori	B8 Ia	0	Cd481(W), 721(T,W)
ε CMa	B2 II	1	Cd689(T,W), 690(T,W), 729(W)
γ Peg	B2.5 IV	0	Cd461(W), 555(W)
τ Her	B5 IV	0	Cd733(W), 740(W)
ζ Dra	B8 ...	0	Cd737(W)

calibration-curve is essentially the same for all wave lengths. Only plates of good density for photometric work were used, so that the densities fell on the linear part of the calibration-curve except in a few cases for the cores of the strongest lines. Since the transmission of the coudé spectrograph for light of wave length less than 4100 A decreases rapidly, a number of plates which were of usable density at λ 4300 were too thin for the accurate determination of the profiles of $H\delta$, λ 4026 and λ 4009. The measures given for these lines are only from plates of good density in these regions. The Yerkes microphotometer was used with both amplifying systems, the new circuit[4] being used for thin plates.

Some of the microphotometer tracings were reduced to intensities by means of the semi-automatic recording intensitometer of the Dominion Astrophysical Observatory, Victoria, B.C. I am grateful to Dr. J. A. Pearce for the privilege of using this instrument, thus speeding the tedious job of reducing all the microphotometer tracings to intensities point by point. No systematic differences were found between the profiles derived from the intensitometer tracings and those obtained in the conventional manner.

To correct for the instrumental broadening, the following integral equation must be solved:

$$f(x) = \int_{-\infty}^{+\infty} f'(x-y)\, g(y)\, dy\,, \tag{1}$$

[3] *Photometric Atlas of Stellar Spectra* (Ann Arbor: University of Michigan Press, 1946), Book I.

[4] *Pub. A.S.P.*, **58**, 373, 1946.

where $f(x)$ is the measured intensity distribution in a spectral line, $g(y)$ is the true intensity distribution in the line, and $f'(x - y)$ is the instrumental profile. The problem is to obtain $g(y)$, knowing $f(x)$ and $f'(x - y)$. Van de Hulst and Reesinck[5] discuss this problem and give a method of solution, using Voigt functions. The present semi-empirical method, which is based on the well-known half-breadth method, was worked out before the more elegant method of van de Hulst and Reesinck came to the notice of the writer. Tests of the two methods show that they yield similar results. For the lines under discussion the simpler method used is sufficiently accurate.

If we can assume that

$$g(y) = A_c e^{-(y/a)^2}, \tag{2}$$

where A_c is the true central absorption of the line and a is the half half-width of the line, and if we assume that the instrumental profile is given by

$$f'(x-y) = \frac{1}{b\sqrt{\pi}} e^{-(x-y)^2/b^2}, \tag{3}$$

where b is the half half-width of the instrumental profile, we find from equation (1) that

$$\frac{1}{A_c^2} = \frac{1}{A_m^2} - \frac{\pi b}{W}. \tag{4}$$

Here A_m is $f(0)$, the measured central absorption of the line, and W is the equivalent width of the line. We have

$$W = \sqrt{\pi}\, a A_c. \tag{5}$$

From equation (4) we see that, if we know b, we can obtain the true central absorption of a line from measurement of its apparent central absorption and its equivalent width. For strong lines, $W \gg b$, the correction is negligible. Since the moderately strong lines in B-type stars are closely Gaussian in apparent form (as can be seen from the profiles of Figure 4 by plotting $\log A/A_c$ against Δx^2, where Δx is the distance from the center of the line), the assumption expressed in equation (2) is valid. If we can find a b such that equation (3) represents the instrumental profile reasonably well, equation (4) can be used to obtain corrected central absorptions of the lines. This correction will be small so long as $1/A_m^2$ is large with respect to the term containing W. For the lines in B-type stars this is nearly always the case on coudé dispersion. Since the correction is small, it does not have to be critically determined, and the relatively crude method outlined is sufficient.

The half half-width, b, of the instrumental profile was determined empirically in the following manner. Microphotometer tracings were made of several sharp lines in the iron-arc comparison spectrum on the spectrogram, and a mean profile was derived. This was called the "instrumental profile" and is identical with that given by Hiltner and Williams.[3] Actually, the iron-arc lines used are not infinitely sharp, but they are sufficiently so for our purpose. The instrumental profile has somewhat broader wings than a Gaussian profile with the same half-width and central intensity would have. To find a half half-width that would reproduce the effect of this profile, equation (1) was solved graphically for $f(0)$, which is A_m, when an arbitrary $g(y) = A_c e^{-(y/a)^2}$ was used with the observed instrumental profile $f'(x - y)$. Then equation (1) was solved with the same $g(y)$ but with $f'(x - y)$ given by equation (3) and the constant b was adjusted until the same $f(0)$ was obtained. The constant b thus determined is the effective half half-width of the instrumental profile. The arbitrary constants A_c and a in the expression for $g(y)$ were given a series of values such that line profiles typical of B stars resulted. The effec-

[5] *Ap. J.*, **106**, 121, 1947.

TABLE 2

EQUIVALENT WIDTHS AND CENTRAL ABSORPTIONS

STAR	WT.	W	A_m	A_c	WT.	W	A_m	A_c	WT.	W	A_m	A_c
	$H\gamma$				$H\delta$				*He* I λ 4471			
ρ Leo	2	2.276	50	50	1	1.543	46	46	2	0.953	43	43
χ^2 Ori	2.5	1.601	51	51	1	1.148	40	40	2.5	0.905	46	47
o^2 CMa	1.5	1.818	53	54	1	1.351	44	44	1.5	0.906	50	51
χ Aur	1	1.458	42	42	.....	.....	.....	.....	1	0.560	34	35
η CMa	4	1.597	49	49	3	1.606	53	54	3	0.781	50	51
β Ori	2	1.526	52	53	2	1.767	61	61	2	0.395	34	35
ϵ CMa	3	2.546	54	54	3	2.290	49	49	3	0.941	50	51
γ Peg	2	4.002	62	62	2	5.113	62	62	2	1.222*	57	58
τ Her	2	7.520	70	70	.....	.....	.....	.....	2	1.014†	46	46
ζ Dra	1	8.623	77	77	1	9.315	86	86	1	0.671‡	32	32
	He I λ 4026				*He* I λ 4388				*He* I λ 4144			
ρ Leo	1	0.704	38	39	2	0.398	26	26	2	0.364	24	24
χ^2 Ori	.....	.....	.....	.....	2.5	.607	37	37	2.5	.307	23	24
o^2 CMa	1	0.597	50	50	1.5	.494	33	34	1.5	.376	30	30
χ Aur	.....	.....	.....	.....	1	.437	31	32	1	.275	23	23
η CMa	4	0.547	42	42	3	.439	32	32	4	.346	29	30
β Ori	1	0.397	32	32	2	.249	22	23	2	.153	19	20
ϵ CMa	3	0.884	45	45	3	.605	39	39	3	.447	32	32
γ Peg	1	1.311§	54	54	2	.767	50	50	2	.658	44	44
τ Her	.....	.....	.....	.....	1	.428	24	24	2	.412	23	23
ζ Dra	1	0.760	43	43	1	0.295	18	18	1	0.210	19	19
	He I λ 4009				*Si* II λ 4130				*Si* II λ 4128			
ρ Leo	1	0.262	18	18	.....	.....	.....	.....	.....	.....	.....	.....
χ^2 Ori	.....	.....	.....	.....	.....	.....	.....	.....	.....	.....	.....	.....
o^2 CMa	.....	.....	.....	.....	1.5	0.196	16	16	1.5	0.174	16	16
χ Aur	.....	.....	.....	.....	1	.143	15	15	1	.164	16	16
η CMa	4	.264	24	24	4	.237	23	24	4	.238	25	26
β Ori	1	.165	16	16	2	.252	27	28	2	.253	27	27
ϵ CMa	3	.405	27	27	1	.076	13	14	1	.056	9	10
γ Peg	1	.640	32	32	2	.030	13	20	2	.031	14	22
τ Her	.....	.....	.....	.....	2	.211	24	24	2	.166	19	20
ζ Dra	1	0.221	13	13	1	0.249	24	24	1	0.225	25	25
	Si III λ 4574				*Si* III λ 4568				*Si* III λ 4552			
ρ Leo	2	0.310	22	22	1	0.461	29	30	2	0.594	35	36
χ^2 Ori	2.5	.231	19	20	2.5	.396	29	29	2.5	.522	34	34
o^2 CMa	1	.176	12	13	1.5	.256	19	19	1.5	.300	22	23
χ Aur	1	.075	9	10	1	.136	13	14	1	.159	15	16
η CMa	2	.099	10	10	2	.156	14	15	2	.198	18	19
β Ori	.....	.....	.....	.....	.....	.....	.....	.....	.....	.....	.....	.....
ϵ CMa	2	.254	26	27	3	.346	36	38	3	.418	41	43
γ Peg	2	0.088	23	.....	2	0.112	32	.....	1	0.162	38	.....
τ Her	.....	.....	.....	.....	.....	.....	.....	.....	.....	.....	.....	.....
ζ Dra	.....	.....	.....	.....	.....	.....	.....	.....	.....	.....	.....	.....

* The equivalent width of λ 4471 only is 0.911 A; of λ 4470 it is 0.311 A.

† The equivalent width of λ4471 only is 0.776A; of λ4470 it is 0.238A.

‡ The equivalent width of λ 4471 only is 0.486 A; of λ 4470 it is 0.185 A.

§ The equivalent width of λ 4026 + [*He* I] only is 0.947 A.

TABLE 2—*Continued*

Star	Wt.	W	A_m	A_c	Star	Wt.	W	A_m	A_c
	Mg II λ 4481					*Mg* II λ 4481			
ρ Leo	2	0.252	15	15	β Ori	2	0.490	43	45
χ^2 Ori	2.5	.241	19	19	ε CMa	3	.223	26	27
o^2 CMa	1.5	.415	32	33	γ Peg	2	.172	38	.....
χ Aur	1	.370	26	27	τ Her	2	.370	38	39
η CMa	4	0.511	39	40	ζ Dra	1	0.428	38	39

tive b is that value which gave the best representation of the blurring effects of the true instrumental profile on all these lines. As a final check, arbitrary wings such as might occur for strong lines were drawn on $g(y)$, and the integration of equation (1) was performed graphically for $f(0)$ when the actual $f'(x - y)$ was used and when a Gaussian $f'(x - y)$ with the half half-width determined above was used. These two integrals agreed satisfactorily.

With the half half-width, b, thus determined, a family of curves giving A_c as a function of W was plotted from equation (4), for a series of values of A_m. The observed A_m's were corrected to A_c's by interpolation in this graph. To avoid the difficulties of the changing dispersion, it is convenient to express b and W as millimeters on the tracing. An example of the order of magnitude of the instrumental correction may be of interest. For tracings magnified thirty times from the plate, $b = 1.26$ mm. A typical weak line is λ 4128 in ε CMa on Cd729. For this line $W = 0.72$ mm; $A_m = 9$ per cent. From the graph we estimate $A_c = 10$ per cent. From equation (4), $A_c = 9.2$ per cent. The correction is smaller than the probable error of measurement. Only the *Mg* II line and the *Si* III lines in γ Peg are so narrow and sharp that the corrections are very large and uncertain. For these lines the correction obtained is very sensitive to the shape of the apparent profile. Since the apparent profile cannot be determined accurately enough, the central absorptions of these lines are not corrected. The central absorptions of all the other lines have been corrected by the graphical method described.

2. *Observed line intensities and central absorptions.*—The measured equivalent widths and central absorptions are given in Table 2. Weights are assigned according to the number of plates used in the determination. A few of the plates which are weak or streaked by poor guiding are given half-weight. The mean equivalent width, W, is given in equivalent angstroms; the mean measured central absorption, A_m, and the mean corrected central absorption, A_c, are given in percentages of the continuum. The average percentage deviation of any single measured W from the mean W for the line is ± 9.2 per cent of the mean W. The average deviation of any single central absorption from the mean measured central absorption for the line is ± 1.8 per cent of the continuum. The rather large average error in a single measurement of equivalent width reflects the graininess of the plates. It is advisable to use finer-grained plates than 103*a*-O if the brightness of the object and the speed of the spectrograph will permit. The average error in a measurement of central absorption is small and is of the order of the correction for instrumental profile. It is mostly caused by uncertainty in placing the continuum. Since the lines have relatively wide wings for their depths, this uncertainty in placing the continuum is sufficient to account for most of the uncertainty in the equivalent widths, as much of the equivalent width arises in the wings.

The equivalent widths of Table 2 may be compared with those of E. G. Williams.[6]

[6] *Ap. J.*, **83**, 279, 1936.

We have 59 lines in common. The mean value of the ratio $(ABU - EGW)/ABU$ is -13.1 ± 2.9 per cent. Thus the present measures are a little smaller, on the average, than those of E. G. Williams. This is not surprising, as on microphotometer tracings of high-dispersion spectra one is inclined to draw the continuum low and thus cut off part of the extensive wings of the lines. This is particularly true when, as in the present case, only short regions of the plate around the lines of interest are run through the microphotometer. The comparisons given in the accompanying table are of interest. The mean value of the ratio $(ABU - x)/ABU$ with its probable error is tabulated, where x denotes the work to which comparison is being made. The equivalent widths of Table 2 are referred to as "*ABU*."

Lines	No. of Measures in Common	x	$(ABU-x)/ABU$
Hydrogen	10	E. G. Williams*	+ 1.1±5.2 per cent
Hydrogen	12	S. Günther†	− 6.5±5.3
He I	23	E. G. Williams*	−22.4±3.9
He I	10	A. B. Underhill‡	+ 9.2±4.4
Mg II, *Si* II, and *Si* III	26	E. G. Williams*	−10.2±6.6

* *Ap. J.*, **83**, 279, 1936.
† *Zs. f. Ap.*, **7**, 106, 1933. ‡ *J.R.A.S. Canada*, **38**, 385, 1944.

The rather large negative difference, −22.4 per cent, between the equivalent widths of the *He* I lines given in this paper and those given by E. G. Williams is partly due to his inability to resolve the blends at λ 4026 and λ 4144 on his dispersion. The effect of these blends is discussed in my earlier paper[7] on the *He* I lines. It would seem that the equivalent widths obtained from McDonald coudé plates are substantially in systematic agreement with measures of equivalent widths obtained elsewhere.

The equivalent widths given for λ 4471 in Table 2 for the main-sequence stars include the forbidden line λ 4470. On the profiles it is possible to estimate where the violet wing of λ 4471 might lie. If this is done, subtraction gives the equivalent width due to λ 4470. The equivalent widths obtained in this way are given in notes to Table 2. The mean measured central absorptions for λ 4470 are 24 in γ Peg, 17 in τ Her, and 11 in ζ Dra. The equivalent width of the whole feature at λ 4026 is given in Table 2 for the main-sequence stars. In γ Peg it is possible to separate on the profile the combined feature λ 4026 + the forbidden *He* I lines from λ 4024 of *He* I and the *Fe* III line at λ 4025. The equivalent width of λ 4026 + [*He* I] is given in a note to Table 2. In the supergiants λ 4024 and λ 4026 of *He* I can be seen clearly separated. There is a number of *O* II and *S* II lines in the wings of λ 4144. On coudé spectra one can resolve these features; hence the equivalent widths given in Table 2 for λ 4144 are for the *He* I line only, as the blending lines have been separated out.

The one plate for χ Aur, Cd684, is well exposed and should yield reliable equivalent widths and line profiles. In forming the mean values for η CMa, the plates Cd126 and Cd134 are not used, since on these plates some of the lines appear double and all the lines are shallower than usual. These plates were taken by Greenstein in February, 1941; and none of the plates taken at scattered intervals since that date have shown this phenomenon again. Although Cd126 and Cd134 are not very dense, it seems improbable that the observed line-shape changes are due to photographic effects. These two plates give a radial velocity near that obtained from the rest of the plates. At present there are insufficient data to discuss possible variations in the spectrum of η CMa further.

[7] *J.R.A.S. Canada*, **38**, 385, 1944.

The one plate for ζ Dra, Cd737, is of good density and should yield quite reliable measures.

i) *Hydrogen lines.*—The data in Table 2 show that the depths of the hydrogen lines in all the supergiants studied are around 50 per cent, whereas in the dwarf stars the central absorptions are deeper and increase from 62 per cent at B2.5 to about 80 per cent at B8. Typical profiles of $H\gamma$ for the supergiant stars are shown in Figure 1, and for the other stars in Figure 2. The difference in shape caused by Stark broadening in the stars of lower luminosity is obvious. Comparison of $H\gamma$ in ϵ CMa with $H\gamma$ in the supergiants shows that a luminosity class II star has hydrogen-line profiles quite different from those of the supergiants, the Stark wings already being prominent. The difference between luminosity classes I*a* and II is large. The stars ϵ CMa, γ Peg, and τ Her give profiles that are very much the same from plate to plate and, on the whole, symmetrical. However, the profiles of the hydrogen lines in the supergiants seem to change from plate to plate and tend to show small asymmetries which also change from time to time. For this reason a profile from one plate only is given for the supergiants, whereas a mean profile

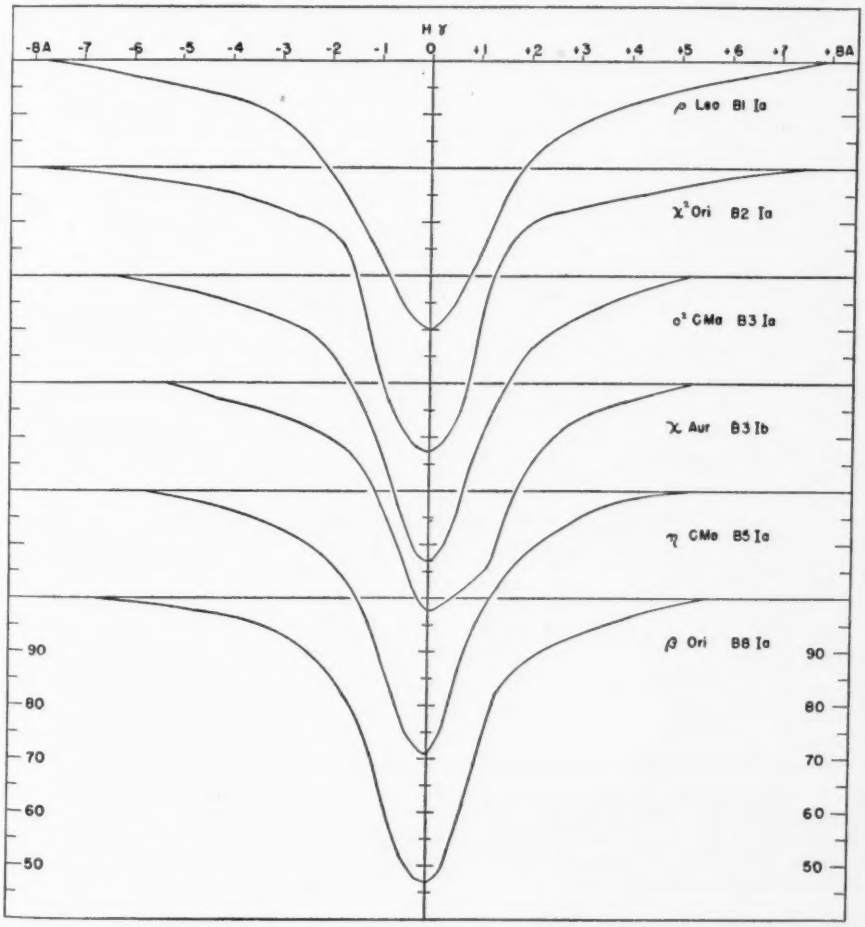

FIG. 1.—$H\gamma$ in the supergiants. The scale for residual intensity is given only for β Ori. Each profile is displaced 20 per cent below the preceding one. The residual intensity is in percentages of the continuum.

is drawn for the other stars. The slight variability and asymmetry of $H\gamma$ in χ^2 Ori and β Ori may be related to the fact that $H\alpha$ is in emission in these stars; and χ Aur has been reported to be a spectroscopic binary by R. K. Young,[8] which may account for the peculiar shape observed for $H\gamma$. There is no defect apparent on the plate or the microphotometer tracing that can account for the observed shape of the line. In χ Aur all the lines are weaker than in the comparable stars, o^2 CMa and ϵ CMa. It is possible that the observed weakening is due to the overlying spectrum of the companion.

ii) *Helium lines.*—The *He* I lines have been thoroughly discussed by many investigators.[9] The present observations are in accord with their results. The data of Table 2

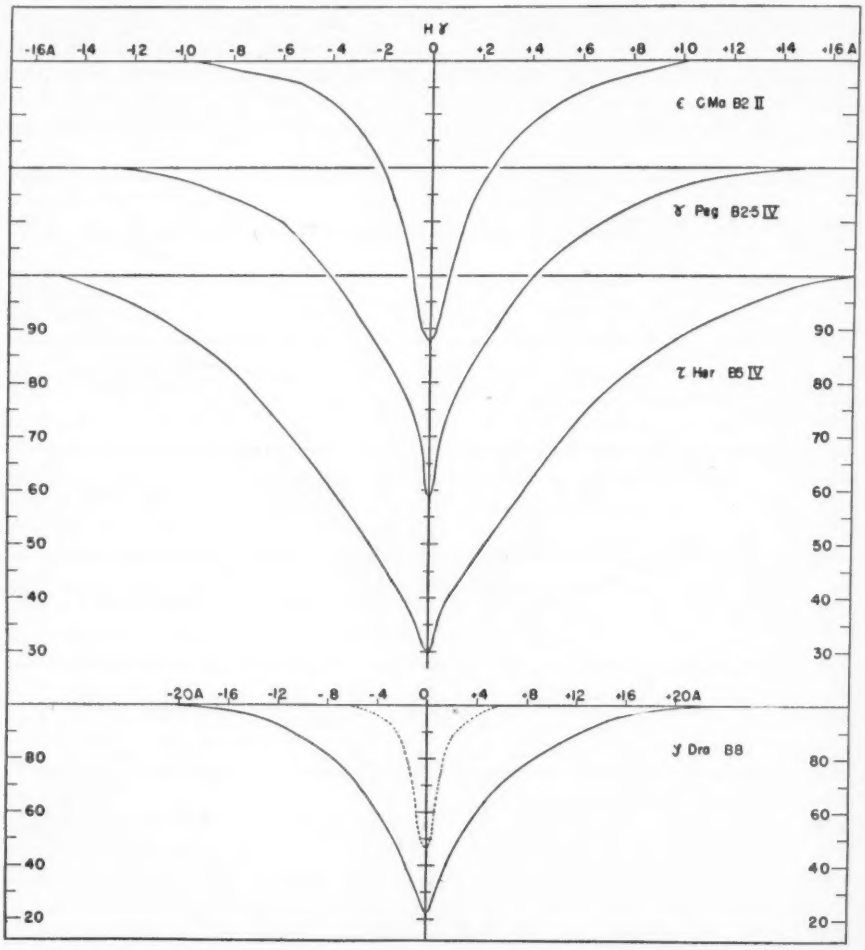

FIG. 2.—$H\gamma$ for ϵ CMa, γ Peg, τ Her, and ζ Dra. For ϵ CMa, γ Peg, and τ Her the wave-length scale is half its value in Fig. 1. For ζ Dra the wave-length scale has been reduced by a factor 4 from Fig. 1. The profiles for ϵ CMa, γ Peg, and τ Her are each displaced vertically by 20 per cent. The profile for β Ori, B8 I*a*, is dotted in for comparison with $H\gamma$ in the main-sequence star ζ Dra. The residual intensity is in percentages of the continuum.

[8] *Pub. Dom. Obs., Ottawa*, **4**, 1, 1920.

[9] See, e.g., O. Struve, *Ap. J.*, **74**, 225, 1931; E. G. Williams, *Ap. J.*, **83**, 305, 1936; P. Rudnick, *Ap. J.*, **83**, 439, 1936; and A. B. Underhill, *J.R.A.S. Canada*, **38**, 385, 1945.

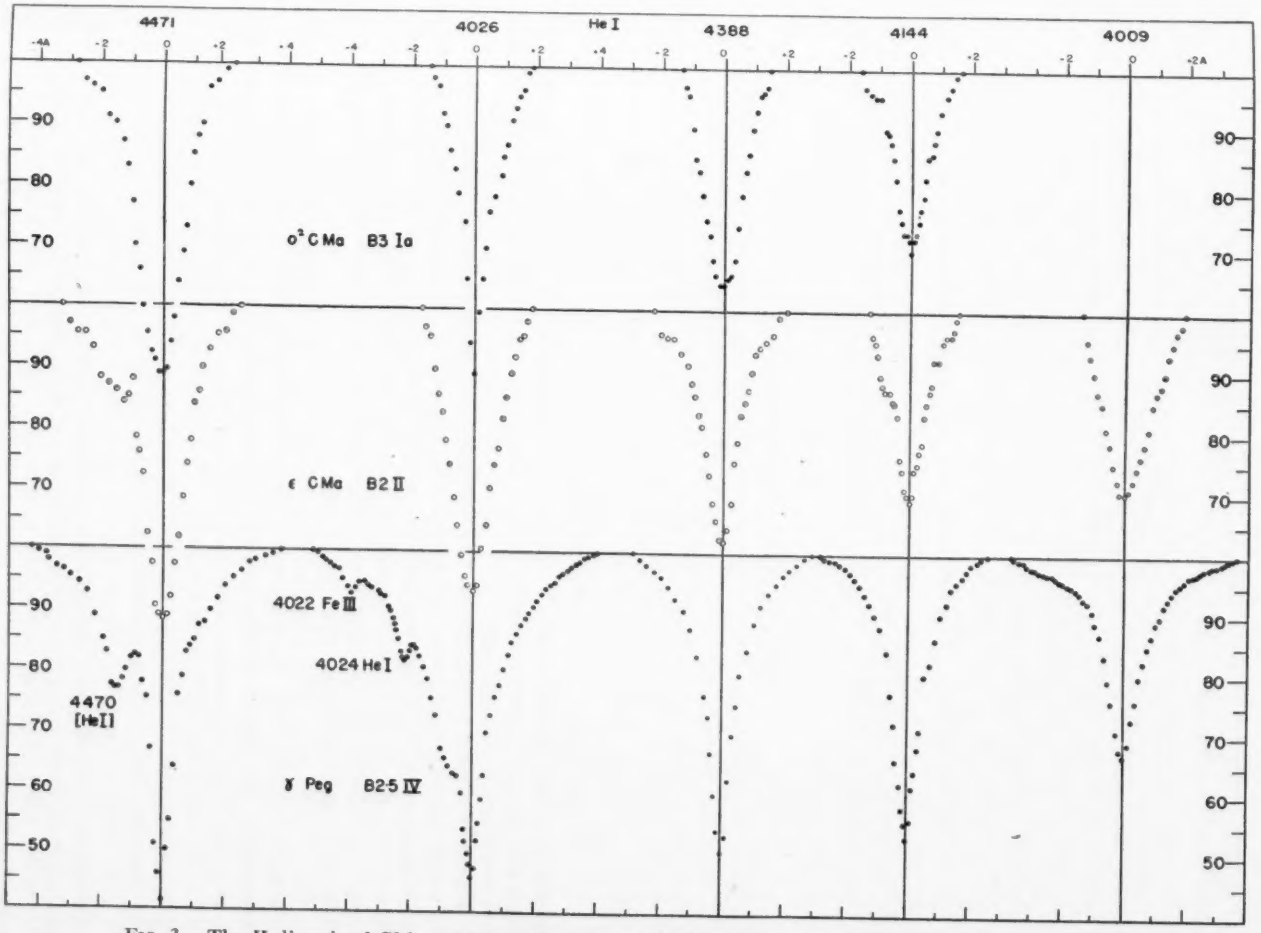

FIG. 3.—The *He* lines in o^2 CMa, ϵ CMa, γ Peg. The residual intensity is in percentages of the continuum

indicate the increase in equivalent width of the *He* I lines due to Stark effect as one goes from supergiants to main-sequence stars. The well-known maximum of the *He* I lines at about type B2 is better indicated in the main-sequence stars than in the supergiants. The observations indicate that at B2 the *He* I lines are deeper in the main-sequence stars than in the supergiants, whereas at B5 and B8 the *He* I lines are deepest in the supergiants. A decrease in central absorption with increasing serial number is indicated for the singlet lines. Since only two triplet lines are observed, a similar trend cannot be confirmed for the triplets. Figure 3 shows the profiles observed for the *He* I lines in o^2 CMa, ϵ CMa, and γ Peg. The development of the Stark wings as the luminosity of the star decreases is clearly indicated. The strong forbidden lines of *He* I are marked on the diagrams for γ Peg. The profiles for o^2 CMa are from Cd727, for ϵ CMa from Cd729, and for γ Peg from Cd461. This cross-section of line shapes at about type B2.5 is typical of the cross-sections at later types.

iii) *The Mg II line and the Si II and Si III lines.*—The data of Table 2 confirm and extend the observations of these lines made on lower-dispersion plates by other investigators.[9] At spectral types B2 and B5 the *Mg* II line λ 4481 is stronger in luminosity class I*a* than in class IV. At B8 there is little luminosity effect. The line strengthens generally

TABLE 3

RELATIVE INTENSITIES OF THE *Si* III LINES

Line	ρ Leo	χ^2 Ori	o^2 CMa	χ Aur	η CMa	ϵ CMa	γ Peg
λ 4552	1.92	2.26	1.70	2.12	2.00	1.64	1.84
λ 4568	1.49	1.71	1.49	1.81	1.58	1.36	1.27
λ 4574	1.00	1.00	1.00	1.00	1.00	1 00	1.00

toward class B8. At B2, λ 4481 is shallower in luminosity class I*a* than in class IV. At B5, λ 4481 is about the same depth in class I*a* and IV. At B8 it is deeper in class I*a* than it is in the main-sequence star.

The *Si* II lines λ 4128 and λ 4130 show a general strengthening from spectral type B2 to B8. The data of Table 2 indicate for all spectral types studied that the depths of the lines are about the same in supergiant and in main-sequence stars. The *Si* II and particularly the *Si* III lines vary sharply with spectral type; thus, in estimating differences of behavior due to luminosity differences, care must be taken to compare only stars of the same spectral type.

The *Si* III lines λλ 4552, 4568, and 4574 are first measurable at about B5 and increase in strength toward B1. They show a definite luminosity effect, being strongest in the supergiants. The depths of the lines increase from B5 to B1. At B2 the lines are deeper in class IV than in the other luminosity classes. Since the theoretical relative strengths of λ 4552, 4568, and 4574 are in the ratio 5:3:1, the observed relative intensities of these lines will indicate on what part of the curve of growth these lines fall. If the lines fall on the damping part, their relative intensities should be in the ratio $\sqrt{5}:\sqrt{3}:1$ or 2.24:1.73:1. Table 3 gives the relative intensities of the *Si* III lines; the intensity of λ 4574 is unity in each case. Only the values for χ^2 Ori are close to the ratios which would be expected if all the lines of the multiplet fell on the damping part of the curve of growth. However, the probable errors in the measures of equivalent width do not exclude observed relative intensities in the range 1.84–2.69 for λ 4552, and 1.42–1.84 for λ 4568 from being interpreted as pure damping gradients. It is probable that the lines lie on the transition part of the curve of growth. If the lines fell near the point where the curve of growth changes from the Doppler part to the transition part, one might expect the ratio λ 4568:λ 4574 to approach the value 3:1 for stars in which the *Si* III lines were weak.

Since there is no evidence of this behavior, it seems most likely that the *Si* III lines lie closer to the damping part of the curve of growth than to the Doppler part. From the evidence of Table 3 it is doubtful if damping is the predominant broadening agent for the *Si* III lines in any of the stars studied. This view is supported by the fact that the line profiles do not show damping wings.

The relative intensities of the lines in the *Si* III multiplet have been investigated by I. H. Abdel-Rahman.[10] If his relative intensities are expressed in the same form as are the relative intensities in Table 3, they are seen to be closely the same as the data given here. He finds that an abnormally large damping constant is required if the lines are to lie on the damping portion of the curve of growth. It is more probable that λ 4574 does not lie on the damping part of the curve of growth; then such a large damping constant is not required to account for the observations. The present data and the more extensive data of Abdel-Rahman agree in indicating that λ 4574, and possibly λ 4568 in some cases, are relatively too strong for the multiplet to lie completely on the damping part of the curve of growth.

Typical line profiles for λ 4481 and the *Si* lines at about spectral type B2.5 are shown in Figure 4. The profiles are from the same plates that were used to give the *He* I line contours. The change of shape in going from luminosity class I*a*, o^2 CMa, to class II, ϵ CMa, to class IV, γ Peg, is conspicuous. However, its direct interpretation is difficult. Observed points are plotted in Figures 3 and 4.

In Table 4 are given the half half-widths of the *Mg* and *Si* lines, calculated according to equation (5) from the data of Table 2. These could be interpreted literally as Doppler widths if we knew the relation between the true profiles and the absorption coefficient. Expressed as velocities, these half half-widths, particularly for the supergiants, are quite large. In any case, these numbers, being proportional to W/A_c, give a measure of the sharpness of the lines. It is interesting to note that, although the *Mg* II line λ 4481 is a close doublet, it is very little wider on the average than the *Si* lines are. However, it is notable that the lines in the supergiants are generally wider than those in the less luminous stars. The numbers given for γ Peg indicate a minimum sharpness, as the central absorptions in this case have not been corrected for the instrumental profile. The broad lines in ρ Leo are largely due to rotation,[2] but the source of broadening for the other supergiants is difficult to decide. The effects of turbulence,[11] of expansion or contraction of the atmosphere,[12] and of the sphericity of the atmosphere[13] should all be considered. First, it should be demonstrated whether the ordinary theory of radiation transfer and line formation predicts suitable contours for the lines in B stars when adequate account is taken of collision and radiation damping, as well as of pure Doppler broadening. If it does not, then the above phenomena must be invoked to account for the observed line shapes.

3. *The interpretation of the line profiles.*—It can be shown[14] that, if Stark broadening is important, the line-absorption coefficient per atom in state $n = 2$ for the wings of the Balmer lines of hydrogen may be represented by

$$k^{(S)}(\Delta\lambda) = C\,\frac{F_0^{3/2}}{(\Delta\lambda)^{5/2}}, \tag{6}$$

where F_0 is the "normal field strength" and depends on the density of charged particles and their velocity and $\Delta\lambda$ in angstroms is the distance from the center of the line. The

[10] *M.N.*, **101**, 312, 1941.

[11] Struve and Elvey, *Ap. J.*, **79**, 409, 1934.

[12] Underhill, *Ap. J.*, **106**, 128, 1947. [13] *Ibid.*, **107**, 247, 1948.

[14] See Unsöld, *Physik der Sternatmosphären* (Berlin: Julius Springer, 1938), pp. 180 ff.

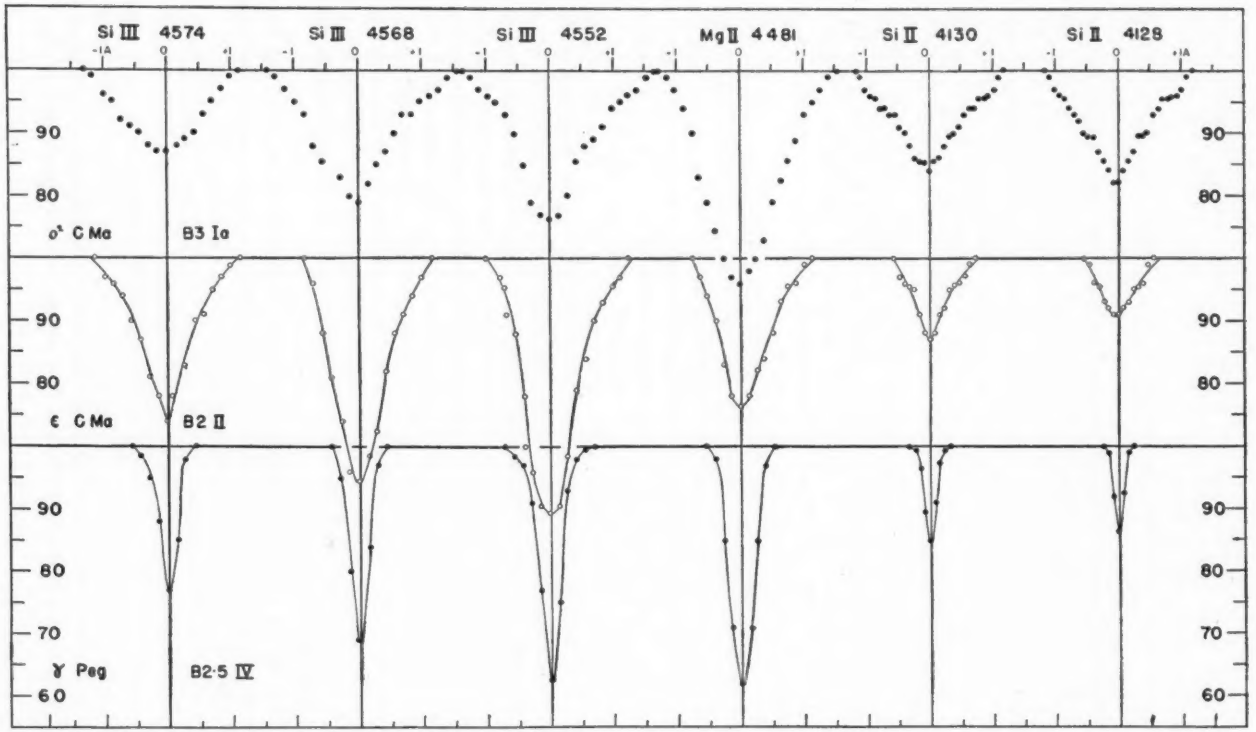

FIG. 4.—The *Si* III, Mg II, and *Si* II lines in o^2 CMa, ϵ CMa, and γ Peg. The residual intensity is in percentages of the continuum

constant C is evaluated by Unsöld for several of the Balmer lines. Inserting the numerical values given by Unsöld, we find for $H\gamma$ that

$$k^{(S)}(\Delta\lambda) = 1.42 \times 10^{-14} \frac{p_e}{T} (\Delta\lambda)^{-5/2}, \tag{7}$$

where p_e is the electron pressure in bars and T is the temperature. This expression differs from that quoted by Unsöld by a factor 2, since now it is known that only the field from protons causes the broadening of the hydrogen lines. The electrons do not contribute to the Stark effect of the hydrogen lines in the high-temperature stars.

Following Unsöld's discussion of radiation damping,[15] we see that, if radiation damping is important in forming the wings of the Balmer lines of hydrogen, the line-absorption coefficient per atom in state $n = 2$ for the wings of $H\gamma$ is

TABLE 4

HALF HALF-WIDTHS OF THE *Mg* AND *Si* LINES IN ANGSTROMS

Star	*Mg* II λ 4481	*Si* II λ 4130	*Si* II λ 4128	*Si* III λ 4574	*Si* III λ 4568	*Si* III λ 4552
ρ Leo	0.98A	.....	.....	0.82A	0.89A	0.96A
χ^2 Ori	.74	.....	.....	.67	.80	.89
o^2 CMa	.73	0.71A	0.63A	.78	.78	.76
χ Aur	.80	.55	.59	.44	.56	.57
η CMa	.74	.58	.53	.57	.60	.60
β Ori	.63	.52	.53	.....	.....	.....
ε CMa	.49	.31	.33	.55	.53	.56
γ Peg	.26	.09	.08	0.22	0.20	0.25
τ Her	.55	.51	.48	.....	.....	.....
ζ Dra	0.64	0.60	0.52	.....	.....	.....

$$k^{(R)}(\Delta\lambda) = 7.31 \times 10^{-18} (\Delta\lambda)^{-2}, \tag{8}$$

where the appropriate numerical values for $H\gamma$ have been introduced. For radiation damping to be predominant we must have

$$k^{(R)}(\Delta\lambda) \geqslant k^{(S)}(\Delta\lambda). \tag{9}$$

This leads to the inequality

$$\frac{p_e}{T} \leqslant 5.12 \times 10^{-4} (\Delta\lambda)^{1/2}. \tag{10}$$

The maximum values that log p_e may reach if at $\Delta\lambda = 1$ A, or at $\Delta\lambda = 4$ A, the line-absorption coefficient is to be determined chiefly by radiation damping are given in Table 5. Since the expected electron pressures in B-type stars are greater than these values, it follows that the hydrogen-line profiles even in supergiants should be predominantly determined by Stark effect. Acting upon this assumption, Unsöld[16] derived electron pressures for a number of B-type stars. He derived[17] a relation between the equivalent width of a hydrogen line and the electron pressure, by using the empirical formula

$$\frac{1}{A} = \frac{1}{A_c} + \frac{1}{x_\nu}, \tag{11}$$

[15] *Ibid.*, pp. 152 ff. [16] *Zs. f. Ap.*, **23**, 100, 1944. [17] *Ibid.* **21**, 22, eqs. (27)-(31), 1944.

where A is the absorption at any point in the line, A_c is the central absorption, and

$$x_\nu = k^{(S)}(\Delta\lambda)\, N_{0,2} H\ , \tag{12}$$

is the optical thickness of the equivalent Schuster atmosphere. Here $N_{0,2} H$ is the number of hydrogen atoms in the second quantum state. Since we have profiles of the hydrogen lines, we may test the validity of Unsöld's assumptions. From equations (6) and (12) we note that, when Stark broadening is important,

$$\frac{1}{x_\nu} = \text{Constant}\ (\Delta\lambda)^{5/2}; \tag{13}$$

hence a plot of log $1/x_\nu$ as obtained from equation (11) against log $\Delta\lambda$ should yield a straight line with slope 5/2. If radiation damping is the most important broadening agent, we should get a straight line with slope 2.

TABLE 5

MAXIMUM ELECTRON PRESSURES IF RADIATION DAMPING IS TO PREDOMINATE

T	$(\log p_e)_{max}$		T	$(\log p_e)_{max}$	
	$\Delta\lambda = 1$ A	$\Delta\lambda = 4$ A		$\Delta\lambda = 1$ A	$\Delta\lambda = 4$ A
10,000°	0.71	1.01	20,000°	1.01	1.31
16,000°	0.92	1.21	24,000°	1.09	1.39

Figure 5 shows such plots for $H\gamma$ in o^2 CMa, ϵ CMa, and γ Peg. The points are chosen for $\Delta\lambda \geqslant 1$ A. The slope of the best straight line for o^2 CMa is 2.05, for ϵ CMa it is 1.53, and for γ Peg it is 1.91. In the latter case one has no doubt that the profile is the result of Stark effect. The two or three points in each case to the right of log $[(1/A) - (1/A_c)] = 1.2$ represent absorptions of less than 5 per cent; hence it is not significant that they deviate from the straight line. Similar results are obtained from the profiles of $H\gamma$ and $H\delta$ in the other stars. The slope is generally less than 2 and is in no case greater than 2.3. Since we expect that even in the supergiants the absorption coefficient is largely determined by Stark effect, we must conclude that equation (11) does not represent the process of line formation for the hydrogen lines in B stars. Consequently, electron pressures deduced from formulae based on equation (11) should be regarded only as indications of order of magnitude.

We shall now investigate an atmosphere in which the classical temperature distribution of a gray body is valid, and we shall show how the intensities of some typical lines may be computed. Chandrasekhar[18] has shown that the gray-body temperature distribution remains valid in a nongray atmosphere to a good approximation if the proper mean absorption coefficient,

$$\bar{\kappa} = \int_0^\infty \kappa_\nu \frac{F_\nu^{(1)}}{F}\, d\nu\ , \tag{14}$$

is used. In forming $\bar{\kappa}$, the monochromatic absorption coefficients are weighted by the monochromatic fluxes in a gray body. It has been assumed that

$$\frac{\kappa_\nu}{\bar{\kappa}} = \delta_\nu + 1\ , \tag{15}$$

[18] *Ap. J.*, **101**, 328, 1945.

where δ_ν, a small quantity independent of depth, measures the departure from grayness. The relation (14) has been developed for an atmosphere in which the equation of transfer,

$$\cos\vartheta \frac{dI_\nu}{\rho dz} = -\kappa_\nu I_\nu + \kappa_\nu B_\nu , \tag{16}$$

is valid. For a B-type atmosphere, electron scattering is important; hence the appropriate equation of transfer is

$$\cos\vartheta \frac{dI_\nu}{\rho dz} = -(\kappa_\nu + \sigma) I_\nu + \kappa_\nu B_\nu + \sigma J_\nu , \tag{17}$$

where σ is the electron-scattering coefficient and is independent of frequency. It can be shown, following Chandrasekhar,[18] that the gray-body temperature distribution can be

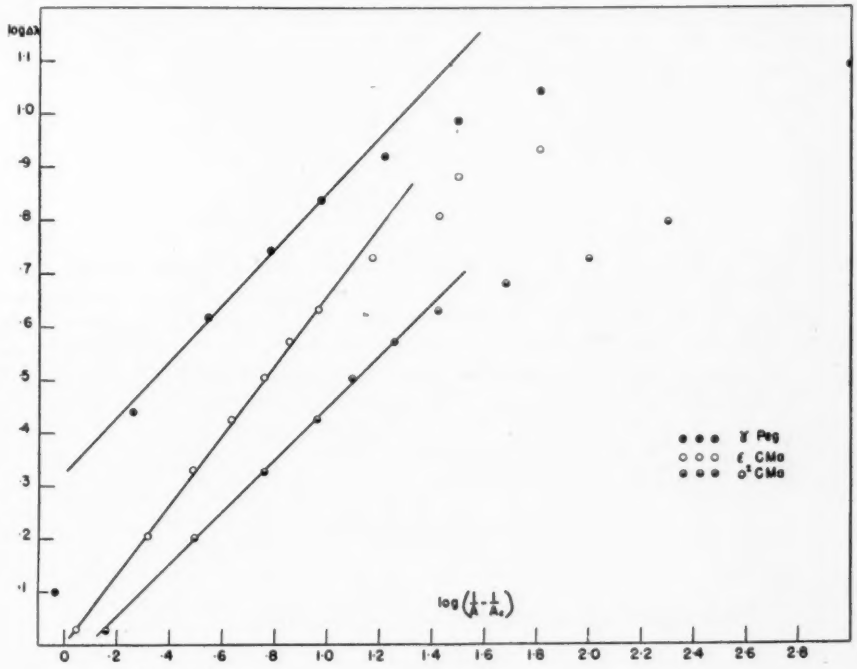

FIG. 5.—Log $\left(\frac{1}{A}-\frac{1}{A_c}\right)$ − log Δλ plots for $H\gamma$ in σ^2 CMa, ϵ CMa, and γ Peg. Δλ is measured in angstroms.

maintained as a good approximation if the optical depth, τ, is given by

$$d\tau = -(\bar{\kappa} + \sigma)\rho dz , \tag{18}$$

where $\bar{\kappa}$ is the mean absorption coefficient defined in equation (14) and there are the same restrictions on δ_ν, the departure from grayness, as before.

We shall consider a pure hydrogen atmosphere with boundary temperature $\theta_0 = 0.30$. The monochromatic mass absorption coefficient per gram of star material is

$$\kappa_\nu = k_\nu (1 - x) , \tag{19}$$

where k is the mass absorption coefficient per gram of neutral hydrogen (corrected for stimulated emissions), and $1-x$ is the fraction of neutral hydrogen atoms at any level in the star. The quantity $1-x$ is obtained from the ionization equation for hydrogen and is dependent on the temperature and electron pressure. The absorption coefficient k is dependent only on the temperature. The electron-scattering coefficient per gram of star material, σ, is given by

$$\sigma = \sigma_e \frac{x}{m_H}, \tag{20}$$

where σ_e is the electron-scattering coefficient per electron. For the temperatures and pressures of the atmospheres to be investigated, hydrogen is so highly ionized that

$$\sigma = \text{Constant} = 0.40 \tag{21}$$

throughout.

We evaluate the mean absorption coefficient by putting

$$\bar{\kappa} = \bar{k}\,(1-x) = (1-x)\,\frac{\int_0^{\nu_1} k_\nu \frac{F_\nu^{(1)}}{F}\,d\nu}{\int_0^{\nu_1} \frac{F_\nu^{(1)}}{F} d\nu}, \tag{22}$$

where ν_1 is the frequency of the Lyman limit. If the integration is carried out over all frequencies less than the Lyman limit, the departures from grayness are always small. If the integration is performed over frequencies from zero to infinity as in equation (14), then, because k is very large in the Lyman continuum and $F_\nu^{(1)}$ is not vanishingly small, the part of the integral with ν running from ν_1 to infinity will far outweigh the rest of the integral, and the departures from grayness in the usual regions will become large. Since the fraction of the total flux emergent in the Lyman continuum is not very large, it is permissible to neglect this flux in an approximate theory. In this way $\bar{k}$ was calculated at $\tau = 0$, 0.5, and 1.0. The classical relation

$$T^4 = T_0^4\,(1 + \tfrac{3}{2}\tau) \tag{23}$$

was assumed.

Since hydrogen is almost completely ionized, we can write

$$p_e = \tfrac{1}{2} p\ , \tag{24}$$

where p is the total pressure. If radiation pressure is neglected, the equation of hydrostatic equilibrium gives

$$\frac{dp_e}{d\tau} = \frac{g}{2}\,\frac{1}{\bar{\kappa} + \sigma}, \tag{25}$$

where g is the surface gravity. We have

$$\bar{\kappa} = \bar{k}\,(\tau)\,(1-x)\,, \tag{26}$$

where $\bar{k}(\tau)$ is known graphically as a function of τ from the calculations discussed above and $1-x$ is a known analytic function of τ and p_e. To obtain p_e as a function of optical depth, an initial p_e, compatible with the surface gravity and mean absorption coefficient, is assumed, and equation (25) is integrated step by step. Each stage is iterated to get

the best dp_e before advancing to the next stage of the integration. When p_e has been determined, $\bar{\kappa}+\sigma$ and $\kappa_\nu+\sigma$ are obtained at each optical depth, and thence the ratio

$$n_\nu = \frac{\kappa_\nu + \sigma}{\bar{\kappa} + \sigma} \tag{27}$$

is found. If the standard theory of line formation is to be used, strictly this ratio should be independent of optical depth. However, small variations of n_ν will not invalidate the theory. In order to predict the intensity at any point in a line, the ratio

$$\eta_\nu = \frac{l_\nu}{\kappa_\nu + \sigma}, \tag{28}$$

where l_ν is the line-absorption coefficient per gram of star material, must be known. Strömgren[19] has shown that, if η_ν is reasonably constant with increasing optical depth, the residual intensity at any point in the line is given by

$$R_\nu = \frac{1 + \frac{2}{3}\sqrt{3}}{\frac{4}{3}\sqrt{3} + \frac{1}{2}\frac{x_0}{n_\nu}} \frac{\frac{4}{3}\sqrt{3}\,\overline{\sqrt{\lambda_\nu}} + \frac{1}{2}\frac{x_0}{n_\nu}\overline{\lambda_\nu}}{1 + \frac{2}{3}\sqrt{3}\,\overline{\sqrt{\lambda_\nu}}}, \tag{29}$$

where

$$x_0 = \frac{h\nu}{kT_0}(1 - e^{-h\nu/kT_0})^{-1}, \tag{30}$$

and

$$\lambda_\nu = \frac{1}{1 + \eta_\nu}. \tag{31}$$

The quantities $\bar{\lambda}_\nu$ and $\overline{\sqrt{\lambda_\nu}}$ are suitable mean values of λ_ν and $\sqrt{\lambda_\nu}$. In a later paper[20] Strömgren gives a practical method of forming these mean values by using the weighted values of λ_ν and $\sqrt{\lambda_\nu}$ at five representative points. Equation (29) has been derived on the assumption that absorption plays no role in line formation but that the lines are formed by a pure scattering process. That is, the quantity ϵ, which is usually introduced to allow for the absorption processes, has been put equal to zero.

The line-absorption coefficient in the center of a line is given by

$$l_{\text{center}} = \frac{\sqrt{\pi}\,e^2}{mc}\frac{f}{v}\lambda\frac{N^*}{N}N, \tag{32}$$

where

$$v = 1.289 \times 10^4 \sqrt{\frac{T}{\mu}}\ \text{cm/sec} \tag{33}$$

is the most probable thermal velocity of the atoms, N^*/N is the relative number of atoms excited to the lower level of the line, and N is the number of atoms per gram of star material in the proper stage of ionization. (Here λ is the wave length of the line.) The quantity μ is the atomic weight of the atom in question. Table 6 gives θ, log p_e, log $(1-x)$, $\bar{\kappa}+\sigma$, and n_ν at λ 4340 as functions of τ for an atmosphere in which log $g = 4.09$; also given are log η at the center of the *Si* II line λ 4128, the *Si* III line λ 4552,

[19] *Ap. J.*, **86**, 1, 1937.

[20] *Pub. Copenhagen Obs.*, No. 127, p. 243, 1940.

the *He* I line λ 4471, and *Hγ*. The *f*-values of the silicon lines and the relative abundance by number, $a(Si)$, of silicon are unknown. The tabulated η's are for the case in which $fa(Si) = 10^{-6}$. Similarly, the relative abundance by number, $a(He)$, of helium must be known; it is assumed to be 10^{-1}, and the *f*-value for λ 4471 given by Goldberg[21] is used. A model in which log $g = 2.00$ is given in Table 7.

TABLE 6

$\theta_0 = 0.300$; LOG $g = 4.09$

τ	θ	LOG p_e	LOG $(1-x)$	$\bar{\kappa}+\sigma$	n_ν λ 4340	LOG η_{center}				WING OF $H\gamma$ LOG η(4 A)
						Si II* λ 4128	*Si* III* λ 4552	*He* I† λ 4471	*H* λ 4340	
0.01...	0.299	1.70	−4.34	1.21	0.717	+0.34	0.85	2.84	3.29	−0.82
0.02...	.298	1.94	−4.13	1.72	0.686	+0.47	.74	2.99	3.37	−0.51
0.04...	.296	2.15	−3.95	2.46	0.650	+0.56	.62	2.96	3.41	−0.26
0.06...	.294	2.26	−3.87	3.02	0.871	+0.34	.55	2.83	3.39	−0.17
0.08...	.292	2.34	−3.83	3.45	0.863	+0.39	.52	2.85	3.38	−0.10
0.10...	.290	2.40	−3.80	3.81	0.811	+0.42	.48	2.87	3.38	−0.04
0.20...	.281	2.59	−3.77	4.66	0.989	+0.32	.38	2.81	3.33	+0.09
0.40...	.267	2.80	−3.80	5.07	1.21	+0.28	.52	2.81	3.26	+0.22
0.60...	.256	2.94	−3.86	4.96	1.46	+0.21	.61	2.79	3.15	+0.32
0.80...	.246	3.06	−3.91	4.68	1.81	+0.09	.67	2.76	3.20	+0.40
1.00...	0.238	3.15	−3.96	4.48	2.06	−0.08	0.92	2.75	3.21	+0.50

* $fa(Si) = 10^{-6}$.
† $a(He) = 10^{-1}$.

TABLE 7

$\theta_0 = 0.300$; LOG $g = 2.00$

τ	θ	LOG p_e	LOG $(1-x)$	$\bar{\kappa}+\sigma$	n_ν λ 4340	LOG η_{center}				WING OF $H\gamma$ LOG η(4 A)
						Si II* λ 4128	*Si* III* λ 4552	*He* I† λ 4471	*H* λ 4340	
0.01.....	0.299	0.08	−5.97	0.419	0.981	−1.66	0.55	1.60	1.60	−3.75
0.02.....	.298	0.37	−5.69	.436	0.966	−1.15	0.75	1.87	1.88	−3.19
0.04.....	.296	0.66	−5.44	.466	0.966	−0.71	0.90	2.11	2.13	−2.69
0.06.....	.294	0.82	−5.31	.494	0.972	−0.82	0.92	2.21	2.36	−2.32
0.08.....	.292	0.93	−5.24	.518	0.960	−0.65	0.97	2.30	2.43	−2.15
0.10.....	.290	1.02	−5.18	.539	0.946	−0.53	1.00	2.34	2.49	−2.03
0.20.....	.281	1.27	−5.08	.605	0.996	−0.51	0.94	2.46	2.68	−1.65
0.40.....	.267	1.54	−5.07	.651	1.09	−0.49	1.08	2.54	2.78	−1.40
0.60.....	.256	1.70	−5.11	.657	1.20	−0.63	1.07	2.56	2.84	−1.21
0.80.....	.246	1.82	−5.14	.652	1.32	−0.86	1.00	2.55	2.96	−1.08
1.00.....	0.238	1.92	−5.19	0.639	1.43	−1.17	1.11	2.53	2.94	−0.97

* $fa(Si) = 10^{-6}$.
† $a(He) = 10^{-1}$.

[21] *Ap. J.*, **90**, 414, 1939.

In the wing of $H\gamma$ the line-absorption coefficient per gram of star material is

$$l(\Delta\lambda) = 1.42 \times 10^{-14} \frac{p_e}{T} (\Delta\lambda)^{-5/2} \frac{N_H(2)}{N} \frac{(1-x)}{m_H} \tag{34}$$

(cf. eq. [7]), where $N_H(2)/N$ is the relative number of hydrogen atoms in the state $n = 2$, and m_H is the mass of a hydrogen atom. Here $\Delta\lambda$ is in angstroms. From this expression $\eta(\Delta\lambda)$ may be obtained. Log η(4 A) for the two models is given in the last columns of Tables 6 and 7.

In the log $g = 4.09$ model, η for *Si* II increases inward at first for a short distance and then decreases regularly as greater optical depths and higher ionization are reached. For *Si* III the trend of η with τ is the opposite of this, η decreasing rapidly at first as the increasing electron pressure decreases the ionization, and then increasing again as the effects of increasing temperature predominate. For *He* I and the center of $H\gamma$, η is reasonably constant with increasing optical depth. In these two cases η is so large that complete absorption effectively occurs at the outermost fringes of the atmosphere. In the wing of $H\gamma$, the line-absorption coefficient is pressure-dependent; thus η increases rapidly with increasing optical depth. Since $\eta(\Delta\lambda)$ can be obtained from η(4 A) by multiplying η(4 A) by $4^{5/2}\,(\Delta\lambda)^{-5/2}$, η has quite different values at different points in the wing of the line.

In the log $g = 2.00$ model, the variations of η with increasing depth are greater in all cases than in the log $g = 4.09$ model. The *Si* II line is weakened with respect to the *Si* III line because of the low electron pressure which favors the ionization of *Si* II. For *Si* II, η reaches a maximum at a greater depth than in the log $g = 4.09$ model. For *Si* III, η rises rapidly with increasing optical depth and at a τ of about 0.08 becomes nearly independent of optical depth. The η for *He* I, λ 4471, behaves in a similar manner. It is smaller than in the log $g = 4.09$ model, because at the low pressures of the log $g = 2.00$ model the ionization of helium is advanced. The η_{center} for *H* behaves similarly and shows the advancement of the ionization of hydrogen in the log $g = 2.00$ model. Thus, apart from the broadening effects of Stark effect which must be considered in the denser model, we should expect the helium and hydrogen lines to be weaker in early supergiants than in main-sequence stars of the same temperature, because there are fewer neutral atoms to absorb the lines. Observations[7] of λ 5876, the leading member of the triplet diffuse series of *He* I, do not confirm this conclusion for helium, the line being significantly stronger in the early supergiants than in the main-sequence stars. Since this line is very little affected by Stark effect, we should expect abundance effects, such as those indicated above, to be detectable. To account for the observations, we might postulate some strong broadening agent in the supergiant stars or that there is some process, such as proposed by Foster and Douglas,[22] making λ 5876 abnormally weak in the main-sequence stars. We should also recognize that λ 5876 may have a tendency to appear in emission in some supergiants, much as $H\alpha$ does. In the wing of $H\gamma$, in the log $g = 2.00$ model, η varies very greatly with increasing optical depth. We have considered Stark broadening only as a broadening agent. At the low pressures of this model it is possible that some other source of broadening may be dominant. A comparison of the predicted profile with observations may indicate whether this is so.

Equation (29) has been used to predict absorptions for the various lines from the values of η tabulated in Tables 6 and 7. The predicted absorptions are given in Table 8. They are listed as A_5 when $\bar{\lambda}_\nu$ and $\overline{\sqrt{\lambda_\nu}}$ have been found from the values of λ_ν and $\sqrt{\lambda_\nu}$ at five representative points as suggested by Strömgren, and as A_1 when the values of λ_ν and $\sqrt{\lambda_\nu}$ at one optical depth have been inserted in equation (29). In this latter case

[22] *M.N.*, 99, 150, 1939.

the atmosphere is assumed to be homogeneous, with the properties of the model atmosphere at the one representative point. The single representative point in the log $g = 4.09$ model is at $\tau = 0.11$. For the log $g = 2.00$ model, the single representative point is at $\tau = 0.22$. The selection of these single representative points is arbitrary, and the intention of their use is to show the effects of stratification. When η changes fairly rapidly with optical depth, the predicted absorptions are sensitive to the representative points chosen. The difference of A_1 from A_5 illustrates this point.

Log g for a star can be estimated from the prediction of the wings of $H\gamma$ and from the relative intensities of the silicon lines. Thus comparison of the observed profile for $H\gamma$ in γ Peg with the predicted absorptions, A_5, in both models, suggests a value of g intermediate between the two values chosen. The predicted relative central absorptions of the silicon lines also suggest this. When the mean of the observations for χ^2 Ori and o^2 CMa are compared with the predicted $H\gamma$ in the log $g = 2.00$ model, it would seem that log $g = 2.00$ is a fairly good estimate for the supergiants. If the predicted points are plotted to form a profile, the shape of the predicted line is rather different from the observed shape, and there is a question of whether there is some other broadening agent active.

TABLE 8

PREDICTED ABSORPTIONS

Line	log $g = 4.09$		log $g = 2.00$		Wing of $H\gamma$ $\Delta\lambda$	log $g = 4.09$			log $g = 2.00$		
	A_{c_5}	A_{c_1}	A_{c_5}	A_{c_1}		A_5	A_1	A_{obs}	A_5	A_1	A_{obs}
Si II λ 4128...	36	42	7	10	1 A.....	69	78	42	20	20	32
Si III λ 4552..	43	43	58	63	2.....	50	55	34	8	4	13
He I λ 4471...	95	95	83	92	4.....	26	24	21	3	2	4
H λ 4340.....	97	97	87	95	8.....	2	8	7	.....	.....	.....

The absorption coefficient from radiation damping only is comparable in size to that from Stark broadening for the low electron pressures of the log $g = 2.00$ model. The observed relative central absorptions of the *Si* II lines suggest a slightly larger g-value than that used in the model. However, since the observations show that the shape of $H\gamma$ in supergiants is significantly different from the shape of $H\gamma$ in main-sequence stars, g cannot be increased much, or the typical Stark-broadened shape will result.

When a reasonable estimate of log g has been made in this way, abundances of the elements may be derived by finding that abundance which will give a predicted profile which fits the observed profile. Such a procedure would not entail a prohibitive amount of work, for the abundance enters η as a multiplicative factor only. This method of finding abundances has the advantage that account may be taken of the variation of η through the atmosphere, that is, of stratification, if it is important, and use is made of the shape of the absorption line, as well as of its equivalent width. We are assuming that the boundary temperature θ_0 is known. In practice the best pair of θ_0 and log g can be estimated by fitting the wings of the hydrogen lines; and then the relative abundances of the elements can be derived upon the assumption of a suitable form for the line-absorption coefficient. If the f-value of the line is not known, then it is the product of the f-value and the abundance that will be determined. This method of determining abundances should be quite critical for elements which are present in two stages of ionization, for then the intensities of the lines in both spectra must be predicted satisfactorily.

Our model atmosphere computations also allow us to derive the shape of the line-absorption coefficient from observations. When the predicted values of A_1 are plotted

against η and the predicted A_5 are plotted against $\bar{\eta}$, where $\bar{\eta}$ is the value of η corresponding to $\bar{\lambda}_\nu$, both sets of points are found to lie on a single curve with very little scatter. The same curve can be used for both models up to absorptions of about 60 per cent. The reason that one curve can be so constructed is that the predicted absorptions are not very sensitive to the change of darkening, $\frac{1}{2}x_0/n_\nu$, with wave length or gravity, or to a fairly large variation of η with optical depth. The values of η corresponding to the observed absorptions in a line profile can be read from this mean curve, as a function of $\Delta\lambda$, the displacement from the center of the line. The variation of η with $\Delta\lambda$ will represent the variation of the line-absorption coefficient with $\Delta\lambda$. Since we have seen that

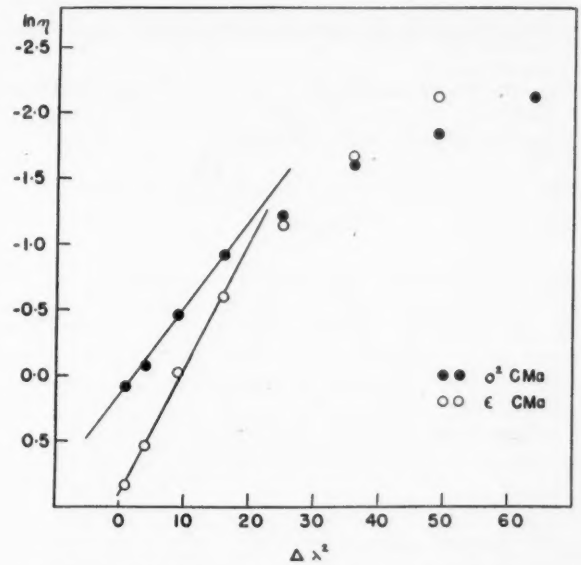

FIG. 6.—$ln\ \eta - (\Delta\lambda)^2$ plot for λ 4552 in o^2 CMa and ε CMa. Δλ is expressed as millimeters on the microphotometer tracing.

the line profiles have very closely a Gaussian shape, we shall see if $\eta(\Delta\lambda)$ itself is Gaussian. Let us assume

$$\eta = \eta_0\, e^{-(\Delta\lambda/\Delta\lambda_D)^2}\ , \tag{35}$$

where λ_D is the width of the line-absorption coefficient due to the most probable velocity of the atoms. Then

$$ln\,\eta = ln\,\eta_0 - \left(\frac{\Delta\lambda}{\Delta\lambda_D}\right)^2; \tag{36}$$

hence a plot of $ln\eta$ against $(\Delta\lambda)^2$ should yield a straight line with slope $(\Delta\lambda_D)^{-2}$, if the line-absorption coefficient is Gaussian in shape. The intercept at $\Delta\lambda = 0$ gives η_0, from which the abundance of the element may be deduced if the f-value of the line is known. Figure 6 gives such plots for λ 4552 in o^2 CMa and ε CMa. The core of the line can be represented by a Gaussian line-absorption coefficient, but in the wings the form of the line-absorption coefficient may be different. The present observations are not accurate enough to determine unambiguously the shape of the absorption coefficient in the wings of the lines, as in the wings the uncertainty in any measure of absorption is a large

fraction of the measured absorption. Such plots were made for the *Si* II and *Si* III lines in o^2 CMa and ϵ CMa; and $\Delta\lambda_D$ in kilometers per second was derived from the slope of the first part of the curve. The mean $\Delta\lambda_D$ from the five determinations in each case is 37 ± 2 km/sec for o^2 CMa, and 27 ± 2 km/sec for ϵ CMa. These values, if interpreted as turbulent velocities, are considerably larger than the mean values of v_t found by Goldberg[23] from curves of growth for B2 supergiants. They are significantly less than the half half-widths of Table 4 give, if these half-widths are interpreted directly as $\Delta\lambda_D$. This is because the relation between absorption and line-absorption coefficient is not, in general, linear. The large Doppler widths of the lines in the supergiant o^2 CMa and the giant ϵ CMa appear to be an example of the phenomenon discussed by Struve,[24] K. O. Wright,[25] and M. Schwarzschild[26] for F supergiants—that the lines are broader than the turbulent velocity found from the curve of growth would suggest.

I am very grateful to Dr. Jesse L. Greenstein for many helpful and fruitful discussions of the problems dealt with here. His encouragement and aid in dealing with the problems of line interpretation are particularly acknowledged.

[23] *Ap. J.*, **89**, 623, 1939.

[24] *Ap. J.*, **104**, 138, 1946.

[25] *J.R.A.S. Canada*, **41**, 49, 1947

[26] Unpublished.

A POLARIGRAPHIC STUDY OF THE REFLECTION NEBULA NGC 6729

WALTER T. WHITNEY AND EDWIN B. WESTON
Frank P. Brackett Observatory, Pomona College
Received January 5, 1948

ABSTRACT

The variable nebula NGC 6729 was photographed through a sheet of Polaroid and its polarization determined. Visual examination of the plates indicated that polarization was definitely present. Reduction of microphotometer traces over the nebulosity yielded a mean maximum of about 15 per cent. There is an indication that the nebula close to T CrA may derive a little of its light from that star as well as from R CrA. To the southwest of R CrA is located a wisp of nebulosity extending away from two brighter spots, one of which is surrounded by a faint ring. The wisp and bright spots show polarization, the latter having a mean of 11 per cent and a maximum of about 15 per cent. The apparent radial polarization in NGC 6729 and the wisp of nebulosity to its southwest, with R CrA as center, is everywhere between zero and 35 per cent, and for the most part it is less than 20 per cent.

PREVIOUS WORK

Investigations to determine the amount of polarization in nebulae have not been very extensive, and the earliest studies yielded uncertain results. These include Perrine's[1] observations of the nebulosity near Nova Persei and Reynolds'[2] and Green's[3] observations of the bright spiral nebula NGC 4826. Meyer,[4] using improved equipment and technique, photographically investigated several spiral and planetary nebulae, the Orion nebula, and Hubble's variable nebula (NGC 2261). The last-mentioned nebula, for which Meyer found small polarization effects (less than 10 per cent), is similar to the variable nebula studied by the authors of this paper. Sinclair Smith[5] analyzed the extragalactic elliptical nebula M32 for polarization effects. Struve, Elvey, and Roach[6] and Henyey[7] made qualitative studies of the nebulosities about ρ Ophiuchi and γ Cygni, respectively, for polarization effects. In the same year Henyey[8] also made a more extensive examination of the nebulosity about the Pleiades and of NGC 7023. In the latter object he obtained an average maximum polarization of 12 per cent but found little polarization for the most part in the former. More recently, Walter[9] found polarization effects up to 11 per cent for the reflection nebula around FU Orionis. Öhman[10] has measured polarization effects up to 6 per cent or less in several clouds in the extragalactic Andromeda nebula, M31.

OBSERVATIONS OF NGC 6729 FOR POLARIZATION EFFECTS

The investigation of the reflection nebula NGC 6729 for polarization effects was suggested by Struve. In the summer of 1946, plates of this nebula were taken at the prime focus of the 82-inch reflector (focal length, 324 inches) at the McDonald Observatory by the senior author. Just in front of the plateholder a sheet of Polaroid (clear aperture of 72 mm) of photographic quality, cemented between two glass plates, was mounted in a plastic rim which could be rotated in an aluminum frame. An aesculine gelatine filter was separated from the outer surface of one of the Polaroid cover plates and a third

[1] *Lick Obs. Bull.*, No. 23, p. 180, 1902.
[2] *M.N.* **72**, 553, 1912.
[3] *Pub. Lick Obs.*, **13**, Part II, 53, 1918.
[4] *Lick Obs. Bull.*, No. 328, p. 68, 1920.
[5] *Mt. W. Contr.*, No. 524; *Ap. J.*, **82**, 192, 1935.
[6] *Ap. J.*, **84**, 219, 1936.
[7] *Ap. J.*, **84**, 609, 1936.
[8] *Ibid.*
[9] *Zs. f. Ap.*, **20**, 256, 1941.
[10] *Stockholms Obs. Ann.*, **14**, No. 4, 1–29, 1942.

glass plate by means of thin separators about the edge of the Polaroid-filter combination. The guiding was accomplished in the usual manner.

Two exposures were taken in focus through the Polaroid-filter combination. The exposures were taken on the same night (July 29, 1946, U.T.) approximately symmetrically with respect to the meridian passage of the object, of equal exposure time (90 minutes), and with approximately uniform atmospheric conditions. The plane of polarization of the Polaroid was rotated through 90° between exposures. In the first exposure (index position angle, 135°) the transmission axis of the Polaroid was placed along the direction of the axis of the nebula (which is fan-shaped and extends away from the star R CrA toward and beyond T CrA). A third plate (for comparison purposes) was taken of the nebula on August 2, 1946, U.T., without the Polaroid-filter combination. All the plates were 103 *a*-F Eastman Spectroscopic plates. Those exposed through the Polaroid were developed together in the same tank of D11 developer. Before development, photometric standards were impressed upon an unexposed portion of each of the plates in the tube photometer.

EXAMINATION AND MEASUREMENT OF PLATES

The plates were examined visually for polarization effects. This examination was made difficult by the fact that the sky intensity on the first plate was greater than that on the second. For convenience, we shall call the first plate (with the position angle of the transmission plane of the Polaroid at 135°) "W1" and the second (position angle of Polaroid at 225°) "W2." Figures 1, *a* and *b*, are nearly seven-fold enlargements of NGC 6729 on W1 and W2, respectively. Figure 1, *c*, is a second seven-fold enlargement of W2 upon which significant details are indicated.

Microphotometer measurements of the original plates and of enlargements of them have been made. The errors introduced in enlarging the standards made their measurement unreliable. The measurement of the original plates was made difficult by the small size of the objects. The method finally adopted was to orient the plates so that the galvanometer deflection of the microphotometer was a maximum when each of two stars was placed over the slit. The effective slit length employed was about 0.11 mm, and its effective width somewhat less than 0.02 mm. Only those microphotometer traces most free from random fluctuations were employed in the reductions.

Measurements of the standards on each plate showed some systematic differences; therefore, the intensity of the background sky was used as the unit of brightness. A weighted mean was obtained from traces made of the background sky on each plate near ten different stars which appeared to be free from surrounding nebulosity. The polarization, p, was computed by the usual formula,

$$p = \frac{1 - \frac{I_A}{I_B}}{1 + \frac{I_A}{I_B}},$$

where I_A is less than I_B, I representing the mean intensity of a single, very small area on plates A and B. The polarization was taken as positive when the intensity on W2 was less than that on W1, negative when that on W1 was less than that on W2.

At the head of the nebula is the irregular variable R CrA. Five seconds of right ascension east and 0.8′ south of R CrA is the irregular variable T CrA. On the first plate the condensation of nebulosity, designated as area B (see Fig. 1, *c*), is much stronger than it is on the second plate. Microphotometer measurements yield a value of 17 per cent positive polarization for this area. This is the largest polarization value found in NGC 6729 and is most readily apparent from a comparison of Figures 1, *a* and *b*. Despite the difference in the intensity of the sky background, areas F, G, and K seem more intense

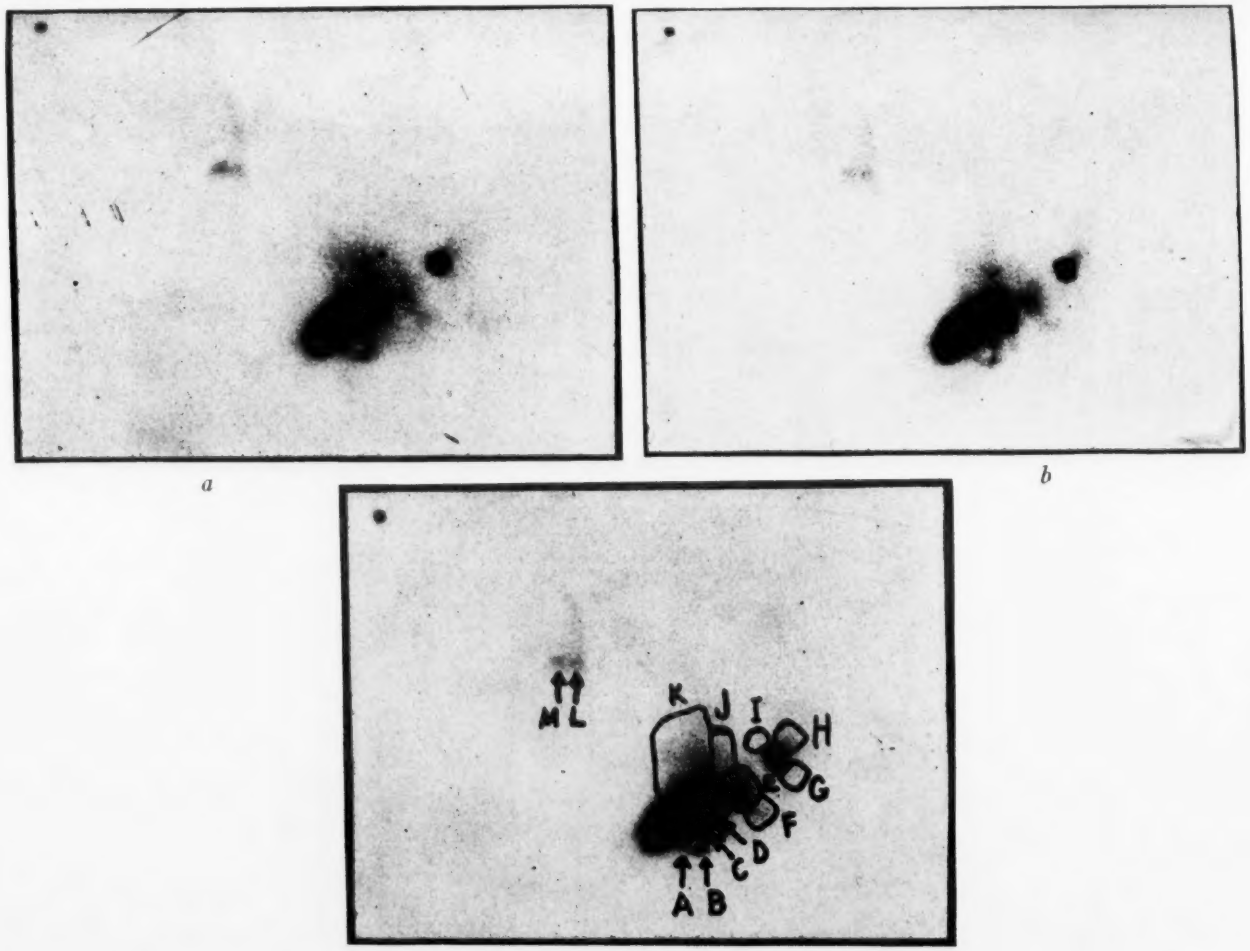

FIG. 1.—NGC 6729. *a*, plate W1; *b*, plate W2; *c*, identification of regions on plate W2. Enlarged about seven times. North is at bottom, east at right.

on plate W1 (or on Fig. 1, *a*). Measurement yields positive polarizations of 9 per cent for areas *F* and *G*, while for area *K* it varies from 5 to 8 per cent, showing an increase toward the southwest. Areas *A* and *C* exhibit positive polarizations of 7 and 4 per cent. The densest portion of NGC 6729 southeast of R CrA (along the axis of the Polaroid on plate W1) shows definite negative polarization, and measurement yields a mean maximum of about 12 per cent. Areas *J* and *I* (also along the axis) show mean positive polarizations of 4 and 10 per cent, respectively, the value for area *I* (along an axis through T CrA and perpendicular to the one through R CrA) showing large variation, however. The small density of the plates made measurements of the latter area quite uncertain. Measurement of areas *G* and *H* gives positive polarizations of 9 and 3 per cent. Previous visual examination had indicated that in area *G* positive polarization should be expected, while in area *H* negative polarization, becoming positive away from T CrA, should be found. The measured value for *H* is an average for that area. Areas *D* and *E*, for which visual examination indicated greater intensity on plate W2 (Fig. 1, *b*), both yield measured mean values of 3 per cent negative polarization, the latter varying from +2 to −7 per cent, however. In the case of each area, larger negative mean values had been anticipated, which suggests that the negative polarization values may all be too small. Between T CrA and area *E* the polarization is about 5 per cent positive. The edges of the nebula to the northeast and to the southwest of R CrA (along the axis of the Polaroid on plate W2) exhibit a mean of 10 per cent positive polarization, with a maximum of about 12 per cent.

The polarization values found for the more dense portion of the nebula between R CrA and T CrA, for the edges of the dense portion to the northeast and to the southwest of R CrA, and for areas *A* and *B* indicate quite definitely that most of the light scattered by these regions of the nebula comes from R CrA. While areas *D* and *E* and several other regions suggest that all the polarization values for the faint areas may be systematically too positive by a few per cent, the distribution of the values about T CrA leads one to the tentative suggestion that T CrA may provide a small amount of light that is scattered by near-by nebulosity.

The wisp of nebulosity to the southwest of NGC 6729, especially area *M*, is definitely more intense on W1 (Fig. 1, *a*).[11] Upon measurement, area *L* exhibits about 6 per cent polarization, and area *M*, about 17, both positive. The wisp of nebulosity extending north from area *L* shows only about 7 per cent polarization near this area. Farther out, the polarization is probably about the same, but extensive measurements of it were not made. It was determined, however, that it was positive and less than 10 per cent within 45″ of area *L*. The ring of radius 20″ about area *M* (lost, for the most part, in the enlargements but readily apparent upon the original plates) shows polarization up to a maximum of about 15 per cent positive, but with sufficient variation at different points along the ring to warrant further investigation upon plates of greater density.

We conclude that, at all points in NGC 6729 and the nebulosity to its southwest, the apparent polarization by reflection, including certain corrections, does not exceed 20 per cent and has a mean maximum of about 15 per cent. With only negligible departures, the radial polarization with R CrA as center is everywhere between zero and 35 per cent, and for the most part it is less than 20 per cent.

ERRORS OF MEASUREMENT

No precise value can be given for the probable error of measurement of polarization because the errors from plate grain, plate irregularities, uncertainties in the sky background and in the standards, uncertainties in the orientation of the plates upon the microphotometer carriage, and erratic fluctuations and drift of the microphotometer cannot be accurately evaluated. The probable error was estimated to be less than 3 per

[11] This wisp of nebulosity is reported verbally by Hubble to have been recently increasing in brightness.

cent for nebula intensities from two to eight times the background sky. For fainter nebulosity the probable error increases quite rapidly, being about 5 per cent at one and one-half times the sky background. Systematic errors up to possibly as much as 5 per cent may be present in the nebulosities brighter than twice the sky background, and slightly more for fainter nebulosity. For this reason, further refinement of the measurements already made seems useless. Uncertainty of the position of R CrA at the head of the nebula, the small size of the nebula upon the plates, the difficulty of determining the ratio of polarized to unpolarized light, and the uncertainty of the source of illumination of some parts of the nebula make the determination of radial polarizations unreliable.

TABLE 1*

SUMMARY OF MEAN APPARENT POLARIZATION VALUES FOUND IN AND NEAR NGC 6729

Area	Weighted Mean Intensity of Plate W1 (Per Cent)	Weighted Mean Polarization (Per Cent)
Dense region S.E. of R CrA	More than 6.0	−5 to −13 −12 (mean maximum)
Edge of dense region N.E. and S.W. of R CrA	2.8 (1.8–5.0)	10
A	4.5	7
B	5.0	17
C	4.8	4
D	4.5	− 3
E	3.8	− 3
F	2.2	9
G	2.1	9
H	2.6	3
I	2.5	10
J	3.5	4
K	3.2	7
L	2.6	6
M	3.4	17
Wisp of nebulosity south of *L*	2.2 (maximum)	7
Ring of nebulosity about *M*	1.9 (maximum)	Up to 15

* The areas are defined on Fig. 1, *c*. The nebula intensities are expressed in terms of the background sky. The polarization is positive when the nebula is more intense on plate W1, negative when it is more intense on plate W2.

It has been assumed that the efficiency of Polaroid as an analyzer is very high. The data given by Ingersoll[12] and his associates indicate that the efficiency of the Polaroid and aesculine filter should certainly be greater than 90 per cent. This high efficiency was verified by the authors for the filter combination used with F-type Eastman Spectroscopic plates.

The authors wish to express their appreciation to Dr. Otto Struve for suggesting the problem and making it possible to obtain the necessary photographs of the nebula and to Dr. George Van Biesbroeck for assistance in the taking of the photographs. Their appreciation is also extended to Dr. Ira S. Bowen for authorizing the use of the Mount Wilson microphotometer in these investigations.

[12] *J. Opt. Soc. Amer.*, **26**, 234, 1936.

STARS IN DIFFUSE NEBULAE*

JESSE L. GREENSTEIN
Yerkes and McDonald Observatories
Received February 4, 1948

ABSTRACT

Slit spectrograms of a group of stars in bright and dark nebulosity have been obtained; taken with a wide slit, they are suitable for spectrophotometric comparison of the nebulous objects with B stars of known color. In a field near o Per, nine stars of types B6–A8, magnitudes 10–12.5, were observed; no trace of emission was found. Two B5 stars, heavily involved in NGC 2068, also showed normal spectra. Spectra of $-6°1253$, R Mon, and NGC 2261 were measured to obtain relative gradients and the intensities of the Balmer emission and absorption lines. From the space reddening and from distances determined by other means, both $-6°1253$ and R Mon seem too bright to be normal T Tauri objects; it is possible that there is an extra-stellar source of luminosity in R Mon. The line $H\gamma$ is stronger in absorption in NGC 2261 than it is in R Mon; line absorption may occur in the nebula. The Balmer emission decrement, after correction for space reddening, is steeper than in planetary nebulae (recombination spectrum); it more nearly resembles that in the chromosphere or Be stars. Theoretical decrements under conditions approaching thermodynamic equilibrium fit moderately well; this suggests a higher space density and less dilution than in planetary nebulae. Possible sources of continuous emission are discussed, and it is shown that the normally expected Paschen continuum is negligible.

In previous investigations I have discussed[1,2] the spectroscopic properties of stars intimately involved with bright and dark nebulae of the reflection type. A few such stars, notably the T Tauri variables discussed by Joy,[3] have shown strong emission lines superposed on a late-type dwarf absorption spectrum. The present investigation contains further spectroscopic and spectrophotometric observations made at the McDonald Observatory in November, 1947. The $f/1$ camera with two glass prisms gives a dispersion of 150 A/mm at $H\gamma$; by using a slit 1″.5–6″ in width, the slit spectrograms were made suitable for spectrophotometric measurement. The effects of atmospheric dispersion were small; an attempt was made to observe the stars at nearly constant zenith distance. For every series of films on one night, several spectra of B stars of known[4] photoelectric color, C_1, were obtained. Photometric calibration was provided by a tube photometer with blue and red filters. The wide slit prevents accurate radial-velocity measurement or new line identifications.

After reduction of microphotometer tracings the gradients of the nebulous stars were determined with respect to the standard B stars. Rather complex relations exist between gradients, short-base-line C_1 colors and the long-base-line V − I colors[5] of the six-color photoelectric photometry. An indirect method of reduction must therefore be adopted. The relative gradients, ϕ, measured at Greenwich were found[6] to be proportional to the V − I color if the redness of a star is caused either by space reddening or by low temperature; this is not true for the C_1 colors. For space-reddened stars, we find

$$\phi = 1.45 + 0.682\,(\mathrm{V}-\mathrm{I})\,, \tag{1}$$

$$C_1 = 0.16 + 0.159\,(\mathrm{V}-\mathrm{I})\,. \tag{2}$$

From these we derive

$$\mathrm{V}-\mathrm{I} = 1.47\phi - 2.13\,. \tag{3}$$

* *Contributions from the McDonald Observatory, University of Texas*, No. 148.

[1] "Harvard Symposium on Interstellar Matter, Dec., 1946" (in press).

[2] *Pub. A.S.P.*, **59**, 139, 1947. [3] *Ap. J.*, **102**, 168, 1945.

[4] Stebbins, Huffer, and Whitford, *Ap. J.*, **91**, 20, 1940.

[5] Stebbins and Whitford, *Ap. J.*, **102**, 318, 1945. [6] Greenstein, *Ap. J.*, **104**, 403, 1946.

Our comparison stars were reddened B stars, and we obtain their gradients from

$$\phi = 0.76 + 4.28\, C_1 . \qquad (4)$$

The wave-length region covered was 6600–3900 A, about the same as that used at Greenwich. Consequently, I adopted the above group of relationships for my gradient measures. The zero-point is essentially that of Stebbins and Whitford, which makes the color temperature of an A0 star 11,000°. The procedure is as follows: the mean gradient of the comparison B stars is determined from equation (4); relative gradients, $\Delta\phi$, for the unknown star give ϕ, which determines the V − I color from equation (3); color excesses on the V − I scale were determined with Stebbins and Whitford's mean colors as a function of spectral type; color excesses, Δ(V − I), could be transformed into International color excesses by multiplication by 0.33; from[6] a "minimum" value of the absorption A_{pg} is equal to 1.64 Δ(V − I). The accuracy of a color determination from one plate is not high, and the colors are quite preliminary; nevertheless, they permit some progress in an otherwise unexplored field.

THE NEBULOUS STARS

Stars in the dark nebula near o Persei.—The *Barnard Atlas of Selected Regions of the Milky Way*, Plate 3, shows an interesting region of the dark nebula in Taurus and Perseus. This nebula is at a distance of 100 or 150 psc. Several stars in this field are immersed in patches of bright nebulosity, which are obviously part of the larger dark nebula. Some have been observed by Hubble,[7] and data on a group near +31°643 are given by Gingrich.[8] The nebula IC 348 envelops +31°643, but the other stars in Gingrich's field are not nebulous. I have obtained spectra and, in some cases, colors based on one plate per star for nine of these objects, with results given in Table 1. Photographic magnitudes, color excesses (C.E.), and spectra were obtained at Mount Wilson by Hubble and Seares. Stars near +31°643 are tabulated as G 6–G 12; they apparently form a cluster, together with brighter, unobscured B stars. My new types and color excesses (C.E.), as reduced to the International scale, are tabulated. All the diffuse nebulae listed are probably of the reflection type. The new spectral types are systematically later than the old in the field near +31°643, effectively reducing the color excesses. Adopting main-sequence luminosities, we find the stars to be at a mean distance of 160 psc, in moderately good agreement with that of the dark nebulosity. The first four stars are certainly inside or

TABLE 1

STARS IN THE DARK NEBULA NEAR o PER

Star	Mt. Wilson			McDonald		
	m_{pg}	C.E.	Type	C.E.	Type	Nebula
+29°565	9.6	0^{m}33	A5	0^{m}48	A8	Barnard nebulous star
+30°540	.....	.....	.....	.....	A0:	Barnard nebulous star
+30°549	10.9	.30	B9p	.84	B8	NGC 1333
+31°643	9.1	.79	B6	.91	B5	IC 348
G 6	12.3	.64	A2	.51	A7	IC 348 Field
G 9	12.1	.79	A1	0.51	A8	
G 10	12.3	.74	B9	.....	A2:	
G 11	11.4	.95	B9	.....	A3:	
G 12	10.8	0.83	B9	.....	B9	

[6] *Ap. J.*, **56**, 400, 1922.

[8] *Ap. J.*, **56**, 139, 1922.

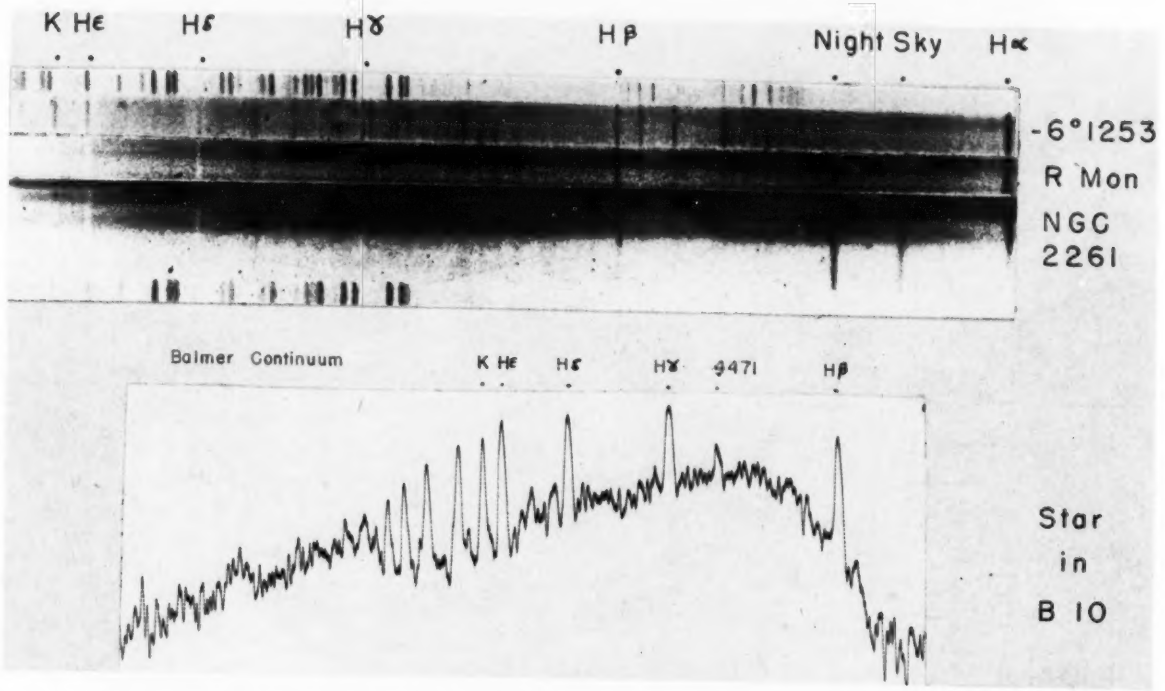

FIG. 1.—Spectra of −6°1253, R Mon, and NGC 2261 from $H\alpha$ to K. The $H\gamma$ absorption line in R Mon is weaker than in NGC 2261. Below is reproduced a microphotometer tracing of the star in the faint nebula, B 10, from an original film kindly loaned by Struve and Swings. The Balmer decrement is very slow in this object, compared to the other two stars, and a strong Balmer emission continuum exists.

close behind the dark material and suffer absorption up to 4 mag. Nevertheless, there is no trace of emission *Hα* or of H and K in any of the spectra; +31°643 was observed with 75 A/mm dispersion, also with negative results. In all spectra the absorption *Hα* was clearly seen. Thus association of rather late A-type dwarfs with nebulosity does not necessarily result in the emission-line characteristics of a T Tauri star. Many fainter stars in neighboring regions of the Taurus nebula have been found by Joy[9] to show T Tauri emission features; spectral types of B8e–dMe occurred. We may conclude that not all A stars involved in bright nebulosity show emission features. A survey of fainter stars below 12 mag. in this field would be of great interest.

NGC 2068.—This is one of the brightest and largest reflection nebulae. Hubble[7] remarked on the discrepancy between the large size of the nebula and the apparent magnitude of the illuminating star. The star (10.8 mag.) is 2.2 mag. fainter than the average star illuminating a nebula of the size of NGC 2068, as computed from the Hubble relation. It is also very red. We have a clear case for location of a star inside or close behind a reflection nebula. The theory of reflection nebulae[10] predicts that such a nebula would be very blue, compared to the star. According to Collins' measures,[11] NGC 2068 proves, in fact, to be the nebula which is bluest, compared to the illuminating star. Unfortunately, a 90-minute exposure gave me only an underexposed nebular spectrum. By inspection the color difference is seen to be very large; the relative brightness of nebula and star should be observed over a wide range of wave length, since it would give important information on the scattering by interstellar particles. Two stars of spectral types B5 and B8 are located inside the brightest part of the nebula. The fainter (north-following) of the two is the earlier and is very red; I find C.E. of +1.3 and +0.6 mag., respectively, and Hubble gave +1.0 mag. In spite of the very close connection between the stars and the nebulosity, there is no trace of emission in either star.

−6°1253.—This T Tauri star[12] in NGC 1999 has strong emission lines superposed on a stellar spectrum of dwarf A spectral type. Broad absorption wings of the hydrogen lines can be seen (Fig. 1), with superposed strong emission lines. Two accordant spectrophotometric comparisons are available. An attempt was made to eliminate known emission lines, so as to permit measurement of the background continuum. The mean observed V − I color is −0.34 mag. From the strength of the hydrogen lines the spectral type is later than A0 and, from the absence of wings of an absorption K line, earlier than F0. The color excess, Δ(V − I), is between 1.46 and 0.80 mag.; the C.E. is between 0.47 and 0.27 mag. The distance of the star, so derived, is only about 150 psc, which seems much too small. The star must have $M \approx -0.5$ to permit it to be at a distance of 400 psc. Morgan and Sharpless point out that NGC 1999 seems to be associated with the dark and bright nebulosity of the Orion region, at a distance near 400 psc. If such a distance is established, either the correction for absorption as derived from the color excess is too large, or the star is about 2 mag. brighter than a normal dwarf A star. The contribution of the emission lines to the total photographic magnitude is not large enough to account for this discrepancy. We shall later examine the theoretical intensity of continuous emission by hydrogen around the star. The underlying hydrogen absorption lines in −6°1253 correspond to a dwarf; they are at least 20 A wide.

R Mon and NGC 2261.—The spectral changes of R Mon have been reported previously.[1,2,3] In November, 1947, the star was relatively bright, $m_v \approx 10$, and probably near maximum. The *Ca* II emission in the star and the K-line absorption in the nebula, observed in January, 1946, when the star was near minimum, have disappeared; all emission lines seem somewhat weaker. The cometary nebula, NGC 2261, showed considerable

[9] *Pub. A.S.P.*, **58**, 244, 1946.

[10] Henyey and Greenstein, *Ap. J.*, **88**, 580, 1938.

[11] *Ap. J.*, **86**, 529, 1937; Greenstein, *Ap. J.*, **87**, 581, 1938.

[12] Morgan and Sharpless, *Ap. J.*, **103**, 249, 1946; Herbig, *Pub. A.S.P.*, **58**, 163, 1946.

structure, visually; Figure 1 shows several streaks caused by bright knots. The slit was along the long axis of the nebula, in declination. Three good spectrophotometric comparisons of the nebula and the star R Mon were available; B stars provide a zero-point for the color of R Mon. The color of the continuous spectrum of NGC 2261 was found nearly constant along the nebula over about 40″ of its 150″ extension, although some changes in line intensity exist. The relative gradient—*nebula minus star*, $\Delta\phi = -0.55 \pm 0.07$ (m.e.)—corresponds to $\Delta(V - I) = -0.81 \pm 0.11$, or -0.27 mag. on the International scale. In 1946, when R Mon was faint ($m_v \approx 13$), I obtained $\Delta\phi = -1.2$; unfortunately, no comparison spectra were then taken to fix the color of R Mon. By inspection it seems probable that the color of the nebula remained nearly constant; the star then became bluer as it became brighter. Both nebula and star should be followed photoelectrically. The color of R Mon is poorly determined by the November, 1947, observations; three plates give a deduced V − I color of -0.16 ± 0.45. It may have varied during the series of observations. The relative gradients of the nebula and the star, compared to normal B stars, are approximately linear.

TABLE 2

EQUIVALENT WIDTHS OF EMISSION AND ABSORPTION LINES

LINE	NGC 2261		R MON		−6°1253
	Emission (A)	Absorption (A)	Emission (A)	Absorption (A)	Emission (A)
$H\alpha$	126	.....	148	.....	147
$H\beta$	13	.....	14	.....	16
$H\gamma$	.....	2.4	<0.2	0.9	5.0
$H\delta$	.....	3.3	.....	2.2	2.0
H, H+$H\epsilon$	.....	3.4	.....	3.1	7.4
K	.....	.....	<0.1	.....	9.6

The theory of the colors of reflection nebulae[10] suggests that, if a star is in front of most of the nebulous material, the maximum International color difference, *nebula minus star*, is about −0.25 mag. However, if the star is inside or behind most of the nebulosity, the nebula may become much bluer than the star (e.g., NGC 2068). Denser clouds of absorbing material may drift, or form, near R Mon; then faintness would be correlated with redness, as is probably observed. The variations of the nebula need not be correlated with those of the star. Let us assume that the nebula is a 60° cone; its distance is near 400 psc, so that its extension in the line of sight is about 0.08 psc, at 40″ from the star. Consider only starlight scattered once, contributing to a given element of surface. A total range of about 100 days exists between the time of origin, at the star, of light coming from the front and that from the back of the nebula. Further, the brightness of the star as seen at different points inside the nebula will differ. Variations of the star occur in much less than 100 days, so the nebula integrates the light of the star over a wide range in time and in space.

The spectrum of the nebula is not a pure reflection of that of the star. In January, 1946, the K line was clearly strengthened[1] in absorption in the nebula beyond about 30″ from the star. In November, 1947, $H\gamma$ consisted of an absorption line on the violet wing of a weak emission. Equivalent widths, in angstroms, measured in R Mon and in NGC 2261 are given in Table 2 (with data also for −6°1253). The emission intensities are expressed in units of the intensity within 1 A.U. of the continuous spectrum near each line. Note that all hydrogen absorptions are stronger in NGC 2261 than in R Mon; $H\gamma$ is most clearly affected because of the almost complete filling-in by the emission, in R Mon.

Because of the strength of emission lines, $H\alpha$ and $H\beta$ are not seen in absorption. The hydrogen absorption is produced either in the nebula itself or in an envelope between the nebula and the region near or at the star where the emission lines are produced. These measures support the strong impression[1] obtained from the January, 1946, spectra that the hydrogen absorption lines increase outward from the star; if the latter is true, the hydrogen absorption lines are produced in the body of the nebula.

Most of the reddening and obscuration of R Mon is produced in its immediate neighborhood. This region of the Milky Way is quite transparent to large distances, except for a dark nebula found[13] to be at about 400–500 psc. Examination of direct photographs shows clearly that R Mon lies in an extension of the dark nebula which envelops the nebulous cluster NGC 2264 (S Mon). The distance of this cluster is about 450 psc according to Trumpler;[14] his distance requires negligible correction for space reddening. This large distance for R Mon leads to a serious problem. If the absorption is A_{pg} and if we take $m_{pg} \approx 10$, then

$$M_{pg} = m_{pg} + 5 - A_{pg} - 5 \log r , \tag{5}$$

$$M_{pg} = +1.3 - A_{pg}. \tag{6}$$

Adopt $A_{pg}/E_{int} = 5$; assume the usual relations between spectral type, luminosity, and color along the main sequence. We have no clue to the spectrum of the underlying star; by adopting a series of trial spectral types we can obtain the intrinsic color and then A_{pg}

TABLE 3

DERIVED LUMINOSITY OF R MON

Assumed Spectrum	Color Excess $\Delta(V-I)$	M_{pg}	Assumed Spectrum	Color Excess $\Delta(V-I)$	M_{pg}
B0	$+2^m.3$	-2.5	F0	$+0^m.9$	-0.1
B5	$+2.1$	-2.1	G0	$+0.1$	$+1.1$
A0	$+1.6$	-1.3			

and M_{pg}. From the observed V − I color, -0.16 ± 0.45, we obtain the luminosities given in Table 3. Thus, over a wide range of type, we require a star of rather high luminosity, i.e., a main-sequence B or a giant A, F, or G star. In this, R Mon seems to differ from the other T Tauri stars, which are mainly dwarf stars of late type. If we interpret $H\delta$ and $H\epsilon$ as the undisturbed stellar lines, their equivalent widths, in Table 2, correspond to about spectral type B3. The ultraviolet spectra obtained in 1946, however, show higher members of the Balmer series strong and sharp, with H 15 still resolvable on low dispersion. It seems most probable that the hydrogen lines are produced in a nearly opaque extended shell.

It is interesting that $-6°1253$ is also too bright for its distance after correction is made for obscuration. We may ask whether the apparent excess brightness, the observed continuous spectrum, the emission lines, and the hydrogen-line absorption arise in a nonstellar source of energy. The emission lines may indicate a fluorescent transfer of radiation from the ultraviolet into the visual region; for cool stars this is a negligible source of energy. On the other hand, shock-wave collisional processes may occur in the dense clouds of gas and dust particles as they move past the star at high velocities.

The other variable nebula, NGC 6729, with R CrA involved, is very similar to NGC 2261 in spectral peculiarity. No estimate of the reddening is now available; since it is nearer the sun, we can estimate its absolute magnitude as about $+4 - A_{pg}$. Any ap-

[13] Bok and Rendall-Arons, *Ap. J.*, **101**, 280, 1945.

[14] *Lick Obs. Bull.*, No. 420, 1930.

preciable reddening will make R CrA brighter than a normal dwarf F or G star; like R Mon, it may also prove too bright to be grouped with the late-type T Tauri stars. It also shows sharp absorption lines[1] with apparently shell or nebular characteristics.

HYDROGEN ABSORPTION AND EMISSION

The actual Balmer decrement in −6°1253 and R Mon can be estimated from Table 2. Direct measurement gives the strength of a line in units of the energy per angstrom in the neighboring continuous spectrum. The gradients give the observed relative energy per angstrom in different parts of the continuum, since we can adopt a black-body energy distribution for the star. The intensities under "Obs." in Table 4 express the emission lines in units of the emission in 1 A.U. of continuum at $H\beta$. These intensities are still affected by space reddening; the observed color temperature of −6°1253 was 6000° and of R Mon, 5700°. Table 4 also gives "Corr." intensities obtained on the assumption that, if it were not for space reddening, −6°1253 would have had a color temperature of 9000° and R Mon of 15,000°. The corrected intensities, relative to $H\beta$, are given under "Rel."; these are on an energy scale. In −6°1253, $H\gamma$, $H\delta$, and $H\epsilon$ are superposed on broad ab-

TABLE 4

BALMER EMISSION DECREMENTS

LINE	−6°1253			R MON			ORION. NEB.	PLAN. NEB.	NEB. THEORY	T.E. THEORETICAL		
	Obs.	Corr.	Rel.	Obs.	Corr.	Rel.				20,000°	10,000°	7,000°
$H\alpha$	119	78	4.9	126	56	4.0	4.5	3.3	2.04	3.12	4.60	6.62
$H\beta$	16	16	1.0	14	14	1.0	1.0	1.0	1.00	1.00	1.00	1.00
$H\gamma$	4.9	5.9	0.37	<0.2	<0.2	<0.01	0.54	0.48	0.58	0.43	0.36	0.31
$H\delta$	1.9	2.5	0.16	.....	.....	.....	0.28	0.24	0.31	0.24	0.19	0.14

sorption lines, and their intensities as given have been corrected for this fact; $H\alpha$ and $H\beta$ are so strong relative to the absorption that this was not possible. Consequently, $H\alpha$ and $H\beta$ are underestimated, and the true Balmer decrement is steeper than the tabulated one. In R Mon superposed absorption weakens the higher series members and distorts the Balmer gradient in a manner similar to a Be shell star. Nevertheless, the decrements in both stars are clearly steeper than in the Orion nebula[15] and planetary nebulae.[16] The Orion nebula still requires correction for space reddening, so that its true decrement is less steep than that tabulated. Berman[16] has corrected the data on planetary nebulae approximately for reddening.

For comparison, I list theoretical relative intensities in a recombination spectrum, as computed by Baker and Menzel[17] for their case A_1 at an electron temperature, T_e = 10,000°. The last three columns give the computed decrement under conditions of thermodynamic equilibrium (abbreviated as "T.E."),

$$\frac{I_{n2}}{I_{42}} = \frac{n^2}{16}\frac{A_{n2}h\nu_{n2}}{A_{42}h\nu_{42}}\, e^{-(E_n-12.69)/kT}, \qquad (7)$$

where E_n is the nth excitation potential and $A_{nn'}$ the transition probability. The T.E. decrements are steeper than the nebular recombination type. The observed decrements in −6°1253 and R Mon tend to resemble those predicted under conditions approaching

[15] Greenstein and Henyey, *Ap. J.*, **89**, 654, 1939.

[16] *M.N.*, **96**, 898, 1936. [17] *Ap. J.*, **88**, 52, 1938.

T.E. for temperatures 10,000° or less. We may conclude that the hydrogen emission originates relatively near the star under physical conditions more like an extended chromosphere or Be star envelope than a nebula. It should be noted, however, that steep Balmer decrements also occur in laboratory spectra, where molecular dissociation or collisional excitation is the source of energy.

An obvious possible source of continuous emission is the recombination spectrum to the violet of the Paschen and higher series. To simplify the theoretical computation, let us consider only the emission at frequency, ν, arising from electron captures on the level $n = 3$ of hydrogen, as measured per A.U.:

$$\text{Pac } d\lambda = 10^{-21.90} \frac{N_i N_e}{T_e^{3/2}} e^{(\chi_3 - h\nu)/kT_e} d\lambda , \tag{8}$$

where χ_3 is the ionization potential from the third level. We can now compute the intensity of a line, say, $H\gamma$, in units of the intensity within 1 A.U. of the Pac continuum at $H\gamma$. We find, under conditions of T.E.,

$$I_{52} \approx 1000 \times 10^{1.89\theta_e} \text{ A.U. of Pac} . \tag{9}$$

If we allow for the higher series, the coefficient in equation (9) becomes about 800. If we compute this ratio for a pure recombination spectrum, the line emission would be about one-fourth as strong, relative to the continuum. At 10,000°, $\theta_e = 0.5$, $H\gamma$ has an equivalent width near 1000 A.U. of Pac. Since $H\gamma$ in $-6°1253$ is observed to have a strength of only 5 A.U., the continuous spectrum in that star is *not* produced by hydrogen captures. Another computation was made to estimate the total Pac emission in the entire photographic region (5000–4000 A). Even in a pure nebular recombination spectrum at 20,000°, this integrated continuous emission equals only $H\gamma$. We must conclude that in T.E. or in pure recombination, hydrogen-emission continua play a negligible role. It is not excluded that other mechanisms, such as collisional emission, shock waves, or fluorescence, may provide another source of photographic energy.

The two objects investigated differ strongly from the interesting object in the nebula B 10, described by Struve and Swings.[18] In this spectrum, which they very kindly permitted me to examine, the Balmer decrement is very slow, and a strong Balmer emission discontinuity is visible. The decrement and the Balmer jump seem, by inspection, to be very similar to those in the Orion nebula. The physical conditions in the star in B 10 may more closely resemble those in a nebula, with high dilution and with rather high excitation. It would be valuable to attempt to correlate the Balmer decrement and emission continuum in T Tauri stars with the excitation and the appearance of forbidden lines. Even in B 10 the predicted Pac emission is too small to provide a significant contribution to the light of the star. It should be mentioned, however, that apparently a still unexplained continuous spectrum exists in planetary nebulae and perhaps[19] in the Orion nebula.

A preliminary estimate of the density and extent of the regions producing the hydrogen emission can be obtained. Let us neglect self-absorption and assume that both ionization and excitation are given by the usual formulae, modified solely by the dilution factor. Compute the emission of a line by a spherical nebula of radius R, expressing the intensity as an equivalent width, W, in units of the emission within $d\lambda$ by a black body of radius r and temperature T:

$$W = \frac{R^3}{3r^2} \frac{N_n A_{nn'} h\nu_{nn'}}{B(\lambda, T)} . \tag{10}$$

[18] *Pub. A.S.P.*, **60**, 61, 1948.

[19] Greenstein, *Ap. J.*, **104**, 414, 1946.

Here N_n is the population of the upper level producing the line, and $B(\lambda, T)$ is the Planck function. We introduce the Boltzmann distribution, modified by the dilution, and obtain

$$N_0 R = \frac{12\, W\, B\,(\lambda, T)}{A_{nn'} h\nu_{nn'}} \frac{1}{n^2}\, e^{E_n/kT}. \tag{11}$$

For $-6°1253$ and R Mon, $W \approx 15$ A.U. for $H\beta$, and with $T = 10{,}000°$ the number of neutral atoms, N_0, is

$$N_0 \approx \frac{6 \times 10^{19}}{R}. \tag{12}$$

The ionization formula is

$$\frac{N_i N_e}{N_0} = \frac{r^2}{4R^2} \left(\frac{2\pi m kT_e}{h^2}\right)^{3/2} e^{-\chi_1/kT_e}. \tag{13}$$

Then, combining equations (12) and (13), we find that the ionization is high ($N_i = N_e$) and

$$N_e \approx 10^7 \frac{r}{R} N_0^{1/2}. \tag{14}$$

For the probable spectral types, r is near 3×10^{11}; by adopting the ratio r/R (essentially the dilution), we obtain a set of values of N_0 and N_e. The results are not sensitive to choice of the dilution. For $R = 10r$, $N_0 \approx 2 \times 10^7$ and $N_e \approx 5 \times 10^9$. The ionization is high, only 0.4 per cent of hydrogen being neutral. The space density is low, much less than in the solar chromosphere, but high compared to interstellar space ($N_e \approx 10$) and planetary nebulae ($N_e \approx 10^4$). The total masses involved are negligibly small.

We may wish to estimate the strength of the absorption lines of hydrogen produced within the nebulous envelope of the star. If the metastability of the 2s-level is neglected, the number of excited atoms decreases rapidly with distance from the star as does the ionization. We can write the number of hydrogen atoms in the second level as

$$N_2 \approx 4 N_i N_e\, e^{\chi_2/kT} \left(\frac{h^2}{2\pi m kT_e}\right)^{3/2}. \tag{15}$$

If we insert the values of N_e obtained above in the case in which the nebula has a radius $R = 10r$, we find $N_2 \approx 2$ cm^{-3}. If such a nebula had constant space density, the effective number of absorbing atoms would be $N_2 R$, or about 6×10^{12} cm^{-2}. It is probable that the velocity of the atoms is very large; emission-line widths[1,2] correspond to 150 km/sec. We can then use the thin-layer formula for the equivalent width of an absorption line:

$$W \approx \pi^{1/2} 10^{-13} N_2 R f. \tag{16}$$

We find that $W \approx 0.05$ A.U. for $H\gamma$. While this is too small to be observed, it is surprisingly large. The nebula NGC 2261 has the very large extension of 2×10^{17} cm. The hydrogen absorption lines could be extremely strong, if the space density remained high and if the excitation were comparable to that given by equation (15). Unfortunately, there is no direct means of estimating the density in the outer regions of NGC 2261, since the amount of hydrogen emission contributed by the nebula is not known. Any weak emission lines produced in the nebula would be masked by the intense reflected emission of the star and its nebulous envelope.

SOME *f*-VALUES FOR IONIZED OXYGEN AND IONIZED SILICON

D. R. BATES AND AGNETE DAMGAARD
University College, London
Received January 12, 1948

ABSTRACT

In this paper the transitions $3s - 3p$ and $3p - 3d$ in *O* II and $4s - 4p$ in *Si* II are studied by a standard method. The *f*-values and the mean square radii of the orbitals involved are tabulated.

INTRODUCTION

The authors are undertaking a comprehensive program on evaluating *f*-values for the transitions of systems in *L-S* coupling. A general method is being used that avoids the necessity of having to treat each atom or ion separately. In order to test the accuracy of the technique being employed, it was thought desirable, first, to extend the data already available for comparison by carrying through a few individual calculations by the normal procedure. The transitions studied were as shown in the accompanying tabulation.

$3s - 3p$ . . . . . *O* II
$3p - 3d$ . . . . . *O* II
$4s - 4p$ . . . . . *Si* II

These were chosen mainly because of their importance in certain astrophysical applications. The present paper presents the results obtained for the *f*-values and also gives the mean square radii of the orbitals involved (which are of interest in connection with the estimation of the effective collision-broadening constant in stellar atmospheres)[1].

THE CALCULATIONS

1. The *f*-value associated with a line is given in terms of the strength $\mathfrak{S}$ by the formula,[2]

$$f = \frac{1}{\omega_i} \cdot \frac{1}{3R\lambda a_0^2 e^2} \mathfrak{S} \tag{1}$$

ω_i being the statistical weight of the system in its initial state, R the Rydberg constant, λ the wave length of the radiation absorbed, a_0 the radius of the first Bohr orbit of hydrogen, and e the electronic charge. $\mathfrak{S}$ itself can be expressed as

$$\mathfrak{S} = S(\mathfrak{M})\, S(\mathfrak{L})\, \sigma^2 , \tag{2}$$

where $S(\mathfrak{M})$ is a factor depending on the particular multiplet of the transition array, $S(\mathfrak{L})$ is a factor depending on the particular line of the multiplet, and σ^2 is the quantity

$$\frac{a_0^2 e^2}{(4l_>^2 - 1)} \left| \int_0^\infty R_i R_f r\, dr \right|^2 . \tag{3}$$

Here $l_>$ is the greater of the two azimuthal quantum numbers involved in the transition, and R_i/r and R_f/r are, respectively, the initial and final radial wave functions of the active electron normalized in atomic units.

[1] Cf. B. Strömgren, *Pub. og mindre Meddel. fra Københavns Obs.*, No. 127, 1940.

[2] Cf. E. U. Condon and G. H. Shortley, *Theory of Atomic Spectra* (Cambridge: The University Press, 1935).

The quantity $S(\mathfrak{M})$ can be obtained from the two sets of tables compiled by Goldberg,[3] and $S(\mathfrak{P})$ from the papers either of White and Eliasen[4] or of Russell.[5] The determination of the absolute f-values therefore requires only the computing of the relevant wave functions and the evaluation of the integral occurring in equation (3).

2. The wave functions of the $3s$, $3p$, and $3d$ orbitals of O II and the $4s$ and $4p$ orbitals of Si II were obtained by numerical integration of the standard nonexchange equation,

$$R''+\left(2v-\frac{l(l+1)}{r^2}-\epsilon\right)R=0\,, \tag{4}$$

the potentials v being assumed to be the same as those of the undistorted cores and being taken from the publications of Hartree, Hartree, and Swirles[6] on O III and of Donley[7] on Si III. In Table 1 are given (a) the values found for ϵ, the energy parameter, and also the

TABLE 1

Orbital	Units I_H (13.53 e.v.)		$\overline{r^2}$ (Units a_0^2) (2.79×10^{-17} cm^2)	
	Energy Parameter ϵ	Greatest and Least Ionization Potentials	Derived Directly	Calculated from Hydrogenic Formula
O II $3s$	0.779	0.907–0.861	17.4	12.7–14.1
$3p$	.601	.725– .632	24.0	15.5–21.1
$3d$	.448	.476– .436	30.6	26.2–33.0
Si II $4s$	.529	.605	37.5	28.1
$4p$	0.410	0.461	54.0	41.6

greatest and least ionization potentials i of the various terms as observed in the case of O II by Edlén[8] and, in the case of Si II, by Fowler[9]; and (b) the mean square radii $\overline{r^2}$ of the orbitals as derived directly from the wave functions and as calculated from the hydrogenic formula

$$\overline{r^2}=\frac{a_0^2}{2i}\left\{\left[\frac{5z^2}{i}+1-3l(l+1)\right]\right\}, \tag{5}$$

z being the excess nuclear charge of the parent-ion (2 for O III and Si III). The quantities ϵ and i are not, of course, to be identified, but it is likely that the difference between them arises to a considerable extent from the defects in the theoretical treatment. A general tendency for the energy parameter to be too small is characteristic of the approximation employed. It is reflected in the well-known overdiffuseness of the wave functions. This, in turn, yields too high mean square radii for the orbitals. The true magnitudes of $\overline{r^2}$ probably lie between the values given in the fourth and those in the fifth columns. It may perhaps be mentioned here that if in the hydrogenic formula i is replaced by ϵ, the values of $\overline{r^2}$ obtained are (because the major part of the potential is closely coulomb) al-

[3] *Ap. J.*, **82**, 1, 1935, and **84**, 11, 1936.

[4] *Phys. Rev.*, **44**, 753, 1933.

[5] *Ap. J.*, **83**, 129, 1936.

[6] *Phil. Trans. R. Soc., London, A*, **238**, 229, 1939.

[7] *Phys. Rev.*, **50**, 1012, 1936.

[8] *Nova. Acta Reg. Soc. Scient. Upsal.*, Vol. 9, No. 6, 1934.

[9] *Phil. Trans. R. Soc., London, A*, **225**, 1, 1925.

most identical with the values obtained directly. This serves as a useful (though not complete) check on the work.

With the wave functions, derived as described, the transition integrals were computed. The extent of the cancellation that occurs in them is inappreciable, so that no gross inaccuracy can arise. However, the magnitudes of the integrals are likely to be rather too great because of the overdiffuseness already mentioned. The *f*-values for the complete transition arrays were finally obtained by substituting in

TABLE 2

Transition Array	$\sigma^2/a_0^2e^2$	Mean Wave Length $\bar{\lambda}$ (Units A)	*f*-Value
O II $3s-3p$.....	5.5	4393	1.14
O II $3p-3d$.....	1.48	4294	1.05
Si II $4s-4p$.....	11.4	6357	1.64

$$f = \frac{1}{\Sigma\omega_i}\Sigma\left(\frac{1}{3R\lambda a_0^2 e^2}\mathfrak{S}\right) \tag{6}$$

and using equations (2) and (3). They are given in Table 2, together with σ^2 and for convenience the mean wave lengths $\bar{\lambda}$ defined by the relation

$$\frac{1}{\bar{\lambda}}\Sigma\mathfrak{S} = \Sigma\left(\frac{1}{\lambda}\mathfrak{S}\right). \tag{7}$$

If the *f*-value for any particular line is required, it can, of course, be got at once from these data and from the work of Goldberg[3] and of White and Eliasen[4] or of Russell.[5]

VIBRATIONAL ENERGY LEVELS OF THE CARBON DIOXIDE MOLECULE*

ROBERT C. HERMAN
Applied Physics Laboratory, The Johns Hopkins University, Silver Spring, Maryland
Received February 27, 1948

ABSTRACT

The positions are tabulated of a number of vibrational energy levels of the CO_2 molecule in the ground electronic state. These were calculated by the methods of Dennison. The calculations concern principally energy levels between which Fermi-Dennison resonance exists.

During the course of an investigation, a number of vibrational energy levels were calculated for the CO_2 molecule in the ground electronic state. The calculations were carried out principally for those energy levels between which there exists Fermi-Dennison[1,2] resonance. The procedure followed in calculating the shifts of the unperturbed levels due to this type of resonance interaction has been given by Dennison[2,3] and later by Adel and Dennison.[4,5] The vibrational constants employed are those recalculated by Dennison.[6] After expansion of the appropriate secular determinants in polynomial form, the shifts produced by the resonance perturbation were obtained in a straightforward manner by means of standard methods.[7]

The results are presented in Table 1. In the first column the vibrational energy-level designation is given in terms of the quantum numbers, v_1, v_2^l, and v_3, which refer to the three fundamental frequencies ν_1, ν_2, and ν_3, respectively. The quantum number l denotes the angular momentum, in units of $h/2\pi$, which arises from the doubly degenerate mode of vibration ν_2. The second column gives the value of the energy level as measured above the ground state, $(W - W_0)/hc$, in cm^{-1}. The levels listed are of species $\sum_u^+$ or $\sum_g^+$, according to whether v_3 is odd or even. The ground state $(0\,0^\circ\,0)$ is of species $\sum_g^+$. Several of the energy levels listed in Table 1, namely,

$$\left\{\begin{matrix}(2\,0^\circ\,5)\\(1\,2^\circ\,5)\\(0\,4^\circ\,5)\end{matrix}\right\}, \quad (0\,0^\circ\,7), \quad \left\{\begin{matrix}(0\,2^\circ\,7)\\(1\,0^\circ\,7)\end{matrix}\right\}, \quad (0\,0^\circ\,9), \quad \text{and} \quad \left\{\begin{matrix}(0\,2^\circ\,9)\\(1\,0^\circ\,9)\end{matrix}\right\},$$

have been calculated by Adel and Dennison[4] on the basis of earlier vibrational constants. The difference between the energy levels calculated with the two sets of constants is only several cm^{-1}. Since the calculation of most of the energy levels under considera-

* The work described in this paper has been supported by the Bureau of Ordnance, United States Navy, under Contract NOrd-7386.

[1] E. Fermi, *Zs. f. Phys.*, **71**, 250, 1931.

[2] D. M. Dennison, *Phys. Rev.*, **41**, 304, 1932.

[3] D. M. Dennison, *Rev. Mod. Phys.*, **12**, 175, 1940.

[4] A. Adel and D. M. Dennison, *Phys. Rev.*, **43**, 716, 1933.

[5] A. Adel and D. M. Dennison, *ibid.*, **44**, 99, 1933.

[6] These constants are given on p. 187 of Dennison, *Rev. Mod. Phys.*, **12**, 175, 1940, and are also listed as Eq. III 54 in G. Herzberg, *Infrared and Raman Spectra of Polyatomic Molecules* (New York: D. Van Nostrand Co., Inc., 1945).

[7] J. B. Scarborough, *Numerical Mathematical Analysis* (Baltimore: Johns Hopkins Press, 1930).

tion involves an extrapolation of the potential function, the differences to be expected between the observed and the calculated positions of the vibration bands will increase, the greater the vibrational quantum numbers. Although energy levels such as $\left\{\begin{matrix}(0\ 2^\circ\ 7)\\(1\ 0^\circ\ 7)\end{matrix}\right\}$ may be in error by about 1 or 2 cm^{-1}, the higher energy levels are probably in error by an amount of the order of 10 cm^{-1}.

TABLE 1

CALCULATED VIBRATIONAL ENERGY LEVELS* OF CO_2

(v_1, v_2^l, v_3)	$(W-W_0)/hc$ in cm^{-1}	(v_1, v_2^l, v_3)	$(W-W_0)/hc$ in cm^{-1}	(v_1, v_2^l, v_3)	$(W-W_0)/hc$ in cm^{-1}	(v_1, v_2^l, v_3)	$(W-W_0)/hc$ in cm^{-1}
(0 6° 0)	3787.5	(0 6° 4)	12,772	(0 0° 7)	15,921	(0 0° 9)	20,245
(1 4° 0)	3951.9	(1 4° 4)	12,936				
(2 2° 0)	4074.8	(2 2° 4)	13,059	(0 2° 7)	17,053	(0 2° 9)	21,333
(3 0° 0)	4231.8	(3 0° 4)	13,216	(1 0° 7)	17,156	(1 0° 9)	21,436
(0 6° 1)	6071.0	(0 4° 5)	13,825	(0 4° 7)	18,161	(0 4° 9)	22,397
(1 4° 1)	6235.5	(1 2° 5)	13,954	(1 2° 7)	18,290	(1 2° 9)	22,526
(2 2° 1)	6358.4	(2 0° 5)	14,077	(2 0° 7)	18,413	(2 0° 9)	22,649
(3 0° 1)	6515.4						
		(0 6° 5)	14,955	(0 6° 7)	19,247	(0 6° 9)	23,439
(0 0° 2)	4673.9	(1 4° 5)	15,120	(1 4° 7)	19,412	(1 4° 9)	23,604
		(2 2° 5)	15,243	(2 2° 7)	19,535	(2 2° 9)	23,728
(0 2° 2)	5915.9	(3 0° 5)	15,400	(3 0° 7)	19,692	(3 0° 9)	23,884
(1 0° 2)	6018.1						
		(0 8° 5)	16,067	(0 8° 7)	20,315	(0 8° 9)	24,463
(0 4° 2)	7133.6	(1 6° 5)	16,266	(1 6° 7)	20,513	(1 6° 9)	24,662
(1 2° 2)	7262.2	(2 4° 5)	16,411	(2 4° 7)	20,659	(2 4° 9)	24,808
(2 0° 2)	7385.1	(3 2° 5)	16,551	(3 2° 7)	20,799	(3 2° 9)	24,948
		(4 0° 5)	16,741	(4 0° 7)	20,990	(4 0° 9)	25,138
(0 6° 2)	8329.6						
(1 4° 2)	8494.1						
(2 2° 2)	8617.1	(0 10° 5)	17,162	(0 10° 7)	21,367	(0 0° 10)	22,370
(3 0° 2)	8774.0	(1 8° 5)	17,391	(1 8° 7)	21,595		
		(2 6° 5)	17,569	(2 6° 7)	21,774	(0 2° 10)	23,436
(0 4° 3)	9389.1	(3 4° 5)	17,708	(3 4° 7)	21,912	(1 0° 10)	23,538
(1 2° 3)	9517.7	(4 2° 5)	17,880	(4 2° 7)	22,084		
(2 0° 3)	9640.6	(5 0° 5)	18,099	(5 0° 7)	22,303	(0 0° 11)	24,469
(0 6° 3)	10,563	(0 0° 6)	13,722	(0 0° 8)	18,096	(0 2° 11)	25,513
(1 4° 3)	10,728					(1 0° 11)	25,616
(2 2° 3)	10,851	(0 2° 6)	14,876	(0 2° 8)	19,206		
(3 0° 3)	11,008	(1 0° 6)	14,978	(1 0° 8)	19,308	(0 4° 11)	26,533
						(1 2° 11)	26,662
(0 0° 4)	9,247.8	(0 4° 6)	16,006	(0 4° 8)	20,292	(2 0° 11)	26,785
		(1 2° 6)	16,135	(1 2° 8)	20,421		
(0 2° 4)	10,446	(2 0° 6)	16,257	(2 0° 8)	20,543	(0 0° 12)	26,543
(1 0° 4)	10,548						
		(0 6° 6)	17,114	(0 6° 8)	21,356		
(0 4° 4)	11,620	(1 4° 6)	17,279	(1 4° 8)	21,521		
(1 2° 4)	11,748	(2 2° 6)	17,402	(2 2° 8)	21,644		
(2 0° 4)	11,871	(3 0° 6)	17,558	(3 0° 8)	21,801		

* The values given in Table 1 for the levels $\left\{\begin{matrix}(0\ 6^\circ\ 1)\\(1\ 4^\circ\ 1)\\(2\ 2^\circ\ 1)\\(3\ 0^\circ\ 1)\end{matrix}\right\}$ differ slightly from those previously given by Dennison (*Rev. Mod. Phys.* **12**, 175, 1940). A correction for a small numerical error leads to the values given above, which are in agreement with the latest computations of Dennison (private communication).

The transition probabilities for vibration bands arising from transitions between the ground state $(0\,0^{\circ}\,0)$ and the tabulated levels of species $\sum_u^+$ are, for the most part, very small and probably decrease somewhat more slowly than proportionately from one harmonic or combination band to the next higher one. Adel[8] has calculated the transition probability for the absorption bands $(0\,0^{\circ}\,0) \rightarrow (0\,0^{\circ}\,5)$, $(0\,0^{\circ}\,0) \rightarrow (1\,0^{\circ}\,5)$, and $(0\,0^{\circ}\,0) \rightarrow (0\,2^{\circ}\,5)$, discovered in the atmosphere of Venus by Adams and Dunham.[9] To within the approximation involved in employing a potential function containing terms up to and including those of fourth degree, the matrix element of the electric moment for the transition $(0\,0^{\circ}\,0) \rightarrow (0\,0^{\circ}\,7)$ is found to be

$$\epsilon_{0 \rightarrow 7\nu_3} = \int_\tau \psi_{00^{\circ}0} \alpha \xi \psi_{00^{\circ}7} d\tau = -5.0 \times 10^{-6} \alpha ,$$

where α is the electric moment and ξ is the normal co-ordinate which describes the vibrational motion, ν_3. The notation is that employed by Adel.[8] This result is clearly an estimate only, since it includes the contributions from but a few of the many terms which should properly be considered. The neglected terms contain molecular constants which are at present not known. In spite of this circumstance, it is believed that the calculated result may give an indication of the order of magnitude of the actual transition probability.

The author wishes to express his appreciation and thanks to Professor D. M. Dennison for his aid and stimulating discussions and to Drs. A. Adel and E. O. Salant for their interest in these calculations. Finally, we acknowledge our indebtedness to Mmes E. M. Eichelberger, B. M. Grisamore, and H. S. Hopfield for assistance in performing many of the computations.

[8] A. Adel, *Ap. J.*, **85**, 345, 1937.

[9] W. S. Adams and T. Dunham, *Pub. A.S.P.*, **44**, 243, 1932.

A NEW BAND SYSTEM OF THE C_2 MOLECULE

JOHN G. PHILLIPS
Yerkes Observatory
Received January 27, 1948

ABSTRACT

Five new bands in the spectrum of the C_2 molecule have been discovered in the laboratory, with heads at λλ 7715, 7908, 8108, 8751, and 8980. They are all degraded to the red. An analysis of the bands has shown that they are due to a $^1\Pi_u$–$^1\Sigma_g^+$ transition. The two electronic states involved in the transition are the lower states of the $^1\Pi_g$–$^1\Pi_u$ Deslandres-D'Azambuja system and the $^1\Sigma_u^+$–$^1\Sigma_g^+$ Mulliken system. The excitation energy, ν_{00}, of the $^1\Pi_u$ state relative to the $^1\Sigma_g^+$ state is 8268.50 cm^{-1} (1.025 e.v.). Improved molecular constants for the two states are given in Table 6.

A. INTRODUCTION

The spectrum of the C_2 molecule is of such astrophysical importance that it is being reinvestigated in the laboratory at Yerkes Observatory. The eventual aim is to obtain a reliable value for its heat of dissociation. While this problem has as yet not been solved, during the course of the investigation a new system of bands was discovered in the near infrared which has proved to be of considerable interest, since an analysis of the bands has shown that they arise from a transition between the lower states of the two previously known singlet transitions of the C_2 molecule.

B. EXPERIMENTAL

The C_2 spectrum was obtained in a discharge tube through which argon and benzene vapor were streamed. The tube was a modification of the type employed by Pearse and Gaydon[1] to produce the spectrum of *MnH*. The outer Pyrex tube was 84 cm long and 5 cm in external diameter. It contained two tubular aluminum electrodes, spaced 30 cm apart and concentric with the tube. Between the electrodes a quartz tube, 10 cm long and 8 mm in external diameter, was supported concentric with the Pyrex tube by two fused quartz rings. Owing to the very low coefficients of expansion and thermal conductivity of quartz, the use of this material rather than iron for the rings made it possible to fit them more tightly into the Pyrex tube without danger of the tube's cracking during use. This closer fit made it easier to maintain the path of the discharge through the quartz tube.

It was necessary to purify the argon before streaming it through the tube because the trace of nitrogen present in the commercially produced gas that was used gave rise to strong *CN* bands. This purification was accomplished by passing the argon over red-hot calcium metal. With fresh calcium it was possible by this means to obtain spectra completely free of *CN* bands.

The spectrum of carbon was the most intense when the mixture of argon and benzene vapor was streamed through the tube rather rapidly, being completely replaced every 10 seconds. If the streaming was slower than this the *CH* and H_2 spectra increased in strength. The pressure in the tube was held at between 1.0 and 1.5 cm of mercury. Very little benzene vapor was required, the amount evaporating from solid benzene at −15° C being sufficient for greatest strength of the bands. Under these conditions the deposit of carbon in the tube was slight, and the tube did not require cleaning during the exposures.

The discharge tube was connected directly to the secondary of a 4800-volt, 5-kva

[1] R. W. B. Pearse and A. G. Gaydon, *Proc. Phys. Soc.*, **50**, 201, 1938.

transformer. With a current of 15 amp in the 220-volt primary, the intensity was sufficient to give a well-exposed spectrum in 1 minute at λ 4000 in the second order of the 21-foot grating spectrograph. Sensitized I-N plates were used in the region of the new bands, from λ 7700 to λ 9300. The first order of the spectrograph was used, with a dispersion of 2.5 A per millimeter. With a slit width of 0.02 mm, a 5-minute exposure was sufficient at λ 7700, while a 4-hour exposure was necessary at λ 9300.

C. ROTATIONAL ANALYSIS

Five bands of the new system were observed and measured, with heads at λλ 7715, 7908, 8108, 8751, and 8980. They were all degraded to the red. A reproduction of the bands at λ 8751 and λ 8980 is given in Figure 1. As can be seen, the λ 8751 band consists of three series of singlets, forming an intense Q branch and weaker R and P branches. The R branch is slightly more intense than the P branch. All the five bands exhibit this intensity distribution, which is characteristic of a Π–Σ transition.

The wave numbers in vacuum of all the measured lines are given in Table 1. Gaps that appear in some of the branches are due to the presence in the spectrum of heavily overexposed argon lines.

The usual procedure[2] was followed in the assignment of the rotational quantum numbers J. It was found that a consistent assignment could be made only if lines of odd J were assumed missing. This immediately suggested that the C_2 molecule was the carrier of the system, since only homonuclear molecules with zero nuclear spin produce bands with alternate missing lines. Examples of molecules with this characteristic are C_2 and O_2. The latter molecule could be immediately eliminated from consideration, since, if oxygen had been present in the discharge, bands of CO would have been observed in the visible and ultraviolet parts of the spectrum, and no trace of these bands was found.

As can be seen from Table 1, for the three bands at λλ 8751, 8980, and 8108, the R branches begin with $J = 0$. There is no reason to suppose that the R branches of the other two bands at λ 7715 and λ 7908 do not also begin with this same quantum number, the corresponding lines being unobserved because they are faint and are blended with the background lines, which are unusually strong in this part of the spectrum. Thus the rotational level with $J = 0$ must be present in the lower state, indicating that it must be a Σ state. This fact, together with the observed intensities of the branches, as mentioned above, and the fact that the lines are single even for high J-values, unambiguously identifies the system as being due to a $^1\Pi$–$^1\Sigma$ transition.

Four steps were made in the evaluation of the rotational constants, B_v and D_v, of the upper and lower level of each band and of the band origins, ν_0.

1. From the combination differences, $\Delta_2F'(J) = R(J) - P(J)$ and $\Delta_2F''(J) = R(J-1) - P(J+1)$, approximate values for the rotational constants, B_v and D_v, were obtained by the usual methods. The constants B_v found in this way were accurate to 2 or 3 in the fourth decimal place. This accuracy was improved by the use of the methods presented in steps 3 and 4 below, after the band origins, ν_0, had been determined. The resulting final values of B_v were uncertain by 2 or 3 in the fifth decimal place. The constants D_v were correspondingly improved.

2. The band origins ν_0 were evaluated by two different methods, through the independent use of the two following equations:

$$Q(J) - \overline{(B_v' - B_v'')}J(J+1) = \nu_0 + (B_v' - B_v'')_{\text{corr}} J(J+1),$$

$$R(J) + P(J) - 2\overline{(B_v' - B_v'')}J(J+1) = 2(\nu_0 + B_v') + 2(B_v' - B_v'')_{\text{corr}} J(J+1).$$

[2] G. Herzberg, *Molecular Spectra and Molecular Structure* (New York: Prentice-Hall Book Co., Inc., 1939), Vol. 1.

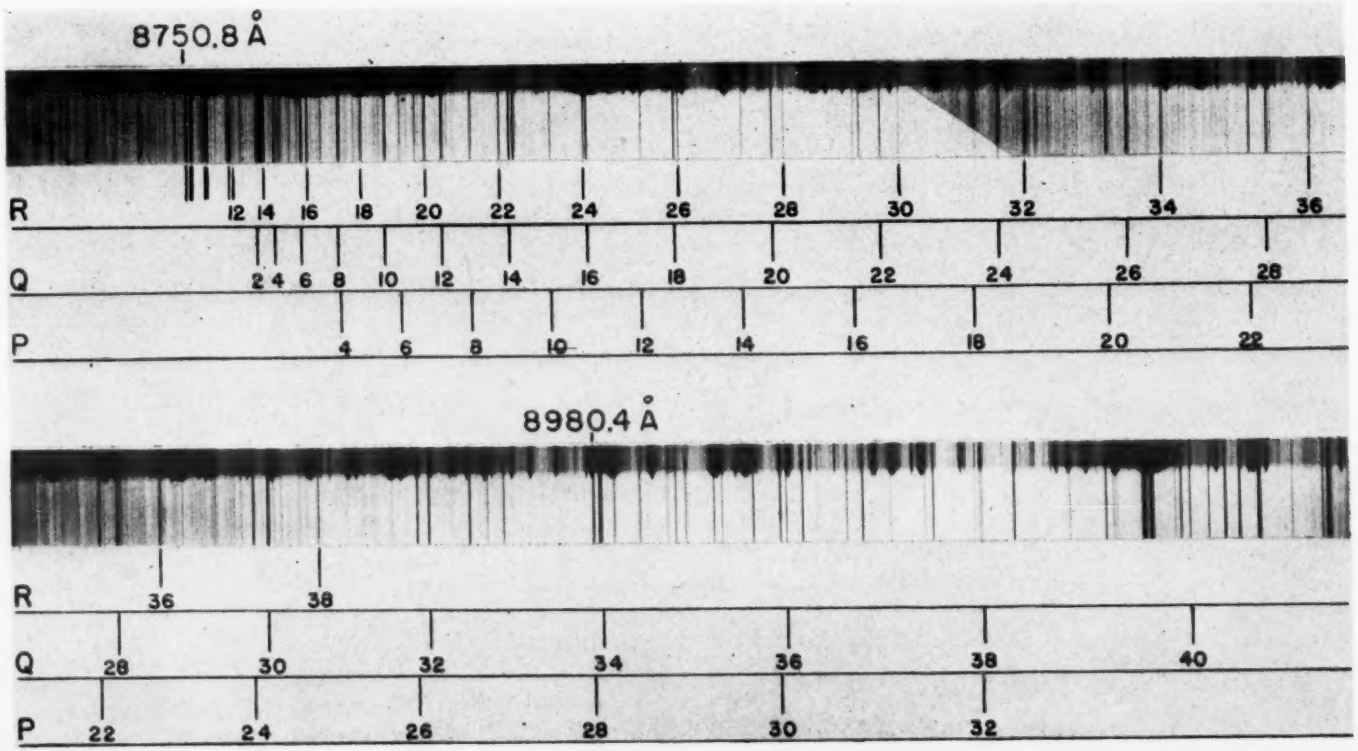

FIG. 1.—The spectrum of the C_2 bands at λ8750.8 and λ8980.4. The narrow, more heavily exposed spectrum is an iron-arc comparison spectrum. The rotational analysis of the λ8750.8 band is given. The numbers below the leading lines are the J-values.

TABLE 1

WAVE NUMBERS OF THE LINES IN THE NEW BANDS OF THE C_2 MOLECULE

J	2–0 Band $\lambda_{head} = 8750.8$			3–1 Band $\lambda_{head} = 8980.5$			3–0 Band $\lambda_{head} = 7714.6$		
	$R(J)$	$Q(J)$	$P(J)$	$R(J)$	$Q(J)$	$P(J)$	$R(J)$	$Q(J)$	$P(J)$
0	11,415.44	.....	.....	11,123.50	.....	.....	.....	.....	.....
2	420.32	11,410.88	.....	128.28	11,118.57	11,112.71	12,955.57	.....	.....
4	423.29	407.58	11,394.98	131.24	115.64	103.33	958.29	.....	.....
6	424.36	402.36	383.46	132.24	110.42	091.75	958.94	12,937.14	12,918.42
8	423.56	395.24	370.08	131.24	103.33	078.45	957.52	929.51	904.59
10	420.79	386.24	354.77	128.58	094.40	063.25	954.03	919.84	888.70
12	416.17	375.36	337.58	123.95	083.54	046.17	948.52	908.17	870.81
14	409.66	362.56	318.51	117.38	070.79	027.21	.....	894.43	850.87
16	401.22	347.87	297.55	108.95	056.17	11,006.37	.....	878.67	828.93
18	390.82	331.29	274.73	098.58	039.66	10,983.63	919.84	860.89	804.94
20	378.62	312.83	249.96	086.34	021.29		906.18	841.10	778.97
22	364.47	292.48	223.36	072.26	11,000.96		890.43	819.28	750.95
24	348.41	270.23	194.90	056.17	10,978.80		872.71	795.43	720.96
26	330.46	246.11	164.59				852.94	769.55	688.93
28	310.63	220.09	132.36				831.11	741.65	654.88
30	288.88	192.22	098.33				807.25	711.73	618.87
32	265.23	162.47	062.40				781.39	679.78	.....
34	239.66	130.85					753.44	645.83	540.83
36	212.22	097.36					723.52	609.92	498.82
38	182.90	061.95					691.51	571.98	454.82
40		024.73					657.46	531.98	
42							621.46	.....	
44							.....	446.04	
46							543.39	400.10	
48								352.06	
50								302.15	

J	4–1 Band $\lambda_{head} = 7907.7$			5–2 Band $\lambda_{head} = 8108.2$		
	$R(J)$	$Q(J)$	$P(J)$	$R(J)$	$Q(J)$	$P(J)$
0	.....	.....	.....	12,322.15	.....	.....
2	12,639.23	12,630.06	.....	326.80	.....	.....
4	641.87	626.46	.....	329.28	.....	.....
6	642.44	620.91	12,602.42	329.86	12,308.57	12,290.27
8	640.98	613.31	588.69	328.31	301.00	276.38
10	637.48	603.70	.....	324.84	291.41	260.99
12	631.98	592.03	555.12	.....	279.80	243.30
14	624.44	.....	535.30	311.73	266.21	223.61
16	.....	562.68	513.48	302.15	250.58	
18	603.21	544.96	.....	290.52	232.95	
20	589.53	525.21	463.78	276.90	213.29	
22	.....	503.46	435.98	261.24	191.62	
24	556.13	479.67	406.06	243.53	167.95	
26	536.36	453.91	374.17	223.73	142.28	
28	514.58	426.11	340.35	202.01	114.66	
30		396.27		178.29	084.92	
32		364.47				
34		330.70				
36		294.86				
38		257.02				
40		217.21				
42		175.39				
44		131.57				
46		085.78				

In these equations, $\overline{(B'_v - B''_v)}$ is an approximate value for the difference $(B'_v - B''_v)$, derived by using the approximate values for the constants B_v found above; $(B'_v - B''_v)_{\text{corr}}$ is the correction to be applied to $\overline{(B'_v - B''_v)}$ to get the true difference $(B'_v - B''_v) = \overline{(B'_v - B''_v)} + (B'_v - B''_v)_{\text{corr}}$. The other symbols have the usual meanings.

By using the first equation, a plot was made, taking $Q(J) - \overline{(B'_v - B''_v)}J(J+1)$ as ordinate and $J(J+1)$ as abscissa. The intercept for $J = 0$ then gave ν_0. Similarly, through the use of the second equation, a plot of $R(J) + P(J) - 2\overline{(B'_v - B''_v)}J(J+1)$ against $J(J+1)$ gave $2(\nu_0 + B'_v)$ as intercept, from which ν_0 was found, by the use of the approximate B'_v found in the first step above, which was sufficiently accurate for this purpose. The two values of ν_0 found in this way for each band should, of course, agree with each other. This provided a valuable check of the computation. The final values found are given in Table 4.

Accurate values for the correction $(B'_v - B''_v)_{\text{corr}}$ could not be derived from the slopes of the resultant curves, since the points did not fall on a straight line but showed marked curvature. This was due to the fact that the rotational constants D_v were neglected in the derivation of the two equations given above. Therefore, in order to find accurately the differences $(B'_v - B''_v)$, more complete equations had to be used, as given in the next step.

3. The equations, taking into account the rotational constants D_v, took the following forms:

$$\frac{Q(J) - \nu_0}{J(J+1)} = (B'_v - B''_v) - (D'_v - D''_v)J(J+1),$$

$$\frac{R(J) + P(J) - 2(\nu_0 + B'_v - 2D'_v)}{J(J+1)} = 2(B'_v - B''_v - 6D'_v) - 2(D'_v - D''_v)J(J+1).$$

A plot of the left side of each of these equations versus $J(J+1)$ produced straight lines, the intercept providing a value of $(B'_v - B''_v)$ and the slope a value of $(D'_v - D''_v)$. This value of $(B'_v - B''_v)$ was accurate to the fifth decimal place. The differences as evaluated by these two independent methods did not agree exactly. Since the band system is due to a $^1\Pi$–$^1\Sigma$ transition, such a discrepancy is to be expected on account of Λ-type doubling of the $^1\Pi$ state, which produces a splitting of the rotational levels of this state into two components. Owing to the selection rule, $+ \leftrightarrow -$, the lines of the Q branches have one Λ-component as upper state, while the lines of the R and P branches have the other component as upper state, producing a slight difference in the quantities $(B'_v - B''_v)$ and $(D'_v - D''_v)$ as evaluated by the two different methods above. The magnitude of the Λ-doubling constant and the identification of the components of the $^1\Pi$ state will be discussed later.

4. The quantities $(B'_v - B''_v)$ and $(D'_v - D''_v)$ were then used to find more accurate rotational constants, B_v and D_v, for the upper and lower states of each band. Throughout the following procedure, the two sets of differences, $(B'_v - B''_v)$ and $(D'_v - D''_v)$, derived from the Q branches and the P and R branches were used independently, to give separate rotational constants for the two Λ-components of the $^1\Pi$ state. Since a $^1\Sigma$ state does not exhibit Λ-type doubling, the constants as found for this state by these independent methods should be exactly the same. This gave a good check on the computation.

An inspection of the approximate constants found in step 1 above showed that most of the bands had upper and lower states in common with others of the bands. This can be seen in the first column of Table 2. Thus the λ 7715 band has an upper state in common with the λ 8980 band and a lower state in common with the λ 8751 band, and the bands at λ 7908 and λ 8980 have a lower state in common.

In order to determine the constants B_v and D_v from the differences $(B'_v - B''_v)$ and $(D'_v - D''_v)$, it was necessary to know in advance the constants for some one state. Then, by using the corresponding differences, the constants could be determined for all the bands having an upper or lower state in common with one of the others. In the present case the best possible constants B_v and D_v were found for the lower state which the bands at λ 8751 and λ 7715 had in common by using the combination differences $\Delta_2 F''(J)$, as in step 1 above, and combining the data from both these bands. The resulting constants are given in Table 2. The constant B''_v thus found was uncertain in the

TABLE 2

ROTATIONAL CONSTANTS

UPPER STATE $^1\Pi_u$

Band	Infrared Bands: From Q Branches B_v (Cm^{-1})	From Q Branches $D^c_v \cdot 10^6$ (Cm^{-1})	From P, R Branches B^d_v (Cm^{-1})	From P, R Branches $D^d_v \cdot 10^6$ (Cm^{-1})	From $^1\Pi$-$^1\Pi$ Transition v''	B''_v (Cm^{-1})	$D''_v \cdot 10^6$ (Cm^{-1})
.....	.....	.....	.....	.....	0.....	1.6084	6.6
.....	.....	.....	.....	.....	1.....	1.5912	6.5
8751.....	1.5743_2	6.7	1.5740_9	6.6	2.....	1.5738	6.4
7715, 8980.....	1.5571_6	6.8	1.5569_2	6.7	3.....	1.5564	6.9
7908.....	1.5397_0	6.3	1.5395_3	6.3	4.....	1.5400	7.2
8108.....	1.5216	.....	1.5214	.....	5.....	1.5223	6.7

LOWER STATE $^1\Sigma^+_g$

Band	Infrared Bands B''_v (Cm^{-1})	$D''_v \cdot 10^6$ (Cm^{-1})	$^1\Sigma^+_u$–$^1\Sigma^+_g$ v''	B''_v (Cm^{-1})	$D''_v \cdot 10^6$ (Cm^{-1})
8751, 7715.....	1.8113_8	7.2	0.....	1.8125	7.39
7908, 8980.....	1.7930_6	6.8	1.....	1.7927	6.47
8108.....	1.7733	.....	2.....	1.7735	5.50

fifth decimal place, hence this fifth place has been indicated by a subscript. The constants for the upper states of these two bands were then evaluated, using their corresponding differences $(B'_v - B''_v)$ and $(D'_v - D''_v)$ found in step 3. This immediately gave the constants for the upper state of the λ 8980 band and, with the differences for this band, the constants for its lower state. With this procedure the constants for the lower state and the two Λ-components of the upper state of all the bands except the one at λ 8108 were found. They are given in Table 2.

The λ 8108 band had no state in common with any of the others, so the following method had to be used to obtain its constants. Since only a few members of the P branch

of this band were observed, the R and Q branches were used in the following equations:

$$\frac{R(J)-Q(J)}{(J+1)}-2\bar{B}'_v+4\bar{D}'_v(J+1)^2=2B'_{v_{\text{corr}}}-4D'_{v_{\text{corr}}}(J+1)^2,$$

$$\frac{R(J)-Q(J+1)}{(J+1)}-2\bar{B}''_v+4\bar{D}''_v(J+1)^2=2B''_{v_{\text{corr}}}-4D''_{v_{\text{corr}}}(J+1)^2.$$

For each state, $\bar{B}_v$ and $\bar{D}_v$ are the approximate constants found in step 1 above, and $B_{v_{\text{corr}}}$ and $D_{v_{\text{corr}}}$ their corresponding corrections. These equations were used in a manner similar to the ones used in step 3 to give the constants presented in Table 2 for this band.

The constant difference between the rotational constants B_v of the two Λ-components of the $^1\Pi$ state is known as the "Λ-type doubling constant, q." An independent determination of q was made, through the use of the combination defects ϵ[3]

$$\epsilon=[R(J)-Q(J)]-[Q(J+1)-P(J+1)].$$

Since the lines $Q(J+1)$ and $P(J+1)$ were not observed, their wave numbers were computed by the use of interpolation between the lines $Q(J)$ and $P(J)$. After this was done, the quantities ϵ were found. According to the equation

$$\epsilon=2qJ(J+1),$$

a plot of ϵ against $J(J+1)$ gave $2q$ as the slope of the resulting straight line. The average of the quantities q found for the five bands was -0.00020 cm^{-1}, in good agreement with the value -0.00021 cm^{-1} found above from the differences of the B'_v values for the Λ-components of the $^1\Pi$ state.

The rotational constants for the upper $^1\Pi$ state that were found in this way from the new band system were in close agreement with those reported by Herzberg and Sutton[4] for the lower state of the $^1\Pi_g$–$^1\Pi_u$ Deslandres-D'Azambuja system. Their data for this lower state are given in the last two columns of the upper part of Table 2. Similarly, the constants for the lower $^1\Sigma$ state agreed with those found by Landsverk[5] for the lower state of the $^1\Sigma_u$–$^1\Sigma_g$ Mulliken system, given in the last two columns of the lower part of Table 2. Thus it was concluded that the new system was due to a $^1\Pi$–$^1\Sigma$ transition connecting these two previously known transitions. This conclusion was confirmed when the corresponding combination differences were compared. As an example, in Table 3 the combination differences, $\Delta_2F'(J)$, of the λ 8751 band are compared with $\Delta_2F''(J)$ of the $v''=2$ state of the $^1\Pi$–$^1\Pi$ system as given by Herzberg and Sutton. Similarly, the combination differences $\Delta_2F''(J)$ of the λ 7715 and λ 8751 bands are compared with $\Delta_2F''(J)$ of the $v''=0$ state of the $^1\Sigma$–$^1\Sigma$ system as reported by Landsverk. Similar comparisons were made for all the bands, confirming unambiguously the identification mentioned above. On the basis of these comparisons, vibrational quantum numbers were assigned to each band, as given in Table 4.

The lower $^1\Sigma$ state is the lowest observed singlet state of the C_2 molecule. According to Mulliken,[6] it is a $^1\sum_g^+$ state. Therefore, the new system is due to a $^1\Pi_u$–$^1\sum_g^+$ transition. This makes it possible to identify the two series of rotational levels into which each of the upper states is divided because of the Λ-type doubling. According to the rules

[3] *Ibid.*, p. 278.

[4] G. Herzberg and R. B. Sutton, *Canadian J. Research, A*, **18**, 74, 1940.

[5] O. G. Landsverk, *Phys. Rev.*, **56**, 769, 1939.

[6] R. Mulliken, *Phys. Rev.*, **56**, 778, 1939.

given by Mulliken,[7] the negative sign of the constant q found above shows that the series of levels in each upper state from which the Q branch arises is a (c) series, while the P and R branches arise from a (d) series. The (c) series of each upper state is composed of the upper components into which each rotational level is divided, while the (d) series is composed of the lower components.

In order to obtain the best possible rotational constants, the new data and the old were combined. In Table 5 are presented those constants which, for various reasons,

TABLE 3

COMPARISON OF COMBINATION DIFFERENCES

J	Upper State $^1\Pi_u$		J	Lower State $^1\Sigma_g^+$		
	Infrared Bands	$^1\Pi$-$^1\Pi$ Transition		Infrared Bands		$^1\Sigma$-$^1\Sigma$ Transition
	$\Delta_2F'(J)$ from λ 8751 Band	$\Delta_2F''(J)$ ($v''=2$)		$\Delta_2F''(J)$		$\Delta_2F''(J)$ ($v''=0$)
				λ 7715 Band	λ 8751 Band	
4	28.31 cm^{-1}	28.34 cm^{-1}	3	.....	25.34 cm^{-1}	25.5 cm^{-1}
6	40.90	40.87	5	39.87 cm^{-1}	39.83	39.9
8	53.48	53.50	7	54.35	54.28	54.4
10	66.02	66.08	9	68.82	68.79	68.7
12	78.59	78.65	11	83.22	83.21	83.2
14	91.15	91.07	13	97.65	97.66	97.5
16	103.67	103.68	15	.....	112.11	112.2
18	116.10	116.08	17	.....	126.49	126.7
20	128.66	128.66	19	140.87	140.86	140.8
22	141.11	141.09	21	.....	155.26	155.2
24	153.51	153.48	23	169.47	169.57	169.6
26	165.87	165.84	25	183.78	183.82	183.8
28	178.27	178.24	27	198.06	198.10	198.0
30	190.55	190.65	29	212.24	212.31	212.2
32	202.83	202.85	31	.....	226.48	226.5
			33	240.56	.....	240.4
			35	254.62	.....	254.7
			37	268.70	.....	268.5

TABLE 4

BAND ORIGINS AND VIBRATIONAL QUANTUM NUMBERS

λ_{head} in Air	ν_0	v', v''	Approximate Relative Intensity in Discharge
7715 A	12,947.81 cm^{-1}	3–0	5
7908	12,631.55	4–1	3
8108	12,319.16	5–2	1
8751	11,412.31	2–0	10
8980	11,120.34	3–1	5

[7] R. Mulliken, *Rev. Mod. Phys.*, **3**, 89, 1931.

appeared most reliable. When a choice was necessary, it was made principally on the basis of the amount of material available for the determination of each constant. Whenever this was equal, the constants as derived from the $^1\Pi$–$^1\Sigma$ system were favored, since presumably the measurements were more accurate because of the fact that the system was at longer wave lengths. The constants for the (*c*) and (*d*) series of each upper level of the $^1\Pi$–$^1\Sigma$ transition were averaged to give the constants presented in Table 5.

These were the data that were used in the determination of the rotational constants, B_e and D_e, α, β, and the equilibrium nuclear separations, r_e, given in Table 6. They rep-

TABLE 5

THE MOST PROBABLE ROTATIONAL CONSTANTS

FOR THE $^1\Pi_u$ STATE

v'	Observed			Computed	
	B_v (Cm^{-1})	$D_v \cdot 10^6$ (Cm^{-1})	Source	B_v (Cm^{-1})	$D_v \cdot 10^6$ (Cm^{-1})
0	1.6084	6.6	$^1\Pi$–$^1\Pi$	1.6084	6.41
1	1.5912	6.5	$^1\Pi$–$^1\Pi$	1.5912	6.53
2	1.5742_0	6.6	$^1\Pi$–$^1\Sigma$	1.5740	6.65
3	1.5570_4	6.8	$^1\Pi$–$^1\Sigma$	1.5568	6.77
4	1.5396_2	7.2*	$^1\Pi$–$^1\Sigma$	1.5396	6.89
5	1.5223	6.7	$^1\Pi$–$^1\Pi$	1.5224	7.01

* Taken from the $^1\Pi$–$^1\Pi$ transition.

FOR THE $^1\Sigma_g^+$ STATE

v''	Observed			Computed	
	B_v (Cm^{-1})	$D_v \cdot 10^6$ (Cm^{-1})	Source	B_v (Cm^{-1})	$D_v \cdot 10^6$ (Cm^{-1})
0	1.8113_8	7.16	$^1\Pi$–$^1\Sigma$	1.8113_8	7.16
1	1.7930_6	6.75	$^1\Pi$–$^1\Sigma$	1.7930_6	6.75
2	1.7735	5.50	$^1\Sigma$–$^1\Sigma$	1.7747_2	6.34
3	1.754	.....	$^1\Sigma$–$^1\Sigma$	1.7564_0	5.92

resent no significant change over corresponding constants for these same states, as reported earlier, but may be considered to be somewhat more accurate, since they are based upon more material.

The accuracy with which the molecular constants so derived reproduce the rotational data is shown to the right in both parts of Table 5.

D. VIBRATIONAL ANALYSIS

The wave numbers for the origins of the five new bands are given in Table 4. The corresponding vibrational quanta in the upper and lower states, $^1\Pi_u$ and $^1\Sigma_g^+$, respectively, are given in Table 7. The quantities $\Delta G'_{1/2}$ and $\Delta G'_{3/2}$ are the values determined by

Herzberg and Sutton from the Deslandres-D'Azambuja system. A comparison between $\Delta G'_{5/2}$, as obtained from the $^1\Pi$–$^1\Sigma$ system, and the $^1\Pi$–$^1\Pi$ system showed the former to fit much better into a smooth series, and it was therefore adopted. It is probable that perturbations in the upper state of the $^1\Pi$–$^1\Pi$ system have very slightly falsified the value obtained by Herzberg and Sutton. With an average Δ^2G' of 24.29 cm^{-1}, $\Delta G'_{9/2}$ was obtained by extrapolation, which was necessary in order to compute $\Delta G''_{3/2}$, since neither the 5–1 nor the 4–2 bands were observed. Therefore, the quantum $\Delta G''_{3/2}$ is uncertain to

TABLE 6

MOLECULAR CONSTANTS

	Upper $^1\Pi_u$ State	Lower $^1\Sigma_g^+$ State
B_e	1.6170_0 cm^{-1}	1.8205_2 cm^{-1}
D_e	$6.35 \cdot 10^{-6}$ cm^{-1}	$7.36 \cdot 10^{-6}$ cm^{-1}
α_e	0.0172_0 cm^{-1}	0.0183_2 cm^{-1}
β_e	$0.12 \cdot 10^{-6}$ cm^{-1}	$-0.41 \cdot 10^{-6}$ cm^{-1}
q	-0.00020 cm^{-1}	.....
r_e	1.3180 A	1.2422 A
ν_e	8391.66 cm^{-1}	0
ν_{00}	8268.50 cm^{-1}	0
ω_e	1608.33 cm^{-1}	1855.63 cm^{-1}
$\omega_e x_e$	12.14 cm^{-1}	14.08 cm^{-1}

TABLE 7

VIBRATIONAL QUANTA IN THE UPPER AND LOWER STATES

v	Upper State $^1\Pi$		Lower State $^1\Sigma$	
	$\Delta G'_{v+1/2} = G'(v+1) - G'(v)$	Δ^2G'	$\Delta G''_{v+1/2} = G''(v+1) - G''(v)$	Δ^2G''
0	1584.08 cm^{-1}	24.33 cm^{-1}	1827.47 cm^{-1}	(28.16 cm^{-1})
1	1559.75	24.25	(1799.31)	
2	1535.50	24.29	.....	.....
3	1511.21	(24.29)	.....	.....
4	(1486.92)		.....	.....

the extent that the aforementioned extrapolation is uncertain; but the error is probably not greater than 2 or 3 in the second decimal place.

The vibrational constants for the upper and lower states and the excitation energies, ν_e and ν_{00}, derived from the ΔG values of Table 7 and the ν_0 values of Table 4, are given in the lower part of Table 6. The values found for the upper $^1\Pi_u$ state differ only very slightly from those of Herzberg and Sutton. The vibrational constants of the lower state were not previously known with any accuracy, Landsverk's value being obtained from the rotational constants, D and B. The value of ν_e is entirely new.

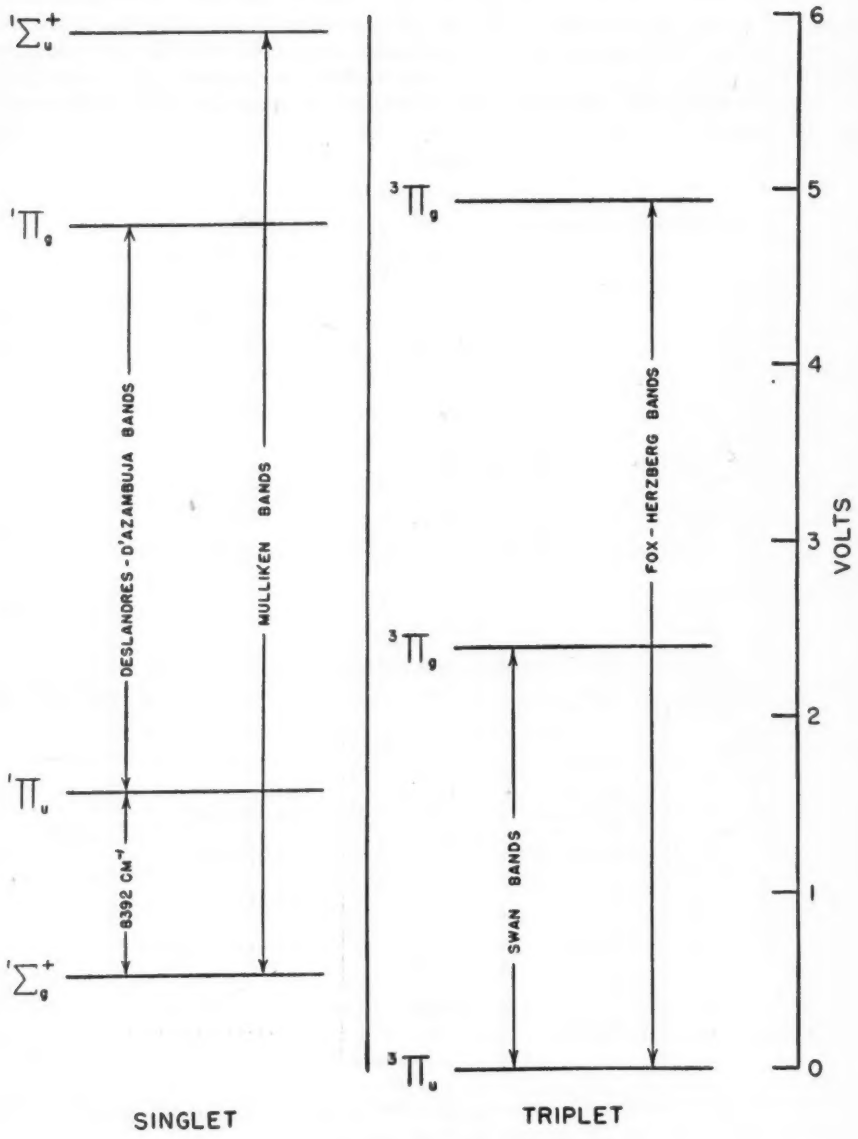

FIG. 2.—Energy-level diagram of the C_2 molecule

E. ELECTRONIC STRUCTURE

The electron configurations of the two states involved in the new bands are

$$(K)\,(K)\,(\sigma_g 2s)^2\,(\sigma_u 2s)^2\,(\pi_u 2p)^4 \qquad {}^1\Sigma_g^+,$$

$$(K)\,(K)\,(\sigma_g 2s)^2\,(\sigma_u 2s)^2\,(\pi_u 2p)^3\,(\sigma_g 2p)\;{}^1\Pi_u\,.$$

On the assumption of equal energy for the two configurations, Mulliken[6] predicts that the ${}^1\Pi_u$ state would be 0.8 e.v. above the ${}^1\Sigma_g^+$ state, which is in satisfactory agreement with the observed value, 1.04 e.v.

F. ENERGY-LEVEL DIAGRAM

The determination of the excitation energy of the ${}^1\Pi_u$ state above the ${}^1\Sigma_g^+$ state, as given in Table 6, makes it possible to complete the energy-level diagram of the C_2 molecule, as far as the known singlet levels are concerned. In Figure 2 is presented all that is known at present about the energy-level diagram of this molecule. Altogether, three triplet and four singlet electronic levels are known. The observed transitions are as shown. The ${}^3\Pi_u$ level is considered to be the ground level of the molecule, mainly due to the great strength of the Swan bands in absorption in the spectra of the N-type stars. On account of the fact that no intercombination system has been found, the relative position of the triplet and singlet levels is still in doubt. Therefore, a vertical line has been drawn in the diagram separating the singlet and triplet systems. Mulliken[6] predicts from theoretical considerations that the ${}^1\Pi_u$ level should be 1.6 e.v. above the ${}^3\Pi_u$ level, and the diagram has been drawn to conform to this prediction. There still remains, however, the possibility of a slight vertical shift of the singlet levels with respect to the triplet levels.

The analysis of the ${}^1\Pi_u$–${}^1\Sigma_g^+$ transition gives $\nu_e = 8391.66\ \mathrm{cm}^{-1}$ as the energy difference between these two states. Similarly, the energy difference between the two known ${}^1\Pi$ states is given by the analysis of the Deslandres-D'Azambuja bands; and the analysis of the Mulliken bands gives the energy difference between the two ${}^1\Sigma$ states. Thus, from these three observed band systems, the relative positions of the four known singlet levels can be determined. The resulting energy-level diagram is shown in Figure 2.

This investigation was carried out under the guidance of Dr. G. Herzberg. I am greatly indebted to him for many helpful suggestions and valuable advice.

METHANE IN THE EARTH'S ATMOSPHERE*

MARCEL V. MIGEOTTE†
Mendenhall Laboratory of Physics, Ohio State University
Received February 23, 1948

ABSTRACT

A study of the solar spectrum, under high resolving power, in the 3.3-μ region has revealed the presence of thirteen regularly spaced lines which have been identified as methane lines.

In 1943, G. B. B. M. Sutherland and G. S. Callendar[1] pointed out that the 3.3-μ region of the atmospheric spectrum was of special interest for the discovery of new compounds in the earth's atmosphere. However, for such a study, high resolution is needed because of the presence of many intense water-vapor lines.

On January 10, 1948, the solar spectrum was mapped in the 3.3-μ region by using a prism-grating spectrograph equipped with an echelette grating having 7200 lines per inch. Figure 1 gives a reproduction of one of the records obtained between 3.49 and 3.31 μ, the principal feature of this region being the presence of thirteen regularly spaced lines about 10 cm^{-1} apart. These lines are indicated by arrows in Figure 1. Their wave lengths and wave numbers are given, respectively, in the first and second columns of Table 1. In the third column are reproduced the wave numbers corresponding to vibration-rotation lines of the 3.3-μ absorption band of methane (lines of the P branch). The first wave number, $\nu = 2876.0$ cm^{-1}, in this column is taken from a publication by J. P. Cooley.[2] The other measurements given in the same column are more accurate and were published by A. H. Nielsen and H. H. Nielsen[3] in 1935. The last column of Table 1 indicates the differences between the wave numbers measured in the solar spectrum and those measured in the laboratory. All the differences fall within the errors of measurements. Because of this fact, it may be stated that the regularly spaced lines found in the 3.4-μ region of the solar spectrum are due to atmospheric methane.

During the months of January and February, only four other opportunities presented themselves to record the 3.3-μ region of the solar spectrum, and the same lines have been observed on each of the records obtained.

In the 3.3-μ region, there is a band of water vapor which has been measured under high resolving power by H. H. Nielsen.[4] At the present time the fine structure of this band is not known for wave numbers shorter than 3011 cm^{-1}. However, as the water-vapor absorption extends farther than this limit, it is possible that water-vapor lines are superposed on some of the methane lines in the atmospheric spectrum, between 3000 and 2870 cm^{-1}.

The position of the Q branch of the 3.3-μ methane band is indicated in Figure 1. It corresponds to a region of strong absorption in the solar spectrum. However, a comparison with the spectrum of water vapor obtained by H. H. Nielsen shows that there are six lines of water vapor in the same region (between 3011 and 3019 cm^{-1}).

* The present investigation was supported by the Air Materiel Command, Wright Field, Dayton, Ohio.

† From the Institut d'astrophysique de Cointe, University of Liége, Belgium.

[1] *Reports on Progress in Physics*, **9**, 18, 1943.

[2] *Ap. J.*, **62**, 73, 1925.

[3] *Phys. Rev.*, **48**, 864, 1935.

[4] *Phys. Rev.*, **59**, 565, 1941.

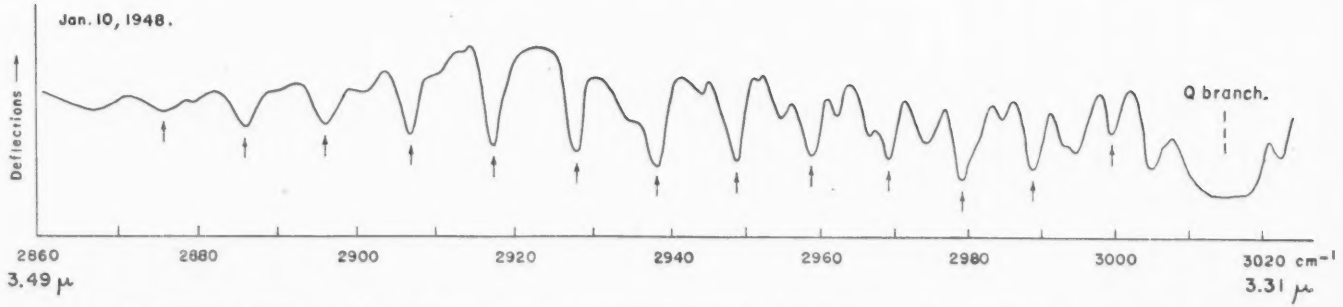

FIG. 1.—The solar spectrum in the 3.4-μ region. Echelette grating: 7200 lines per inch. Slits: 0.2 mm; 0.52 cm^{-1}. The methane lines are indicated by arrows.

The lines of the R branch of the 3.3-μ methane band have been measured by A. H. Nielsen and H. H. Nielsen[3] between 3000 and 3155 cm^{-1}. In the solar spectrum they fall at places where there are strong water-vapor lines or very close to such lines. To identify methane lines in this region, still higher resolution is needed, as well as solar spectra taken when the water-vapor content in the atmosphere is very low.

The solar spectrum given in Figure 1 was obtained by using a new prism-grating spectrograph designed by Dr. R. Nobel, under the direction of Professor H. H. Nielsen. The optics of the grating spectrograph are of the "Pfund type."[5] The parabolic mirrors have an aperture of $f/5$ and a focal length of 100 cm. The detector was a thermistor bolometer, connected to a Bell Telephone amplifier. The records were obtained with a Brown electronic recorder.

The 3.3-μ band of CH_4 has been attributed to the fundamental vibration, ν_3, the other fundamental band, ν_4, being situated in the 7.7-μ region. As this last band is more intense

TABLE 1

LINES OF METHANE

Wave Lengths in Angstroms (Solar Spectrum)	Wave Numbers in Cm^{-1} (Solar Spectrum)	Wave Numbers of CH_4 in Cm^{-1} (Laboratory)	Differences in Wave Numbers (Solar−Lab.)
34774.4	2875.7	2876.0	−0.3
34648.8	2886.1	2886.1	0
34530.0	2896.0	2896.7	− .7
34400.3	2906.9	2907.0	− .1
34277.7	2917.3	2917.7	− .4
34149.8	2928.2	2927.8	+ .4
34035.3	2938.1	2938.1	0
33912.5	2948.7	2948.3	+ .4
33798.9	2958.7	2958.6	+ .1
33677.6	2969.3	2968.8	+ .5
33566.4	2979.2	2979.1	+ .1
33455.9	2989.0	2989.2	− .2
33337.4	2999.6	2999.7	−0.1

than the first one, a band of methane may be predicted in the 7.7-μ region of the solar spectrum.

In 1941, A. Adel[6] discovered a band at 7.6 μ when mapping the solar spectrum under low resolution. He proposed N_2O and perhaps N_2O_5 as possible identifications.[7] The 7.6-μ region of the solar spectrum was also mapped by A. Adel,[8] under high resolving power, using a grating with 2400 lines per inch; and he attributed part of the observed fine structure to N_2O.[9] Concerning this identification, Sutherland and Callendar[1] have stated that the evidence of N_2O, while very strong, is not entirely conclusive.

The 7.7-μ band of CH_4 was measured, under high resolving power, by A. H. Nielsen and H. H. Nielsen,[3] from 1253 to 1365 cm^{-1}. A comparison between these laboratory measurements and the one obtained by A. Adel[8] in the solar spectrum shows that, within the limit of accuracy of the measurement, it is possible to find lines in the solar spectrum corresponding to all the methane lines. However, by mapping the water-vapor spectrum

[5] For a description of a spectrometer using the same kind of optics see *Phys. Rev.*, **38**, 2162, 1931.

[6] *Ap. J.*, **87**, 198, 1938.

[7] *Ibid.*, **90**, 627, 1939.

[8] *Ibid.*, **94**, 451, 1941.

[9] *Ibid.*, **93**, 509, 1941.

in the 7.7-μ region, it has been found that nearly all the intense lines observed by Adel in the solar spectrum between 1250 and 1365 cm^{-1} can be attributed to water vapor.

Preliminary results have been obtained on the solar spectrum in the 7.7-μ region by using a grating with 3600 lines per inch. Up to the present, the resolution is not higher than that found in the spectra published by A. Adel.[8] These spectra were obtained in Flagstaff, Arizona, in 1940. From a comparison with the new spectrograms recorded in Columbus, Ohio, there are reasons to believe that the detected methane is not due to a local impurity of the atmosphere. More details concerning this question will be published as soon as better spectrograms are obtained in the 7.7-μ region.

Experiments are under way for a quantitative determination of the atmospheric methane. The change of intensities of the CH_4 lines for different heights of the sun is also being studied.

I acknowledge important suggestions of Professor H. H. Nielsen and I am grateful to him for giving me the opportunity to work in his laboratories.

ANHARMONIC PULSATIONS OF THE CEPHEID VARIABLE

H. K. SEN
Harvard College Observatory
Received December 8, 1947

ABSTRACT

It has been shown that only homogeneous stars are capable of uniform, radial, adiabatic pulsations. Rosseland's theory of anharmonic oscillations (to the second order of approximation) has been found to work better with the nonhomogeneous models than with the homogeneous one and has been applied to different stellar models, including Roche's and the standard model. Close accord with observation regarding period, skewness of velocity-curve, and amplitude has been found for δ Cephei, regarding it as a polytrope of index $n = 4$. The analysis indicates a high degree of compressibility, in general, for the cepheids.

I. INTRODUCTION

Eddington[1] initiated the consideration of the square of the amplitude in the cepheid's oscillation, and a dependence of period on amplitude was envisaged by Miss Kluyver.[2] Rosseland,[3] in his George Darwin Lecture, developed a general theory of anharmonic pulsations. Considering the second-order terms for the homogeneous star of radius R, he obtained $\frac{1}{4}R$ as the limit to the semi-amplitude, which was about three or four times the observed one (about $\frac{1}{16}R$). In Rosseland's opinion the discrepancy would hardly be bridged over by considering Roche's model, and he suggested the carrying-out of further approximations.

Kothari and Bhatnagar,[4] in a recent paper, have found that the equations of motion for the homogeneous star are exactly integrable for the value $\frac{5}{3}$ of the ratio of specific heats (γ) and that, for the observed degree of skewness ($\delta \sim 5$), the semi-amplitude would be about $0.8R$. They have found Roche's model to give the same result as the homogeneous one with $\frac{5}{2}M$ in place of M (mass of star). Their conclusion is: "The theory of anharmonic oscillations (for $\gamma = \frac{5}{3}$) cannot account for the observed skewness."

It appears that the workers mentioned above have considered only uniform radial oscillations, for which the displacement at every point is proportional to the radial distance of the point. It will be shown below that only homogeneous stars are capable of uniform, adiabatic oscillations. Thus this assumption imposes a severe restriction on the stellar model, reducing it, in fact, to a homogeneous one; and it is not surprising that the results so far have been found to be independent of the distribution of density in the model.

The application of Rosseland's theory to the nonhomogeneous star is complicated, since the functional dependence, appropriate to the assumed stellar model, of the amplitude on the radial distance has to be ascertained. This would involve extensive numerical integrations in any given case. As it is, a simpler method of approach is possible, starting from the differential equation of motion and the usual boundary conditions. The method has been outlined in the following pages and applied to different stellar models. Roche's model gives a better limit to the semi-amplitude than does the homogeneous one; and δ Cephei is found to be a polytrope of index $n = 4$, and a high degree of compressibility is indicated, in general, for the cepheids.

[1] *M.N.*, **79**, 183, 1919.

[2] *B.A.N.*, **7**, 265, 1937.

[3] *M.N.*, **103**, 233, 1943.

[4] *M.N.*, **104**, 292, 1944.

II. UNIFORM OSCILLATIONS AND THE HOMOGENEOUS STAR

We shall first show that only homogeneous stars are capable of uniform, adiabatic oscillations.

The equation of motion for radial oscillation is

$$\ddot{\xi} = -g_0 \frac{\xi_0^2}{\xi^2} - \frac{1}{\rho}\frac{dP}{d\xi}, \tag{1}$$

where ξ, g, ρ, and P denote distance from center, gravity, density, and pressure, respectively, at a point and where the suffix zero denotes the corresponding values in the initial (undisturbed) state of the star.

Let the amplitudes ξ_1, ρ_1, and P_1 be given by

$$\xi = \xi_0(1+\xi_1), \qquad \rho = \rho_0(1+\rho_1) \qquad \text{and} \qquad P = P_0(1+P_1). \tag{2}$$

The equation of the conservation of mass is

$$\rho_0 \xi_0^2 d\xi_0 = \rho \xi^2 d\xi. \tag{3}$$

As the oscillations are adiabatic, we have the relation

$$P \propto \rho^\gamma, \tag{4}$$

where γ is the effective ratio of the specific heats[5] (regarding the matter and inclosed radiation as one system).

From equations (2), (3), and (4) we have

$$1+\rho_1 = \frac{1}{(1+\xi_1)^2(1+\xi_1+\xi_0\xi_1')} \tag{5}$$

and

$$1+P_1 = \frac{1}{(1+\xi_1)^{2\gamma}(1+\xi_1+\xi_0\xi_1')^\gamma}, \tag{6}$$

where

$$\xi_1' = \frac{d\xi_1}{d\xi_0}.$$

Hence we have

$$\ddot{\xi} = -\frac{g_0}{(1+\xi_1)^2} - \frac{(1+\xi_1)^2}{\rho_0}\left\{(1+P_1)\frac{dP_0}{d\xi_0} + P_0\frac{dP_1}{d\xi_0}\right\}. \tag{7}$$

The equation of hydrostatic equilibrium is

$$\frac{dP_0}{d\xi_0} = -g_0\rho_0. \tag{8}$$

From equations (7) and (8) we have

$$\begin{aligned}\ddot{\xi} = &-g_0\left[\frac{1}{(1+\xi_1)^2} - \frac{1}{(1+\xi_1)^{2\gamma-2}(1+\xi_1+\xi_0\xi_1')^\gamma}\right] \\ &-\frac{P_0}{\rho_0}(1+\xi_1)^2\frac{d}{d\xi_0}\left[\frac{1}{(1+\xi_1)^{2\gamma}(1+\xi_1+\xi_0\xi_1')^\gamma}\right].\end{aligned} \tag{9}$$

[5] Eddington, *The Internal Constitution of the Stars* (Cambridge: At the University Press, 1926), p. 190.

For uniform oscillation we have

$$\xi_1 = \eta q \qquad \text{and} \qquad \xi_1' = 0 \,, \tag{10}$$

where η is a constant and q is a function of time only.

It follows from equations (2), (9), and (10) that

$$\eta \ddot{q} = -\frac{g_0}{\xi_0}\left[\frac{1}{(1+\eta q)^2} - \frac{1}{(1+\eta q)^{3\gamma-2}}\right]. \tag{11}$$

From equation (11) we have

$$g_0 = \mu \xi_0 \,, \tag{12}$$

where μ is a constant.

Hence we have

$$\mu \xi_0 = g_0 = \frac{GM(\xi_0)}{\xi_0^2} \,, \tag{13}$$

where $M(\xi_0)$ is the mass interior to the sphere of radius ξ_0.

It follows from equation (13) that

$$M(\xi_0) = \frac{\mu}{G}\xi_0^3 . \tag{14}$$

Also for the mass of the shell of radius ξ_0 and thickness $d\xi_0$ we have

$$dM(\xi_0) = 4\pi \xi_0^2 \rho_0 d\xi_0 \,, \tag{15}$$

where ρ_0 is the density of the shell.

From equations (14) and (15) we have

$$\rho_0 = \frac{3\mu}{4\pi G} = \text{Constant} \,. \tag{16}$$

Thus we reach the conclusion that only the homogeneous star is capable of uniform, adiabatic oscillation.

For the homogeneous star of mass M and radius R, equation (11) reduces to

$$\eta \ddot{q} = -\frac{GM}{R^3}\left[\frac{1}{(1+\eta q)^2} - \frac{1}{(1+\eta q)^{3\gamma-2}}\right]. \tag{17}$$

Equation (17) is easily seen to be equivalent to the equation of motion derived by Kothari and Bhatnagar[6] for the homogeneous star.

III. ANHARMONIC OSCILLATIONS OF THE NONHOMOGENEOUS STAR

As we have shown above, the oscillations would not remain uniform for nonhomogeneous stars; and this is so for the higher modes of oscillation even of the homogeneous star.[7] It is necessary to investigate the application of Rosseland's theory to nonuniform oscillations. In what follows we shall consider only the second-order approximation, reserving the higher orders for a later communication.

[6] *Op. cit.*, p. 293, eq. (8).

[7] Sterne, *M.N.*, **97**, 582, 1937.

Retaining terms up to the second order in equation (9), we have

$$\ddot{\xi} = g_0\Big[\{-(3\gamma-4)\,\xi_1 - \gamma\xi_0\xi_1'\} + \Big\{\Big(\frac{9}{2}\gamma^2 - \frac{9}{2}\gamma - 2\Big)\,\xi_1^2 + \gamma(3\gamma-1)\,\xi_0\xi_1\xi_1' + \frac{\gamma(\gamma+1)}{2}\,\xi_0^2\xi_1'^2\Big\}\Big] + \frac{P_0}{\rho_0}\,\gamma\,[(4\xi_1' + \xi_0\xi_1'') \tag{18}$$
$$-\{4(3\gamma-1)\,\xi_1\xi_1' + 2(2\gamma+1)\,\xi_0\xi_1'^2 + (3\gamma-1)\,\xi_0\xi_1\xi_1'' + (\gamma+1)\,\xi_0^2\xi_1'\xi_1''\}\,].$$

This equation has been obtained by Banerji[8] in a paper in which he gave his cepheid theory of the origin of the solar system.

We shall consider the oscillation of the surface of the star and introduce the appropriate boundary condition into equation (18). This is

$$\frac{P_0}{\rho_0} \to 0\,. \tag{19}$$

We assume the pressure to vanish on the surface. As the density does not vanish for the homogeneous star, the boundary condition (19) is satisfied in this case. For the polytrope

$$P_0 = K\rho_0^{1+1/n} \qquad (0 < n < 5)\,, \tag{20}$$

P_0 and ρ_0 both vanish on the surface, but

$$\frac{P_0}{\rho_0} = K\rho_0^{1/n} \to 0\,.$$

Hence equation (19) is the appropriate boundary condition for the polytropic stellar models as well. It follows from Sterne's[9] derivation of the limit for P_0/ρ_0 that equation (19) holds also for Roche's model. It is to be noted that equation (19), when substituted in equation (18), gives, with the help of equation (16), Sterne's boundary condition[10] for small oscillations.

We shall assume that the semi-amplitude

$$\xi_1 = \eta q\,, \tag{21}$$

where q is a function of time only and η is a function of ξ_0.

From equations (2), (18), (19), and (21) we now have

$$\eta\ddot{q} = \frac{GM}{R^3}\Big[\{-(3\gamma-4)\,\eta - \gamma\eta'\}\,q + \Big\{\Big(\frac{9}{2}\gamma^2 - \frac{9}{2}\gamma - 2\Big)\,\eta^2 + \gamma(3\gamma-1)\,\eta\eta' + \frac{\gamma(\gamma+1)}{2}\,\eta'^2\Big\}\,q^2\Big], \tag{22}$$

as $g_0/\xi_0 = GM/R^3$ on the star's surface.

[8] *Proc. Nat. Inst. Sci. Ind.*, **8**, 179, 1942.

[9] *Op. cit.*, p. 590:

$$\frac{P_0}{\rho_0} \to \frac{4\pi R^2 G\bar{\rho}(1-x^3)}{9x} = 0 \text{ at } x = 1 \text{ (boundary)}\,.$$

[10] *Ibid.*, p. 585, eq. (1.9):

$$P_1 = -\Big(4 + \frac{n^2 R}{g_0}\Big)\,\xi_1\,.$$

In equation (22) the differentiation is with regard to the variable

$$x = \frac{\xi_0}{R}, \tag{23}$$

and η and η' are no longer functions of space but stand for their values on the star's surface.[11]

The application of equation (22) is comparatively easy, as η' need be known only at the boundary of the star. The boundary value of η' can be estimated for the usual stellar models as follows:

Rosseland's[12] equation, to the second order of approximation, is

$$\ddot{q} = -\sigma^2 q + Dq^2, \tag{24}$$

where the period of the star's pulsation is

$$P = \frac{2\pi}{\sigma}. \tag{25}$$

Comparing equations (22) and (24), we have

$$\sigma^2 = \frac{GM\gamma}{R^3}\left(\alpha + \frac{\eta'}{\eta}\right), \tag{26}$$

where

$$\alpha = 3 - \frac{4}{\gamma}. \tag{27}$$

Thus η' can be found by equation (26) for stars for which σ is known. It is to be noted that equation (26) enables us to get a period-amplitude relation and facilitates the calculation of the semi-amplitude and skewness for stars with known periods of *small* oscillation.

Again comparing equations (22) and (24) and applying Rosseland's criterion for appreciable skewness of oscillation, viz., $D/\sigma^2 = 1$, we have

$$\eta = \frac{\alpha + \dfrac{\eta'}{\eta}}{\dfrac{\alpha(3\gamma+1)}{2} + (3\gamma - 1)\dfrac{\eta'}{\eta} + \dfrac{\gamma+1}{2}\left(\dfrac{\eta'}{\eta}\right)^2}, \tag{28}$$

for appreciable skewness of the velocity-curve.

Elimination of η'/η between equations (26) and (28) would give the requisite period-amplitude relation.

[11] It may be noted that eq. (22) is supposed not to hold generally, but only at the boundary of the star. In fact, η and η' in that equation stand for the boundary values of these quantities. We can make the derivation of eq. (22) more explicit as follows: We assume that any point from the center initially at radial distance ξ_0 suffers a displacement of relative amplitude $\xi_1 = q_1\eta_1 + q_2\eta_2$, where η_1 and η_2 are first- and second-order terms (amplitude of excited mode and that of higher mode, suitably chosen), respectively, and q_1 and q_2 are purely functions of time. The justification for this assumption has been given by Rosseland (*M.N.*, **103**, 241, sec. 3, 1943) and by Eddington (*M.N.*, **79**, 183, sec. 15, 1919). Substitution of this expression for ξ_1 in eq. (18) would lead (retaining terms only up to second order) to an equation in η_1, q_1, equivalent to eq. (22), and an equation in η_2, q_2, which is the boundary condition for oscillation in the higher mode (second-order term), viz.,

$$\eta_2 q_2 = \frac{GM}{R^3}\{(4 - 3\gamma)\,\eta_2 - \gamma\eta_2'\}q_2.$$

[12] *Op. cit.*, p. 241, eq. (19).

IV. ROCHE'S AND STERNE'S MODELS OF A STAR

We shall now consider Roche's model and Sterne's model of a star in which the density at a point varies inversely as the square of the radial distance of the point. As σ and η'/η are known for both these models,[13] it may easily be verified that they satisfy equation (26).

For Roche's model,

$$\eta = b_0 x^{\sqrt{3\alpha}} . \tag{29}$$

Hence we have

$$\frac{\eta'}{\eta} = \sqrt{3\alpha} . \tag{30}$$

For the other model we have

$$\frac{\eta'}{\eta} = \tfrac{1}{2} [(1 + 8\alpha)^{1/2} - 1] . \tag{31}$$

Thus η can be evaluated for the two models (for an assumed value of γ) from equations (28), (30), and (31).

The semi-amplitude[14]

$$\xi_1 = \tfrac{3}{4}\eta . \tag{32}$$

Thus we have Table 1 for ξ_1, in which we have given Rosseland's result for the homogeneous model for comparison.

TABLE 1

Model	γ	
	$\frac{4}{3}$	$\frac{5}{3}$
Roche's	0.25	0.15
Sterne's	.4	.3
Homogeneous	0.3	0.25

It is seen that the semi-amplitude depends on the assumed value of γ, the optimum results obtained being for the maximum value ($\frac{5}{3}$).

V. THE POLYTROPIC STAR

We shall now consider polytropic stellar models for different values of α. We shall use Schwarzschild's[15] results for the standard model given in the accompanying tabulation.

α	0.2	0.4	0.6
ω^2	0.05882	0.10391	0.13670

Here

$$\omega^2 = \left(\frac{2\pi}{P_3}\right)^2 (\pi G \gamma \rho_c)^{-1} , \tag{33}$$

and P_3 is the period for the standard model of central density ρ_c.

[13] Sterne, *op. cit.*, pp. 588–91.

[14] Rosseland, *op. cit.*, p. 243, eq. (39).

[15] *Ap. J.*, **94**, 245, 1941.

From equation (33) we have

$$P_3^2\bar{\rho} = \frac{\pi}{13.59\omega^2 G\gamma}\,, \tag{34}$$

as

$$\frac{\rho_c}{\bar{\rho}} = 54.36 \tag{34a}$$

for the standard model.

For a polytrope of index n and period P we have Miller's[16] formula:

$$\frac{P}{P_3} = c^{3-n}\,, \tag{35}$$

where

$$c = 1.703\ (1 < n < 3) \tag{36}$$

and

$$c = 1.751\ (3 < n < 4)\,. \tag{37}$$

From equations (34) and (35) we have

$$P^2\bar{\rho} = \frac{\pi c^{6-2n}}{13.59\omega^2 G\gamma}\,. \tag{38}$$

From equations (25) and (26) we have

$$P^2\bar{\rho} = \frac{3\pi}{G\gamma\left(\alpha + \dfrac{\eta'}{\eta}\right)}\,. \tag{39}$$

From equations (38) and (39) we have

$$\frac{\eta'}{\eta} = \frac{40.77\omega^2}{c^{6-2n}} - \alpha\,. \tag{40}$$

It may be noted that a numerical check has shown equation (40) to be fairly closely satisfied (even for the higher modes of oscillation) by Schwarzschild's tabulated values of η'/η for different values of α, e.g., for $\alpha = 0.6$, Schwarzschild's table[17] gives $\eta'/\eta = 4.78$, whereas from equation (40) we have $\eta'/\eta = 4.97$.

Equation (40) enables us to calculate η'/η for different values of α and n. This value of η'/η when substituted in equation (28) will give the semi-amplitude[13]

$$\xi_1 = \tfrac{3}{4}\eta\,.$$

We have given in Table 2 (correct to the first significant figure only) the values of ξ_1 for $n = 1$, 2, 3, and 4, and $\alpha = 0.2$, 0.4, and 0.6. The values for $n = 0$ (homogeneous star) have been given for comparison.

It is found that, for values of ξ_1 very close to those tabulated above, there is considerable latitude in the lengthening of the period and the skewness (the range being from about two and four times, respectively, to infinity). Thus from Table 2 we can get the polytropic index of best fit for the cepheids given in Eddington's[18] table. We shall calculate it for the case of the typical cepheid, δ Cephei.

[16] *M.N.*, **90**, 62, 1929, eqs. (5.1) and (5.2).

[17] *Op. cit.*, p. 248, Table 4.

[18] *The Internal Constitution of the Stars*, p. 182, Table 25.

VI. THE POLYTROPIC INDEX OF BEST FIT FOR δ CEPHEI

For δ Cephei, according to Eddington,[19]

$$1-\beta=0.45\ , \qquad (\gamma a)^{1/2}=0.493\ .$$

The quantity a is close to the value 0.2. We shall take $a = 0.2$ and $\gamma = 1.43$. For this value of a and the observed value[18] of the semi-amplitude (0.063), Table 2 gives $n = 4$.

TABLE 2

a	n				
	0	1	2	3	4
0.2	0.28	0.26	0.20	0.13	0.063
.4	.27	.25	.17	.094	.039
0.6	0.25	0.24	0.15	0.076	0.030

Substituting these values in equation (38), we have

$$P^2\bar{\rho}=\frac{\pi}{13.59\,(1.751)^2\omega^2G\gamma}, \tag{41}$$

or, if P is expressed in days,

$$P^2\bar{\rho}=\frac{0.00631}{13.59\,(1.751)^2\omega^2\gamma}. \tag{42}$$

The observed value is given by

$$P^2\bar{\rho}=\frac{(0.89)^2}{54.36}. \tag{43}$$

Equation (43) has been obtained from Eddington's[18] table which gives $P\sqrt{\rho_c}=0.89$, and from equation (34a) above.

Comparing equations (42) and (43), we find that the theoretical period has to be increased 2.86 times to agree with observation. From a table of elliptic integrals we find that, for this increment in period, the skewness (ratio of time of expansion phase to that of contraction phase) is

$$\delta=5.9\ . \tag{44}$$

This is comparable to the asymmetry observed in the velocity-curve of cepheids ($\delta\sim 5$). It is true that ξ_1 will be less than its limiting value 0.063, which gives infinite skewness and lengthening of period; but the difference will be less than 1 per cent, as a 1 per cent difference gives lengthening of period = 2.5 and $\delta = 5$. We conclude that, to the second order of approximation in Rosseland's theory, the constitution of δ Cephei as a polytrope of index $n = 4$ accords fairly well with the observed values of the period, semi-amplitude, and skewness of the velocity-curve.

The polytropic index n, as we see from Table 2, depends on the assumed value of a. In Table 3 we give results for δ Cephei ($\xi_1 = 0.063$).

We can similarly calculate the polytropic indices of best fit for the other cepheids in Eddington's table.[18] This would be an extension, to the second order of approximation, of Miller's[20] results (first order). However, in view of the approximations involved (stated

[19] *Ibid.*, p. 193. [20] *Op. cit.*, p. 64.

below), we shall merely indicate the general trend of the results to be obtained by detailed calculation.

VII. GENERAL REMARKS AND CONCLUSION

Table 2 allows us to make an estimate of the index of best fit for the cepheids. For $a = 0.6$, most of the cepheids wou d be polytropes of indices $3 < n < 4$. The polytropic index would increase with the lowering of the value of a. For $a = 0.2$, most of them would be polytropes of index greater than 4. As the cepheids are supergiants of high radiation pressure, a should be close to the value[21] 0.2 ($\gamma = 1.4$), and our analysis indicates a high degree of central condensation for the cepheids.

We have only estimated the orders of magnitude in our investigation, as we do not think precise calculations would be worth while at this stage—for two reasons: first, it is well known that the adiabatic approximation breaks down for large values of the amplitude of oscillation; and, second, as pointed out by Kothari and Bhatnagar[22] for the

TABLE 3

c	n	δ
0.2	4	5.9
.4	3.5	6.2
0.6	3.25	6.4

homogeneous star, the results may require modification when the calculations are extended to higher orders of approximation. We remark that, in the third- and higher-order approximations, the interaction of the higher modes with the fundamental would have to be considered, and the oscillations would no longer remain uniform ($\eta =$ Constant) even for the homogeneous star. It is conceivable that a suitable value of the semi-amplitude and phase of a higher mode may counteract the effect of the third-order term in the fundamental and considerably lessen the discrepancy between the theoretical and the observed values of the semi-amplitude. At any rate, the case is open, in the author's opinion, for an investigation of the interaction of the higher modes of oscillation with the fundamental of different stellar models.

The author's best thanks are due to Professor A. C. Banerji for his keen interest in the paper and for useful suggestions. He also desires to thank Dr. Kopal for kindly going through the paper and Dr. Shapley for giving him the opportunity to work at the Harvard Observatory.

[21] Eddington, *The Internal Constitution of the Stars*, p. 191, Table 28.

[22] *Op. cit.*

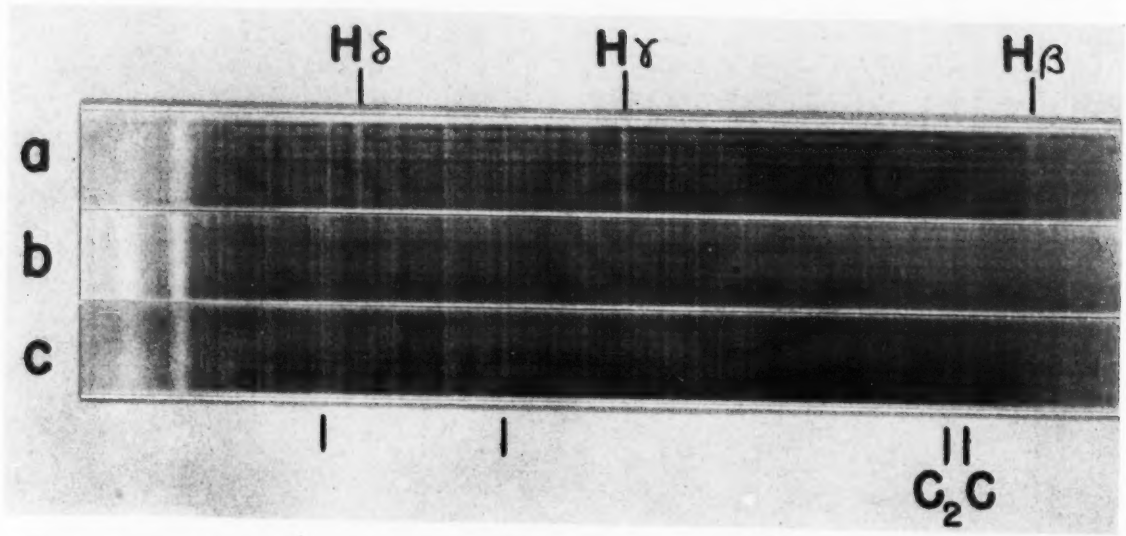

FIG. 1.—Spectra in the photographic region of (*a*) a normal F8 supergiant, γ Cygni; (*b*) the variable star R CrB; and (*c*) the star HD 25878. The features marked and others are very similar in the two peculiar stars; at least two of those indicated are principally due to the element carbon. The spectrogram of R CrB was obtained on June 18, 1947, and that of HD 25878 on November 26, 1947.

NOTES

NOTE ON THE PECULIAR SPECTRUM OF HD 25878

The star HD 25878[1] has been classified as a supergiant by Mrs. Gaposchkin[2] and by the authors of the Mount Wilson Observatory catalogue of spectroscopic parallaxes,[3] who had previously noted narrow bright hydrogen lines in its spectrum.[4] In the course of a low-dispersion investigation of the spectral characteristics of middle-type supergiants, a spectrogram of this star was obtained at the McDonald Observatory. The most striking peculiarity seen in the spectrum was an abnormal weakness of the hydrogen lines; but a number of other features were also noted which are not characteristic of normal stars.

Upon further study it was found that the spectrum of HD 25878 resembles that of the well-known variable star R CrB, at maximum light, to a marked degree. To illustrate this fact, Figure 1 shows the spectra of R CrB and HD 25878, with that of a normal supergiant of type F8, γ Cygni, for comparison. These spectrograms were obtained with the small spectrograph attached to the 40-inch telescope and have a dispersion of 125 A/mm at $H\gamma$. It is apparent upon inspection that the features which distinguish the spectrum of R CrB from that of a normal supergiant are also present in practically the same intensity in the spectrum of HD 25878.

Many of the characteristic features in the spectrum of R CrB are due to the element carbon, a fact which has been taken to indicate an abnormal abundance of that element in the star.[5] The comparable strength of the carbon lines and bands in the spectrum of HD 25878 thus insures the membership of this star in the small group of the "hot carbon stars." Since all other known members of this group are intrinsically variable, an inquiry was made to the Harvard College Observatory concerning possible light-variations of HD 25878. The results of a photometric study of the star are described in the following note.

W. P. Bidelman

Yerkes Observatory
January 29, 1948

LIGHT-CURVE OF A NEW VARIABLE OF R CORONAE BOREALIS TYPE

It was pointed out by Dr. Bidelman, of the Yerkes Observatory, that the star HD 25878 (BD+52°771) has a spectrum with the same characteristics as those of the hot carbon star, R Coronae Borealis, and might show similar variability.

Encouraged by this suggestion, I examined over 1,170 Harvard plates of the region, from 1898 to the present, and found only a single minimum between JD 2429586 and 2429680. The lowest observed magnitude is at JD 2429631.573. At all other times the

[1] $\alpha = 4^h0^m9$; $\delta = +53°6'$ (1900); $m_v = 7.07$; HD type K0.

[2] *The Stars of High Luminosity* (1930).

[3] *Ap.J.*, **81**, 187, 1935; *Mt. W. Contr.*, No. 511.

[4] *Pub. A.S.P.*, **37**, 162, 1925.

[5] Berman, *Ap. J.*, **81**, 369, 1935.

TABLE 1

COMPARISON STARS

BD	HD				Steps	IPg
	No.	Ptm.	Ptg.	Sp.		
+52°755					0	10.30
+52°766					4	9.94
+53°730	25551	8.5	8.5	A0	10	9.12
+52°750	25292	7.6	8.1	F8	13	8.60
+53°732	25602	6.42	7.42	K0	19	7.30

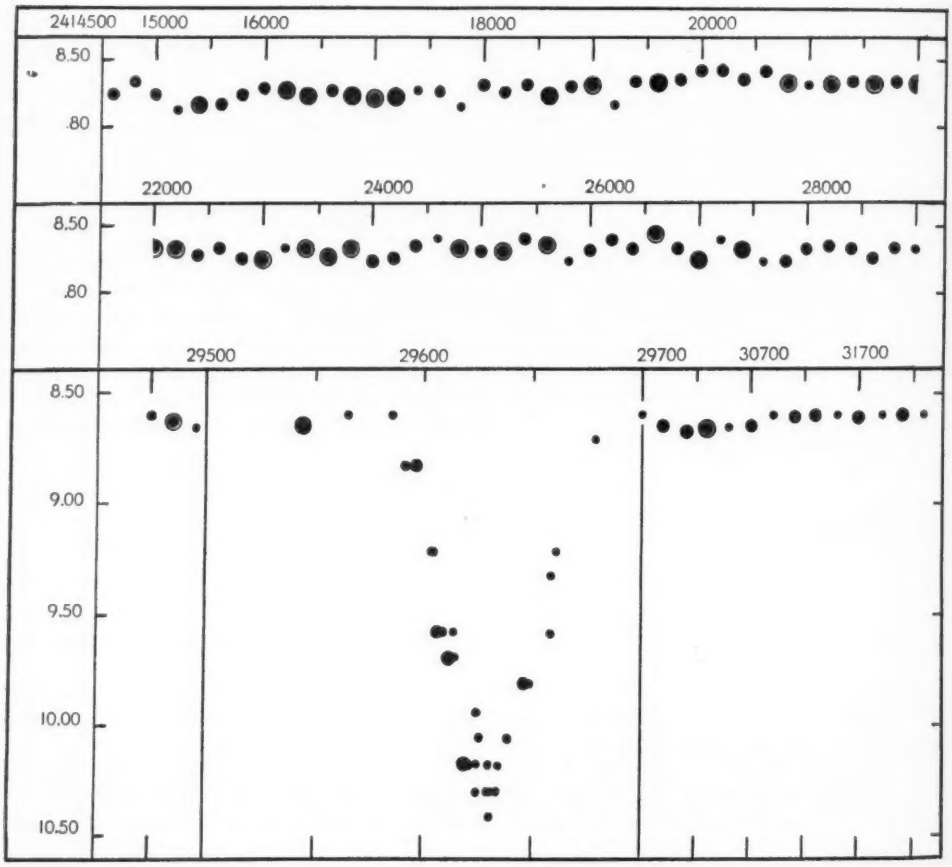

FIG. 1.—*Small dots*, less than five observations; *medium dots*, between six and fifteen observations; *circled dots*, between sixteen and twenty-five observations; *large dots*, more than twenty-five observations.

star appears to have been of constant brightness, between 8.6 and 8.7 mag. on the International photographic scale. The range of variation at minimum is about 1.7 mag.

The position, magnitude, and spectral class of the star in the *Henry Draper Catalogue* are as follows:

R.A. = 4^h0^m9, Dec. = +53°6′,

Ptm. = 7.07, Ptg. = 8.07,

Sp. = K0.

Five stars were used for comparison, as shown in Table 1.

TABLE 2

MAXIMUM OF HD 25878

JD	Mag. (IPg)	No.	JD	Mag. (IPg)	No.	JD	Mag. (IPg)	No.
2414501–700	8.65	5	2420901–100	8.62	4	2427301–500	8.61	26
701–900	8.60	1	1101–300	8.62	8	501–700	8.66	2
901–100	8.67	8	301–500	8.60	7	701–900	8.66	8
5101–300	8.72	1	501–700	8.62	23	901–100	8.60	11
301–500	8.71	31	701–900	8.60	10	8101–300	8.59	16
501–700	8.70	6	901–100	8.60	17	301–500	8.61	9
701–900	8.67	15	2101–300	8.60	23	501–700	8.65	8
901–100	8.64	9	301–500	8.64	12	701–900	8.60	10
6101–300	8.64	23	501–700	8.60	12	901–100	8.60	3
301–500	8.66	36	701–900	8.64	7	9101–300	8.64	12
501–700	8.65	5	901–100	8.65	22	301–500	8.66	2
701–900	8.65	54	3101–300	8.60	2	501–564	8.64	28
901–100	8.67	23	301–500	8.60	24			
7101–300	8.66	50	501–700	8.64	19			
301–500	8.64	3	701–900	8.61	17		Minimum	
501–700	8.66	8	901–100	8.67	12			
701–900	8.72	1	4101–300	8.64	15			
901–100	8.61	8	301–500	8.58	13	681–800	8.60	1
8101–300	8.66	14	501–700	8.56	3	801–000	8.65	29
301–500	8.61	8	701–900	8.60	16	2430001–200	8.67	7
501–700	8.66	29	901–100	8.62	5	201–400	8.67	17
701–900	8.61	9	5101–300	8.61	25	401–600	8.66	2
901–100	8.62	18	301–500	8.55	8	601–800	8.65	11
9101–300	8.72	1	501–700	8.58	20	801–000	8.60	1
301–500	8.59	15	701–900	8.66	2	1001–200	8.60	10
501–700	8.60	5	901–100	8.62	13	201–400	8.60	3
701–900	8.58	12	6101–300	8.56	10	401–600	8.60	6
901–100	8.55	7	301–500	8.60	8	601–800	8.62	5
2420101–300	8.55	11	501–700	8.54	24	801–000	8.60	3
301–500	8.58	11	701–900	8.60	6	2001–200	8.60	6
501–700	8.56	12	901–100	8.65	27	201–400	8.60	1
701–900	8.60	17	7101–300	8.56	3			

Each step is equivalent, on the average, to 0^m12 IPg; all magnitudes are computed with this scale. The light-curve in Figure 1 is plotted from JD 2414501–2432400, and each point represents an average value of observations (Table 2) for 200 days, excepting from JD 2429550–2429700, where the minimum appeared; in this interval they (Table 3) represent individual estimates.

The numbers of observations in each interval of 200 days are quite different, and four kinds of symbols are used to show the mean values in the light-curve.

The light-curve is typical of a star of R Coronae Borealis type. The star apparently

decreased in brightness from JD 2429586 on, and recovered on JD 2429680. The duration of the minimum is 94 days. The faintest magnitude observed occurred at JD 2429631.573, about in the middle of the minimum. The shape of the minimum is very symmetrical and resembles that of an eclipsing variable. It is interesting to note

TABLE 3

MINIMUM OF HD 25878

JD	Mag (IPg)	JD	Mag (IPg)	JD	Mag (IPg)
2429566	8.60	2429613	9.70	2429632	10.18
586	8.60	614	9.70	633	10.30
592	8.84	621	10.18	634	10.30
596	8.84	622	10.18	636	10.18
596	8.84	622	10.18	639	10.06
603	9.22	625	9.94	646	9.82
605	9.22	625	10.18	646	9.82
607	9.58	625	10.30	649	9.82
607	9.58	626	10.06	658	9.34
608	9.58	630	10.30	659	9.58
613	9.58	632	10.30	661	9.22
613	9.70	632	10.42	678	8.72
613	9.70				

TABLE 4

UNOBSERVED INTERVALS

JD	Year	JD	Year
2414800– 900	May–Aug., 1899	2426800– 900	Apr.–July, 1932
15100– 200	Apr.–July, 1900	27200– 300	May–Aug., 1933
15500– 600	May–Aug., 1901	27900–8000	Apr.–July, 1935
17700– 800	May–Aug., 1907	28300– 400	Apr.–July, 1936
18400– 500	Apr.–July, 1909	29000– 100	Apr.–July, 1938
19100– 200	Mar.–June, 1911	29400– 500	May–Aug., 1939
19500– 600	Apr.–July, 1912	29700– 800	Mar.–June, 1940
20200– 300	Mar.–June, 1914	30100– 200	Apr.–July, 1941
21000– 100	May–Aug., 1916	30800– 900	Mar.–June, 1943
22800– 900	Apr.–July, 1921	31200– 300	Apr.–July, 1944
23900–4000	Apr.–July, 1924	31900–2000	Mar.–June, 1946
24600– 700	Apr.–July, 1926	32300– 400	Apr.–Aug., 1947
25700– 800	Apr.–July, 1929		

that the star shows only one minimum from 1898 up to the present; but another minimum of duration about 100 days is not impossible because of some seasonal gaps in the observations. Table 4 shows some intervals of 100 days in which there was not even one observation from Harvard patrol plates.

CHANG YUIN

HARVARD COLLEGE OBSERVATORY
January 28, 1948

REPLY TO D. TER HAAR'S REMARKS ON MY PAPER "THE PHYSICS OF COSMIC GRAINS"

1. I quite agree that, as the radiation in interstellar space is dilute, there does not exist thermodynamic equilibrium. From formulae (2) and (3) of my paper, which are equivalent to one given by S. Rosseland,[1] we may obtain the average number of molecules in quasi-equilibrium with the atoms and the diluted radiation. This fact is shown by equation (4) of my paper, which gives exactly the same order of magnitude for the *CH* molecules in interstellar space as does the one obtained by the detailed theory for the formation of diatomic molecules in interstellar space, developed by Kramers and ter Haar.[2]

2. I then applied similar reasoning to obtain equations (2) and (3) of my paper for the formation of larger molecules. The results are given in relation (5) of my paper. The important point is that the number of molecules with only five atoms is of the order of $10^{-26}/\text{cm}^3$, which is much smaller than the average number of grains ($10^{-11}/\text{cm}^3$). My main objection to the theories which try to explain the formation of the cosmic grains from existing atoms in the gaseous state in its average present conditions is this: How can the grains be formed by the continuing aggregation of atoms if the number of molecules with five atoms is already of the order of 10^{-15} smaller than the number of grains? Dr. ter Haar's theory for the formation of cores of condensation is not satisfactory because it implicitly accepts the theory that a process of condensation does take place.

3. My equation (10) was deduced for the following problem: What is the critical pressure for the formation of drops in a gas in quasi-equilibrium with diluted radiation? The value which T therefore takes in equation (9) is 10,000° K; and the dilution factor cannot also be omitted. Therefore, Dr. ter Haar's application of my formula (9) is not correct. The important point is that from equation (9) I arrive at the same conclusion as by the earlier method; the interstellar gas in the physical conditions considered is far from saturation.

4. At the end of Dr. ter Haar's remarks he says, referring to my calculations of the accommodation coefficient, α: "However, even if the theoretical result were correct, this should only mean that the number of atoms sticking to the surface of an interstellar smoke particle would be reduced by a factor α." This statement implies a misunderstanding of the meaning of α which is given by relation (12) and Figure 1 in my paper.

5. I did not apply directly the theory of Lennard-Jones, but I introduced the necessary modifications to obtain a first approximation for the case when the difference in temperature is great.

6. The experimental results are not yet in disagreement with the results of Section III of my paper. Besides this, it has been shown that the probability of having a second layer of adsorbed atoms is very small.[3]

7. At the end of Section III of my paper I suggested experiments which, when carried out, may give definite information about this whole question. Similar experiments should also be carried out to find out the accurate electrical charge of the cosmic grains.

F. CERNUSCHI

MONTEVIDEO, URUGUAY
DECEMBER 1947

[1] *Theoretical Astrophysics* (Oxford: Clarendon Press, 1936), p. 247.

[2] *B.A.N.*, **10**, 139, 1946.

[3] F. Cernuschi, *Proc. Cambridge Phil. Soc.*, **34**, 392, 1938.

A FAINT S-TYPE STAR IN THE CLEAR REGION IN CYGNUS

During our study[1] of the M-type stars in the Cygnus region we encountered a faint S-type star situated close to a region where a number of faint cepheids have been found.[2] Since the region is relatively free from absorption up to fairly large distances,[3] the star must be far away.

The position of the star in the sky is indicated in the two accompanying charts (Fig. 1), one made from the Eastman 103*a*-O plate and the other from a I-N plate with No. 89 Wratten filter. Three BD stars are shown in both prints. The S-type star has a galactic latitude of 3°.3. Two infrared spectra on hypersensitized I-N plates were secured. A 4° prism plate was taken with an exposure of 30^m on June 17, 1947, and a 2° prism plate with an exposure of 60^m on September 19, 1947. The 4° prism plate shows some continuum to the violet of the A-band, while the 2° prism plate shows no continuum in this region. The band at λ 7950, referred to in another note in this issue of the *Journal*, is very well defined and strong in the 2° prism plate. In the other plate it is also clearly visible, although not quite so strong.

TABLE 1

Date (1947)	No. of Plates	Infrared Magnitude
June 29	2	13.0
July 18	2	13.4
Dec. 14	1	14.2

The infrared magnitudes (determined with I-N plate and with No. 89 filter) of the star, which is variable, are shown in Table 1. Plates on 103*a*-O emulsion were taken on October 15 and 16, 1946, May 23, 1947, and on July 17, 1947. The limiting photographic magnitude on these plates was about 18.0. The star was not recorded on any of these plates. Similarly, a photored plate (103*a*-E plate with No. 22 filter) obtained on October 15, 1946, fails to show the star. The limiting magnitude of this plate is about 17.0.

J. J. NASSAU
G. B. VAN ALBADA

WARNER AND SWASEY OBSERVATORY
CASE INSTITUTE OF TECHNOLOGY
CLEVELAND, OHIO
April 5, 1948

A NEW BAND IN THE INFRARED SPECTRA OF S-TYPE STARS

In connection with our survey[1] of red stars in the Milky Way, some infrared standard spectra have been obtained of M, carbon, and S-type stars. The spectral range extends from about λ 6800 to λ 8700. Both the 2° and the 4° objective prisms have been used;

[1] Nassau and van Albada, *A.J.*, **53**, 115, 1948.

[2] Baade, *Ap. J.*, **79**, 481, 1934.

[3] Oort and Oosterhoff, *B.A.N.*, **9**, 325, 1942.

[1] Nassau and van Albada, *A.J.*, **53**, 115, 1948.

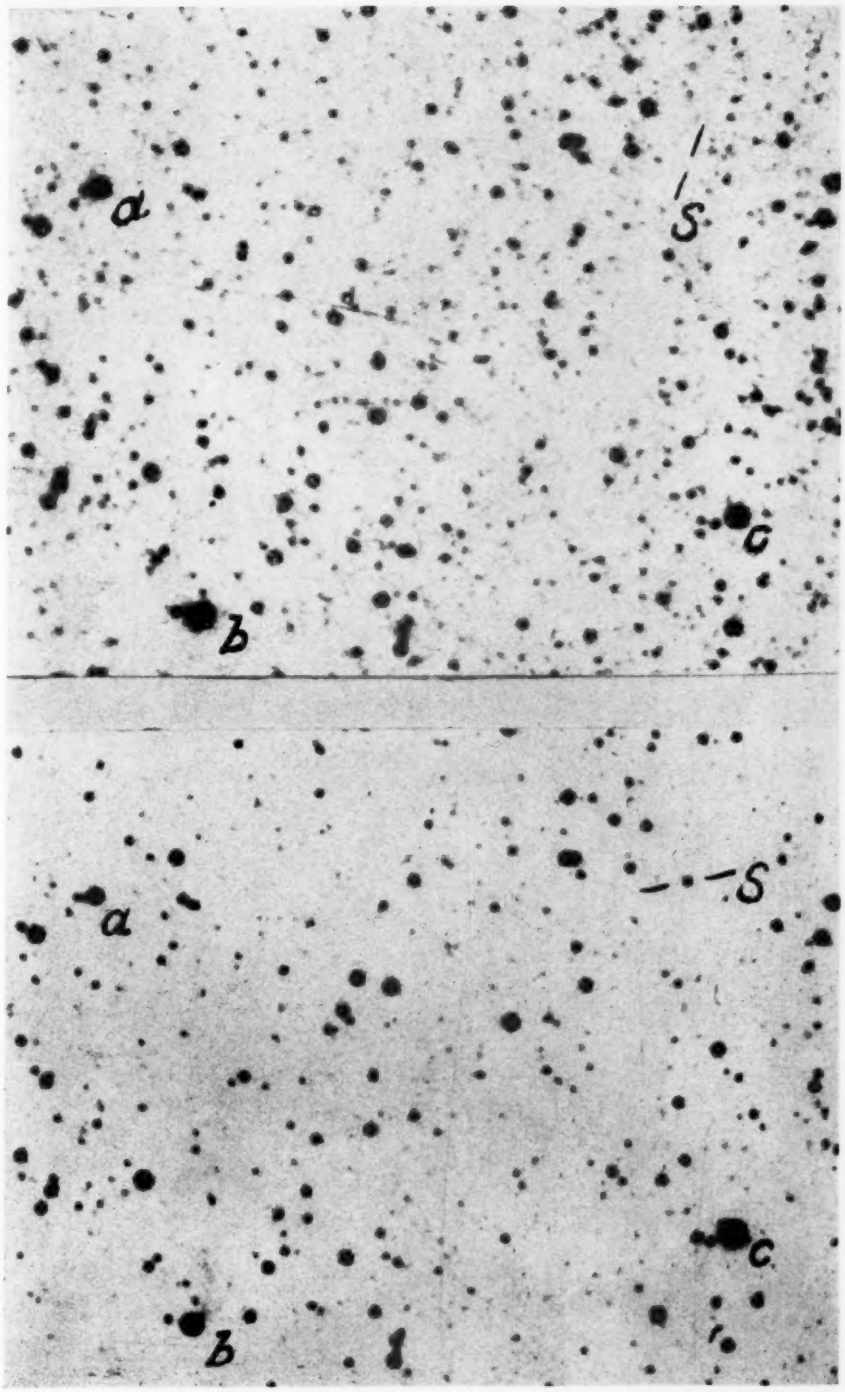

FIG. 1.—Field of S-type star in blue light (*upper*) and in infrared light (*lower*). North is up. The names of the three stars marked are: *a*, BD +36° 3800; *b*, BD +36° 3798; *c*, BD +36° 3792.

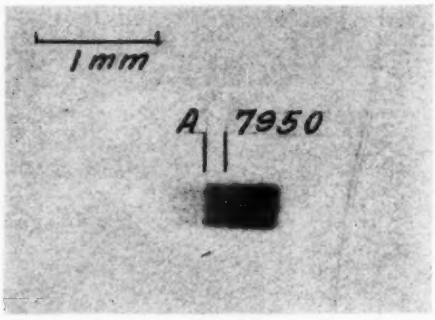

a

FIG. 1, (*a*) Infrared spectrum of S UMa

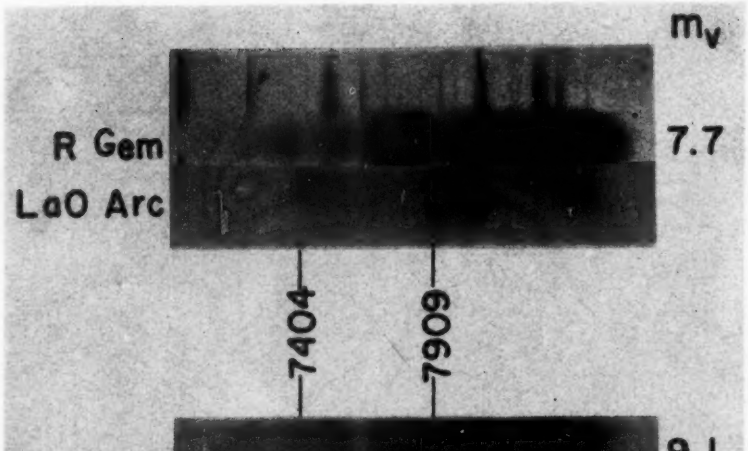

b

c

FIG. 1.—(*b*) Comparison of absorption bands in R Gem (March 25, 1948) with emission bands in *LaO* arc. (*c*) S UMa at 9.1 mag. (March 14, 1948) and at 8.0 mag. (April 22, 1948).

the dispersion at the A-band is 3300 A/mm and 1660 A/mm, respectively. Wave lengths are measured from the A-band which is near the middle of the spectrum.

Table 1 gives seventeen S-type stars used for standards. The spectra may be divided into three classes. Five of them show the bands of *TiO;* their general appearance in this spectral region at low dispersion is very similar to that of M-type stars, although in some cases slight peculiarities have been detected. R CMi shows the bands characteristic to N-type stars.

The remaining eleven stars show a conspicuous break in the continuum at the A-band and a second break at about 0.2 mm to the violet, near λ 7300. The continuum at this side of the A-band is much weaker than that at the long-wave-length side of the band.

TABLE 1

Name	α(1900)	δ(1900)	Variability	Date	Strength of λ 7950
BB And	0^h13^m	+44°.6	Long per.	Nov. 19, 1946	Very strong
R Lyn	6 53	+55.5	Long per.	Mar. 29, 1948	Moderately strong
R Gem	7 01	+22.9	Long per.	Mar. 26, 1948	Very strong
R CMi	7 03	+10.2	Long per.	Mar. 29, 1948	N characteristics
HD 58881	7 22	−11.5	None	Mar. 26, 1948	Very weak
SU Mon	7 38	−10.6	Irr.	Mar. 29, 1948	Weak
HD 64332	7 48	−11.4	None	Jan. 19, 1948	*
V Cnc	8 16	+17.6	Long per.	Mar. 29, 1948	Moderately strong
S UMa	12 40	+61.6	Long per.	Apr. 8, 1947	Strong
R Cam	14 25	+84.3	Long per.	Mar. 26, 1948	Moderately strong
RW Lib	15 17	−23.7	Long per.	June 21, 1947	†
HD 172804	18 37	+ 6.7	None	July 26, 1947	Moderately strong
HD 177175	18 58	+12.1	None	July 25, 1947	‡
Vyssotsky 19	19 29	+23.4	None	Sept. 24, 1947	Very strong
R Cyg	19 34	+50.0	Long per.	July 25, 1947	Very strong
χ Cyg	19 47	+32.7	Long per.	June 23, 1947	§
CN Cyg	20 16	+59.5	Long per.	June 4, 1947	‖

* The *TiO* present makes the star equivalent to the M2 type. The band at λ 7054 gives the appearance of abnormal strength.

† Classed as M7.

‡ Classed as M4.

§ Classed as M5.

‖ Classed as M7.

In addition to these peculiarities, a conspicuous absorption band has been observed at a distance of 0.18 mm from the A-band, with a wave length of about λ 7950. No reference to this band has been found in the literature. The band varies greatly in strength from one star to another as indicated in Table 1. The presence or absence of this band in the *TiO* stars cannot be settled from our spectra. In the stars which do not show the *TiO* or show it weakly, the band is easily observed in spectra made with either prism, even when they are unwidened (Fig. 1, *a*).

J. J. Nassau
G. B. van Albada

Warner and Swasey Observatory
Case Institute of Technology
Cleveland, Ohio
April 5, 1948

ON THE OCCURRENCE OF LANTHANUM OXIDE IN S-TYPE STARS

The new band found near λ 7950 by Nassau and van Albada in the spectra of certain S-type stars[1] has since been observed on low-dispersion slit spectrograms taken with the Perkins reflector. This band and a weaker one centered near λ 7440 can be seen, even on spectrograms of such small scale (≈450 A/mm), to degrade to the red from well-defined main heads. The positions of these heads as measured on spectrograms of R Gem (S3e) and S UMa (S2e) are given in Table 1. It should be emphasized that the accuracy of measurements of prismatic spectra in the infrared is very low and that the measured wave lengths are uncertain by perhaps 2 angstroms.

In position and appearance these bands correspond to the two strongest sequences observed in the infrared arc spectrum of *LaO*. The wave lengths of these bands in the $A^2\Pi$–$X^2\Sigma$ system as measured by Meggers and Wheeler[2] are given in the third line of the table. It will be noticed that two values are tabulated for the λ 7900 band; 7910.50 A was given by Meggers and Wheeler as the wave length of the strongest head, while the

TABLE 1

BANDS OBSERVED IN S-TYPE STARS AND IN *LaO* ARC

SOURCE	WAVE LENGTH OF MAIN HEADS	
	λ 7400 Band	λ 7900 Band
Stars:		
S UMa	7404.4	7908.6
R Gem	7407.0	7910.2
LaO arc:		
Bur. Standards	7403.5	7908.8 7910.5
Perkins (low dispersion)	7405.8	7908.2

fainter head at 7908.77 A undoubtedly merges with the other on spectra of such small scale as ours.

Since it is risky to make identifications by comparing low-dispersion stellar spectrograms with high-dispersion laboratory results, an attempt was made to photograph the emission spectrum of *LaO* through the same spectrograph that was used for the stellar observations. The source of light was an iron arc coated with wet La_2O_3, the stable oxide of lanthanum. The experiments were made by Mr. W. B. Decker, who obtained an almost pure *LaO* spectrum (superposed on a faint continuum) by using a current of about 5 amp. In the reproduction (Fig. 1, *b*) the bands show some structure, including the much fainter secondary heads observed by Meggers and Wheeler at 7380 A and 7877 A. When the current was increased to 6 amp., a number of lines of *Fe* I made their appearance, and these were used as wave-length standards in determining the positions of the *LaO* band heads. These values are given in the last line of Table 1.

The agreement in position between the stellar and the laboratory bands is close enough to make the identification appear probable. It is interesting to note that the bands excited in the arc are less concentrated toward their heads than are the stellar absorption bands. This is to be expected from the lower temperatures of the stars, which

[1] Cf. the preceding note in this issue.

[2] *Bur. Standard J. Res.*, **6**, 239, 1931.

are presumably in the neighborhood of 3000° K. The high melting-point of lanthanum oxide, nearly 4500° K, made it necessary to use an arc of about this temperature.

The sensitivity of the *LaO* bands to atmospheric conditions is shown in Figure 1, *c*. As S UMa brightened from 9.1 mag. to its maximum near 8.0 mag., the bands almost completely disappeared. The lower spectrogram shows a faint, broad feature near the position of the λ 7909 band, but shifted perceptibly toward shorter wave lengths. Examinations of a weak plate of S UMa taken with the grating spectrograph (scale 50 A/mm) on April 18 shows that this absorption marking is not the *LaO* band but is due to a group of strong atomic lines—*Zr* I 7849, 7870, 7945; *Ti* I 7852, 7885, 7895, 7949; *Fe* I 7912; and others—along with a few water-vapor bands. The enhancement of the *Zr* I lines accounts for its appearance in S-type stars. Whether the *LaO* bands are weakly present at all times in S-type stars, and possibly in M-type stars, cannot be established from the existing evidence, for faint bands of *TiO* and atmospheric H_2O are found close to the position of the *LaO* heads.

When the infrared system of *LaO* is conspicuous, the yellow and blue systems of this molecule should also be present, for they all originate from the ground state. Further observations will be necessary to settle this question. The blue bands are difficult to observe in these faint red stars, while the strongest head of the yellow system, at 5600 A, lies in the midst of strong bands of *ZrO* and close to a group of intense *Ca* I lines.

The author is grateful to Professor J. D. Kurbatov for making available the La_2O_3 used in the arc. Mr. W. C. White gave valuable help with the exposures and in the measurement of the plates.

PHILIP C. KEENAN

PERKINS OBSERVATORY
April 1948

NOTICE CONCERNING Be STARS

A *Catalogue and Bibliography of Stars of Classes B and A Whose Spectra Have Bright Hydrogen Lines* (*Mt. W. Contr.*, No. 471; *Ap.J.*, **78**, 87, 1933) was published in 1933; a *Supplement* (*Mt. W. Contr.*, No. 682; *Ap.J.*, **98**, 153, 1943) was published in 1943. A second supplement is being compiled and may be printed in 1949. In order that the new supplement may be as complete as possible, we request observers to send us lists of recent discoveries and of references to published material on Be and Ae stars.

PAUL W. MERRILL
CORA G. BURWELL

CARNEGIE INSTITUTION OF WASHINGTON
MOUNT WILSON OBSERVATORY
PASADENA 4, CALIFORNIA

REVIEWS

Achievements in Optics. By A. BOUWERS. Amsterdam and New York: Elsevier Pub. Co., 1946. Pp. 135+64 Figs. $2.50.

This little book is the first of a series entitled "Monographs on the Progress of Research in Holland during the War." It is of considerable interest to the scientist and also to the amateur astronomer. It reports on a wide variety of results in theoretical optics and in the design of fast cameras. The research was conducted under difficult circumstances; apparently some publication was withheld to prevent enemy use during the war. The book includes outlines of work by Bouwers, L. E. W. van Albada, Korringa, Stephan, van Heel, Nijboer, and Zernike.

Considerable attention is paid to the theory of aberrations and to the compounded effects of diffraction and aberration on the distribution of light in an image. Actual resolving power cannot be predicted from a few ray-tracings of a lens system or from the maximum extension of the confusion disk. The book contains a report on some experimental work on resolving power as dependent on the concentration of light in an image and also detailed computation of diffraction patterns in the presence of third-order spherical aberration, coma, and astigmatism. Zernike gives a brief discussion of the increase in visibility obtained by phase contrast in microscopes. Bouwers describes new microscope objectives made with two concentric mirrors (and also with an additional concentric thin lens). They resemble an inverted Cassegrain telescope and can be used up to N.A. 0.6. The pure mirror type is completely achromatic and usable to N.A. 0.4. I may suggest its application in the ultraviolet or in microphotometers; the latter possibility originates in the prevalent use of red- or infrared-sensitive receivers or photocells and the use of visual radiation for focusing. Almost certainly, some loss of resolution must occur with ordinary microscope objectives. Bouwers also describes some new cameras, telescopes, and field glasses which contain both lenses and mirrors.

For astronomers and spectroscopists the most interesting sections concern fast cameras employing a mirror and one or more lenses. If a spherical mirror is used as the main image-forming component, lenses can be used to correct the residual aberrations. If we accept a curved field, then fast wide-field cameras are possible. The conventional Schmidt is the best known of these; Bouwers gives a useful résumé of its theoretical performance and computes the off-axis spherical aberration (the "arrow-aberration") which ultimately limits the fast Schmidt to a field of about 5° at $f/1$. During the war several independent workers found that fast cameras of wider field can be obtained by using lenses to balance most of the spherical aberration of the mirror. I will not attempt to discuss priority for the various types, but a brief list of the workers may be of value. (I am indebted to Dr. James G. Baker for several of the references.) Maksutov[1] patented an achromatic single meniscus-plus-mirror combination in 1941 in the U.S.S.R. These systems have a relatively limited field but are achromatic. Bouwers has patent applications in the Netherlands in 1940, 1941, and 1945. Van Lear and Swings used such systems in their fast spectrographs (Ray Control Co.) in 1943. In 1943–1944 J. G. Baker developed (patents pending) some very fast systems for television and recently[2] for meteor photography; he also used "concentric" pure lens systems[3] for ultra-wide field photography from 1940 on. Henyey and Greenstein (1944–1946) made a general survey[4] of a wide range of possible combinations of mirrors (one or two) and lenses, with or without aspheric correctors. Hawkins and Linfoot,[5] Wynne,[6] Colacevich, and Bennett have also designed related types.

The new principle adopted by Bouwers and the others is to correct the positive spherical

[1] *J. Opt. Soc. Amer.*, **34**, 270, 1944.

[2] See F. L. Whipple, *Harvard Meteor Program Technical Report*, No. 1 ("Harvard Reprints," Ser. II, No. 19).

[3] *O.S.R.D. Report No. 6016.*

[4] *O.S.R.D. Report No. 4504*, 1945.

[5] *M.N.*, **105**, 334, 1945.

[6] *Nature*, **158**, 583, 1946.

aberration of the mirror by the negative spherical aberration of a meniscus lens. One practical advantage over the Schmidt is that no aspherical surface is usually required; the practicably attainable definition is then better than that of a Schmidt, in view of the inevitable imperfections of the aspheric surface. Maksutov designs his lens to be achromatic, although single; this is possible by a proper choice of the difference of the radii. The field of the Maksutov type is not better than that of the Schmidt. (For visual use and ordinary photography, the Maksutov is quite suitable and can be recommended to the amateur.) Bouwers and many others obtain correction over an unlimited field, by using a lens where the centers of curvature of both surfaces coincide and are at the entrance pupil or stop, which is also the center of the mirror and of the curved focal surface. The system is then completely "concentric"; since it is unaltered by a rotation around the common center, the performance is the same at all field angles. The meniscus lens is chosen so as to balance the spherical aberration of the mirror. A simple concentric system cannot be completely achromatic; if a meniscus is made achromatic by using a doublet, it is found that a small lateral color appears at large fields (10°–20° field angle). If two doublet menisci are used (one concave and the other convex to the mirror), this can be largely eliminated. If exact concentricity is abandoned, achromatism can be obtained at the expense of wide field.

Bouwers gives examples of many such systems. His first $f/1$ experimental system (1940) was made with spectacle lenses. Thin shells suffice for speeds near $f/2$. The shells may be convex or concave to the mirror. Thicker systems can reach $f/1$. Bouwers does not give the final radii for his sytems but derives the necessary approximate formulae. With even an elementary knowledge of optics, it should be possible to compute the exact radii of the lens and mirror required to build a satisfactory $f/1$ camera. He discusses (see also Hawkins and Linfoot[5]) the combination of a centered system with an aspheric corrector at the stop and finds that the asphericity of the corrector need be only about one-fourteenth of that of a Schmidt at comparable speed, $f/0.65$; further, the off-axis spherical aberration is much smaller, and a field of 30° diameter is attainable. This speed seems near the limit that can be reached at present. Henyey and Greenstein[4,7] have developed a thick concentric system with no aspheric surface. The lens lies between the focal surface and the mirror and is traversed twice by the light. This is $f/0.62$ and has a 26° field; it is being built for use in photofluorographic work (an $f/0.9$, 40° field, is already in use). J. G. Baker[2] has designed an $f/0.67$, 52° field, for meteor photography, which uses two thick shells, on either side of an achromatizing aspherical correcting plate. Wynne[6] uses two decentered achromatic menisci to reach $f/0.7$ and 24° field. The types with chromatic aberration are quite satisfactory for spectrographic cameras, in which a curved and tilted field may be provided. Bouwers has built an $f/2$. An $f/0.8$ single thick shell has been designed by Greenstein and built for the Perkins Observatory, and $f/0.7$ would be possible. Such fast cameras are usable only for $\lambda > 3600$ because of the lack of high-quality ultraviolet glass; while natural or fused quartz is unsatisfactory, artificial fluorite may possibly be used. The cost of large thick blocks of glass and the practical difficulties in their use limit the astronomical application of Bouwers', and other, meniscus systems to small focal lengths. It is technologically very difficult and expensive to obtain glass for apertures larger than 12 or 15 inches. The material for spectrographic sizes, however, is easily available. An $f/2$ camera (Bouwers, Fig. 12) of 4-inch aperture can have a meniscus only 0.8 inch thick and would have an aberration disk of about 5 μ. These cameras, like the Schmidt, involve some light-loss by obscuration of part of the aperture by the filmholder.

The book is clearly written and contains elementary derivations of the formulae required. It can be recommended as an introduction into a new field of optical design for both professional and amateur astronomers.

JESSE L. GREENSTEIN

Yerkes Observatory

Studies and Essays, Presented to R. Courant on His Sixtieth Birthday, January 8. New York: Interscience Publishers, Inc., 1948. Pp. 470. $5.50.

The present volume is a collection of papers presented to Professor Richard Courant on his sixtieth birthday by his friends and colleagues "as a token of esteem and friendship." Most of the contributions are of a mathematical nature. But one paper of general astronomical interest to which attention may be drawn is that by O. Neugebauer on "Arithmetical Methods for the

[7] *Amer. J. Roentgenol. and Radium Therapy*, in press.

Dating of Babylonian Astronomical Texts," in which the problem is considered of the dating of Babylonian texts of the last three centuries B.C. relating to lunar and planetary ephemerides from which the dates are missing. The method consists in "continuing the numerical values from a dated text until the values in the fragment are reached. Because each step in the computation of an ephemeris corresponds to a known time unit (e.g., a mean synodic month), the number of steps directly determines the distance in time."

Tables of Spherical Bessel Functions, Vol. II. Prepared by the MATHEMATICAL TABLES PROJECT, NATIONAL BUREAU OF STANDARDS. New York: Columbia University Press, 1947. Pp. xx+328. $7.50.

This volume lists the functions $\sqrt{\pi/2x}J_{n+1/2}(x)$ and $\Lambda_{n+1/2}(x) = \Gamma(n+\frac{3}{2})J_{n+1/2}(x)/(\frac{1}{2}x)^{n+1/2}$, known in the literature as "spherical Bessel functions." The main table contains the functions of orders $\pm(n+\frac{1}{2})$, where $n = 14\ (1)\ 30$ and $x = 0(0.01)\ 10\ (0.1)\ 25$. The majority of the entries are given to eight significant figures for $x < 10$ and to seven significant figures for $x > 10$, except near the zeros of the functions. In some regions a few additional places are given for the sake of uniformity in format.

Tables of the Bessel Functions $J_0(z)$ *and* $J_1(z)$ *for Complex Arguments*. Prepared by the MATHEMATICAL TABLES PROJECT, NATIONAL BUREAU OF STANDARDS. New York: Columbia University Press, 1947. Pp. xliv+403. $7.50.

The volume lists both the real and the imaginary parts of the Bessel functions $J_0(\rho e^{i\varphi})$ and $J_1(\rho e^{i\varphi})$ for $\rho = 0(.01)\ 10$ and $\varphi = 0(5°)\ 90°$. The entries are all given to ten decimals.

INDEX TO VOLUME 107

INDEX TO SUBJECTS

Z Andromedae in 1946 and 1947, The Spectrum of. *Paul W. Merrill* 317

Atmosphere of the K-Type Component of Zeta Aurigae, The Structure of the. *O. C. Wilson* 126

Zeta Aurigae, The Structure of the Atmosphere of the K-Type Component of. *O. C. Wilson* 126

B-Type Stars, The Intensities and Profiles of Lines in Some. *Anne B. Underhill* . . . 349

Be Stars, Notice Concerning. *Paul W. Merrill and Cora G. Burwell* 421

TZ Bootis, Spectrographic Observations of the Eclipsing Binaries of the W Ursae Majoris Type: AH Virginis and. *Y. C. Chang* 96

UY Bootis, The Velocity-Curve of the Cluster-Type Variable. *A. Virginia Farquhar* . 276

C_2 Molecule, A New Band System of the. *John G. Phillips* 389

Carbon Dioxide Molecule, Vibrational Energy Levels of the. *Robert C. Herman* . . . 386

Cepheid Variable, Anharmonic Pulsations of the. *H. K. Sen* 404

"Color-Difference," The Method of. *W. Becker* 278

Color Indices of Proper-Motion Stars. *W. J. Luyten and P. D. Jose* 269

55 Cygni, The Higher Members of the ($2^3P^0-n^3D$) Series of *He* I in the Spectrum of. *O. Struve and H. Chun* 109

SS Cygni, The Parallax of. *K. Aa. Strand* 106

Eclipsing Binaries of the W Ursae Majoris Type: AH Virginis and TZ Bootis, Spectrographic Observations of the. *Y. C. Chang* 96

Fe II Emission Lines in α Herculis and α Scorpii. *G. Herzberg* 94

He I in the Spectrum of 55 Cygni, The Higher Members of the ($2^3P^0-n^3D$) Series of. *O. Struve and H. Chun* 109

α Herculis and α Scorpii, *Fe* II Emission Lines in. *G. Herzberg* 94

Hyades, Radial Velocities of 204 Stars in the Region of the. *Ralph E. Wilson* 119

Interstellar Absorption-Curve, An Extension of the. *A. E. Whitford* 102

Interstellar Matter, The Temperature of. I. *Lyman Spitzer, Jr.* 6

Lanthanum Oxide in S-Type Stars, On the Occurrence of. *Philip C. Keenan* 420

Light-Curve of a New Variable of R Coronae Borealis Type. *Chang Yuin* 413

Lines in Some B-Type Stars, The Intensities and Profiles of. *Anne B. Underhill* . . . 349

"Metallic-Line" Stars, The Classification of the. *Nancy G. Roman, W. W. Morgan, and Olin J. Eggen* 107

Methane in the Earth's Atmosphere. *Marcel V. Migeotte* 400

Milky Way in Northern Cassiopeia and Cepheus, Analysis of the. *Elaine Nantkes and Robert H. Baker* . . . 113

Nebula NGC 6729, A Polarigraphic Study of the Reflection. *Walter T. Whitney and Edwin B. Weston* . . . 371

Nebulae, Stars in Diffuse. *Jesse L. Greenstein* . . . 375

Novae and Planetary Nebulae. *R. Minkowski* . . . 106

Nuclear Reaction, Astrophysical Evidence for the Probability of a. *E. Schatzman* . . . 110

Oxygen and Ionized Silicon, Some *f*-Values for Ionized. *D. R. Bates and Agnete Damgaard* 383

γ Pegasi, The Spectrum of. *Anne B. Underhill* . . . 337

Photoelectric Guider for Astronomical Telescopes, A. *Horace W. Babcock* . . . 73

Photoelectric Photometers, A Theoretical Discussion of the Ultimate Limits of Astronomical. *Harold L. Johnson* . . . 34

Planetary Atmosphere, Scattering in a. *H. C. van de Hulst* . . . 220

Planetary Nebulae, Novae and. *R. Minkowski* . . . 106

J. S. Plaskett's Star of Large Mass, HD 47129. *Otto Struve* . . . 327

Polarigraphic Study of the Reflection Nebula NGC 6729, A. *Walter T. Whitney and Edwin B. Weston* . . . 371

Radial Velocities of 204 Stars in the Region of the Hyades. *Ralph E. Wilson* . . . 119

Reviews:

BOUWERS, A. *Achievements in Optics* (Jesse L. Greenstein) . . . 422

JOHNSON, MARTIN. *Time, Knowledge, and the Nebulae* (E. L. Hill) . . . 112

JONES, SIR HAROLD SPENCER. *John Couch Adams and the Discovery of Neptune* (S. Chandrasekhar) . . . 112

MATHEMATICAL TABLES PROJECT OF THE NATIONAL BUREAU OF STANDARDS. *Tables of Spherical Bessel Functions*, Vol. II . . . 424

MATHEMATICAL TABLES PROJECT OF THE NATIONAL BUREAU OF STANDARDS. *Tables of the Bessel Functions* $J_0(z)$ *and* $J_1(z)$ *for Complex Arguments* . . . 424

Studies and Essays, Presented to R. Courant on His Sixtieth Birthday, January 8 . . . 423

S-Type Star in the Clear Region in Cygnus, A Faint. *J. J. Nassau and G. B. van Albada* . . . 418

S-Type Stars, A New Band in the Infrared Spectra of. *J. J. Nassau and G. B. van Albada* 418

S-Type Stars, On the Occurrence of Lanthanum Oxide in. *Philip C. Keenan* . . . 420

Schuster Problem for an Extended Atmosphere, The. *Anne B. Underhill* . . . 247

α Scorpii, *Fe* II Emission Lines in α Herculis and. *G. Herzberg* . . . 94

Silicon, Some *f*-Values for Ionized Oxygen and Ionized. *D. R. Bates and Agnete Damgaard* 383

Solar Atmosphere, The Effect of Nongrayness on the Temperature Distribution of the. *Guido Münch* . . . 265

Solar Granulation, On Noise Arising from the. *Martin Schwarzschild* . . . 1

Solar Spectrum, $\lambda\lambda$ 2935–3060, The Ultraviolet. *Harold D. Babcock, Charlotte E. Moore, and Mary F. Coffeen* . . . 287

Spectrophotometry of the F Stars and of τ Ursae Majoris. I. *Jesse L. Greenstein* . . . 151

Spectrophotometry of the Wolf-Rayet Star HD 45166. *F. J. Neubauer and Lawrence H. Aller* . . . 281

Spectrum of Z Andromedae in 1946 and 1947, The. *Paul W. Merrill* . . . 317

Spectrum of HD 25878, Note on the Peculiar. *W. P. Bidelman* . . . 413

Spectrum of γ Pegasi, The. *Anne B. Underhill* . . . 337

Stellar Atmosphere, On the Radiative Equilibrium of a. XXII. *S. Chandrasekhar* . 48, 188

Stellar Atmosphere, On the Radiative Equilibrium of a. XXIII. *S. Chandrasekhar and Frances H. Breen* . . . 216

Sunspot Groups of Irregular Magnetic Polarity. *Robert S. Richardson* . . . 78

D. ter Haar's Remarks on My Paper, "The Physics of Cosmic Grains," Reply to. *F. Cernuschi* . . . 417

τ Ursae Majoris, Spectrophotometry of the F Stars and of. I. *Jesse L. Greenstein* . . . 151

Variable Stars, Wave Lengths of Atomic Absorption Lines in the Spectra of Long-Period. *Paul W. Merrill* . . . 303

Velocity-Curve of the Cluster-Type Variable UY Bootis, The. *A. Virginia Farquhar* . . 276

AH Virginis and TZ Bootis, Spectrographic Observations of the Eclipsing Binaries of the W Ursae Majoris Type. *Y. C. Chang* . . . 96

Wave Lengths of Atomic Absorption Lines in the Spectra of Long-Period Variable Stars. *Paul W. Merrill* . . . 303

Wolf-Rayet Star HD 45166, Spectrophotometry of the. *F. J. Neubauer and Lawrence H. Aller* . . . 281

INDEX TO AUTHORS

ALLER, LAWRENCE H., and F. J. NEUBAUER Spectrophotometry of the Wolf-Rayet Star HD 45166 281

BABCOCK, HAROLD D., CHARLOTTE E. MOORE, and MARY F. COFFEEN. The Ultraviolet Solar Spectrum, λλ 2935–3060 287

BABCOCK, HORACE W. A Photoelectric Guider for Astronomical Telescopes 73

BAKER, ROBERT H., and ELAINE NANTKES. Analysis of the Milky Way in Northern Cassiopeia and Cepheus 113

BATES, D. R., and AGNETE DAMGAARD. Some *f*-Values for Ionized Oxygen and Ionized Silicon 383

BECKER, W. The Method of "Color-Difference" 278

BIDELMAN, W. P. Note on the Peculiar Spectrum of HD 25878 413

BREEN, FRANCES H., and S. CHANDRASEKHAR. On the Radiative Equilibrium of a Stellar Atmosphere. XXIII 216

BURWELL, CORA G., and PAUL W. MERRILL. Notice Concerning Be Stars 421

CERNUSCHI, F. Reply to D. ter Haar's Remarks on My Paper, "The Physics of Cosmic Grains" 417

CHANDRASEKHAR, S. On the Radiative Equilibrium of a Stellar Atmosphere. XXII . 48, 188

CHANDRASEKHAR, S. Review of: *John Couch Adams and the Discovery of Neptune*, Sir Harold Spencer Jones 112

CHANDRASEKHAR, S., and FRANCES H. BREEN. On the Radiative Equilibrium of a Stellar Atmosphere. XXIII 216

CHANG, Y. C. Spectrographic Observations of the Eclipsing Binaries of the W Ursae Majoris Type: AH Virginis and TZ Bootis 96

CHUN, H., and O. STRUVE. The Higher Members of the ($2^3P^0-n^3D$) Series of *He* I in the Spectrum of 55 Cygni 109

COFFEEN, MARY F., HAROLD D. BABCOCK, and CHARLOTTE E. MOORE. The Ultraviolet Solar Spectrum, λλ 2935–3060 287

DAMGAARD, AGNETE, and D. R. BATES. Some *f*-Values for Ionized Oxygen and Ionized Silicon 383

EGGEN, OLIN J., W. W. MORGAN, and NANCY G. ROMAN. The Classification of the "Metallic-Line" Stars 107

FARQUHAR, A. VIRGINIA. The Velocity-Curve of the Cluster-Type Variable UY Bootis . 276

GREENSTEIN, JESSE L. Review of: *Achievements in Optics*, A. Bouwers 422

GREENSTEIN, JESSE L. Spectrophotometry of the F Stars and of τ Ursae Majoris. I. . . . 151

GREENSTEIN, JESSE L. Stars in Diffuse Nebulae 375

HERMAN, ROBERT C. Vibrational Energy Levels of the Carbon Dioxide Molecule . . . 386

HERZBERG, G. *Fe* II Emission Lines in α Herculis and α Scorpii 94

HILL, E. L. Review of: *Time, Knowledge, and the Nebulae*, Martin Johnson 112

JOHNSON, HAROLD L. A Theoretical Discussion of the Ultimate Limits of Astronomical Photoelectric Photometers 34

JOSE, P. D., and W. J. LUYTEN. Color Indices of Proper-Motion Stars 269

KEENAN, PHILIP C. On the Occurrence of Lanthanum Oxide in S-Type Stars . . . 420

LUYTEN, W. J., and P. D. JOSE. Color Indices of Proper-Motion Stars 269

MERRILL, PAUL W. The Spectrum of Z Andromedae in 1946 and 1947 317

MERRILL, PAUL W. Wave Lengths of Atomic Absorption Lines in the Spectra of Long-Period Variable Stars 303

MERRILL, PAUL W., and CORA G. BURWELL. Notice Concerning Be Stars 421

MIGEOTTE, MARCEL V. Methane in the Earth's Atmosphere 400

MINKOWSKI, R. Novae and Planetary Nebulae 106

MOORE, CHARLOTTE E., HAROLD D. BABCOCK, and MARY F. COFFEEN. The Ultraviolet Solar Spectrum, λλ 2935–3060 287

MORGAN, W. W., NANCY G. ROMAN, and OLIN J. EGGEN. The Classification of the "Metallic-Line" Stars 107

MÜNCH, GUIDO. The Effect of Nongrayness on the Temperature Distribution of the Solar Atmosphere 265

NANTKES, ELAINE, and ROBERT H. BAKER. Analysis of the Milky Way in Northern Cassiopeia and Cepheus 113

NASSAU, J. J., and G. B. VAN ALBADA. A Faint S-Type Star in the Clear Region in Cygnus 418

NASSAU, J. J., and G. B. VAN ALBADA. A New Band in the Infrared Spectra of S-Type Stars 418

NEUBAUER, F. J., and LAWRENCE H. ALLER. Spectrophotometry of the Wolf-Rayet Star HD 45166 281

PHILLIPS, JOHN G. A New Band System of the C_2 Molecule 389

RICHARDSON, ROBERT S. Sunspot Groups of Irregular Magnetic Polarity 78

ROMAN, NANCY G., W. W. MORGAN, and OLIN J. EGGEN. The Classification of the "Metallic-Line" Stars 107

SCHATZMAN, E. Astrophysical Evidence for the Probability of a Nuclear Reaction . . 110

SCHWARZSCHILD, MARTIN. On Noise Arising from the Solar Granulation. 1

SEN, H. K. Anharmonic Pulsations of the Cepheid Variable 404

SPITZER, LYMAN, JR. The Temperature of Interstellar Matter. I 6

STRAND, K. AA. The Parallax of SS Cygni 106

STRUVE, O., and H. CHUN. The Higher Members of the (2^3P^0—n^3D) Series of *He* I in the Spectrum of 55 Cygni 109

STRUVE, OTTO. J. S. Plaskett's Star of Large Mass, HD 47129 327

UNDERHILL, ANNE B. The Intensities and Profiles of Lines in Some B-Type Stars . . . 349

UNDERHILL, ANNE B. The Schuster Problem for an Extended Atmosphere 247

UNDERHILL, ANNE B. The Spectrum of γ Pegasi 337

VAN ALBADA, G. B., and J. J. NASSAU. A Faint S-Type Star in the Clear Region in Cygnus 418

VAN ALBADA, G. B., and J. J. NASSAU. A New Band in the Infrared Spectra of S-Type Stars 418

VAN DE HULST, H. C. Scattering in a Planetary Atmosphere 220

WESTON, EDWIN B., and WALTER T. WHITNEY. A Polarigraphic Study of the Reflection Nebula NGC 6729 371

WHITFORD, A. E. An Extension of the Interstellar Absorption-Curve 102

WHITNEY, WALTER T., and EDWIN B. WESTON. A Polarigraphic Study of the Reflection Nebula NGC 6729 371

WILSON, O. C. The Structure of the Atmosphere of the K-Type Component of Zeta Aurigae 126

WILSON, RALPH E. Radial Velocities of 204 Stars in the Region of the Hyades . . . 119

YUIN, CHANG. Light-Curve of a New Variable of R Coronae Borealis Type 413